INFORMATION TO USERS

This manuscript has been reproduced from the microfilm master. UMI films the text directly from the original or copy submitted. Thus, some thesis and dissertation copies are in typewriter face, while others may be from any type of computer printer.

The quality of this reproduction is dependent upon the quality of the copy submitted. Broken or indistinct print, colored or poor quality illustrations and photographs, print bleedthrough, substandard margins, and improper alignment can adversely affect reproduction.

In the unlikely event that the author did not send UMI a complete manuscript and there are missing pages, these will be noted. Also, if unauthorized copyright material had to be removed, a note will indicate the deletion.

Oversize materials (e.g., maps, drawings, charts) are reproduced by sectioning the original, beginning at the upper left-hand corner and continuing from left to right in equal sections with small overlaps.

Photographs included in the original manuscript have been reproduced xerographically in this copy. Higher quality 6" x 9" black and white photographic prints are available for any photographs or illustrations appearing in this copy for an additional charge. Contact UMI directly to order.

ProQuest Information and Learning
300 North Zeeb Road, Ann Arbor, MI 48106-1346 USA
800-521-0600

HYDROGEN SHIFT ISOMERS OF PYRIDINE AND OTHER N-HETEROCYCLES: A TANDEN MASS SPECTROMETRY STUDY.

By

DAVID JOSEPH LAVORATO, B. Sc.

A Thesis

Submitted to the School of Graduate Studies

In Partial Fulfillment of the Requirements

for the Degree

Doctor of Philosophy

McMaster University

A MASS SPECTROMETRIC STUDY OF HETEROCYCLIC IONS AND NEUTRALS

For Selena,

For my parents

DOCTOR OF PHILOSOPHY (1999) McMaster University

(Chemistry) Hamilton, Ontario

TITLE: Hydrogen Shift Isomers of Pyridine and other N-Heterocycles: A Tandem Mass Spectrometry Study.

AUTHOR: David J. Lavorato (McMaster University)

SUPERVISOR: Dr. Johan K. Terlouw

NUMBER OF PAGES: xv, 181

ABSTRACT

Ionic and neutral hydrogen shift isomers of common nitrogen containing heterocycles, such as pyridine, have been generated and identified as stable species in the gas phase. The ionic isomers could be obtained by dissociative electron ionization of carefully chosen precursor molecules. Their structure characterization could be realized using tandem mass spectrometry based techniques. Not only conventional metastable ion (MI), collision-induced dissociation (CID) and neutralization-reionization (NR) techniques were used but also the novel hybrid techniques, CID/CID and NR/CID. The use of deuterium labelled isotopomers and quantum chemical calculations formed an essential component in the interpretation of the results.

The neutral hydrogen shift isomers are ylides, carbenes or betaines. Such species are frequently invoked as key intermediates in synthetic and metabolic pathways but their high reactivity in bimolecular reactions often precludes their identification in condensed phases. However, in the dilute gas phase of the mass spectrometer, where intermolecular reactions do not occur, the structure and intrinsic stability of such species may be examined. The mass spectrometric technique of neutralization-reionization (NR) is ideally suited for this purpose. In this technique fast moving beams of structurally well characterized ions are neutralized by charge exchange. The structures of the resulting neutrals are then probed with subsequent collisional ionization experiments.

The thermodynamic stability of the various ionic hydrogen shift isomers appeared to be comparable to that of the parent isomer of conventional structure. A case in point is the pyridine ion $\mathbf{Ia}^{\bullet+}$ for which ΔH_f = 247 kcal/mol and whose hydrogen shift isomers pyridine-2-ylidene$^{\bullet+}$ ($\mathbf{IIa}^{\bullet+}$), pyridine-3-ylidene$^{\bullet+}$ ($\mathbf{IIb}^{\bullet+}$) and pyridine-4-ylidene$^{\bullet+}$ ($\mathbf{IIc}^{\bullet+}$) have enthalpies of formation of 245, 244 and 242 kcal/mol. CID mass spectrometry provided a convenient and reliable tool for the characterization of these ions. The (distonic) ions $\mathbf{IIa}^{\bullet+}$ and $\mathbf{IIb}^{\bullet+}$ but not $\mathbf{IIc}^{\bullet+}$ could be subjected to reduction by single electron transfer in NR experiments. Intense "survivor" signals were obtained but

collision experiments of the reionized neutrals (NR/CID) were required to establish the carbene structure of the neutral species generated. The experimental results concur with predictions from quantum chemical calculations that the neutral (singlet and triplet) and ionic isomers are minima on the potential energy surfaces which are separated by substantial (1,2-H shift) isomerization barriers.

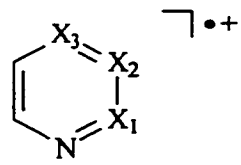

$\mathbf{I}^{\bullet+}$

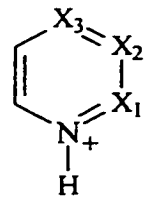

$\mathbf{II}^{\bullet+}$

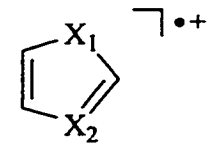

$\mathbf{III}^{\bullet+}$

a: $X_1 = X_2 = X_3 = C\text{-}H$

b: $X_1 = X_2 = C\text{-}H \;\; X_3 = N$

c: $X_1 = X_3 = C\text{-}H \;\; X_2 = N$

a: $X_1 = C^{\bullet} \;\; X_2 = X_3 = C\text{-}H$

b: $X_1 = X_3 = C\text{-}H \;\; X_2 = C^{\bullet}$

c: $X_1 = X_2 = C\text{-}H \;\; X_2 = C^{\bullet}$

a: $X_1 = S \;\; X_2 = N$

b: $X_1 = N\text{-}H \;\; X_2 = N$

The same strategy was used to probe the structure and stability of the H-shift isomers of neutral and ionic pyrazine ($\mathbf{Ib}^{\bullet+}$), pyrimidine ($\mathbf{Ic}^{\bullet+}$), thiazole ($\mathbf{IIIa}^{\bullet+}$) and imidazole ($\mathbf{IIIb}^{\bullet+}$). Among the elusive neutral species identified are the ylides pyrazine-2-ylidene, pyrimidine-2-ylidene, pyrimidine-4-ylidene, thiazol-2-ylidene, imidazol-2-ylidene and imidazol-4-ylidene and the betaine pyrazine-3-ylidene. *Ab initio* calculations on the potential energy surfaces confirm the experimental results but they also reveal that the pyrazine and pyrimidine systems feature additional isomers of comparable stabilities.

The final component of this work deals with the decarbonylation reaction of ionized 2-acetylpyridine, 2-acetylpyrazine and 2-acetylthiazole. Multiple collision experiments were used to show that this reaction does not involve a methyl migration yielding the 2-methyl substituted heterocycle as proposed in the literature. The product ions generated are the 2-methylene heterocycles, ionized 2-methylene-1,2-

dihydropyridine, 2-methylene-1,2-dihydropyrazine, and 2-methylene-2,3-dihydrothiazole, suggesting that the decarbonylation involves a 1,4-H shift followed by an *ipso* substitution. NR/CID mass spectrometry was used to establish that the neutral counterparts of the ionized decarbonylation products retain their structural integrity in the rarefied gas phase.

PREFACE

The larger part of this thesis describes the results obtained by the author during four years of experimental research in gas phase ion chemistry. This field is ideally suited to the investigation by both experimental and theoretical methodologies. Indeed, the common set of conditions involved in mass spectrometric experiments and computational chemistry, i.e. the study of isolated particles, makes the two approaches complementary. Such investigations necessitate the collaboration of both experimental and theoretical chemists. Collaborative contributions from the computational chemists, Prof. Dr. Wolfram Koch (Chapters 2,3 and 6-8), Prof. Dr. Jan Hrusak (Chapter 4), Dr. Christoph Heinemann (Chapter 5), Dr. Lorne Fell (Chapter 7) and Mr. Thomas Dargel (Chapters 2,3 and 6-8) are greatly appreciated. Finally, one individual deserves special mention in the context of collaboration: Dr. Graham McGibbon. His computational contributions (Chapters 2-6), insights, suggestions and critical evaluations have significantly shaped the way in which the results have been presented.

The permission of Elsevier Science, John Wiley & Sons and the American Chemical Society Publication Division to reproduce the data and text which have previously been published is also appreciated.

LIST OF PUBLICATIONS

7. D.J. Lavorato, J.K. Terlouw, G.A. McGibbon, T.K. Dargel, and W. Koch. Observation of Pyrimidine-4-ylidene and Pyrimidine-2-ylidene in the Gas Phase Using Tandem Mass Spectrometry, *Int. J. Mass Spectrom.*, in preparation.

6. D.J. Lavorato, L.M. Fell, J.K. Terlouw, G.A. McGibbon, S. Sen, and H. Schwarz, Identifying Ylide Ions and Methyl Migrations in the Gas Phase: The Decarbonylation Reactions of Simple Ionized N-heterocycles, *Int. J. Mass Spectrom.*, in press.

5. T. Dargel, W. Koch, D.J. Lavorato, G.A. McGibbon, J.K. Terlouw, and H. Schwarz, Pyrazine Diradicals, Carbenes, Ylides, and Distonic Ions Probed by Theory and Experiment, *Int. J. Mass Spectrom.* **1999**, *185/186/187*, 925-930.

4. D.J. Lavorato, J.K. Terlouw, G.A. McGibbon, T. Dargel, W. Koch, and H. Schwarz, The Generation of Neutral and Cationic Hydrogen Shift Isomers of Pyridine. A Combined Experimental and Computational Investigation, *Int. J. Mass Spectrom.* **1998**, *179/180*, 7-14.

3. G.A. McGibbon, J. Hrusak, D.J. Lavorato, H. Schwarz, and J.K. Terlouw, The Thiazole Ylid: A Frequently Invoked Intermediate Is a Stable Species in the Gas Phase, *Chemistry - A European Journal* **1997**, *3*, 232-235.

2. G.A. McGibbon, C. Heinemann, D.J. Lavorato, and H. Schwarz, Imidazol-2-ylidene: Generation of a Missing Carbene and Its Dication by Neutralization-Reionization and Charge Stripping Mass Spectrometry, *Angew. Chem., Int. Ed. Engl.* **1997**, *36*, 1478-1481.

1. D.J. Lavorato, J.K. Terlouw, T. Dargel, W. Koch, G.A. McGibbon, and H. Schwarz, Observation of the Hammick Intermediate: Reduction of the Pyridine-2-Ylide Ion in the Gas Phase, *J. Am. Chem. Soc.* **1996**, *118*, 11898-11904.

ACKNOWLEDGEMENTS

I would like to thank my supervisor and mentor, Professor Johan K. Terlouw, for his guidance, support and patience throughout my graduate studies. I am especially grateful for those times when he recognized that I didn't need a supervisor but rather a friend.

I would also like to thank the members of my supervisory committee: To Prof. John Warkentin, I would like to express my gratitude for allowing me to work out of his lab and for adopting me as a member of his group. I thank Prof. Brian McCarry for his support, inspiration and positive outlook during my studies.

Thanks are also extended to the former and current members of the McMaster Regional Centre for Mass Spectrometry, Dr. Richard W. Smith, Mr. Fajan "Faj" A. Ramelan, Dr. Kirk Green, Mr. Tadek Olech and Ms. Leah Allen for their assistance in the use and maintenance of the mass spectrometers and most importantly their friendship. Many thanks to the members of the NMR facility, Dr. Don Hughes and Mr. Brian Sayer, for always taking the time to answer my questions. I am also indebted to past and present members of the Terlouw research group, Dr. Carol Kingsmill, Dr. James Francis, Dr. Dennis Suh, Dr. Lorne "has fallen" Fell, M. Anna Trikoupis, Suzanne Ackloo and Lisa Heydorn and the Warkentin research group, Paul Venneri, John Pezacki, Phil Couture, Darren Reid, Nadine Merkley and Xiaosong Lu for many valuable scientific and personal discussions.

I would also like to mention a few of the many people whom I have met at McMaster. Paul (aka Chooch): thanks for the great times, conversations, and words of inspiration, you're a great friend! Jamie and John: you made being at McMaster an absolute adventure, thanks for the good times. You do realize that we must come back to win the Phoenix Cup!

Most importantly, I would like to thank my parents, my brother and other family members for their love and encouragement especially in times of stress. Finally, I would like to thank my wife, Selena, without your love, support and understanding I couldn't have completed this thesis.

TABLE OF CONTENTS

LIST OF FIGURES

LIST OF ABBREVIATIONS

AE	=	appearance energy
B	=	magnetic sector
B3LYP	=	hybrid Hartree-Fock/density functional theory
CA	=	collisional activation
CASSCF	=	complete active space self-consistent field
CCSD(T)	=	coupled cluster singles doubles and triples
CE	=	charge exchange
CI	=	chemical ionization
CID	=	collision-induced dissociation
CIDI	=	collision-induced dissociative ionization
CP	=	cyclopropane
CR	=	charge-reversal
CS	=	charge-stripping
DFT	=	density functional theory
EI	=	electron ionization
ESA	=	electrostatic analyser
eV	=	electron Volt (1 eV = 23.061 kcal/mol or 96.487 kJ/mol)
ffr	=	field-free region
ΔH_f	=	enthalpy of formation
HF	=	Hartree-Fock
IE	=	ionization energy
KER	=	kinetic energy release
MI	=	metastable ion
MO	=	molecular orbital
MP	=	Moller-Plesset (perturbation theory)
MS	=	mass spectrometry
NDMA	=	N,N-dimethylaniline
m/z	=	mass to charge ratio
NR(MS)	=	neutralization-reionization (mass spectrometry)
PA	=	proton affinity
q	=	charge
r,R	=	radius
SCF	=	self-consistent field
T	=	kinetic energy release (value)
TPEPICO	=	threshold photoelectron photoion coincidence
TS	=	transition state
ZAB-R	=	BEE three-sector mass spectrometer
ZPVE	=	zero-point vibrational energy

CHAPTER 1

Introduction

Reactive intermediates play a key role in a great many metabolic pathways and organic reactions. Information regarding their intrinsic stability and reactivity is therefore of considerable importance. Traditionally, these species have been studied in condensed phases; however, considerable technological and experimental progress in the area of mass spectrometry has resulted in the gas phase becoming a safe haven for a number of elusive reactive intermediates. By conducting such examinations in the rarefied gas phase intermolecular reactions and solvent effects are virtually eliminated enabling the *unimolecular* properties of the species to be investigated.

In general, mass spectrometric investigations are primarily concerned with providing information regarding two fundamental properties of a molecule, its mass and its structure. Interestingly enough, the structural information is not acquired directly from the neutral molecule, but rather, is based upon the dissociation behaviour of its ionized counterpart. The fragmentation behaviour of various classes of molecules has been extensively studied over the past four decades [1] and forms the basis of molecular structure determination in mass spectrometry. Modern gas phase ion chemistry also focuses on structure elucidation but here the species under study are not simply ionized molecules. In fact, most species studied today have unconventional ion structures and neutral counterparts which are unstable, highly reactive or even non-existent.

The task of ion structure determination has become feasible with the advent of tandem mass spectrometers in conjunction with novel experimental techniques. In section 1.1, the standard techniques of Metastable Ion (MI) [2] and Collision-Induced Dissociation [3] (CID) mass spectrometry used in this work are described. Section 1.2 deals with the more recent technique of Neutralization-Reionization [4] (NR) mass

spectrometry. This technique was originally developed for the tailor-made synthesis of highly reactive neutral species, but in combination with CID it yields a powerful hybrid technique (NR/CID) for the structure analysis of gas phase ions. The methods described rely heavily on comparisons with reference data and are most useful when used collectively and in combination with isotopic labelling experiments.

Isomeric ion structures can also be distinguished on the basis of their ion/molecule reactions [5]. Several approaches have been developed which involve the use of specialized instrumentation including Fourier Transform Ion Cyclotron Resonance (FT-ICR) and tandem quadrupole mass spectrometers [6].

Theoretical chemistry or rather computational chemistry, is being increasingly used as a complementary or even an alternative method for studying gas phase ions [7]. The present day calculations are ideally suited to treat isolated gaseous species providing reliable molecular structure information (3-dimensional geometries, not simply atom connectivities). They can also reliably predict stable isomeric forms and thermochemical data such as relative energies, and be used to elucidate key aspects of reaction mechanisms. Section 1.3 provides a brief overview of the methods used for estimating thermochemical data, particularly enthalpy of formation values.

In recent years, experimental and theoretical studies of reaction mechanisms of ionized molecules have led to the postulation of the existence of several types of remarkably stable intermediates that possess unconventional ion structures. In section 1.4, a particular class of ions known as distonic ions are described. The study of such species forms an integral part of this thesis.

1.1 Structure Elucidation

1.1.1 Ion Formation and Energetics

There are a number of ionization techniques available which are routinely used to generate ions (both positive and negative) for mass spectrometric analysis. Nevertheless, electron impact (EI) ionization remains the most common and certainly the most robust

method for producing positive ions from neutral molecules. The ionization process itself can be viewed as the interaction of solitary neutral molecules with a fast moving beam of electrons (typically 70 eV) resulting in the formation of molecular ions, $M^{\bullet+}$,

$M + e^- \rightarrow M^{\bullet+} + 2e^-$.

For such a process to occur, the impinging electrons must impart a minimum energy to the neutral molecule corresponding to its ionization energy (IE). The removal of an electron occurs in approximately 10^{-16} seconds [8] which is two to three orders of magnitude faster than a molecular vibration (10^{-13} to 10^{-14} seconds). Consequently, ionization occurs at a fixed internuclear distance, a so-called "vertical" ionization, and is governed by the Franck-Condon Principle [9]. If in fact, the energy imparted by the electron is greater than the IE of the molecule, the excess energy is deposited into the newly formed molecular ion as internal energy resulting in transitions to various excited vibrational, rotational and possibly electronic states [10]. It is from these excited states that fragment ions may then be produced.

The formation of fragment ions in the ion source can be described by the Quasi-Equilibrium Theory [11] and may be viewed to occur by a two step mechanism. The first step, as described above, involves the formation of an ensemble of solitary molecular ions which possesses a certain amount of internal energy (0-10 eV). The initial excitation energy is rapidly redistributed over all of the degrees of freedom of the ionized molecule. If a molecular ion possesses sufficient internal energy, dissociation ensues by a series of competing and consecutive unimolecular reactions. Statistical methods such as the Quasi-Equilibrium Theory (QET) and the Rice, Ramsperger, Kassel and Marcus (RRKM) Theory [12] have also been employed attempting to rationalize the unimolecular fragmentations observed in mass spectra. Unfortunately, these methods have met with limited success stemming from the fact that such investigations require an intimate knowledge of the reaction mechanism. For example, key parameters such as transition state energies are routinely estimated using computational chemistry. The accuracy of the estimation ultimately determines the success of the statistical method.

1.1.2 The Mass Spectrometer

Before discussing the various techniques used in ion structure characterization, it is useful to provide an overview of the salient features of the mass spectrometer used in this study, the VG Analytical ZAB-R instrument (see Figure 1.1). The ZAB-R is a custom built three sector, double focusing mass spectrometer of B(q⊥)EE geometry (B = magnetic analyzer, q⊥= orthogonal quadrupole and E = electrostatic

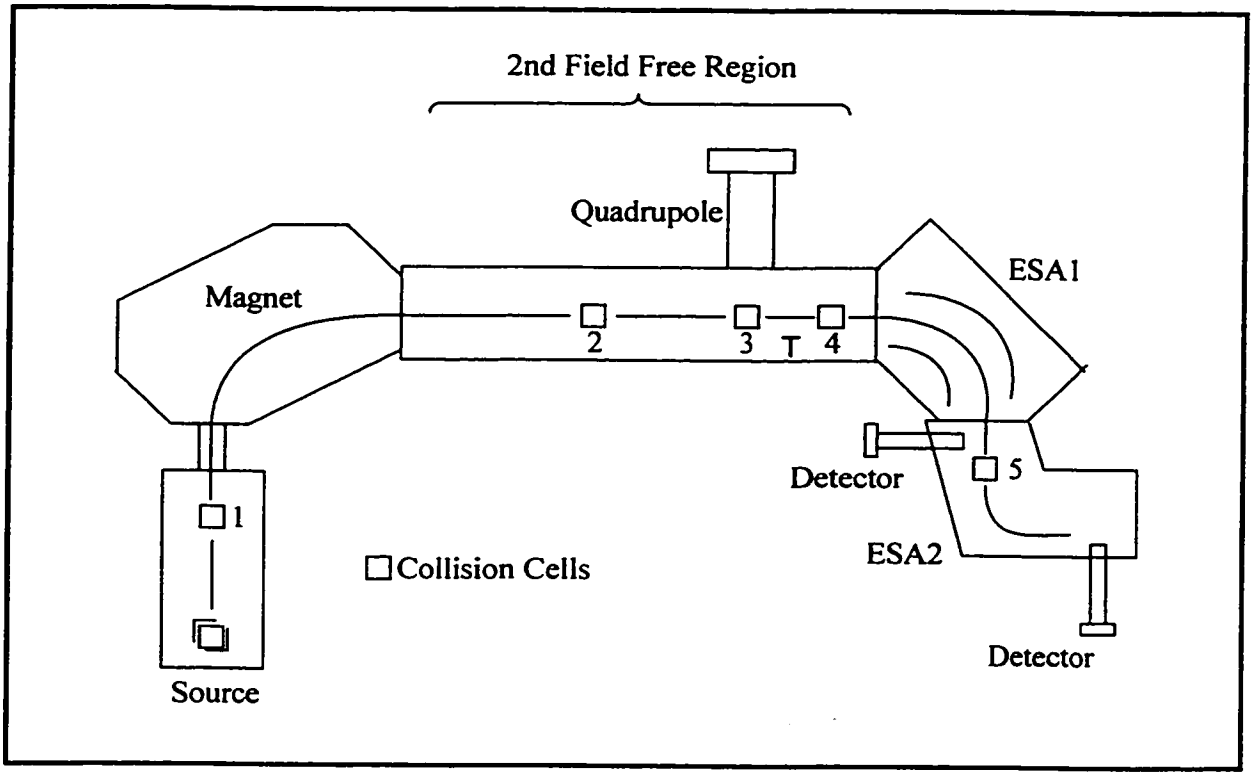

Figure 1.1: Schematic diagram of the VG Analytical ZAB-R instrument.

analyzer) [13]. The extraction of the positive molecular and fragment ions generated in the ion source is accomplished by means of a repeller electrode located in the ionization chamber which carries a small positive potential. Upon exiting the source, the ions are accelerated to 6-10 kilo-electron volts (keV) through a potential drop V. Thus, the kinetic (or translational) energy of the ions can be defined as: $zeV = \frac{1}{2} mv^2$

where m is the mass of the ion, v is its terminal velocity, e is the charge of a single electron and z is the charge of the ion. As a result, ions possessing equal charge must also possess equal kinetic energy. An ion beam which has a kinetic energy equal to that of the full accelerating energy, V, is known as the "main ion beam" or simply the "main beam". The newly formed fast moving ion beam then enters a drift region, preceding the magnet, free of any applied fields (electric or magnetic) which is appropriately termed the first field free region (1ffr). There are two other field free regions in this instrument, the 2ffr and the 3ffr, located between the magnet and the first electrostatic analyzer (ESA1) and between ESA1 and ESA2, respectively (see Figure 1.1). As will be discussed below, it is in these field free regions where the unimolecular dissociations, either spontaneous or collision-induced, are monitored.

In order to acquire any one of the various types of mass spectra, it is necessary to analyze an incoming ion beam by separating ions of different mass to charge ratios. A magnetic analyzer (B) is ideally suited for this purpose, since ion separation is based upon differences in momentum (mv). The overall relationship governing the separation of ions by a magnetic field is: $m/z = B^2r^2/2V$

where B is the magnetic field strength in Tesla (T) and r is the radius of curvature in centimetres. The magnetic analyzer can be operated in one of two modes: a scan or a set mode. In the first instance, ions of increasing mass to charge (m/z) are successively transmitted into the 2ffr by varying the applied magnetic field. In the latter case, the magnetic field is set to allow only those ions possessing a particular m/z ratio to be transmitted.

Along with a magnetic analyzer, the ZAB-R also has two electrostatic analyzers (ESA). In contrast to their magnetic counterpart, the mode of ion separation of an ESA is independent of the mass of the ion, but rather ions are separated based upon their kinetic energies. Briefly, ions are transmitted through the ESA when the two opposing forces, i.e. the electrostatic and centrifugal forces are balanced. The net result is a condition where the energy of the electrostatic (E_{ESA}) analyzer is equal to the kinetic energy of the ion (E_{ION}) for a given ESA radius r_e, $E_{ESA} = 2E_{ION}/r_e$.

Like the magnetic analyzer, the applied electric field of the electrostatic analyzer can either be scanned or set. Consequently, these "energy filters" are often used in tandem with a magnetic sector when performing so-called MS/MS/MS type experiments by fixing ESA1 and examining the resulting dissociation products by scanning ESA2. A more thorough explanation of MS/MS/MS type experiments and how they apply to structure elucidation is given below.

1.1.3 Metastable Ions

When discussing the various types of ions formed in the ionization chamber of a mass spectrometer, it is often convenient to speak of one of three categories: stable, unstable and metastable. A stable ion is defined as one which is initially formed in the ion source and travels intact through to the detector. Conversely, an unstable ion is one which rapidly dissociates (< 1 μs) in the ion source giving rise to fragment ions. In the case of the third category, the term "metastable" is defined differently in various niches of chemistry as pointed out by McLafferty and Tureček [1a]: "In spectroscopy, a "metastable" state is a thermodynamically unstable state that has not *yet* dissociated for kinetic reasons; in contrast, in mass spectrometry a "metastable" ion is one that *does* dissociate but whose dissociation is delayed for kinetic reasons". Simply stated, a metastable ion refers to an ion which is sufficiently stable to leave the ion source, but which dissociates before reaching the detector. In general, metastable ions account for only a small percentage (< 1%) of the overall ion beam intensity.

In magnetic deflection instruments of reversed geometry, such as the ZAB-R, metastable ion (MI) mass spectra are routinely obtained in the 2ffr by mass selecting the ions of interest using the magnetic sector and analyzing the subsequent product ions by scanning ESA1. MI spectra can also be obtained in the 3ffr by mass selecting the ions using both the magnetic sector and ESA1 and by scanning the second electrostatic analyzer, ESA2. Metastable transitions are representative of only low energy dissociation pathways, a consequence of the narrow range of internal energies (< 2 eV above threshold) of the ions. Typically, ions reside in the ion source for ~ 1 μs and require

approximately 10 μs to traverse the remainder of the instrument. Thus, the observation of metastable dissociations is restricted to processes having rate constants of 10^5 - 10^6 s^{-1}. The minimum energy required to observe a particular dissociation is known as its appearance energy (AE) and is dependent on the enthalpy of formation, ΔH_f, of both the reactant and product ions. If we consider the dissociation: $ABC^{\bullet+} \rightarrow AB^+ + C^\bullet$, the appearance energy of AB^+, denoted $AE[AB^+]$, is defined as:

$$AE[AB^+] = \Delta H_f[AB^+] + \Delta H_f[C^\bullet] - \Delta H_f[ABC^{\bullet+}] + \varepsilon_{excess}$$

where ε_{excess} is the excess energy, i.e. the kinetic shift [14], required to observe the reaction for a given rate. It is important to note that the above expression assumes a negligible energy barrier for the reverse reaction. Appearance energy measurements can be determined using photoionization based methods including the powerful threshold technique of photoelectron-photoion coincidence (PEPICO) spectroscopy [15] or through the use of monochromatic electron ionization [16]. Detailed reviews have been published outlining the advantages and disadvantages of these techniques [16a,17].

Upon dissociation, the kinetic energy of the parent ion, $ABC^{\bullet+}$ in the above example, is partitioned between the two fragments generated, AB^+ and $C^\bullet$. The percentage of kinetic energy imparted to a particular fragment is equal to the mass percentage of the newly formed ion. Thus, fragment AB^+ will possess a kinetic energy, E_{AB+}, based on the following: $E_{AB+} = (m_{AB+} / m_{ABC\bullet+}) E_{ABC\bullet+}$
where $E_{ABC\bullet+}$ is the kinetic energy of the parent ion which is typically equal to the accelerating potential, V.

Since their discovery by Hipple and Condon [18] in 1945, metastable ions have been utilized in the structure determination of a great number of species [19]. An early approach used in the mid-1960's by Rosenstock [20] and by Shannon and McLafferty [21] to deduce ion structures was based on the peak intensity ratios of metastable ions and assumed that the internal energy distribution of an ion did not influence the relative peak ratios observed in the MI spectrum. Hence, one may confidently conclude that ions having the same structure would produce identical MI mass spectra; however, the

corollary does not always hold. In the case where the MI spectra are characteristically different, it is concluded that the ions possess different structures.

In fact, to deduce ion structures from metastable spectra, one must differentiate the ions based on both the relative peak intensities as well as the peak shape of the resulting fragments [22]. The most common of these peaks are the so-called Gaussian-type peaks. A simple Gaussian shape suggests that only one fragmentation pathway is responsible for producing an ion, whereas a composite Gaussian peak shape indicates: i) that the metastable ions lose two isobaric fragments (e.g. C_2H_4 and CO) or ii) that they yield a pair of isomeric daughter ions. It is also possible that two isomeric ions dissociate via different reacting configurations [22] to yield the same product ion. In other instances, broad dished-shaped peaks are observed. The correct explanation for the observed differences in metastable peak shapes was provided by Hipple and Condon [23] in 1946. They proposed that the broadening of a metastable peak was the result of the conversion of excess internal energy into kinetic energy due to the presence of an appreciable reverse energy barrier associated with a particular dissociation pathway. The amount of energy transferred in this manner, known as the kinetic energy release (KER), is routinely determined from the width of a metastable fragment at half height. Consider the metastable dissociation: $m_1^{\bullet+} \rightarrow m_2^{\bullet+} + m_3$, the kinetic energy release associated with the formation of $m_2^{\bullet+}$ is defined by:

$$T_{0.5} = (m_1^{\bullet+})^2 \cdot V \cdot (\Delta E_{0.5})^2 / 16 \cdot m_2^{\bullet+} \cdot m_3 \cdot (E)^2$$

where $T_{0.5}$ is the KER measured at half peak height, $\Delta E_{0.5}$ is the energy width of the peak at half height and E is the electric sector voltage required for transmission of the main beam [19,22]. Kinetic energy release values are routinely obtained under conditions of high energy resolution, i.e. a main beam energy width of a few volts. This contribution to the overall energy width of the metastable peak may be ignored if it is relatively small. However if the contribution is not negligible the following correction may be applied [19,22]: $\Delta E_{0.5}[\text{corrected}] = [\Delta E_{0.5}^2 (m_2^{\bullet+}) - \Delta E_{0.5}^2 (m_1^{\bullet+})]^{1/2}$.

1.1.4 Rationalizing Dissociation Chemistry in Terms of Potential Energy Surfaces

A relatively simple and elegant method of summarizing the dissociation chemistry of a given set of isomers is the construction of the potential energy surface over which the ions decompose [24]. This method is typically used when only a single electronic state is involved (an adiabatic surface) but can be extended to include cases where more than one electronic state is considered (a diabatic surface). For ions composed solely of first row elements, a single electronic surface is often sufficient to describe the system. However, there are a few notable exceptions, such as the phenyl cation [25] and ionized hexafluoroethane [26], in which the observed ion chemistry must involve the participation of an isolated excited state.

The construction of a potential energy surface for an ionic system is often useful in the rationization of dissociation chemistry. For instance, the metastable ion spectra of ionized acetone ($\mathbf{I}^{\bullet+}$) and its enol ($\mathbf{Ia}^{\bullet+}$) are each dominated by a peak at m/z 42 ($-CH_4$) and m/z 43 ($-\ ^{\bullet}CH_3$) respectively. However, these seemingly simple spectra have been the subject of numerous studies [27] concerned with the mechanism by which the product ions are formed. As depicted in Scheme 1.1, the m/z 43 ions generated from $\mathbf{Ia}^{\bullet+}$ have been determined to possess the acetyl cation structure, $CH_3C^{+}{=}O$ [27e] rather than the

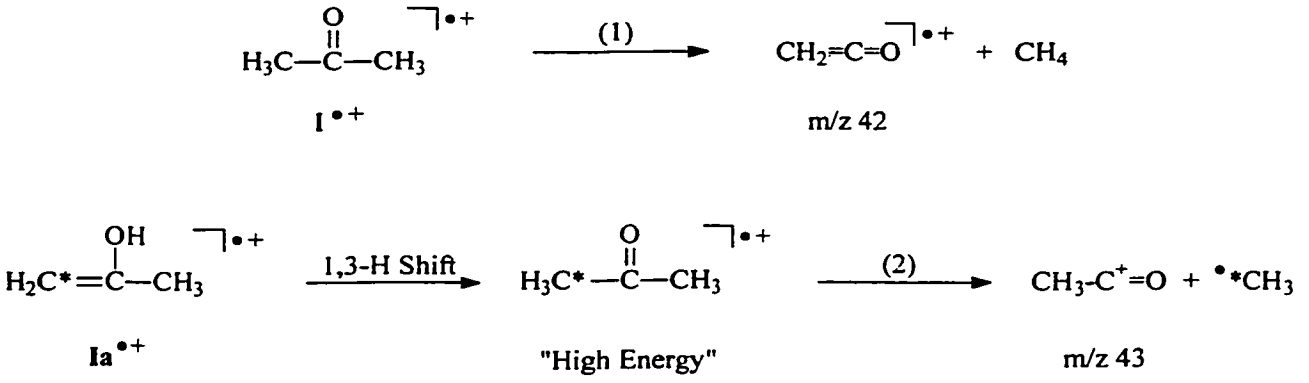

Scheme 1.1

expected connectivity $CH_2=C^+$-OH. In contrast, metastable acetone molecular ions almost exclusively yield a peak at m/z 42 by the loss of CH_4.

This seemingly unusual experimental observation can readily be explained by an examination of the potential energy surface, see Figure 1.2. Unlike its neutral counterpart, ionized acetone is less stable than its enol by 14 kcal/mol [28] and enolization is hindered by an isomerization barrier of 37 kcal/mol [29]. In the case of ionized acetone, the isomerization barrier lies 21 kcal/mol [27g] higher in energy than the dissociation limit for the reaction of lowest energy: $CH_2C=O^{\bullet+}$ (m/z 42) + CH_4. Thus, dissociation of the metastable acetone ions prevails via reaction (1). However, the enthalpy of formation of the products $CH_2=C^+$-OH + $^{\bullet}CH_3$ expected from $\mathbf{Ia}^{\bullet+}$ is 18 kcal/mol [30] *higher* in energy than the enol-ketone isomerization barrier. Thus, the enol ions isomerize to their keto counterparts prior to dissociation via reaction (2) in a so-called rate-determining isomerization. In such a process, the nascent acetone ions are formed in a highly excited vibrational state, from which the direct bond cleavage reaction (2) rapidly occurs. Of particular interest in this mechanism is the observation that the methyl loss occurs preferentially from the newly formed methyl group, denoted as $^*CH_3$. Such an observation is an example of "non-ergodic" behaviour, that is, the internal energy imparted to the ion is not evenly distributed over all the degrees of freedom prior to dissociation. It is also interesting to note that the metastable acetone radical cations do not undergo loss of $^{\bullet}CH_3$ to an appreciable extent even though the reaction is nearly isoenergetic with the loss of CH_4 [27d,g] (see Figure 1.2). Heinrich and co-workers [27g] have concluded that the loss of methane occurs below the methyl dissociation limit and consequently must involve "tunneling" through the isomerization barrier.

In the event that the dissociation barrier of both isomers lies higher in energy than the isomerization barrier, the two species may freely interconvert above the isomerization threshold and dissociation can occur from a common ion(s) or transition state. In either case, the resulting MI spectra from the two isomers will be closely similar, including metastable peak shapes. Such a potential energy surface exists for ionized pyridine and its

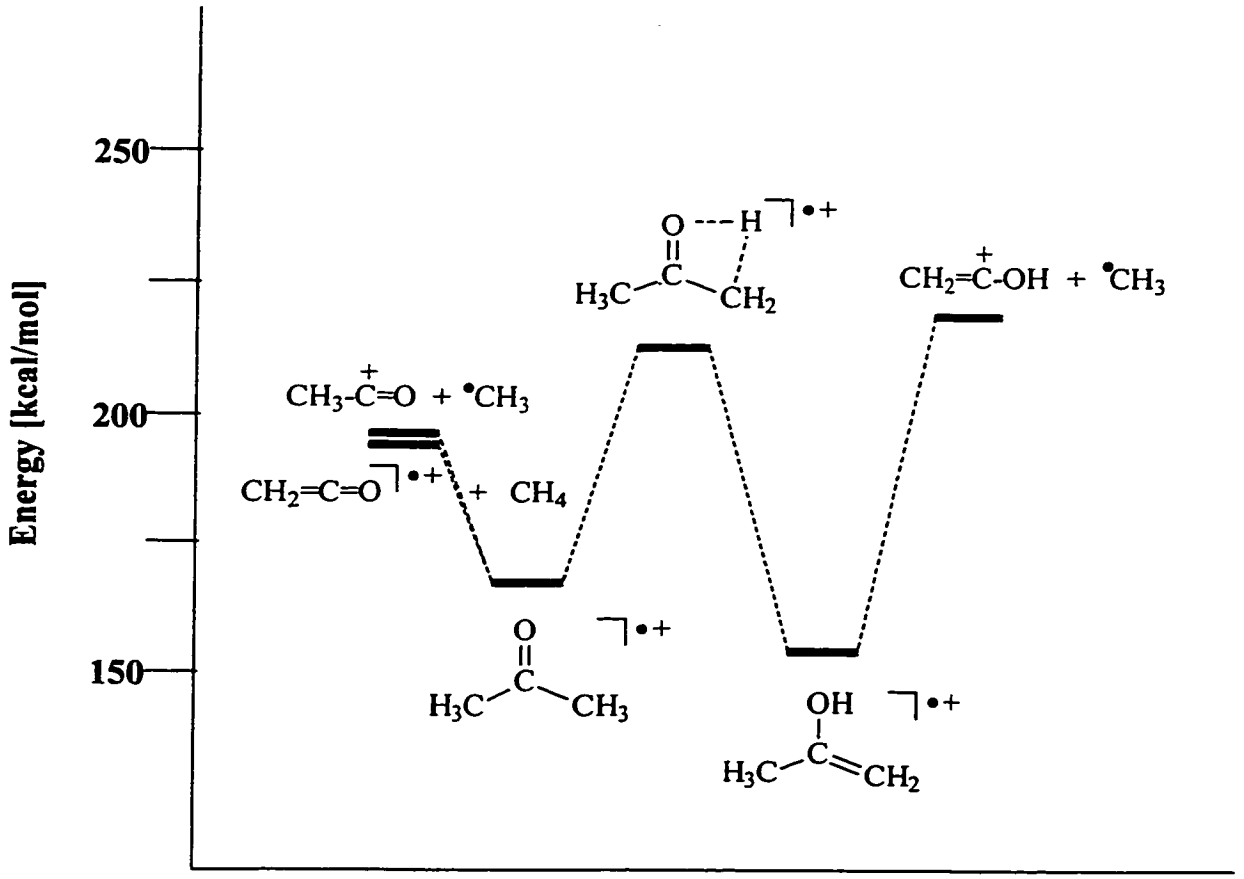

Figure 1.2: Schematic potential-energy surface describing the dissociation chemistry of ionized acetone and its enol.

α-ylide (see Chapter 2). These isomers exhibit a single metastable transition, i.e. loss of HCN, to yield a signal at m/z 52. Characterization of ionized pyridine and its isomer is further complicated using metastable ion mass spectrometry since the partially deuterated pyridines, 2-deuteropyridine and 2,6-dideuteropyridine, undergo hydrogen randomization or "scrambling" prior to dissociation leading to a statistical loss of HCN/DCN [31]. Fortunately, other methods are available to distinguish the isomers, in particular, collision-induced dissociation has been instrumental for this system (Chapter 2) and related N- containing heterocycles (see Chapters 3-8).

1.1.5 Collision-Induced Dissociation

A second method commonly used in the structural elucidation of isomeric ions is the technique of collision-induced dissociation (CID), also known as collisionally activated dissociation (CAD) and collisional activation (CA). As its name implies, structural information is obtained when precursor ions having a high translational energy, i.e. 100 eV - 10 keV, collide inelastically with stationary neutral molecules (N) subsequently leading to the production of fragmentation products ($m_2^{\bullet+}$):

$$m_1^{\bullet+} + N \rightarrow m_2^{\bullet+} + m_3 + N$$

Much of the pioneering work conducted in this area was carried out by Jennings [32] and by Haddon and McLafferty [33]. Since that time, numerous reviews [3,34] have been published evaluating the technique and summarizing the work to date. In this section, some of the important aspects of structural elucidation using collision-induced dissociation will be discussed.

The fragmentation of an ion by collision-induced dissociation can be viewed as a two step process, much like the ionization of a neutral molecule described in section 1.1.1. The first step is ascribed to the collisional excitation (or activation) of the ion in which a portion of its kinetic energy (0 - 10 eV) is transformed into internal energy. Once excited, the energy is redistributed amongst the various vibrational degrees of freedom of the ion. Since both the collisional excitation/redistribution occurs rapidly (~ 10^{-14} - 10^{-15} seconds [3b]) relative to bond cleavage, the process can be viewed as a vertical Franck-Condon excitation. The resulting fragment ions are representative of high as well as low energy dissociation pathways. Direct bond cleavage reactions comprise a majority of the high energy pathways and are often the most structure diagnostic. Unlike metastable ions, collisionally activated ions possess sufficient internal energy to undergo a number of dissociation and/or isomerization reactions. Hence, the height of the activation barriers does not solely determine the reaction pathway, rather it is the rate associated with a particular dissociation and/or isomerization which becomes the dominating parameter.

Similar to their metastable counterparts, collision-induced dissociation mass spectra are obtained in the field free regions of the instrument but differ in that one of the

collision cells (see Figure 1.1) is pressurized with a target (or collision) gas. A number of factors relating to the nature and pressure of the collision gas can markedly change the appearance of a CID mass spectrum [34,35]. For instance, helium is commonly used as a collision gas because of its high target efficiency, that is, competing processes such as neutralization and scattering are kept to a minimum. In contrast, O_2 is considered as a "softer" collision gas, i.e. induces less fragmentation, and is often utilized to observe charge - stripping (see below) peaks in a CID mass spectrum. Furthermore, oxygen is also routinely used as the reionization gas in neutralization-reionization (NR) experiments (see Section 1.2) which allows for direct comparisons of the two spectra. The pressures at which the CID spectra are obtained is also an important consideration. Since the collision pressure can only be estimated using remote ionization gauges located outside the collision cell, the gas concentration is defined in terms of the reduction of the main ion beam. Holmes [34], concluded that a reduction of the main beam by 30 - 40 % was an optimum condition. Further reduction of the main beam results in the occurrence of multiple collisions, which in turn increases the number of high energy dissociations. As the yield of fragment ions increases, the structure specific information in the CID mass spectrum may be reduced or eliminated. This is of considerable importance especially when the differentiation of isomeric ions is based solely on the relative intensities of the fragment ions.

The outcome of a collision-induced dissociation mass spectrum is not solely dependent on the nature of the target gas, but also on the initial kinetic and internal energies of the incoming ion [36]. The kinetic energy of the impinging ions, E_{kin}, is directly proportional to the maximum energy transferred (E_{max}), kinetic $\rightarrow$ internal, in the collision process. Ions possessing high kinetic energies (6 - 10 keV) typically produce similar CID mass spectra whereas their lower energy counterparts (2 - 5 keV) tend to be significantly more sensitive. Consequently, there are often advantages in utilizing either high or low kinetic energies depending upon the energetic requirement of the structure diagnostic fragmentation(s).

There have been reports in the literature which suggest that the internal energy of the ion prior to the collision event may well influence the relative intensities of the fragment ions [3a,b]. A definite answer to this question has not been found to date; however, the present consensus is that in the CID mass spectrum the relative abundances of fragment ions resulting from all reactions of high critical energy are independent of the initial internal energy of the precursor ion [34].

1.1.6 Charge-Stripping

Collision-induced dissociation is the dominant process when a fast moving beam of ions collides with a neutral target molecule. However, competing processes such as neutralization (see section 1.2), charge-stripping and charge inversion also occur to a lesser extent. The charge stripping (CS) process [32,37], $m_1^+ + N \rightarrow m_1^{2+} + N + e^-$, can display characteristically different CS mass spectra for isomeric species, even in cases in which their CID spectra provide little or no information. A case in point is the characterization of isomeric $C_3H_6^{\bullet+}$ and $C_5H_8^{\bullet+}$ radical cations [38]. The relative intensity of charge stripping peaks vary considerably depending on the ion under study and on the nature of the collision gas. The most efficient charge stripping gases are O_2 and N_2 by virtue of their large electron affinities [3b]. The ability to differentiate isomeric nitrogen containing heterocycles based upon charge-stripping forms an integral part of this thesis.

1.1.7 Charge Inversion

The process of charge inversion (or charge reversal), $m_1^- + N \rightarrow m_1^+ + N + 2e^-$, has been successful in the characterization of a number of isomeric species since its discovery by Bowie and Blumenthal [39]. The two vertical ionization processes yields a positive ion, m_1^+, whose geometry is essentially that of its anionic counterpart m_1^-. If the newly formed cation possesses sufficient energy, dissociation may also occur. High energy direct bond cleavage reactions are typically more abundant in cations, allowing for structural characterization of highly unstable species which would be difficult to generate

by other means [40]. Charge inversion experiments are also amenable to the study of neutrals, particularly species which possess short lifetimes ($< 10^{-6}$ sec). A new technique, referred to as Neutral and Ion Decomposition Difference (NIDD) mass spectrometry, has recently been developed for the identification of neutral intermediates using both CR and NR mass spectrometry [41]. However, its application is restricted to systems which are stable in the different oxidation states, i.e. m_1^-, m_1, and m_1^+.

1.1.8 The Collision-Induced Dissociation of Ionized Acetone and its Enol

Unlike their metastable ion counterparts, the collision-induced dissociation spectra of ionized acetone ($\mathbf{I}^{\bullet+}$) and its enol ($\mathbf{Ia}^{\bullet+}$) show quite similar fragmentation pathways (see Figure 1.3). Although the base peak in each case corresponds to m/z 43, structure diagnostic peak intensities in the region of m/z 12 - 15 and 26 - 31 have allowed their differentiation [41] (Figure 1.3 - insets). The question still remains: "Do the ions communicate prior to dissociation ?" To answer this question, the structure of the m/z 43 ions generated in each CID spectrum were analyzed in a subsequent CID experiment, the details of which are described below (see Section 1.1.10). It has been shown that the m/z 43 ions generated from both ionized acetone and its enol exclusively possess the acetyl ion structure, CH_3-C^+=O. This observation provides two conclusions: i) the enol must isomerize, at least in part, to the keto form prior to dissociation and ii) the rate of isomerization is comparable to the rate of dissociation. Quite a different scenario exists, however, for ionized pyridine and its α-ylide isomer.

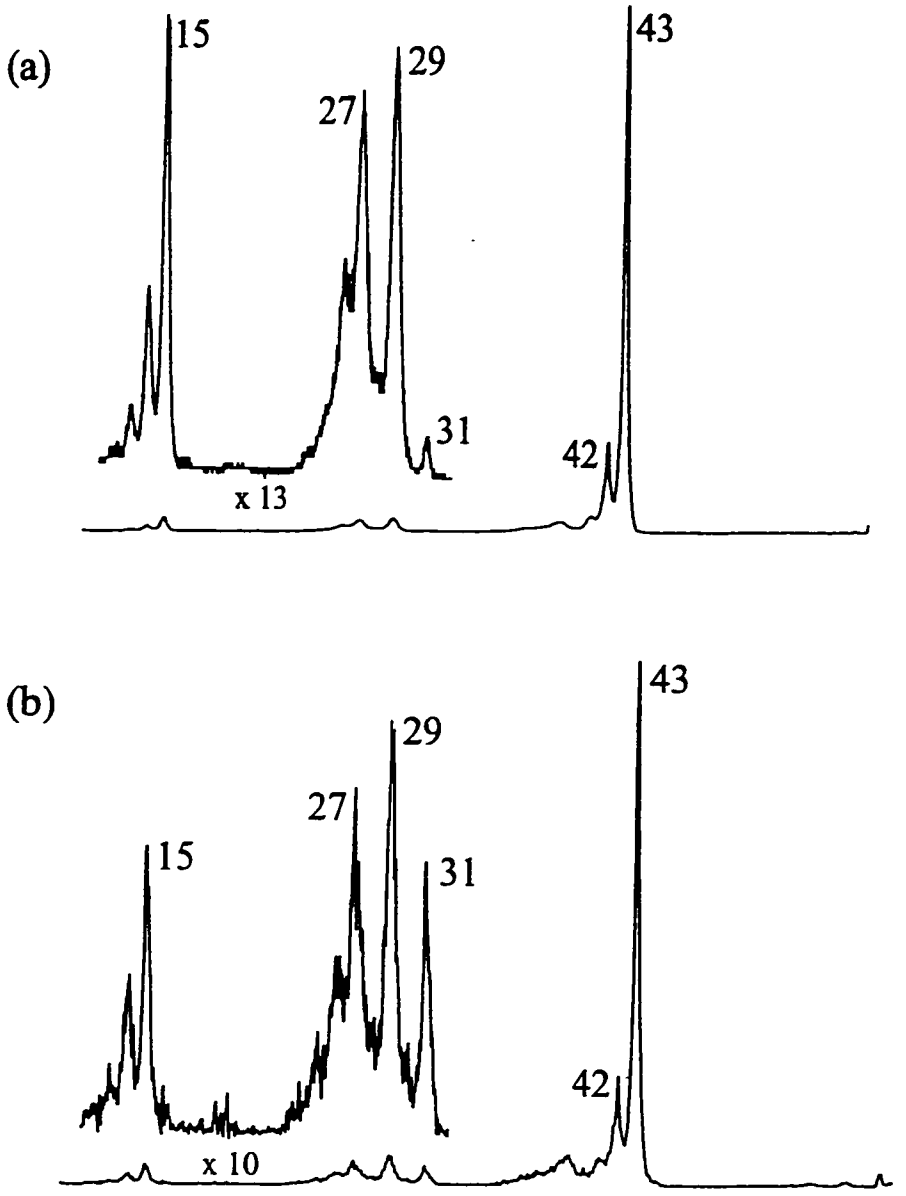

Figure 1.3: CID mass spectra [2ffr/O_2] of the m/z 58 ions generated from ionized (a) acetone and (b) 2-heptanone.

1.1.9 The Collision-Induced Dissociation of Ionized Pyridine and its Ylide Isomer

As stated in section 1.1.4, the dissociation reaction of lowest energy (- HCN) for ionized pyridine and its α-ylide isomer is significantly higher in energy than the isomerization barrier separating the two species. The minimum energy requirement in both cases corresponds to 96 kcal/mol (see Chapter 2), 30 kcal/mol higher than the isomerization barrier. Hence, once collisionally activated, isomerization may well occur for those ions whose internal energy lies above that of isomerization, but below that of dissociation. Considering that the average internal energy imparted to the ion upon collision is on the order of 1-2 eV, only a fraction of the ions possess sufficient energy to dissociate. Also, once ring opening occurs, the possibility of isomerization is reduced since ring closure is highly unlikely. Therefore, it is the relative rates of isomerization/dissociation which determine whether the species communicate prior to dissociation. In fact, as illustrated in Chapter 2, ionized pyridine and its α-ylide ion do yield characteristic CID mass spectra, thus it may be concluded that the ions do not communicate (isomerize) to any significant extent prior to dissociation.

1.1.10 MS/MS/MS experiments

The characterization of structurally interesting ions is not restricted to source generated ions. Often, valuable information regarding the structure of a precursor ion can be obtained by probing the structure of fragment ions generated either metastably or collisionally. Furthermore, this technique readily lends itself to the identification of isomeric or isobaric fragment ions which may be produced in these processes. In order to conduct such MS/MS/MS experiments, a multi-sector mass spectrometer [42] becomes necessary in which sequential collision and/or dissociation reactions may be performed. Although a number of combinations is possible, MI/CID and CID/CID experiments typically provide the most compelling information. To illustrate this point, the identity of m/z 26 and m/z 27 generated from ionized pyridine are determined using a series of "double collision" (CID/CID) experiments. In the case of m/z 26 the two isobaric ions,

$H\text{-}C{\equiv}C\text{-}H^{\bullet+}$ and CN^{+} are considered while for m/z 27, $HCN^{\bullet+}$ and $H_2C{=}C\text{-}H^{+}$ could potentially be generated.

1.1.11 MS/MS/MS Experiments in Ionized Pyridine

When probing the structure of isomers possessing a structurally similar backbone, e.g. ionized pyridine and its α-ylide, it is not unexpected that the two species exhibit similar dissociation pathways. Consequently, their identification is based upon structure characteristic peak intensity ratios. In the case of the above mentioned isomers, one of these diagnostic areas is the m/z 24 - 29 cluster (see Chapter 2). There is little doubt that m/z 24, 25, 28 and 29 correspond to $C_2^{\bullet+}$, C_2H^{+}, CH_2N^{+} and $CH_3N^{\bullet+}$ respectively. However, for m/z 26 two possibilities exist namely $H\text{-}C{\equiv}C\text{-}H^{\bullet+}$ and CN^{+}. The CID/CID mass spectrum of the m/z 26 ions from ionized benzene is given in Figure 1.4a while that of ionized pyridine is given in Figure 1.4b. It is evident that the two spectra are virtually identical indicating that they share a common structure. Thus, the vast majority of the m/z 26 ions generated from ionized pyridine is ionized acetylene. It is also evident that the signal to noise ratio of MS/MS/MS spectra is significantly lower than in single CID experiments. In a similar way, the CID/CID mass spectrum of the m/z 27 ions from ionized benzene (Figure 1.4c) was compared to that of the m/z 27 ions from ionized pyridine (Figure 1.4d). The major dissociation in each case corresponds to successive hydrogen atom losses, m/z 26, 25 and 24, respectively. Since the m/z 27 ions generated from ionized benzene must be $C_2H_3^{+}$ and $HCN^{\bullet+}$ can only produce a single $H^{\bullet}$ loss, the ratio m/z 26 to m/z 25 provides a semi-quantitative indication of the relative abundance of $HCN^{\bullet+}$. It is clear that the two spectra are similar, but possess slight differences, i.e. the ratio m/z 26 to m/z 25 indicates the presence of a second contributor, $HCN^{\bullet+}$. From the analysis of the relative peak intensities, it follows that the m/z 27 ions generated from ionized pyridine are largely $C_2H_3^{+}$ with only a minor component (~ 6 %) of $HCN^{\bullet+}$.

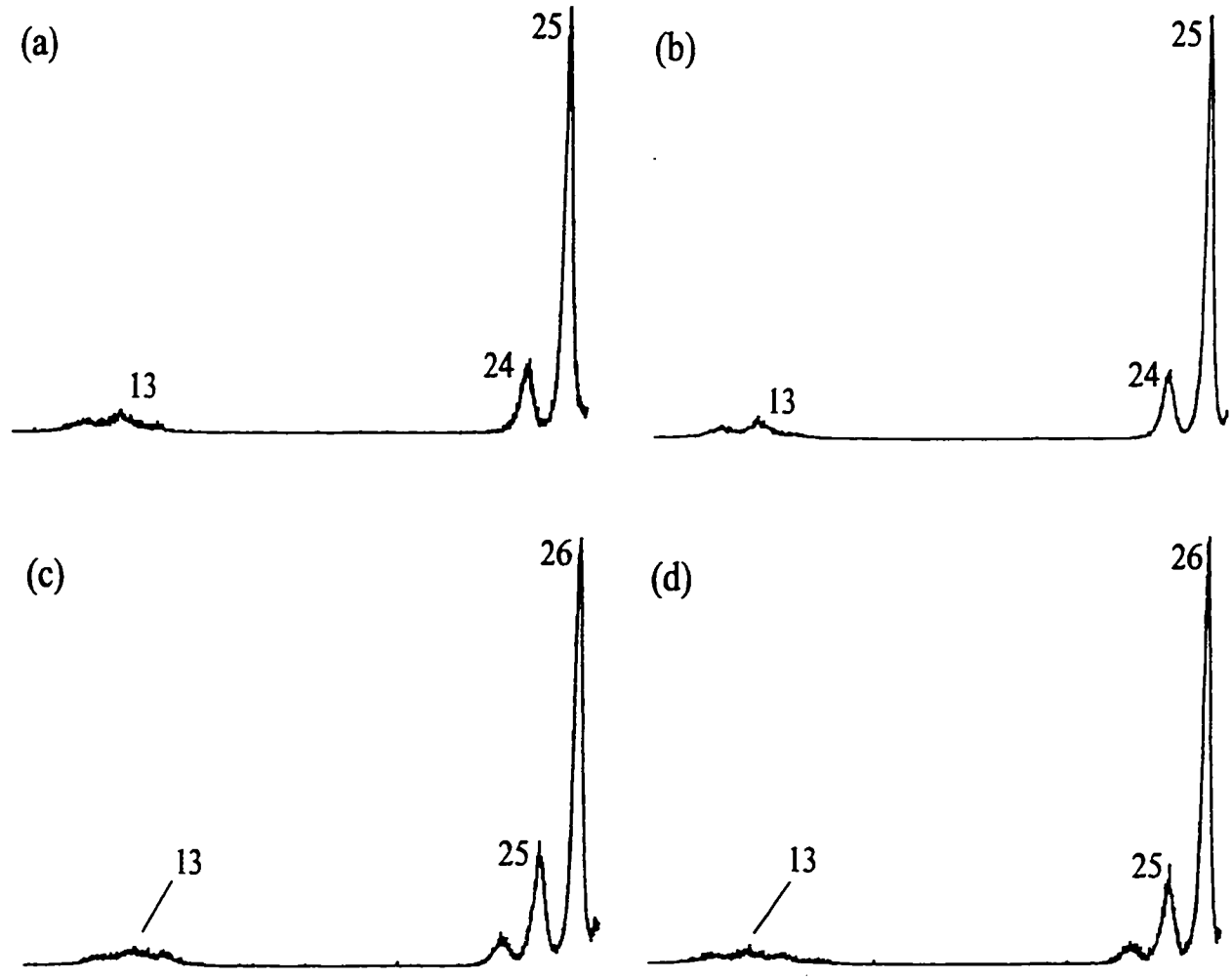

Figure 1.4: CID mass spectra [3ffr/O_2] of the m/z 26 ions generated from the collision-induced dissociation of (a) benzene molecular ions (b) pyridine molecular ions. CID mass spectra [3ffr/O_2] of the m/z 27 ions generated from the collision-induced dissociation of (c) benzene molecular ions (d) pyridine molecular ions.

1.2 Neutralization-Reionization Mass Spectrometry and Related Techniques

1.2.1 Fast Moving Ions

At first sight, the idea of studying neutral species by mass spectrometric techniques may appear to be a contradiction in terms, since traditional techniques were focused solely on the analysis of ionic species. This concept was brought to fruition in the mid-sixties when Lavertu and co-workers [43] discovered that a fast moving (4-10 keV) beam of ions could undergo charge exchange reactions when collided with a thermalized target gas to yield a fast moving beam of *neutrals*. Further instrumental developments conducted by Devienne [44] and Gray and Tomlinson [45] ultimately led to the investigation of small hypervalent species such as $H_3^{\bullet}$, He_2 and HeH [45]. After a period of dormancy, Porter and co-workers utilized this methodology in neutralized ion beam spectroscopic studies of small hypervalent radicals [46]. Trailblazing work by the groups of McLafferty, Holmes, Terlouw and later Schwarz and Harrison developed Neutralization-Reionization mass spectrometry (NRMS) [4] into a powerful technique for the generating and identifying of elusive organic molecules in the gas phase. Among the many entities characterized by NRMS are some molecules which have been presumed to be incapable of independent existence, e.g. H_2CO_3 (carbonic acid), and H_2SO_3 (sulfurous acid), plus a variety of other acids, enols, (hypervalent) radicals, carbenes, cumulenes, ylides and diradicals, which are expected to have extremely small lifetimes in solution, as well as many other species of intersellar, atmospheric and organometalic importance [4j]. One reason why NRMS has been so successfully applied in the generation of the elusive isomers of many well known molecules (i.e. isomers with elevated enthalpies and enhanced reactivities) is the fact that for many ionic systems, in contrast to their corresponding neutral systems, the "rare" isomer can be as stable, or even more stable, thermodynamically than the "common" isomer and thus the ionized form of the "rare" isomer may be accessible by simple dissociative ionization of an appropriate precursor molecule.

The structure of the neutral species produced by dissociation of an ion, be it spontaneous or collision-induced, can be investigated by a related complementary

technique dubbed collision-induced dissociative ionization (CIDI) [4f], although some refer to it under the designation of NRMS.

The standard procedure in an NR experiment is to first generate the (radical) cation in the mass spectrometer and to establish its ion structure and its isomeric purity. Next the NR experiment is performed: neutralization by electron transfer and deflection of the unreacted ionic species is followed (after approximately 1 μs) by collisional reionization of the fast moving neutralized species. Neutralization (oxidation) of and reionization to negative ions has also been demonstrated, giving rise to the nomenclature $^{-}NR^{-}$, $^{-}NR^{+}$, $^{+}NR^{-}$and $^{+}NR^{+}$ [4h], but the latter is generally assumed when just NR is used. Ideally, the collisional reionization step leads to the identification of neutral species which correspond to the recovered ion signal and indeed the resulting NR mass spectrum is often recognizably similar to the CID (or even EI) mass spectrum of reference ions. NR mass spectra can readily be obtained from any ion present in the conventional mass spectrum of the compound under study. However, the combined neutralization-reionization efficiency [47] is fairly low, typically 0.1 - 0.001 % of the main beam intensity, and thus a high sensitivity is often required.

A closer inspection of the events that may occur in an NR experiment, which are summarized [4b,f,g] in Scheme 1.2 and below, illustrates why neutral structure assignment may not always be a matter of straightforward spectral comparison.

Neutralization: after acceleration, typically to 6-10 keV, and mass-selection, the ions ABC^{+} enter the first collision gas chamber (Cell 3) where electron-capture from a target gas, G_1, results in the reduction to the neutral species ABC (Eq. 1.1) in a vertical Franck-Condon transition. All ions ABC^{+} which have been neutralized and also (the relative minor fraction of) their ionic dissociation products (Eq. 1.4 and 1.5) are effectively removed from the beam by using a charged deflector electrode. The only species which enter into the second collision gas chamber (Cell 4) are therefore the neutral molecules ABC (having the momentum of ABC^{+}) and their uncharged dissociation products, e.g. AB and C (having the momentum of AB^{+} and C^{+} respectively).

Cell 3 (Neutralization)

$G_1 + ABC^+ \longrightarrow G_1^+ + ABC$ (Eq. 1.1)

$G_1 + ABC^+ \longrightarrow G_1^+ + ABC^* \longrightarrow AB^\bullet + C^\bullet$ (Eq. 1.2)

$\longrightarrow BAC^*$ (Eq. 1.3)

$G_1 + ABC^+ \longrightarrow G_1^+ + ABC^{+*} \longrightarrow AB^+ + C^\bullet$ (Eq. 1.4)

$AB^\bullet + C^+$

$ABC^+ \longrightarrow AB^+ + C^\bullet$ (Eq. 1.5)

$AB^\bullet + C^+$

Cell 4 (Reionization)

$G_2 + ABC \longrightarrow G_2 + e^- + ABC^+ \longrightarrow AB^+ + C^\bullet$ (Eq. 1.6)

$AB^\bullet + C^+$

$G_2 + AB^\bullet + C^\bullet \longrightarrow G_2 + e^- + AB^+, C^+$ (Eq. 1.7)

Scheme 1.2

Reionization: the fast moving neutrals ABC are reionized by collision with a target gas G_2 in the second collision chamber (Eq. 1.6 and 1.7). This oxidation step should be performed such that molecular (survivor) ions and also charged fragment ions are produced. The latter are recorded by scanning ESA1 and they serve to characterize the structure ABC^+. Because it takes approximately a microsecond for the neutral generated in Cell 3 to travel to Cell 4, the presence of an ABC^+ signal in the NR mass spectrum indicates that the neutral is stable and possesses a lifetime greater than 10^{-6} seconds. However, the mere presence of a recovery (survivor) signal does not prove that the neutral counterpart of ABC^+ is a stable entity. As shown by Equation 1.3, it is also

possible that all or part of the incipient neutral species ABC isomerize to a more stable isomer, BAC, prior to reionization. Therefore, a detailed analysis of the NR and CID mass spectra of isomeric ions is required, particularly in those systems where there is computational or experimental evidence for facile isomerization reactions of the neutral species. When the NR mass spectrum of a given ion is closely similar to its CID mass spectrum, the conclusion is often warranted that no isomerization has taken place, but only if it has been established (computationally) that there are high barriers towards isomerization. On the other hand, discrepancies between the CID and NR mass spectra of a given species may also originate in NR mass spectra, since these spectra may contain, beside the reionized neutrals ABC and their fragment ions, interfering contributions from reionized neutrals $AB^{\bullet}$ and $C^{\bullet}$ produced in the following processes: (i) dissociation of "hot" neutrals ABC* (Eq. 1.2), (ii) collision-induced dissociation of ABC^{+} (Eq. 1.4) and, (iii) spontaneous dissociation of (metastable) ABC^{+} ions (Eq. 1.5). Contributions from (iii) can easily be identified by placing a small voltage (> 100 V) on Cell 4, because most of these neutrals are generated outside the cell, but those resulting from the other two processes are often more difficult to verify.

If the neutralized ion beam is not isomerically pure, the presence of even minor amounts of isomeric (or isobaric) species which have a relatively high NR efficiency [47] may cause additional problems with the interpretation of the NR spectrum. Fortunately, the possibility of obtaining NR/CID mass spectra often resolves these uncertainties (see below).

Apart from a high NR efficiency, a balanced distribution of intact ions ABC^{+} and structurally characteristic fragment ions (see reaction 1.6) is desired in any NR experiment. As will be briefly discussed below, this and the degree of interference from the processes mentioned above, can be influenced to some extent by the appropriate choice of neutralization and reionization target gases.

The nature of the neutralization target gas is a crucial factor in a NRMS experiment since it effects the energy defect, Q, of the neutralization reaction [4c]. Since

Equation 1.1 represents a Franck-Condon process, the energy deficit for the reaction can be defined as: $Q(G_1) = IE_v(G_1) - NE_v(AB^+)$

where the subscript "v" indicates a vertical transition and NE is the neutralization (or recombination) energy for the ion going to the neutral. Three situations can occur: (i) $Q \sim 0$: resonant electron transfer, an efficient process; (ii) $Q < 0$: endothermic electron transfer, the energy deficit is provided from a slight reduction of the translational energy of the fast moving ions; and (iii) $Q > 0$: exothermic electron transfer; leading to the generation of species in (electronically) excited states and/or extensive dissociation thereof. Since charge transfer is a vertical process, the extent of overlap between the neutral and ionic states of the target gas will affect the charge exchange efficiency. Lindholm and co-workers have explored this phenomenon using perpendicularly oriented MS/MS instrumentation [48]. Similar neutralization target (NT) experiments can be realized on the ZAB-R using the quadrupole mass analyzer (q⊥) to detect the ionized target G_1^+ and, in the case of polyatomic targets, any fragment ions derived therefrom; the extent of fragmentation may offer more insight into the energetics of the exchange reaction.

The vertical nature of the neutralization and also the reionization step has another important consequence [49]: if there are large differences in geometry for the ion under investigation and its neutral, the survivor signal in the NR mass spectrum may become quite small. Thus, the absence of a measurable survivor signal does not necessarily imply that a given neutral species is not a stable entity. A case in point is the NR mass spectrum of the long-sought-after molecule ethylenedione, O=C=C=O [50] which has been proposed to be stable in its lowest triplet state but not in its singlet state. It is important to note that a recent computational study by Schröder and co-workers [51] suggested that the triplet state of O=C=C=O is also repulsive and in fact this elusive molecule may not be stable in any electronic state. In other cases, for example carbenes (see Chapters 2-8), it may also be desirable to determine the electronic state of the neutrals generated in NR experiments.

In NR experiments, metal vapours are usually very efficient targets and in particular Hg (IE = 10 eV) has been used extensively. However, their use can have deleterious effects on instrument performance, unless properly contained [52]. This prompted the use of Xe [4b] which is a permanent gas and is quite efficient even though it has a higher IE, 12.13 eV. More recently, vapours from polyatomic organics with lower IE's such as cyclopropane, trimethylamine, N,N-dimethylaniline and dimethyldisulfide (CH_3-S-S-CH_3) have also found favour. They have relatively high neutralization efficiency but are poor targets for collision-induced dissociation. This makes them particularly useful in studies of ions of low recombination energy [47,53]. Many other targets have been studied [54] and even surface-induced neutralization has been attempted [55].

For collisional reionization, He and O_2 (at a pressure corresponding to single collisions) are the target gases of choice. Helium is usually very efficient but, unlike oxygen, it often induces extensive dissociation. Routine NR mass spectra are therefore obtained with oxygen.

1.2.2 Neutralization-Reionization/Collision-Induced Dissociation (NR/CID)

When the identity of the reionized species in a NR experiment and/or the purity of the ions being neutralized is in doubt, the ability to perform MS/MS/MS experiments, especially CID of the NR survivor ion may prove invaluable [4c,e,g]. Such experiments, which are depicted in Figure 1.5, are capable of revealing whether the main beam of ions originally consisted of a single isomeric species or if the neutrals isomerize to a significant extent (Eq. 1.3). In this context, NR/CID mass spectra may be compared directly with CID mass spectra obtained under the same experimental conditions. If the spectra are closely similar, this virtually guarantees that the initial ion flux is pure and that structural integrity is maintained in the NR process. This is because isomeric (or isobaric) species will not normally have identical neutralization and also reionization efficiencies. Unfortunately, when the NR mass spectrum is weak, these experiments may be unattainable due to a lack of sensitivity.

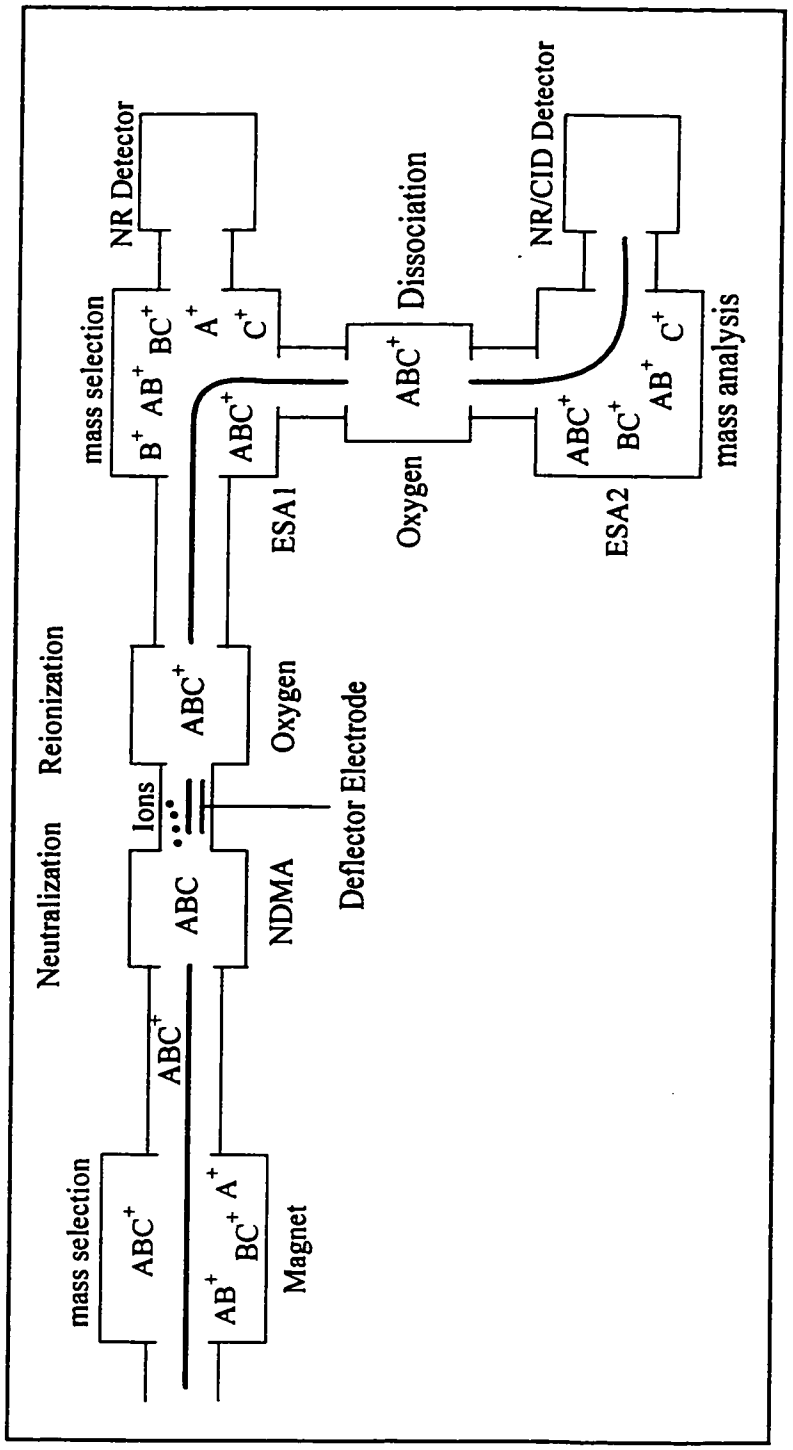

Figure 1.5: Schematic representation of an NR/CID experiment.

1.3 Estimation of Thermochemical Data

The ability to assign structures to gaseous ions and neutrals is not based exclusively on collision experiments (e.g. MI, CID and NR). Quite often the use of thermochemical data, i.e. enthalpy of formation (ΔH_f), ionization potentials (IP) and proton affinities (PA) can be instrumental in this capacity. In 1988, Lias and co-workers [28] completed the monumental task of producing a comprehensive volume of thermochemical data for ionic and neutral species derived largely from experimental methods. However, this does not preclude the need for techniques which are capable of estimating ΔH_f values in cases where none are available. Group additivity is currently the most widely used method for estimating thermochemical data for neutral molecules [56]. One of the most well known and commonly used methods is "Benson's Additivity Scheme" [57]. Other methods such as the use of isodesmic reactions [58] commonly provide satisfactory approximations for enthalpy of formation values for neutral species. Unfortunately, the thermochemistry of gas phase ions is not well-estimated using group additivity schemes [59]. Other empirical schemes for estimating ion thermochemistry, such as the methods developed by Holmes and Lossing [60] for odd electron ions and that developed by Benoit and Harrison [61] for even electron ions, have proven useful in this regard.

Thermochemical data can also be readily obtained using computational chemistry [7,58b]. One important aspect of the theoretical approach is that it can be applied to reactive species, such as ylide ions, distonic ions, and their neutral counterparts, as well as to conventional molecules and ions. Pople and Curtiss [62] have developed an *ab initio* "G2" method which is able to predict chemically accurate (± 2 kcal/mol) enthalpies of formation, ionization energies and proton affinities. This composite method combines results from *ab initio* calculations obtained at several lower levels of theory. However, these calculations are currently impractical for large systems. Very recently, Pople and Curtiss [63] have reported a subsequent method, dubbed "G3", which promises better accuracy and wider applicability. Other composite methods such as CBS-Q [64] and J2

[65] have also been shown to reproduce thermochemical data accurately. Typically, enthalpy of formation (ΔH_f) values for a given set of isomeric ions or neutrals are derived from differences in the relative energies of the isomers obtained at a lower level of theory with at least one value anchored to an experimentally established ΔH_f. In this regard, density functional theory (DFT) [66] and its hybrid (e.g. B3LYP) methods [67] have proven extremely useful since they tend to be far less computationally (time) demanding. *Ab initio* and DFT methods are also capable of providing detailed geometries and energies for dissociation products and transition state structures. From these thermodynamic parameters, a determination of dissociation energies, reaction barriers, ionization energies and proton affinities, can be obtained [7a].

Semi-empirical methods [68] are less computationally intensive and they have proven useful for investigations of larger systems for which *ab initio* and DFT methods cannot be applied. Although, one should be cautious about applying such procedures to organic ions and neutrals since these methods are limited by their parameterization and may yield erroneous energies.

1.4 Unconventional Ion Structures

1.4.1 Distonic Ions, Ylide Ions and Hydrogen Shift Isomers

The dissociation chemistry of many organic radical cations involves the formation of species which, either as an intermediate or a product ion, possess an unconventional ion structure. Thus, the discovery of ion-molecule complexes [69] and distonic ions as stable entities has greatly contributed to our understanding of gas phase reaction mechanisms. Consequently, the generation and characterization of such species, in particular distonic ions, has been the central focus of numerous studies [70] and forms an integral part of this thesis.

The term "distonic" ion was introduced by Radom and co-workers [71] in 1984 to describe the general class of radical cations where the charge and radical sites are located on separate heavy atoms. These species would (formally) arise from the ionization of systems best represented as zwitterions or as biradicals. An ylide ion (commonly denoted

ylidion) [71b], a sub-class of the distonic ion, has been coined to describe the particular case where the charge and the radical site are located on adjacent atoms, analogous to its well known neutral counterpart. As presented in Scheme 1.3, it is often useful to express the degree of separation between the charge and the radical site using prefixes (α, β and γ) for a given set of distonic ions.

α-distonic ion (ylide ion) β-distonic ion γ-distonic ion

Scheme 1.3

Distonic ions are not immediately accessible by direct ionization, but can be formed as a result of isomerization or ring opening of intact molecular ions or by ion-molecule reactions [5b,72]. These species are also routinely generated as product ions resulting from the rearrangement and fragmentation of molecular and daughter ions alike [70a,72b]. As alluded to above, the most striking characteristic property of this well-defined class of compounds is their relative stability. The $^{\bullet}CH_2OH_2^+$ ion was the first distonic (ylide) ion identified both experimentally [73] and computationally [74] to be more stable than its conventional isomer, $CH_3OH^{\bullet+}$. Similar behaviour has been observed for other distonic ions [70] including those described in this work. Furthermore, small distonic ions have been observed to be more susceptible to charge stripping [75] than their conventional isomers which facilitates their characterization.

The term "hydrogen shift isomers" was introduced in the context of this work to describe a particular set of isomers for which the basic structural skeleton remains intact, aside from the position of the hydrogen atoms. To illustrate this point, three hydrogen

shift isomers of ionized pyridine (see Chapter 3) are presented above in Scheme 1.3. It is also important to note that unlike a tautomer, this term does not infer the existence of an equilibrium between any of the isomers.

The work presented in this thesis focuses on the generation and characterization of a series of ionic and neutral hydrogen shift isomers of nitrogen containing heterocycles using a variety of tandem mass spectrometric techniques (MI, CID, NR and NR/CID), deuterium labelling experiments and quantum chemical calculations.

Chapters 2 and 3 describe the generation and characterization of two neutral and three ionic hydrogen shift isomers of pyridine and ionized pyridine respectively. This particular system is an excellent example of molecules which require NR/CID to enable their unambiguous identification.

Chapter 4 describes a combined mass spectrometric and computational study of the hydrogen shift isomer of thiazole, 2,3-dihydrothiazol-2-ylidene. The C_3H_3NS and $C_3H_3NS^{\bullet+}$ potential energy surfaces were also examined to deduce the thermodynamic and kinetic stabilities of the above mentioned and related species.

Chapter 5 describes the characterization of two hydrogen shift isomers of imidazole, including the well known species imidazol-2-ylidene, using NR and multiple collision (NR/CID) experiments in conjunction with quantum chemical calculations.

Chapter 6 describes the generation and characterization of the hydrogen shift isomers of the 1,4-diazine pyrazine which includes both ylide and biradical species. Similar to the pyridine system, NR/CID experiments were required to unambiguously identify the neutral generated and to evaluate the purity of the ions generated in the ion source.

In Chapter 7 the decarbonylation reaction of ionized 2-acetylpyridine, 2-acetylpyrazine and 2-acetylthiazole was studied to determine the structure of the resultant product ions using a variety of mass spectrometric techniques and quantum chemical calculations. A potential mechanism for the decarbonylation reaction is also proposed. Literature proposals involving methyl transfers in the dissociation of ionized dimethyl

pyridine-2,3-dicarboxylate, methyl pyridine-4-carboxylate and methyl pyridine-2-thio-carboxylate were also re-examined.

Chapter 8 describes the characterization of two neutral and three ionic hydrogen shift isomers of pyrimidine using tandem mass spectrometric techniques and isotopic labelling experiments. Quantum chemical calculations were performed to probe both the neutral and ionic potential energy surfaces.

References

[1] a) F.W. McLafferty and F. Tureček, *Interpretation of Mass Spectra*, 4th Ed., Univ. Sci. Books, California, **1993**.

b) H. Budzikiewicz, C. Djerassi and D.H. Williams, *Interpretation of Mass Spectra of Organic Compounds*, Holden-Day, San Francisco, **1964**.

c) *Mass Spectrometry of Organic Ions*, F.W. McLafferty (ed.), Academic Press, New York, **1963**.

d) J.H. Beynon, *Mass Spectrometry and Its Applications to Organic Chemistry*, Elsevier, Amsterdam, **1960**.

[2] a) R.D. Bowen, D.H. Dudley, H. Williams and H. Schwarz, *Angew. Chem., Int. Ed. Engl.* **1979**, *18*, 451.

[3] a) K. Levsen and H. Schwarz, *Angew. Chem., Int. Ed. Engl.* **1976**, *15*, 509.

b) K. Levsen and H. Schwarz, *Mass Spectrom. Rev.* **1983**, *2*, 77.

c) R.G. Cooks, *J. Mass Spectrom.* **1996**, 30, 1216.

d) S.A. McLuckey, *J. Am. Soc. Mass Spectrom.* **1992**, *3*, 599.

[4] a) C. Wesdemiotis and F.W McLafferty, *Chem Rev.* **1987**, *87*, 485.

b) J.K. Terlouw and H. Schwarz, *Angew. Chem., Int. Ed. Engl.* **1987**, *26*, 805.

c) J.L. Holmes *Chem. Rev.* **1989**, *8*, 513.

d) H. Schwarz, *Pure and Appl. Chem.* **1989**, *61*, 685.

e) J.L. Holmes, *Adv. Mass Spectrom.* **1989**, *11*, 53.

f) J.K. Terlouw, *Adv. Mass Spectrom.* **1989**, *11*, 984.

g) F.W. McLafferty, *Science* **1990**, *247*, 221.

h) F.W. McLafferty, *Int. J. Mass Spectrom. Ion Processes*, **1992**, *118/119*, 221.

i) F. Tureček, *Org. Mass Spectrom.* **1992**, *27*, 1087.

j) N. Goldberg and H. Schwarz, *Acc. Chem. Res.* **1994**, *27*, 347.

k) C.A. Schalley, G. Hornung, D. Schröder and H. Schwarz, *Chem. Soc. Rev.* **1998**, *27*, 91.

l) C.A. Schalley, G. Hornung, D. Schröder and H. Schwarz, *Int. J. Mass Spectrom. Ion Processes*, **1998**, *172*, 181.

[5] a) K.M. Stirk, J.C. Orlowski, D.T. Leeck and H.I. Kenttämaa, *J. Am. Chem. Soc.* **1992**, *114*, 8604.

b) H.I. Kenttämaa, *Org. Mass Spectrom.* **1994**, *29*, 1.

c) K.K. Thoen, B.J. Beasly, R.L. Smith and H.I. Kenttämaa, *J. Am. Soc. Mass Spectrom.* **1996**, *118*, 1408.

[6] K.L. Busch, G.L. Glish, and S.A. McLuckey, *Mass Spectrometry/Mass Spectrometry: Techniques and Applications of Tandem Mass Spectrometry,* VCH, New York, **1988**.

[7] a) L. Radom, *Org. Mass Spectrom.* **1991**, *26*, 359.

b) L. Radom, *Int. J. Mass Spectrom. Ion Processes* **1992**, *118/119*, 339 and references therein.

[8] J.H. Beynon, R.A. Saunders and A.E. Williams, *The Mass Spectra of Organic Molecules*, New York, **1968**.

[9] a) E.U. Condon, *Phys. Rev.* **1930**, *35*, 658.

b) M. Krauss and V.H. Dibeler, *Mass Spectrometry of Organic Ions*, F.W. McLafferty (ed.), Academic Press, New York, **1963**, p. 134.

[10] K. Levsen, *Fundamental Aspects of Mass Spectrometry*, Verlag Chemie, New York, **1978**, Vol. 4, p. 25.

[11] H.M. Rosenstock, M.B. Wallenstein, A.L. Wahrhaftig and H. Eyring, *Proc. Nat. Acad. Sci. US* **1952**, *38*, 667.

[12] a) P.J. Robinson and K.A. Holbrook, *Unimolecular Reactions*, Wiley-Interscience, New York, **1971**.

b) C. Lifshitz, *Adv. Mass Spectrom.* **1989**, *11*, 713.

[13] a) T. Wong, J.K. Terlouw, T. Weiske and H. Schwarz, *Int. J. Mass Spectrom. Ion Processes* **1992**, *113*, R23.

b) H.F. van Garderen, P.J.A. Ruttink, P.C. Burgers, G.A. McGibbon and J.K. Terlouw, *Int. J. Mass Spectrom. Ion Processes* **1992**, *121*, 159.

[14] W.A Chupka, *J. Chem. Phys.* **1959**, *30*, 191.

[15] J. Dannacher, *Org. Mass Spectrom.* **1984**, *19*, 253.

[16] a) H.M. Rosenstock, *Int. J. Mass Spectrom. Ion Phys.* **1976**, *20*, 139.

b) K. Maeda, G.P. Semeluk and F.P. Lossing, *Int. J. Mass Spectrom. Ion Phys.* **1968**, *1*, 395.

c) E.M. Clark, *Can. J. Chem.* **1954**, *32*, 764.

d) P. Marmet and L. Kerwin, *Can. J. Chem.* **1960**, *38*, 787.

e) P. Marmet and J.D. Morrison, *J. Chem. Phys.* **1962**, *36*, 1238.

[17] H.M. Rosenstock, K. Draxl, B.W. Steiner and J.T. Herron, J. Phys. Chem. Ref. Data, **1977**, *6*, Supplement 1.

[18] J.A. Hipple and E.U. Condon, *Phys. Rev.* **1945**, *68*, 54.

[19] R.G. Cooks, J.H. Beynon, R.H. Caprioli and G.R. Lester, *Metastable Ions*, Elsevier, Amsterdam, **1973**.

[20] H.M. Rosenstock, V.H. Dibeler and F.N. Harllee, *J. Chem. Phys.* **1964**, *40*, 591.

[21] T.W. Shannon and F.W. McLafferty, *J. Am. Chem. Soc.* **1967**, *88*, 5021.

[22] J.H. Holmes and J.K. Terlouw, *Org. Mass Spectrom.* **1980**, *15*, 383.

[23] J.A. Hipple, R.E. Fox and E.U. Condon, *Phys. Rev.* **1946**, *69*, 347.

[24] J.H. Polanyi, *Acc. Chem. Res.* **1972**, *5*, 161.

[25] J.N. Harvey, M. Aschi, H. Schwarz and W. Koch, *Theor. Chem. Acc.* **1998**, *99*, 95.

[26] C. Lifshitz and F.A. Long, *J. Phys. Chem.* **1965**, *69*, 3746.

[27] a) D.J. McAdoo, F.W. McLafferty and J.S. Smith, *J. Am. Chem. Soc.* **1970**, *92*, 6343.

b) F.W. McLafferty, D.J. McAdoo, J.S. Smith and R. Kornfeld, *J. Am. Chem. Soc.* **1971**, *93*, 3720.

c) C.C. Van de Sande and F.W. McLafferty *J. Am. Chem. Soc.* **1975**, *97*, 4617.

d) C. Lifshitz and E. Tzidony, *Int. J. Mass Spectrom. Ion Phys.* **1981**, *39*, 181.

e) D.J. McAdoo and C.E. Hudson *Int. J. Mass Spectrom. Ion Processes* **1984**, *59*, 77.

f) C. Lifshitz, *Org. Mass Spectrom.* **1988**, *23*, 303.

g) N. Heinrich, F. Louage, C. Lifshitz and H. Schwarz, *J. Am. Chem. Soc.* **1988**, *110*, 8183.

h) T.H. Osterheld and J.I. Brauman, *J. Am. Chem. Soc.* **1992**, *114*, 7158.

[28] S. Lias, J.E. Bartmess, J.F. Liebman, J.L. Holmes, R.D. Levin and W.G. Mallard, *J. Phys. Chem. Ref. Data*, **1988**, *17*, Supplement 1.

[29] a) J.H. Holmes and F.P. Lossing, *J. Am. Chem. Soc.* **1980**, *102*, 1591.
b) W. Bouma, J.K. MacLeod and L. Radom, *J. Am. Chem. Soc.* **1968**, *102*, 2246.
c) F. Tureček, C. J. Cramer, *J. Am. Chem. Soc.* **1995**, *117*, 12243.

[30] a) D.H. Williams, *Acc. Chem. Res.* **1977**, *10*, 280.
b) P.C. Burgers and J.H. Holmes, *Org. Mass Spectrom.* **1982**, *17*, 123.

[31] D.H. Williams and J. Ronayne, *Chem. Commun.* **1967**, 1129.

[32] K.R. Jennings, *Int. J. Mass Spectrom. Ion Processes* **1968**, *1*, 227.

[33] W.F. Haddon and F.W. McLafferty, *J. Am. Chem. Soc.* **1968**, *90*, 4745.

[34] J.L. Holmes, *Org. Mass Spectrom.* **1985**, *20*, 169.

[35] R. Flammang, L. Gallez, Y. van Haverbeke, M.W. Wong and C. Wentrup, *Rap. Comm. Mass Spectrom.* **1996**, *10*, 232.

[36] H.S.W. Massey, *Rep. Prog. Phys.* **1949**, *12*, 248.

[37] R.G. Cooks, J.H. Beynon and T. Ast, *J. Am. Chem. Soc.* **1972**, *94*, 1004.

[38] J. Holmes, J.K. Terlouw, P.C. Burgers and R.T.B. Rye, *Org. Mass Spectrom.* **1980**, *15*, 149.

[39] J.H. Bowie and T. Blumenthal, *J. Am. Chem. Soc.* **1975**, *97*, 2959.

[40] a) M.M. Bursey, *Mass Spectrom. Rev.* **1990**, *9*, 555.
b) S. Hayakawa, H. Endoh, K. Arakawa, N. Morishita and T. Sugiura, *Int. J. Mass Spectrom. Ion Processes* **1995**, *151*, 89.

[41] a) P.C. Burgers, J.H. Holmes, J.E. Szulejko, A.A. Mommers and J.K. Terlouw, *Org. Mass Spectrom.* **1983**, *18*, 254.
b) F. Tureček and F.W. McLafferty, *J. Am. Chem. Soc.* **1984**, *106*, 2525.

[42] S. Villeneuve and P.C. Burgers, *Org. Mass Spectrom.* **1986**, *21*, 733.

[43] R. Lavertu, M. Catté, A. Pentenero and P. Le Goff, *C.R. Acad. Sc. Paris, Sér. C* **1966**, *263*, 1099.

[44] F.M. Devienne, *Entropie* **1968**, *24*, 35.

[45] a) J. Gray and R.H. Tomlinson, *Chem. Phys. Letters* **1969**, *3*, 523.
b) J. Gray and R.H. Tomlinson, *Chem. Phys. Letters* **1969**, *4*, 251.
c) J. Gray and R.H. Tomlinson, *Int. J. Mass Spectrom. Ion Processes* **1969**, *3*, 523.

[46] G.I. Gellene and R.F. Porter, *Acc. Chem. Res.* **1983**, *16*, 200.

[47] C.E.C.A. Hop and J.L. Holmes, *Org. Mass Spectrom.* **1991**, *26*, 476.

[48] a) E Lindholm, in *Ion-Molecule Reactions* Vol. 2, J.L. Franklin (ed.), Plenum, New York, **1972**, Chapter 10, p. 457.

b) E Lindholm, in *Ion-Molecule Reactions in the Gas Phase*, Adv. Chem. Ser., No. 58, P.J. Ausloos (ed.), American Chemical Society, Washington, **1966**, p.1.

c) J.M. Tedder and P.H. Vidaud, *J. Phys. D: Appl. Phys.* **1980**, *13*, 1949.

[49] V.Q. Nguyen and F. Tureček, *J. Mass Spectrom.* **1996**, *31*, 843 and references therein.

[50] a) D. Sülzle and H. Schwarz, *Int. J. Mass Spectrom. Ion Processes* **1993**, *120*, 1.

b) H. Chen and J.L. Holmes, *Int. J. Mass Spectrom. Ion Processes* **1994**, *133*, 111.

[51] D. Schröder, C. Heinemann, H. Schwarz, J.N. Harvey, S. Dua, S.J. Blanksby and J.H. Bowie, *Chem. Eur. J.* **1998**, *4*, 2250.

[52] a) D.E. Drinkwater, A. Fura, M.-Y. Zhang and F.W. McLafferty, *Org. Mass Spectrom.* **1991**, *26*, 1032.

b) P.C. Burgers, W. Kulik, C. Versluis and J.K. Terlouw, *Int. J. Mass Spectrom. Ion Processes* **1990**, *98*, 247.

[53] a) T. Wong, J.K. Terlouw, T. Weiske and H. Schwarz, *Int. J. Mass Spectrom. Ion Processes* **1992**, *113*, R23.

b) M.-Y. Zhang and F.W. McLafferty, *J. Am. Soc. Mass Spectrom.* **1992**, *3*, 108.

c) S.A. Shaffer, F. Tureček and R.L. Cerny, *J. Am. Chem. Soc.* **1993**, *115*, 12117.

[54] a) G.C. Shields, S.H. Wennberg, J.B. Wilcox, T.F. Moran, *Org. Mass Spectrom.* **1986**, *21*, 137.

b) G.C. Shields, P.A. Steiner IV, P.R. Nelson, M.C. Trauner and T.F. Moran, *Org. Mass Spectrom.* **1987**, *22*, 64.

c) J.B. Sedgewick, B.P. Paulson, G.C. Shields and T.F. Moran, *Int. J. Mass Spectrom. Ion Processes* **1987**, *79*, 127.

[55] a) I. Vidavski, R.A. Chorush and F.W. McLafferty, 41st ASMS Conference, San Francisco, May 31st - June 4th **1994**, abst. #492.

b) R.A. Chorush, I Vidavsky and F.W. McLafferty, *Org. Mass Spectrom.* **1994**, *28*, 1016.

[56] K.K. Irikura and D.J. Frurip, *Computational Thermochemistry: Prediction and Estimation of Molecular Thermodynamics*, American Chemical Society, Washington, **1999**, p. 20.

[57] a) S.W. Benson and J.H. Buss, *J. Chem. Phys.* **1958**, *29*, 546.

b) N. Cohen and S.W. Benson, *Chem. Rev.* **1993**, *93*, 2419.

c) N. Cohen, *J. Phys. Chem. Ref. Data* **1996**, *25*, 1411.

[58] a) W.J. Hehre, R. Ditchfield, L. Radom, and J.A. Pople, *J. Am. Chem. Soc.* **1970**, *92*, 4796.

b) W.J. Hehre, L. Radom, P.v.R. Schleyer and J.A. Pople, *Ab Initio Molecular Orbital Theory*, Wiley, New York, **1986**, p. 36.

[59] J.L. Holmes, *Int. J. Mass Spectrom. Ion Processes* **1992**, *118/119*, 381.

[60] a) J.H. Holmes and F.P. Lossing, *Can. J. Chem.* **1982**, *60*, 2365.
b) J.H. Holmes and F.P. Lossing, *Org. Mass Spectrom.* **1991**, *26*, 537.

[61] F.M. Benoit and A.G. Harrison, *J. Am. Chem. Soc.* **1977**, *99*, 3980.

[62] J.A. Pople and L.A. Curtiss, *J. Phys. Chem.* **1987**, *91*, 155, 3637.

[63] A.G. Baboul, L.A. Curtiss, P.C. Redfern and K. Raghavachari, *J. Chem. Phys.* **1999**, *110*, 7650.

[64] J.W. Ochterski, G.A. Petersson and J.A. Montgomery Jr., *J. Chem. Phys.* **1996**, *104*, 2598 and references therein.

[65] B.D. Dunietz, R.B. Murphy and R.A. Friesner, *J. Chem. Phys.* **1999**, *110*, 1921.

[66] R.G. Parr and W. Yang, *Density-Functional Theory of Atoms and Molecules*, Oxford University, New York, **1989**.

[67] a) A.D. Becke, *J. Chem.* Phys. **1993**, *98*, 5648.
b) P.J. Stephens, F.J. Devlin, C.F. Chabalowski, M.J. Frisch, *J. Phys. Chem.* **1994**, *98*, 11623.

[68] M.J.S. Dewar, *Org. Mass Spectrom.* **1993**, *28*, 305.

[69] For leading references see: (a) R.D. Bowen, *Org. Mass Spectrom.* **1993**, *28*, 1577.
(b) T.H. Morton, *Org. Mass Spectrom.* **1992**, *27*, 353.
(c) P. Longevialle, *Mass Spectrom. Rev.* **1992**, *11*, 157.
(d) R.D. Bowen, *Acc. Chem. Res.* **1991**, *24*, 364.
(e) D.J. McAdoo, *Mass Spectrom. Rev.* **1988**, *7*, 363.

[70] For leading references see: (a) S. Hammerum, *Mass Spectrom. Rev.* **1988**, *7*, 123.
(b) B.F. Yates, W.L. Bouma and L. Radom, *Tetrahedron* **1986**, *42*, 6225.

[71] (a) B.F. Yates, W.L. Bouma and L. Radom, *J. Am. Chem. Soc.* **1986**, *106*, 5805.
(b) L. Radom, W.J. Bouma, R.H. Nobes and B.F. Yates, *Pure and Applied Chemistry*, **1984**, *56*, 1831.

[72] (a) K.M. Stirk, L.K. Kiminkinen and H.I. Kenttamaa, *Chem. Rev.* **1992**, *92*, 1649.
(b) J.S. Splitter and F. Tureček, *Applications of Mass Spectrometry to Organic Stereochemistry*, VCH, New York, **1994**.

[73] (a) J.L. Holmes, F.P. Lossing, J.K. Terlouw and P.C. Burgers, *J. Am. Chem. Soc.* **1982**, *104*, 2931.

(b) W.J. Bouma, J.K. MacLeod and L. Radom, *J. Am. Chem. Soc.* **1982**, *104*, 2930.

[74] W.J. Bouma, R.H. Nobes and L. Radom, *J. Am. Chem. Soc.* **1982**, *104*, 2929.

[75] (a) F. Moquin, D. Stahl, A Sawaryn, P. von Schleyer, W. Koch, G. Frenking and H. Schwarz, *J. Chem. Soc. Chem. Comm.* **1984**, 504.

(b) W.J. Bouma and L. Radom, *J. Am. Chem. Soc.* **1985**, *105*, 5484.

(c) B.F. Yates, W.L. Bouma and L. Radom, *J. Am. Chem. Soc.* **1986**, *108*, 6545.

CHAPTER 2

Observation of the Hammick Intermediate: Reduction of the Pyridine-2-ylide Ion in the Gas Phase

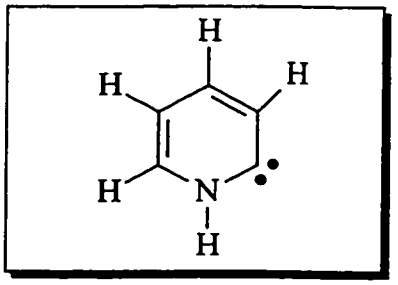

This Chapter describes the generation and characterization of the elusive Hammick Intermediate, azacyclohexatriene-2-ylidene (see inset above). This hydrogen shift isomer of pyridine was generated from its ionic counterpart using the technique of Neutralization-Reionization (NR) mass spectrometry.

The structure of the ionic and neutral species was probed with a variety of mass spectrometry based methods, including analysis of Metastable Ion spectra and Collision-Induced Dissociation (CID) spectra of both the source generated ions and the "survivor" ions resulting from the neutralization-reionization process. For both the ion and the neutral, state-of-the-art computational chemistry was used to determine the stability of the Intermediate and the barrier of isomerization into its pyridine isomer.

From the combined experimental and computational results, it is concluded that the Hammick Intermediate is a stable, non-interconverting species in the gas phase.

The work described here has been published previously in an article under the same title: D.J. Lavorato, J.K. Terlouw, T.K. Dargel, W. Koch, G.A. McGibbon and H. Schwarz, J. Am. Chem. Soc., 1996, 118, 11898-11904.

Introduction

A century ago, Nef [1] made clear his desire to prepare carbenes, and since then they have certainly done anything but languish in obscurity [2,3]. Undoubtedly though, fresh impetus for their further study was provided by the exciting reports of remarkably stable compounds that contain dicoordinate carbon centers [4,5]. Not surprisingly, the question as to which features serve to stabilize (singlet) carbenes was considered long before these reports [6-8]. In addition to considering the parent imidazol-2-ylidene, it was suggested that the 2-isomer of pyridine, i.e., **1**, and other polyene type systems should be stabilized by p-π splitting [8]. Even before this, Hammick [9] and co-workers actually postulated the existence of **1** in its ylidic form to explain the accelerated decarboxylation rate of 2-picolinic acid [10], a reaction which continues to elicit interest [11], although it was Breslow [12] who first explicitly depicted **1** as being stabilized by the carbene resonance contributor. It seems apparent that a rigorous modern analysis of such reactive intermediates benefits from the wide array of theoretical and experimental methods now available to probe and compare their physical and chemical properties. For example, in the case of the imidazol-2-ylidene type carbenes [13] such an analysis even extends to a comparison with related compounds [14], which, for example, include the saturated imidazolin-2-ylidenes [6,15], silylenes (stable analogues of the imidazol-2-ylidene having been recently discovered [16]), and the phosphorus containing ylides synthesized by Bertrand and co-workers [17].

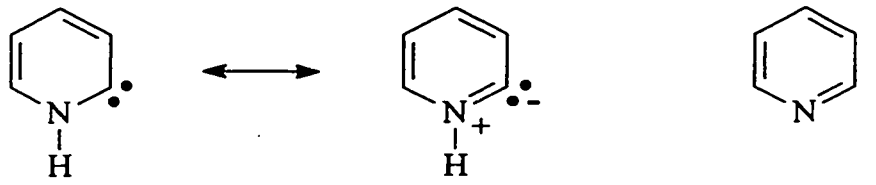

1 **2**

Despite the enormous progress made in the study of such species in condensed phases, there are often advantages, especially for species that are susceptible to bimolecular tautomerization or dimerization, to conduct investigations in the gas phase, particularly in high vacuum where intermolecular interactions are virtually absent. The interior of a mass spectrometer offers such an environment and following the introduction of the neutralization-reionization mass spectrometry (NRMS) [18] technique it has proved to be an ideal place to study a great variety of species, including several carbenes i.e. $H_2N\text{-}\ddot{C}\text{-}NH_2$ [19], $H_2N\text{-}\ddot{C}\text{-}OH$ [20], $H_3C\text{-}\ddot{C}\text{-}OH$ [21], $F\text{-}\ddot{C}\text{-}OH$ [22], $H\text{-}\ddot{C}\text{-}OH$ [23], and ylides i.e. $H\text{-}\bar{C}\text{=}\overset{+}{N}\text{=}NH$ [24], $H\text{-}\bar{C}\text{=}\overset{+}{N}\text{=}CH_2$ [25] that are expected to have only a fleeting existence in solution. One of the advantages of NRMS is that the neutral molecules are accessed by a Franck-Condon type electron transfer to their ionic counterparts, which may be available through the dissociative ionization of a suitable precursor molecule. In the case of the 2-isomer of pyridine, Chen provided strong circumstantial evidence that the radical cation $\mathbf{1}^{\bullet+}$ is formed in this way from 2-picolinic acid as well as its methyl and ethyl esters [26]. It is clear, however, that in order to unambiguously establish the formation of a carbene in a NRMS experiment it is usually necessary to demonstrate that the initial ion beam is not contaminated with interfering ions i.e., species isomeric or isobaric with the ion of interest. Considerable benefits (not the least of which is the chance to assess the purity of the main ion beam) accrue when it is possible to directly probe the structure, usually by collision-induced dissociation (CID), of those ions that survive the neutralization-reionization (NR) process. Furthermore, for both neutral and ionized species there must be energy barriers of sufficient magnitude to prevent the facile equilibration of the carbene with its isomer(s). Sufficiently high level quantum chemical calculations are often an excellent way to obtain insight on the kinetic stability of individual molecules. There is, however, no computational information about the height of the barriers to tautomerization in the present system, although Grigg et al. found a stable structure for **1** with Hartree-Fock calculations using the rather limited STO-3G basis set [27]. It is clear though from the ability to trap **1** in solution with aldehydes (giving secondary alcohols)

that isomerization by a 1,2-hydrogen shift does not proceed immediately upon its formation. Nyulaszi *et al.*, prompted by the observation of phosphorous ylides [17], have recently performed computations on the analogous 2-isomer of phosphinine [28].

In this Chapter, the first direct experimental and theoretical evidence is presented for the identification of the long-invoked [8-10,12], but hitherto unobserved, 2-isomer of pyridine, azacyclohexatriene-2-ylidene, **1.** The structures and stabilities of the two isomeric ions and neutrals and their interconversion barriers were studied by *ab initio* molecular orbital and hybrid density functional theory (DFT) calculations. The existence of the two distinct radical cations and the corresponding neutral species was established by collision experiments, in particular, through the use of neutralization-reionization/collision-induced dissociation (NR/CID) mass spectrometry. Although the possibility of differing descriptive formalism, i.e. carbene vs ylide, exists for **1** we do not concentrate on this aspect in the present work.

Results and Discussion

The proper identification of neutral species by NRMS requires that one can confidently establish the parent ion structure. Fortunately, in this case the search for appropriate precursor molecules from which to attempt to generate the isomeric parent ions, $\mathbf{1}^{\bullet+}$ and $\mathbf{2}^{\bullet+}$, was brief. The carbene ion $\mathbf{1}^{\bullet+}$ was postulated by Chen [26] to explain the differences in the dissociation behaviour of $C_5H_5N^{\bullet+}$ ions generated by dissociative 70 eV electron ionization (EI) mass spectra of various monosubstituted pyridines versus the EI mass spectrum of $\mathbf{2}^{\bullet+}$. The molecular ion $\mathbf{2}^{\bullet+}$ is undoubtedly initially generated by EI of unsubstituted pyridine itself. However, no comparative structural differentiation of the two supposedly distinct isomeric species has been reported despite the fact that the tandem mass spectrometric methods used to accomplish this aim are well known [29]. This is not a trivial point! The process of lowest energy requirement for pyridine is loss of HCN with a reported appearance energy $AE(C_4H_4^{\bullet+}) = 13.28$ eV [30], i.e., the critical energy for the reaction is 4.0 eV. Given this large value, almost 100 kcal/mol, it could

reasonably be expected that the $C_5H_5N^{\bullet+}$ isomers are able to interconvert prior to undergoing their unimolecular dissociation. It is not surprising then that the metastable ion (MI) mass spectra of the m/z 79 ions obtained by EI of pyridine and by dissociative EI of either picolinic acid or its methyl ester, which we had anticipated to represent ions $\mathbf{2}^{\bullet+}$ and $\mathbf{1}^{\bullet+}$ respectively, are the same. Further evidence of isomerization comes from the MI mass spectrum of the isotopologue of $\mathbf{1}^{\bullet+}$, which was generated from ionized d_3-methyl picolinate by subsequent losses of CD_2O and CO and is thereby selectively labelled with a deuterium atom at the nitrogen position. In it, the dominant Gaussian shaped peak in these spectra has split into two components: three parts HCN and one part DCN loss. The situation is not hopeless though, since the collision-induced dissociation (CID) mass spectra of the m/z 79 ions do exhibit minor *but characteristic* differences. The most critical of these are the m/z 26 : 28 ratio and the doubly charged ion intensity. Only $\mathbf{1}^{\bullet+}$ possess a hydrogen on the nitrogen. Thus, it should be able to produce the m/z 28 ion ($HCNH^+$) [31] more easily than $\mathbf{2}^{\bullet+}$ whereas both ions can give m/z 26 fragments ($C_2H_2^{\bullet+}$ and CN^+). For ion $\mathbf{1}^{\bullet+}$, the CID mass spectrum (Table 2.1, see Experimental for details) shows that the characteristic ratio is essentially 1:1 and that m/z 38.5 and 39.5 are the most intense peaks in the cluster at m/z 36-41, whereas for $\mathbf{2}^{\bullet+}$ the ratio is 2:1 and doubly charged ions are really barely visible in the shoulders of the m/z 39 and 40 peaks. More importantly, the CID mass spectrum of the m/z 79 ions generated by the metastable dissociation of picolinic acid molecular ions is the same as the spectrum of the ions which are generated by CO_2 loss in the ion source. Since the parent ions undoubtedly possess different internal energy distributions in the two cases one would expect a variation in the proportion of fragment ions produced if dissociation yielded a mixture of isomers rather than a single species. Thus, we conclude that dissociative ionization of picolinic acid gives preferentially if not exclusively $\mathbf{1}^{\bullet+}$ rather than a mixture of the two isomers. It is clear though from the similarity of the CID mass spectra of the two isomers that large differences are not necessarily to be expected in the NR mass spectra of $\mathbf{1}^{\bullet+}$ and $\mathbf{2}^{\bullet+}$.

Table 2.1. CID and NR Mass Spectra of the ylide ion $1^{\bullet+}$ and its pyridine isomer $2^{\bullet+}$.

	$1^{\bullet+}$			$2^{\bullet+}$		
(m/z)	CID $[O_2]^a$	NR $[\Delta,O_2]^b$	NR $[DA,O_2]^c$	CID $[O_2]^a$	NR $[\Delta,O_2]^b$	CID $[He]^d$
79		24	49		90	
78	14	12	12	11	13	25
77	2	6	3	1	3	5
76	3	7	4	2	4	5
75	2	7	4	2	4	2
53	11	17	9	6	6	7
52	100	100	100	100	100	100
51	45	89	64	44	98	65
50	28	84	47	25	61	51
49	7	34	15	6	20	10
48	2	8	4	2	6	2
40	5	11	6	3	9	4
39.5	12			5		
39	11	25	17	11	24	15
38.5	12					
38	11	41	24	10	35	16
37	9	53	27	8	37	11
36	3	27	12	3	17	2
28	9	12	10	4	11	7
27	6	96	24	4	47	6
26	9	68	27	10	44	20
25	4	36	13	3	20	3
24	2	19	6	2	9	1
13		6	2		4	
12	1	10	3	<1	5	<1

[a]CID $[O_2]$ indicates collision-induced dissociation with O_2 performed between B and E_1. [b]NR $[\Delta,O_2]$ indicates neutralization with cyclopropane and reionization with O_2 performed between B and E_1. [c]NR $[DA,O_2]$ indicates neutralization with N,N-dimethylaniline and reionization with O_2 performed between B and E_1. [d]CID [He] in the third field free region between E_1 and E_2. Since E_1 and E_2 do not have the same energy resolving power, a direct comparison is most appropriate to the spectra presented in Figure 1.1. All spectra refer to source generated ions having 10 keV translational energy.

Indeed, despite the fact that the disparities between the two NR mass spectra are greater than for the corresponding CID mass spectra, the key m/z 26 : 28 ratio is not isomer distinguishing. In fact, using cyclopropane as a neutralization agent the NR ratio is 4:1 for $\mathbf{2}^{\bullet+}$ and even larger, 5.5:1, for $\mathbf{1}^{\bullet+}$. Nevertheless, both spectra do contain peaks at m/z 79, corresponding to reionized $C_5H_5N^{\bullet+}$. Furthermore, the use of organic neutralization agents with low ionization energies, which more closely match the recombination energies of the carbenes, are more likely to give near resonant electron transfer and it was noted that the use of N,N-dimethylaniline as the reducing agent led to considerably less fragmentation in the NR mass spectrum of $\mathbf{1}^{\bullet+}$ (m/z 26:28 ratio 2.7:1), which thus bears a greater resemblance to the CID mass spectrum. It is still not possible though to assign the structure of the stable neutral species at this juncture. Similar problems plague other systems [19,20,32] and it has been shown previously that neutral identification may still be feasible by selectively analyzing the ions recovered after the NR process [18]. This NR/CID type of multiple collision experiment is demanding in terms of sensitivity, but extremely revealing as will be demonstrated. It should be mentioned that NR, but not NR/CID experiments, have been used to probe the structure of the C_5H_5N neutral produced in an interesting nitrogen atom translocation reaction of $(C_5H_5)_2Fe_2NO^+$ and it was suggested that pyridine was the molecule produced [33]. Although it would seem now that the structure of the product cannot be unequivocally assigned on the basis of these results, thermodynamic considerations (vide infra) still favour the earlier suggestion [33].

Partial NR/CID mass spectra of $\mathbf{1}^{\bullet+}$ and $\mathbf{2}^{\bullet+}$ are shown in Figure 2.1 (parts a and b respectively). The former spectrum represents the m/z 79 ions obtained from picolinic acid but it should be noted that the NR/CID mass spectrum of the m/z 79 ions generated from methylpicolinate was essentially superimposable upon it. A comparison of the different NR/CID mass spectra reveals several things. First, two ions ($\mathbf{1}^{\bullet+}$ and $\mathbf{2}^{\bullet+}$) are once again discernable by CID following the neutralization-reionization events. Second, the NR/CID mass spectrum from each isomer is extremely similar to the corresponding

CID mass spectrum (Table 2.1). So, in spite of the common dissociation channels which are accessed by $\mathbf{1}^{\bullet+}$ and $\mathbf{2}^{\bullet+}$ they are sufficiently different from one another to permit isomer identification. That this is undoubtedly the case can be seen from a comparison of the NR/CID mass spectrum (Figure 2.2a) of the labelled ion d_1-$\mathbf{1}^{\bullet+}$ with its CID mass spectrum (Figure 2.2b), which reveals the two to be nearly identical. These results demonstrate that the structural integrity of the species are maintained throughout the NR process and furthermore, the original ion fluxes were constituted of only a single $C_5H_5N^{\bullet+}$ isomer. If this were not the case, since the two isomers are expected to have different efficiencies at each collision step, an enrichment of one relative to the other would take place and the resulting NR/CID spectra would be intermediate in appearance between the CID spectra of the two isomers. The slight difference in the relative intensity of m/z 41 for the labelled ions is thus attributed to a small amount of post-collisional isomerization of the ions, which can occur below the threshold for dissociation. As indicated below by our calculations, neutral tautomerization is in principle also possible since despite its substantial height the barrier is low enough to be surmounted without dissociation [34]. However, the evidence leads us to the conclusion that neutral **1** is a stable species, which does not easily interconvert with **2** although this tautomerization undoubtedly occurs for some of the excited species.

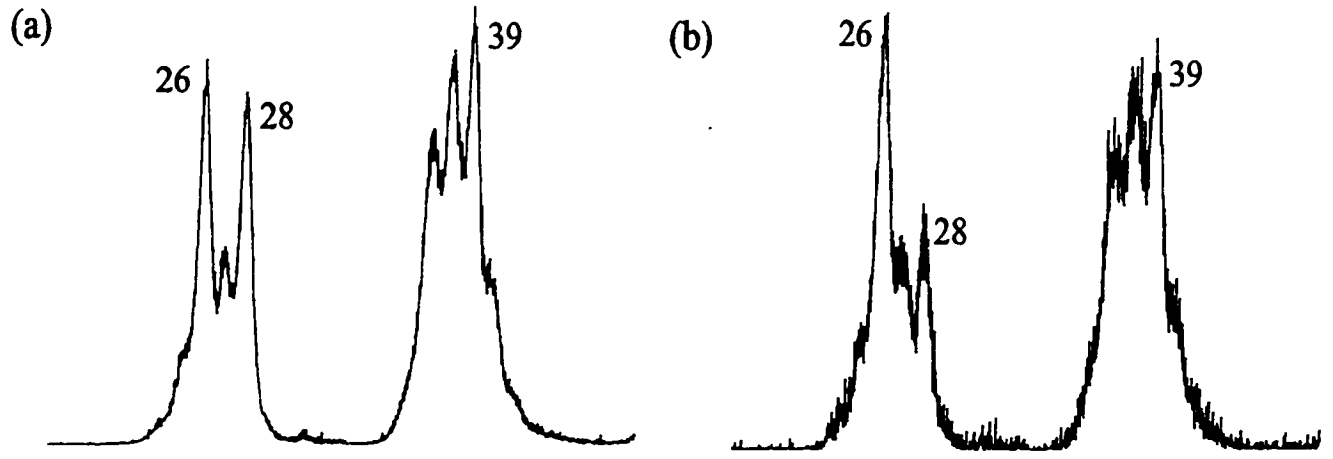

Figure 2.1: NR/CID (see text) mass spectrum of the m/z 79 ions generated from (a) ionized 2-picolinic acid and (b) ionized pyridine.

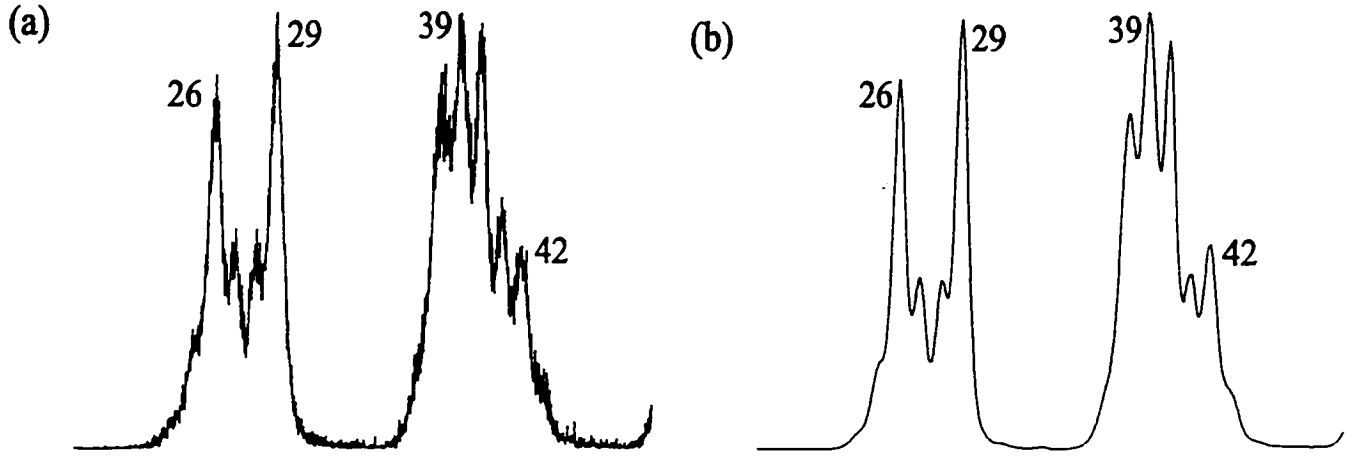

Figure 2.2 : (a) NR/CID (see text) mass spectrum and (b) CID mass spectrum of the $C_5H_4DN^{\bullet+}$ ions (m/z 80) generated from ionized d_3-methyl picolinate.

Theoretical Methods

The calculations of the structures, energetics and frequencies were performed on IBM/RS6000 workstations and a CRAY Y-MP using the Gaussian94 program package [35]. Each method employed in this study was combined with the standard 6-31G** basis set [36], which includes d- and p-type polarization functions on non-hydrogen and hydrogen atoms, respectively. We have considered the effects of valence electron correlation using Møller-Plesset (MP) perturbation theory truncated at second order [36]. For the open shell systems the projected MP2 energy (PMP2), in which the first spin contaminant has been annihilated [37], has been used for the determination of the relative energies. In addition, for the minimum structures calculations employing the multi-reference MP2 procedure based on a complete active space SCF wave function [38] (CASSCF-MP2) as offered in Gaussian94 were performed [39]. The active space consisted of the six π and π^* orbitals and the lone pair at nitrogen or carbon, respectively, thus leading to a distribution of eight (seven for the ions) electrons in seven active orbitals. The CASSCF-MP2 energy calculations were based on CASSCF optimized geometries. We have also used the recently suggested B3LYP hybrid density functional theory (DFT) [40] option employing Becke's [41] empirical three-parameter fit for mixing HF and DFT exchange-energy terms as implemented [42] in Gaussian94. All relative energies were corrected for zero-point vibrational energy (ZPVE) contributions. The ZPVE obtained at the MP2 level were uniformly scaled by a factor of 0.9646, [43] while no scaling was performed for the B3LYP fundamentals. For the CASSCF-MP2 energies the ZPVE obtained at the MP2 level were used.

Emmanuel and Shelvin [44] have recently considered some of the C_5H_5N potential energy surface to explain the production of pyridine in reactions of atomic carbon with pyrrole. Of course, pyridine and its radical cation, i.e. **2** and $\mathbf{2}^{\bullet+}$, are already well known to computational chemists, [45] but by contrast the isomer **1** and its ionized counterpart $\mathbf{1}^{\bullet+}$ are virtually unknown [27]. Of the latter two, there are reports only concerning the neutral species **1** and to our knowledge there have not been any previous

studies of the transition states for interconversion of either the neutral or ionic species. Since one way of looking at **1** is in terms of a carbene, special care has to be taken to adequately describe the electronic structure of this species and single determinant based methods such as MP2 might not be sufficient [46]. We therefore performed CASSCF-MP2 calculations on the neutral and ionic minima species in which degeneracy effects are properly taken care of in order to calibrate the accuracy of the MP2 and B3LYP approaches [47]. However, from the results presented below and the analysis of the CASSCF wave function we can safely conclude that none of the minima considered requires a multi-reference treatment. For the open shell species the CASSCF wave function has the further advantage of being a spin eigenfunction, whereas the unrestricted reference wave functions do show significant spin contamination in the MP2 calculations. The B3LYP approach suffers much less from this problem [48]. The computed total and relative energies together with the $<S^2>$ expectation values in the case of the open shell systems are summarized in Table 2.2.

Table 2.2. Calculated energies for selected C_5H_5N neutrals, radical cations and transition states, employing the 6-31G** basis set.[a,b]

Neutral	MP2	$<S^2>$	ZPVE	E_{rel}	B3LYP	$<S^2>$	ZPVE	E_{rel}	CASSCF-MP2	E_{rel}[d]
1^{s}[c]	-247.44196	0.0	54.5	50.2	-248.21778	0.0	55.6	46.8	-247.40445	49.0
1^{t}[c]	-247.36936	2.395	53.1	94.5	-248.15738	2.037	53.3	82.4	-247.34432	85.4
2	-247.52180	0.0	54.4	0.0	-248.29260	0.0	55.8	0.0	-247.48246	0.0
TS1/2	-247.37542	0.0	50.3	87.9	-248.14978	0.0	51.3	85.1		
$\mathbf{1}^{\bullet+}$	-247.19730	0.956	58.0	207.1	-247.96762	0.758	56.1	204.2	-247.15554	208.6
$\mathbf{2}^{\bullet+}$	-247.18665	1.096	56.8	212.6	-247.96637	0.757	54.2	203.1	-247.14187	216.0
$\mathbf{TS1}^{\bullet+}/\mathbf{2}^{\bullet+}$	-247.09296	0.876	54.5	269.2	-247.86935	0.760	51.4	261.2		

[a] Total energies in Hartree, relative and zero-point energies in kcal/mol. Relative energies include the ZPVE. [b] ZPVE determined at MP2 scaled by 0.9646 [43]. [c] The superscript designates the state of the ylide i.e. singlet or triplet. [d] ZPVE corrections taken from MP2 data.

All four species, **1**, pyridine (**2**) and their respective radical cations are identified as genuine minima characterized by a positive definite Hessian matrix at the MP2 and

B3LYP levels of theory. Neutral pyridine is, of course, much more stable than the isomeric form **1**, the energy difference amounts to 50.2 and 46.8 kcal/mol at MP2/6-31G** and B3LYP/6-31G**, respectively. At the CASSCF-MP2 level, employing the harmonic frequencies as determined at the MP2 level for the ZPVE corrections, we obtain 49.0 kcal/mol for this quantity. The ground state of **1** is undoubtedly a ^{1}A' singlet, the lowest lying (^{3}A") triplet state is theoretically predicted to be 44.3 and 35.6 kcal/mol higher in energy at MP2 and B3LYP, respectively. It should be noted that the MP2 wave function for the ^{3}A" state is severely spin contaminated ($<S^2> = 2.395$) which renders the corresponding triplet energy a bit questionable. Indeed, the CASSCF-MP2 singlet-triplet gap is 36.4 kcal/mol, almost identical to the B3LYP result, but significantly smaller than the result obtained at the MP2 level. These computed energy differences are in line with the singlet-triplet gaps found for other amino carbenes i.e., 50 kcal/mol for amino carbene and 78 kcal/mol for imidazol-2-ylidene [14]. For the cations, the two isomers $\mathbf{1}^{\bullet+}$ (^{2}A') and $\mathbf{2}^{\bullet+}$ ($^2A_1$) are much closer in energy. At MP2 and CASSCF-MP2, the pyridine radical cation is less stable than $\mathbf{1}^{\bullet+}$ by 5.5 and 7.4 kcal/mol, while using our B3LYP results put $\mathbf{1}^{\bullet+}$ just 1 kcal/mol above $\mathbf{2}^{\bullet+}$. It should be noted that the latter stability order results only after inclusion of the ZPVE, the uncorrected total energies slightly favor $\mathbf{1}^{\bullet+}$ (by less than 1 kcal/mol). The relevant optimized geometry parameters of **1**, **2**, $\mathbf{1}^{\bullet+}$, and $\mathbf{2}^{\bullet+}$ are given in Table 2.3 along with the experimental data for neutral pyridine. Overall, all three methods (MP2, CASSCF, B3LYP) yield very similar equilibrium geometries, however, compared to the experimental structure of pyridine, the B3LYP and CASSCF procedures are very similar to each other and slighly outperform the MP2 approach. In spite of the constraint of the ring system, the singlet and the triplet of **1** have slightly different geometries. In particular the NCC bond angle is significantly larger in the triplet as compared to the singlet (ca. 115° versus ca. 110°). The angle in the radical cation $\mathbf{1}^{\bullet+}$, 124.6° (B3LYP), 126.1° (MP2), and 123.7° (CASSCF) is more similar to that of the triplet, which is consistent with the HOMO of the singlet being largely localized at the dicoordinate carbon atom. Compared to pyridine [49], there is thus a noticeable widening of this angle.

The structure of the saddle point for the intramolecular interconversion of the two isomeric forms is very similar at the B3LYP and MP2 levels of theory for the neutral rearrangement **TS1/2**. However, whereas the B3LYP structure is strictly planar and keeps C_s symmetry, at the MP2 level this saddle point adopts a C_1 symmetric structure in which the hydrogen atom migrates very slightly (0.3°) above the plane of the ring (Table 2.4).

Table 2.3. Selected calculated geometric parameters for **1**, $\mathbf{1}^{\bullet+}$, **2** and $\mathbf{2}^{\bullet+}$ at various levels of theory and employing the 6-31G** basis set.[a]

	1 (C_s)			$\mathbf{1}^{\bullet+}$ (C_s)		
Parameter	**B3LYP**	**MP2**	**CASSCF**	**B3LYP**	**MP2**	**CASSCF**
r(C_1N)	1.374	1.374	1.348	1.329	1.317	1.323
r(C_5N)	1.367	1.364	1.371	1.365	1.362	1.350
r(C_1C_2)	1.433	1.429	1.448	1.370	1.340	1.377
r(C_5C_4)	1.371	1.376	1.360	1.381	1.343	1.382
r(C_2C_3)	1.384	1.390	1.372	1.404	1.378	1.397
r(C_4C_3)	1.411	1.403	1.422	1.403	1.391	1.402
a(NC_1C_2)	109.8	109.1	110.6	124.6	126.1	123.7
a(NC_5C_4)	119.0	118.6	119.4	118.6	119.7	118.8
a($C_1C_2C_3$)	124.6	125.2	124.1	115.4	114.1	116.0
a($C_5C_4C_3$)	117.6	117.9	117.6	119.9	118.7	119.7

	2 (C_{2v})				$\mathbf{2}^{\bullet+}$ (C_{2v})		
Parameter	**B3LYP**	**MP2**	**CASSCF**	**exp.**	**B3LYP**	**MP2**	**CASSCF**
r(C_1N)	1.345	1.321	1.332	1.338	1.313	1.302	1.321
r(C_1C_2)	1.395	1.385	1.395	1.394	1.406	1.363	1.394
r(C_2C_3)	1.394	1.384	1.393	1.392	1.397	1.374	1.399
a(CNC)	116.7	117.7	117.6	116.9	132.5	131.3	132.3
a(NC_1C_2)	123.8	123.6	123.5	123.8	114.3	115.0	114.2
a($C_2C_3C_4$)	118.7	118.7	118.6	118.5	121.1	121.8	121.0

[a] Bond lengths in Å, angles in degrees.

However, the deviation from the C_s symmetry is so small that the MP2 **TS1/2** should certainly be looked at as *de facto* planar. The two methods also yield very similar barrier heights. Coming from 1 the 1,2-hydrogen shift via **TS1/2** requires just under 40 kcal/mol, 38.3 or 37.7 kcal/mol according to B3LYP or MP2, respectively. Interestingly, for the ionic transition state $\mathbf{TS1^{\bullet+}/2^{\bullet+}}$, the saddle point geometries turn out to be strongly method dependent as documented in Table 2.4. B3LYP predicts a non-planar, C_1 symmetric structure (dihedral angle H_1-C_1-N-C_5 = 129.8°), see Table 2.4. Using the MP2 scheme instead yields a planar, C_s symmetric transition structure (see Figure 3.2). We note in passing that the structure of $\mathbf{TS1^{\bullet+}/2^{\bullet+}}$ optimized at the Hartree-Fock level with a 6-31G** basis set very closely resembles the non-planar geometry obtained at B3LYP.

Table 2.4. Selected calculated geometric parameters for **TS1/2** and $\mathbf{TS1^{\bullet+}/2^{\bullet+}}$ at the B3LYP and MP2 levels of theory employing the 6-31G** basis set.[a]

	TS1/2		$\mathbf{TS1^{\bullet+}/2^{\bullet+}}$	
Parameter	**B3LYP**	**MP2**	**B3LYP**	**MP2**
$r(C_1N)$	1.387	1.391	1.305	1.265
$r(C_5N)$	1.350	1.353	1.368	1.356
$r(C_1C_2)$	1.410	1.412	1.395	1.352
$r(C_5C_4)$	1.384	1.384	1.386	1.333
$r(C_2C_3)$	1.391	1.392	1.395	1.366
$r(C_4C_3)$	1.407	1.404	1.415	1.405
$r(NH_1)$	1.175	1.164	1.300	1.254
$r(C_1H_1)$	1.360	1.365	1.309	1.360
$a(C_1NC_5)$	125.7	126.7	121.5	125.4
$a(NC_1C_2)$	116.0	115.0	127.0	127.1
$a(NC_5C_4)$	118.4	117.5	115.7	112.8
$a(C_1C_2C_3)$	119.8	120.3	112.1	109.1
$a(C_5C_4C_3)$	121.2	119.6	121.2	120.8
$a(C_1NH_1)$	63.5	64.0	60.3	65.3
$a(NC_1H_1)$	50.7	49.9	59.6	56.9
$d(H_1C_1NC_5)$	180.0	179.7	129.8	180.0

[a] Bond lengths in Å, angles in degrees.

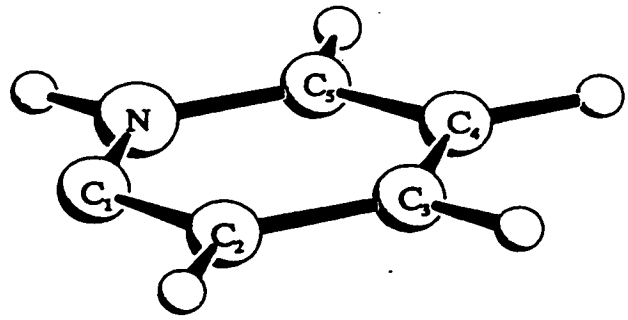

1 and $1^{\bullet+}$ (C_S)

B3LYP / $TS1^{\bullet+}/2^{\bullet+}$ (C_1)

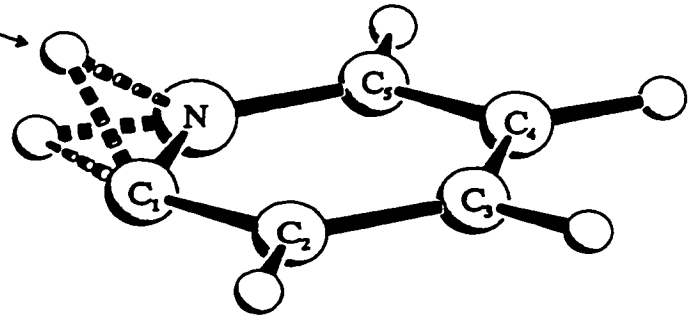

TS1/2 and $TS1^{\bullet+}/2^{\bullet+}$ (C_S)

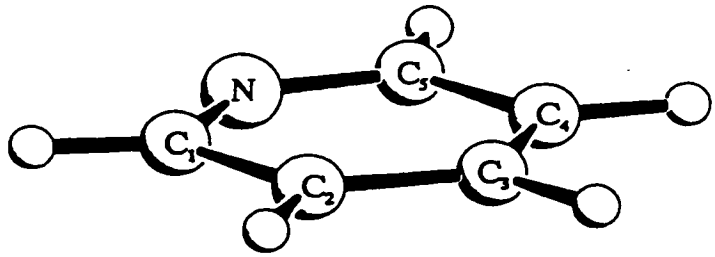

2 and $2^{\bullet+}$ (C_S)

Figure 2.3: Calculated structures of the investigated species (see also Tables 2.3 and 2.4).

Significant activation barriers, which again are similar for both methods, of 57.0 and 56.6 kcal/mol at B3LYP and MP2, respectively, with respect to the least stable $C_5H_5N^{\bullet+}$ isomer are connected with this saddle point. The minimum energy needed for fragmentation of $\mathbf{2}^{\bullet+}$ (which undoubtedly represents the lowest energy dissociation necessary for $\mathbf{1}^{\bullet+}$ as well) has been experimentally determined as 95.6 kcal/mol [50], so it should be possible for some internally excited ions to communicate below the dissociation threshold. This is consistent with the experimental observation that metastable ions $\mathbf{1}^{\bullet+}$ and $\mathbf{2}^{\bullet+}$ freely interconvert giving identical MI spectra whereas most of the ions sampled in the CID and NR/CID experiments reside below the isomerization barrier until activated by the collision, whereupon isomerization is able to occur for some species prior to their dissociation. Nevertheless, the species all have fairly deep energy wells, which should minimize the likelihood of isomerization in NRMS experiments, consistent with the observation of differentiable NR/CID mass spectra for the isomers.

Thermochemistry

A combination of experimental and theoretical approaches have been used to evaluate thermochemical data for species pertinent to the present study. It is not possible to obtain a reliable heat of formation for $\mathbf{1}^{\bullet+}$ using picolinic acid since the peak corresponding to the dissociation of metastable molecular ions is dish-shaped, which indicates that there is a substantial reverse energy term associated with the reaction. Fortunately, this is not the case for methylpicolinate, which shows narrow Gaussian shaped peaks for the successive losses of CH_2O and CO. Therefore, we have used the method of Burgers and Holmes [51] to measure the appearance energy (AE) of the $C_5H_5N^{\bullet+}$ ion produced from metastable methyl picolinate molecular ions (Scheme 2.1). The heat of formation of the precursor molecule, -57 kcal/mol, was estimated from the known ΔH_f of 2-methylpyridine (24 kcal/mol) and the difference between toluene (ΔH_f = 12 kcal/mol) and methyl benzoate (ΔH_f = -68 kcal/mol) under the assumption that there is no unusual effect upon substitution of $-CH_3$ by $-CO_2CH_3$ adjacent to the heteroatom. This

value and the measured AE of 10.14 eV, when combined with the known values for CH_2O (-26 kcal/mol) and CO (-26 kcal/mol), lead to $\Delta H_f(\mathbf{1}^{\bullet+}) = 237 \pm 5$ kcal/mol.

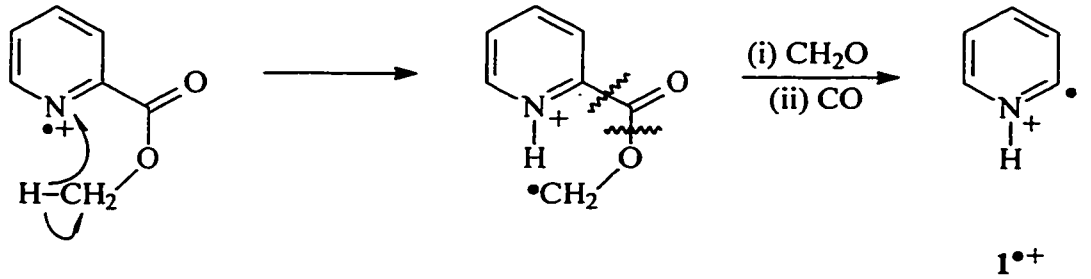

$\mathbf{1}^{\bullet+}$

Scheme 2.1: Generation of ionized pyridine-2-ylidene, $\mathbf{1}^{\bullet+}$, from methylpicolinate molecular ions.

It is also possible to evaluate the $\Delta H_f(\mathbf{1}^{\bullet+})$ from the computational data with reference to the heat of formation of pyridine, either from the differences between the two ions and the ionization energy (IE) of **2** or from the calculated difference between the two neutrals and IE(**1**). Using the former route and $\Delta H_f(\mathbf{2}^{\bullet+})$ = 246 kcal/mol, from the experimental $\Delta H_f(\mathbf{2})$ = 33 kcal/mol and the well established IE(**2**) = 9.25 eV, together with the calculated energy difference between $\mathbf{1}^{\bullet+}$ and $\mathbf{2}^{\bullet+}$, 5.5 (MP2) and 7.4 kcal/mol (CASSCF-MP2), leads to $\Delta H_f(\mathbf{1}^{\bullet+})$ = 240 and 239 kcal/mol, respectively, in excellent agreement with experiment. Employing the B3LYP difference between $\mathbf{1}^{\bullet+}$ and $\mathbf{2}^{\bullet+}$ (1 kcal/mol in favor of $\mathbf{2}^{\bullet+}$) leads to a slightly less satisfactory result of $\Delta H_f(\mathbf{1}^{\bullet+})$ = 247 kcal/mol. Using MP2 or CASSCF-MP2 the calculated adiabatic IEs(**2**) = 9.23 and 9.38 eV are close to the experimental value. On the other hand, at the B3LYP level of theory the IE(**2**) is slightly underestimated, 8.81eV. However, the adiabatic IE(**1**) is essentially the same i.e., 6.81, 6.93 or 6.83 eV, for the three methods, MP2, CASSCF-MP2 and B3LYP, respectively. Since this is the case and the enthalpy difference between **1** and **2** is also quite close for these methods, 50, 49 or 47 kcal/mol, a consistent value for $\Delta H_f(\mathbf{1}^{\bullet+})$ = 237-242 kcal/mol can be derived from these data. The consistency between these

methods and the similarity with the experimentally measured values gives us confidence in the proposed value $\Delta H_f(\mathbf{1}^{\bullet+}) = 237 \pm 5$ kcal/mol.

The energy difference between the two neutrals can be combined with ΔH_f ($C_5H_5NH^+$) = 178 kcal/mol, determined from the proton affinity of pyridine [52], PA(**2**) = 221 kcal/mol, to yield an estimate for PA(**1**) ≅ 270 kcal/mol [53]. This value is even higher than the one predicted for the imidazoline carbene and thus would be one of the largest for a simple organic molecule [13,52].

Finally, the high barriers to isomerization indicated by the computational and experimental results point to the possibility of directly observing **1** in the condensed phase under appropriate conditions i.e. by low temperature matrix isolation.

References

[1] J.U. Nef, *Liebigs Ann. Chem.* **1895**, *287*, 359.

[2] a) C. Wentrup, *Reaktive Zwischenstufen*, Georg Thieme Verlag, Stuttgart, **1979**.
b) W. Kirmse, *Carbene Chemistry*, 2nd. Ed., Academic Press, New York, **1971**.

[3] R.A. Moss, *Acc. Chem. Res.* **1989**, *22*, 15.

[4] a) A.J. Arduengo III, S.F. Gamper, M. Tamm, J.C. Calabrese, F. Davidson and H.A. Craig, *J. Am. Chem. Soc.* **1995**, *117*, 572.
b) A.J. Arduengo III, D.A. Dixon, K.K. Kumashiro, C. Lee, W.P. Power, and K.W. Zilm, *J. Am. Chem. Soc.* **1994**, *116*, 6361.
c) A.J. Arduengo III, H.V.R. Dias, D.A. Dixon, R.L. Harlow, W.T. Klooster and T.F. Koetzle, *J. Am. Chem. Soc.* **1994**, *116*, 6812.

[5] For two recent reports see: a) A. Ghosh, *Angew. Chem.* **1995**, *107*, 1117.
b) D. Enders, K. Breuer, G. Raabe, J. Runsink, J.H. Teles, J.-P. Melder, K. Ebel and S. Brode, *Angew. Chem.* **1995**, *107*, 1119.

[6] H.-W. Wanzlick, *Angew. Chem.* **1962**, *74*, 129.

[7] W.M. Jones and C.L. Ennis, *J. Am. Chem. Soc.* **1967**, *89*, 3069.

[8] R. Gleiter and R. Hoffman, *J. Am. Chem. Soc.* **1968**, *90*, 5457.

[9] a) P. Dyson and D.L. Hammick, *J. Chem. Soc.* **1937**, 1724.

b) M.R.F. Ashworth, R.P. Daffern and D.L. Hammick, *J. Chem. Soc.* **1937**, 809.

[10] a) H. Quast and E. Frankenfeld, *Angew. Chem.* **1965**, *77*, 680.

b) P. Haake and J. Mantecon, *J. Am. Chem. Soc.* **1964**, *86*, 5230.

[11] B. Bohn, N. Heinrich and H. Vorbrüggen, *Heterocycles* **1994**, *37*, 1731.

[12] R. Breslow, *J. Am. Chem. Soc.* **1958**, *80*, 3719.

[13] a) D.A. Dixon and A.J. Arduengo, *J. Phys. Chem.* **1991**, *95*, 4180.

b) R.W. Alder, P.R. Allen and S.J. Williams, *J. Chem. Soc., Chem. Commun.* **1995**, 1267.

c) J. Cioslowski, *Int. J. Quant. Chem., Quant. Chem. Symp.* **1993**, *27*, 309.

[14] a) C. Heinemann, T. Müller, Y. Apeloig and H. Schwarz, *J. Am. Chem. Soc.* **1995**, *118*, 2023.

b) C. Boehme and G. Frenking, *J. Am. Chem. Soc.* **1996**, *118*, 2039.

c) A.J. Arduengo III, H. Bock, H. Chen, M. Denk, D.A. Dixon, J.C. Green, W.A. Herrmann, N.L. Jones, M. Wagner and R. West, *J. Am. Chem. Soc.* **1994**, *116*, 6641.

d) C. Heinemann and W. Thiel, *Chem. Phys. Letters* **1994**, *217*, 11.

[15] a) H.-W. Wanzlick, and E. Schikora, *Angew. Chem.* **1960**, *72*, 494.

b) H.-W. Wanzlick, *Angew. Chem., Int. Ed. Engl.* **1962**, *1*, 75.

c) D.M. Lemal and K.I. Kawano, *J. Am. Chem. Soc.* **1962**, *84*, 1761.

d) D.M. Lemal, R.A. Lovald and K.I. Kawano, *J. Am. Chem. Soc.* **1964**, *86*, 2518.

e) H.J. Schönherr, PhD Thesis, Technische Universität Berlin, D83, 1970.

f) H.J. Schönherr, and H.-W. Wanzlick, *Chem. Ber.* **1970**, *103*, 1037.

[16] a) M. Denk, J.C. Green, N. Metzler and M. Wagner, *J. Chem. Soc., Dalton Trans.* **1994**, 2405.

b) M. Denk, R. Lennon, R. Hayashi, R. West, A.V. Belyakov, H.P. Verne, A. Haaland, M. Wagner and N. Metzler, *J. Am. Chem. Soc.* **1994**, *116*, 2691.

[17] A. Igau, H. Grützmacher, A. Baceiredo and G. Bertrand, *J. Am. Chem. Soc.* **1988**, *110*, 6463.

[18] Recent reviews: a) N. Goldberg and H. Schwarz, *Acc. Chem. Res.* **1994**, *27*, 347.

b) F.W. McLafferty, *Int. J. Mass Spectrom. Ion Processes* **1992**, *118/119*, 211.

[19] G.A. McGibbon, C.A. Kingsmill and J.K. Terlouw, *Chem. Phys. Letters* **1994**, *222*, 129.

[20] a) G.A. McGibbon, P.C. Burgers and J.K. Terlouw, *Int. J. Mass Spectrom. Ion Processes* **1994**, *136*, 191.

b) C.E.C.A. Hop, H. Chen, P.J.A. Ruttink and J.L. Holmes, *Org. Mass Spectrom.* **1991**,*26*, 697.

c) G. Schaftenaar, R. Postma, P.J.A. Ruttink, P.C. Burgers, G.A. McGibbon and J.K. Terlouw, *Int. J. Mass Spectrom. Ion Processes* **1990**, *100*, 521.

[21] C. Wesdemiotis and F.W. McLafferty, *J. Am. Chem. Soc.* **1987**, *109*, 4760.

[22] D. Sülzle, T. Drewello, B.L.M. van Baar and H. Schwarz, *J. Am. Chem. Soc.* **1988**, *110*, 8330.

[23] a) R. Feng, C. Wesdemiotis and F.W. McLafferty, *J. Am. Chem. Soc.* **1987**, *109*, 6521.

b) W.J. Bouma, P.C. Burgers, J.L. Holmes and L. Radom, *J. Am. Chem. Soc.* **1986**, *108*, 1767.

[24] N. Goldberg, A. Fiedler and H. Schwarz, *Helv. Chem. Acta* **1994**, *77*, 2354.

[25] N. Goldberg, M. Iraqi and H. Schwarz, *Chem. Ber.* **1993**, *126*, 2353.

[26] P.H. Chen, *J. Org. Chem.* **1976**, *41*, 2973.

[27] R. Grigg, L. Wallace and J.O. Morley, *J. Chem. Soc., Perkin Trans. 2* **1990**, 51.

[28] L. Nyulaszi, D. Szieberth and T. Veszpremi, *8th International Congress of Quantum Chemistry*, Prague, June 19-23, **1994**.

[29] K.L. Busch, G.L. Glish and S.A. McLuckey, *Mass Spectrometry/Mass Spectrometry, Techniques and Applications of Tandem Mass Spectrometry*; VCH, New York, **1988**.

[30] J.H. Beynon, J.A. Hopkinson and G.R. Lester, *Int. J. Mass Spectrom. Ion Proc.* **1969**, *2*, 291.

[31] a) P.C. Burgers, J.L. Holmes and J.K. Terlouw, *J. Am. Chem. Soc.* **1984**, *106*, 2762.

b) P.C. Burgers, J.K. Terlouw, T. Weiske and H. Schwarz, *Chem. Phys. Lett.* **1986**, *132*, 69.

[32] a) P.C. Burgers, G.A. McGibbon and J.K. Terlouw, *Chem. Phys. Lett.* **1994**, *224*, 539.

b) F.A. Wiedmann, J. Cai and C. Wesdemiotis, *Rapid Commun. Mass Spectrom.* **1994**, *8*, 804.

[33] D. Schröder, J. Müller and H. Schwarz, *Organometallics* **1993**, *12*, 1972.

[34] BDE (C-H) = 134 kcal/mol according to data in S.G. Lias, J.E. Bartmess, J.F. Liebman, J.L. Holmes and R.D. Levin, *J. Phys. Chem. Ref. Data* **1988**, *17*, Suppl. 1.

[35] *Gaussian 94* (Revision B.2), M.J. Frisch, G.W. Trucks, H.B. Schlegel, P.M.W. Gill, B.G. Johnson, M.A. Robb, J.R. Cheeseman, T.A. Keith, G.A. Petersson, J.A. Montgomery, K. Raghavachari, J.B. Foresman, J. Cioslowski, B.B. Stefanov, A. Nanayakkara, M. Challacombe, C.Y. Peng, P.Y. Ayala, W. Chen, M.W. Wong, J.L. Andres, E.S. Replogle,

R. Gomperts, R.L. Martin, D.J. Fox, J.S. Binkley, D.J. DeFrees, J. Baker, J.J.P. Stewart, M. Head-Gordon, C. Gonzalez and J.A. Pople, Gaussian, Inc., Pittsburgh PA, **1995**.

[36] For a complete review on these techniques, see: W.J. Hehre, L. Radom, P.v.R. Schleyer and J.A. Pople, *Ab Initio Molecular Theory*; Wiley Interscience, New York, **1986**.

[37] W. Chen, and H.B. Schlegel, *J. Chem. Phys.* **1994**, *101*, 5957.

[38] For a review on the CASSCF scheme see: B.O. Róos, In Lecture Notes in Quantum Chemistry; B.O. Roos, Springer, Berlin, **1992**.

[39] J.J.W. McDouall, K. Peasley and M.A. Robb, *Chem. Phys. Lett.* **1988**, *148*, 183.

[40] R.G. Parr and W. Yang, *Density Functional Theory of Atoms and Molecules*, Oxford University Press, Oxford, **1989**.

[41] a) A.D. Becke, *J. Chem. Phys.* **1993**, *98*, 1372.
b) A.D. Becke, *J. Chem. Phys.* **1993**, *98*, 5648.

[42] P.J. Stephens, F.J. Devlin, C.F. Chabalowski and M.J. Frisch, *J. Phys. Chem.* **1994**, *98*, 11623.

[43] J.A. Pople, P.A. Scott, M.W. Wong and L. Radom, *Isr. J. Chem.* **1993**, *33*, 345.

[44] C.J. Emmanuel and P.B. Shelvin, *J. Am. Chem. Soc.* **1994**, *116*, 5991.

[45] a) G.F. Tantardini and M. Simonetta, *Int. J. Quant. Chem.* **1981**, *20*, 705.
b) I.C. Walker, M.H. Palmer and A. Hopkirk, *Chem. Phys.* **1990**, *141*, 365.
c) H. Nakano, T. Nakajima and S. Obara, *Chem. Phys. Lett.* **1991**, *177*, 458.
d) J.B. Foresman, M. Head-Gordon, J.A. Pople and M.J. Frisch, *J. Phys. Chem.* **1992**, *96*, 135.
e) M.P. Fulscher, K. Andersson and B.O. Roos, *J. Phys. Chem.* **1992**, *96*, 9204.

[46] See, for instance : J.F. Liebman and J. Simons, In *Molecular Structure and Energetics*, J.F. Liebman, A. Greenberg, Eds., VCH: Deerfield Beach, FL, **1986**; Vol 1.

[47] Due to the loss of symmetry in the saddle points and the importance of the C-H and N-H bonds being formed or broken in the rearrangement processes, no straightforward selection of an active space, which is consistent with the description of the minima and at the time still manageable computationally, was possible. We therefore limited our CASSCF/MP2 calculations to minima.

[48] J. Baker, A. Scheiner and A. Andzelm, *Chem. Phys. Lett.* **1993**, *216*, 380.

[49] D. Spitzner, In *Houben-Weyl*, Band E7b, Teil 2, Georg Thieme Verlag, Stuttgart, Germany **1992**, p. 286.

[50] C. Lifshitz, *J. Phys. Chem.* **1982**, *86*, 606.

[51] P.C. Burgers and J.L. Holmes, *Org. Mass Spectrom.* **1982**, *17*, 123.

[52] S.G. Lias, J.F. Liebman and R.D. Levin, *J. Phys. Chem. Ref. Data* **1984**, *13*, 695.

[53] A purely calculated PA needs to be corrected for ZPVE and thermodynamic contributions (entropy). D.A. Dixon, and S.G. Lias, In *Molecular Structure and Energetics*; J.F. Liebman and A. Greenberg (eds.), VCH, Deerfield Beach, FL, **1987**; Vol 2, Chapter 7, p. 269.

CHAPTER 3

The Generation of Neutral and Cationic Hydrogen Shift Isomers of Pyridine. A Combined Experimental and Computational Investigation

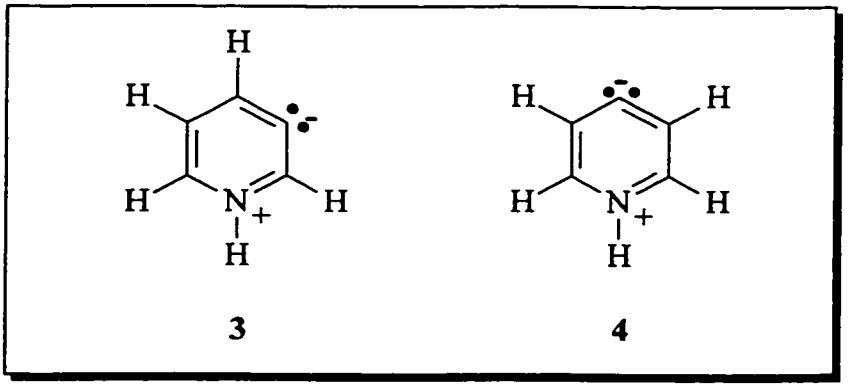

3 4

In this Chapter a second C_5H_5N isomer, azacyclohexatriene-3-ylidene (**3**), has been identified using the experimental approach outlined in Chapter 2. Quantum chemical calculations have also been used to further probe the C_5H_5N and $C_5H_5N^{\bullet+}$ potential energy surfaces (PESs). From this examination of the PESs a third stable isomer, azacyclohexatriene-4-ylidene, **4**, and its radical cation $\mathbf{4}^{\bullet+}$ are shown to be stable entities in the gas phase. However, our experimental investigation was limited only to the ionic species $\mathbf{4}^{\bullet+}$ since an appropriate precursor molecule for the neutral, **4**, could not be realized.

The work described here has been previously published in an article under the same title: D.J. Lavorato, J.K. Terlouw, G.A. McGibbon, T.K. Dargel, W. Koch and H. Schwarz, Int. J. Mass Spectrom. Ion Processes, 1998, 179/180, 7-14.

Introduction

There are many simple molecules that have been studied by computational methods sufficiently often and thoroughly enough that they take on an aura of familiarity but nevertheless still manage to elude experimental observation. Among the most famous of these is OCCO [1], while other candidates for such reactive intermediates are carbenes whose generation and identification has received a great deal of attention over the past decades [2,3]. A case in point concerns the hydrogen-shift isomers **1**, **3** and **4** of pyridine (**2**). The 2-isomer of pyridine, i.e. azacyclohexatriene-2-ylidene (**1**) has been postulated to exist more than 60 years ago by Hammick and co-workers [4,5]; however, unequivocal evidence for its gas phase existence has been presented only recently [6]. While there is neither experimental nor theoretical support in favour of **4**, convincing data for the intermediary formation of **3** in the reaction of gaseous atomic carbon with pyrrole was recently obtained [7]; however, very facile intermolecular isomerization **3** $\rightarrow$ **1** $\rightarrow$ **2** is operative in solution [7,8].

Quite clearly, despite the enormous progress made in the study of these elusive species in condensed phases, there are often advantages, especially for molecules that are susceptible to intermolecular isomerizations (or dimerization), to conduct investigations under high vacuum conditions in the gas phase where intermolecular reactions are virtually absent. Mass spectrometric experiments often provide an opportunity and following the introduction of neutralization-reionization mass spectrometry (NRMS) [9-12], the technique has proved valuable in generating a great variety of remarkable molecules, including several carbenes, e.g. **1** [6], $H_2N\text{-}\ddot{C}\text{-}NH_2$ [13], $H_2N\text{-}\ddot{C}\text{-}OH$ [14-16], $H_3C\text{-}\ddot{C}\text{-}OH$ [17], $F\text{-}\ddot{C}\text{-}OH$ [18], $H\text{-}\ddot{C}\text{-}OH$ [19,20], that are expected to have only a fleeting existence in solution. In addition, the often invoked and long-sought after cyclic heterocarbenes, i.e. 2,3-dihydrothiazole-2-ylidene [21] and imidazol-2-ylidene [22], were generated by one-electron reduction of their corresponding radical cations and characterized by NRMS in conjunction with electronic structure calculations.

Inspired by these findings, we set out to generate and identify the elusive carbene

3, using the combined experimental (NRMS) and computational methodology described in detail in the previous Chapter. This strategy to combine ingenious experimental techniques with powerful computational methods is of particular importance in cases where the spectra of the various species differs only in subtle details. If this experimental information is not backed up by other independent pieces of evidence, it may not suffice for an unequivocal identification of structurally distinct distonic ions. However, if these experimental data is complemented with high-quality calculations, reliable conclusions regarding the system at hand can be drawn.

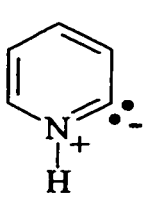

1

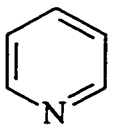

2

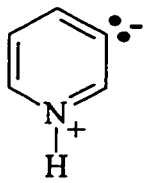

3

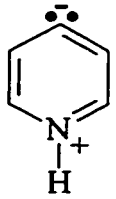

4

Theoretical Methods

The computational determinations of the structures and harmonic frequencies were performed on IBM/RS6000 workstations using the Gaussian94 program package [23]. The popular B3LYP hybrid density functional theory (DFT) [24] option employing Becke's [25] empirical three-parameter fit for mixing HF and DFT exchange-energy terms as implemented [26] in Gaussian94 was combined with the standard 6-31G** basis set [27], which includes d- and p-type polarization functions on non-hydrogen and hydrogen atoms, respectively. All relative energies were corrected for zero-point vibrational energy (ZPVE) contributions. No scaling was performed for the B3LYP fundamentals. Open shell species were treated in the unrestricted Kohn-Sham scheme. The $<S^2>$ expectation values of the non-interacting Kohn-Sham determinant did not exceed 2.037 for the triplet states (exact value = 2.00) and 0.771 for the doublet states (exact value = 0.75). The only species where a larger spin contamination occurred was **TS1**$^{\bullet+}$/**2**$^{\bullet+}$ where $<S^2>$ amounts to 0.876. Improved relative energies based on these optimized structures were obtained by

using the coupled cluster ansatz with single and double excitations and a perturbative estimation of the triple excitations (CCSD(T)) [28-30] to account for the effects of valence electron correlation. For these calculations the MolPro96.4 computer program [31] implemented on a Cray J90 computer at the Konrad-Zuse Zentrum für Informationstechnik, Berlin, was employed. The CCSD(T) method was combined with a more flexible, generally contracted basis set of the atomic natural orbital type [32] (ANO) of polarized triple zeta quality (H: [7s3p]/(3s2p), N, C: [10s6p3d]/(4s3p2d)) [33]. Thus, the final basis set, which will be termed ANO-TZP in the following, consists of 356 primitive gaussians and 183 contractions. For the open shell species, the CCSD(T) calculations were based on ROHF wave functions, as implemented in MolPro96.4 [31]. The CCSD(T)/ANO-TZP relative energies are corrected for ZPVE contributions by using the harmonic fundamentals as obtained at the B3LYP/6-31G** level of theory.

Results and Discussion

Mass Spectrometry.

The proper identification of neutral species by NRMS requires that one can unambiguously establish the parent ion structure. As shown earlier [6], this search was quite brief and successful for the isomeric ions $\mathbf{1}^{\bullet+}$ and $\mathbf{2}^{\bullet+}$. The molecular ion $\mathbf{2}^{\bullet+}$ is undoubtedly generated by electron ionization of **2** while carbene ion $\mathbf{1}^{\bullet+}$ is accessible by consecutive loss of CH_2O and CO from ionized methyl picolinate. Based on labelling experiments, kinetic energy release analyses and collision-induced dissociation studies both isomers are clearly distinguishable. Of particular importance were the minor but structure-indicative differences in the CID mass spectra. The most critical of these are the m/z 28 : 26 ratio and the doubly-charged ion intensities. In the comparison of $\mathbf{1}^{\bullet+}$ and $\mathbf{2}^{\bullet+}$, only $\mathbf{1}^{\bullet+}$ possesses a hydrogen on the nitrogen atom. It should thus be able to produce the m/z 28 ion ($HCNH^+$) [34,35] more easily than $\mathbf{2}^{\bullet+}$, whereas both isomers can give m/z 26 fragments ($C_2H_2^{\bullet+}$ and CN^+). Further, in the CID mass spectrum of $C_5H_4DN^{\bullet+}$ (m/z 80) generated from ionized d_3-methyl picolinate, the m/z 28 signal is also shifted to m/z 29

($HCND^+$). These features were also preserved in the NR/CID spectra of $\mathbf{1}^{\bullet+}$, $\mathbf{2}^{\bullet+}$ and the N-D labelled isotopologue of $\mathbf{1}^{\bullet+}$ thus demonstrating that irrespective of their charge states the two isomers do not easily interconvert, as predicted by extensive electronic structure calculations [6].

For the isomer in question $\mathbf{3}^{\bullet+}$ a related strategy was pursued. Upon electron ionization (EI), methyl-2-carboxypyridine-3-carboxylate, **I**, [36] undergoes consecutive loss of CO_2, CH_2O and CO (Scheme 3.1); the resulting m/z 79 ions may well have the ionized 3-ylidene structure $\mathbf{3}^{\bullet+}$ desired for the NR experiment. To verify the isomeric purity of the putative distonic ion $\mathbf{3}^{\bullet+}$ generated from $\mathbf{I}^{\bullet+}$, these ions were independently produced by the reaction sequence shown in Scheme 3.1, that is from ion-source generated protonated 3-chloropyridine $\mathbf{II}^+$ (chemical ionization (CI) of **II** with methanol); ions m/z 114 were mass-selected and subsequently collisonally decomposed in the second field-free region (2ffr). The isomeric γ-distonic ion $\mathbf{4}^{\bullet+}$ was prepared analogously, i.e. via protonation of 4-chloropyridine **III**. Unfortunately, no suitable precursor molecule could be found to generate ion $\mathbf{4}^{\bullet+}$ by EI, and therefore its neutral counterpart could not be studied by NRMS using the ZAB-R.

As argued before [6], a distinction of ionized pyridine $\mathbf{2}^{\bullet+}$ from its isomer $\mathbf{1}^{\bullet+}$ is readily available on the basis of the m/z 28 : 26 intensity ratio in their CID mass spectra. Items (a) and (b) in Figure 3.1 represent the structure-diagnostic portions of the CID mass spectra of $\mathbf{1}^{\bullet+}$ and $\mathbf{2}^{\bullet+}$, respectively. As reported earlier, isomer $\mathbf{1}^{\bullet+}$ is characterized by a m/z 28 : 26 peak intensity ratio of 0.86 ± 0.03, whereas fewer $HCNH^+$ ions at m/z 28 are generated from $\mathbf{2}^{\bullet+}$ (intensity ratio 0.41 ± 0.03). Note, that the CID spectra also show intensity ratio differences in the m/z 37 - 39 region and that the ylide ion $\mathbf{1}^{\bullet+}$ features a pronounced doubly-charged ion of m/z 39.5 that is virtually absent in the CID mass spectrum of ionized pyridine $\mathbf{2}^{\bullet+}$.

Items (c) and (d) represent the structure diagnostic portions of the CID spectra of the isomeric m/z 79 $C_5H_5N^{\bullet+}$ ions of putative structure $\mathbf{3}^{\bullet+}$ generated from **I** and **II** respectively, as depicted in Scheme 3.1. The two spectra are the same within

experimental error and their m/z 28 : 26 ratio, 1.99 ± 0.04, is characteristically different from that of both $\mathbf{1}^{\bullet+}$ and $\mathbf{2}^{\bullet+}$, attesting to the generation of the β-distonic ion $\mathbf{3}^{\bullet+}$.

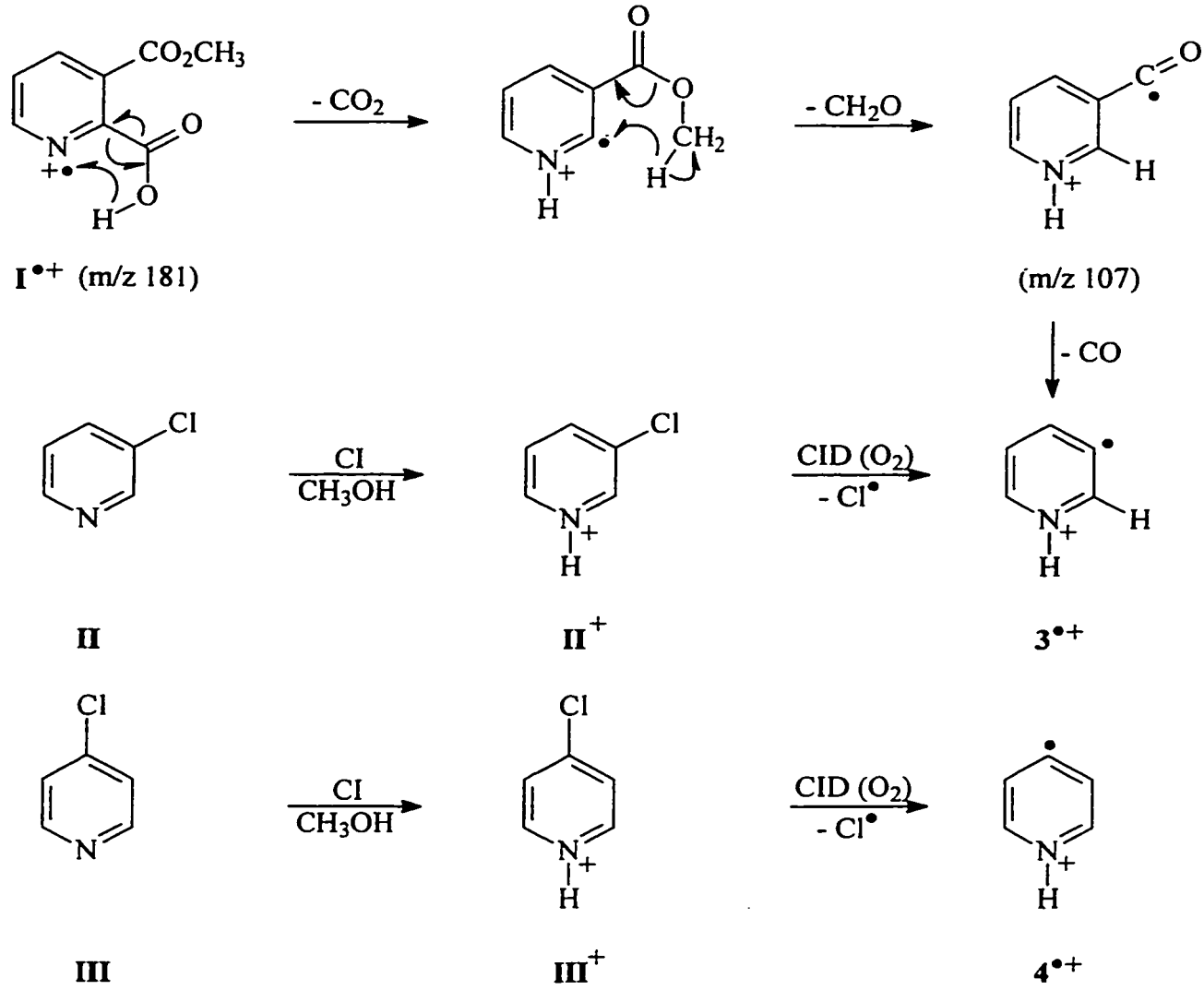

Scheme 3.1

In agreement with this proposal, the CID mass spectrum of the m/z 80 $C_5H_4DN^{\bullet+}$ ions from the OD labelled isotopomer of the ionized ester **I** shows a clean shift of the m/z 28 $HCNH^+$ signal to m/z 29, $HCND^+$. That the β-distonic ions generated by the pathways depicted in Scheme 3.1 are isomerically "pure" is further attested by the observation that

the m/z 79 $C_5N_5N^{\bullet+}$ ions generated by the loss of CO from the low energy (metastable) m/z 107 ions (see Scheme 3.1) yield essentially the same m/z 28 : m/z 26 ratio, 2.02 ± 0.03 (after correcting for the substantial ^{13}C contribution from the transition m/z $106^+ \rightarrow$ m/z 78^+ + CO; result not shown).

The partial mass spectrum of the remaining hydrogen shift isomer of ionized pyridine, i.e. $\mathbf{4}^{\bullet+}$, is shown in Figure 3.1 as item (e). This spectrum exhibits the largest m/z 28 : m/z 26 ratio, 2.27 ± 0.03, and it also features m/z 37 (C_3H^+) as the most prominent peak in the m/z 37 - m/z 39 cluster of ions. Considering the results of our theoretical calculations on the ions - see Table 3.1 which summarizes our computational findings for the ions $\mathbf{1}^{\bullet+}$ - $\mathbf{4}^{\bullet+}$, their neutral counterparts **1** - **4** and the isomerization barriers separating the various species - it is seen (i) that all four isomeric ions have closely similar stabilities, and (ii) that the barriers separating the ionic isomers are uniformly high, 50 - 60 kcal/mol. This reinforces our conclusion that the β-distonic ions $\mathbf{3}^{\bullet+}$ are isomerically pure and also that the γ-distonic ions $\mathbf{4}^{\bullet+}$, whose CID mass spectrum is fairly close to that of $\mathbf{3}^{\bullet+}$, do not effectively communicate with the β-distonic ion $\mathbf{3}^{\bullet+}$.

One-electron reduction of the 6 keV β-distonic ion $\mathbf{3}^{\bullet+}$ from $\mathbf{I}^{\bullet+}$ by neutralization with N,N-dimethylaniline [6] followed by reionization with O_2 yields a NR mass spectrum dominated by a survivor ion at m/z 79. These ions were selectively transmitted to the 3ffr and subjected to CID using O_2. The resulting survivor CID mass spectrum is given as item (f) in Figure 3.1 and its close similarity with the CID mass spectra of the ions $\mathbf{3}^{\bullet+}$ (items (c) and (d)) leaves little doubt that the majority of neutralized ions $\mathbf{3}^{\bullet+}$ have retained their structural integrity and thus that pyridine-3-ylidene **3** is indeed a stable species in the gas phase. This conclusion is fully corroborated by the calculations (see Table 3.1).

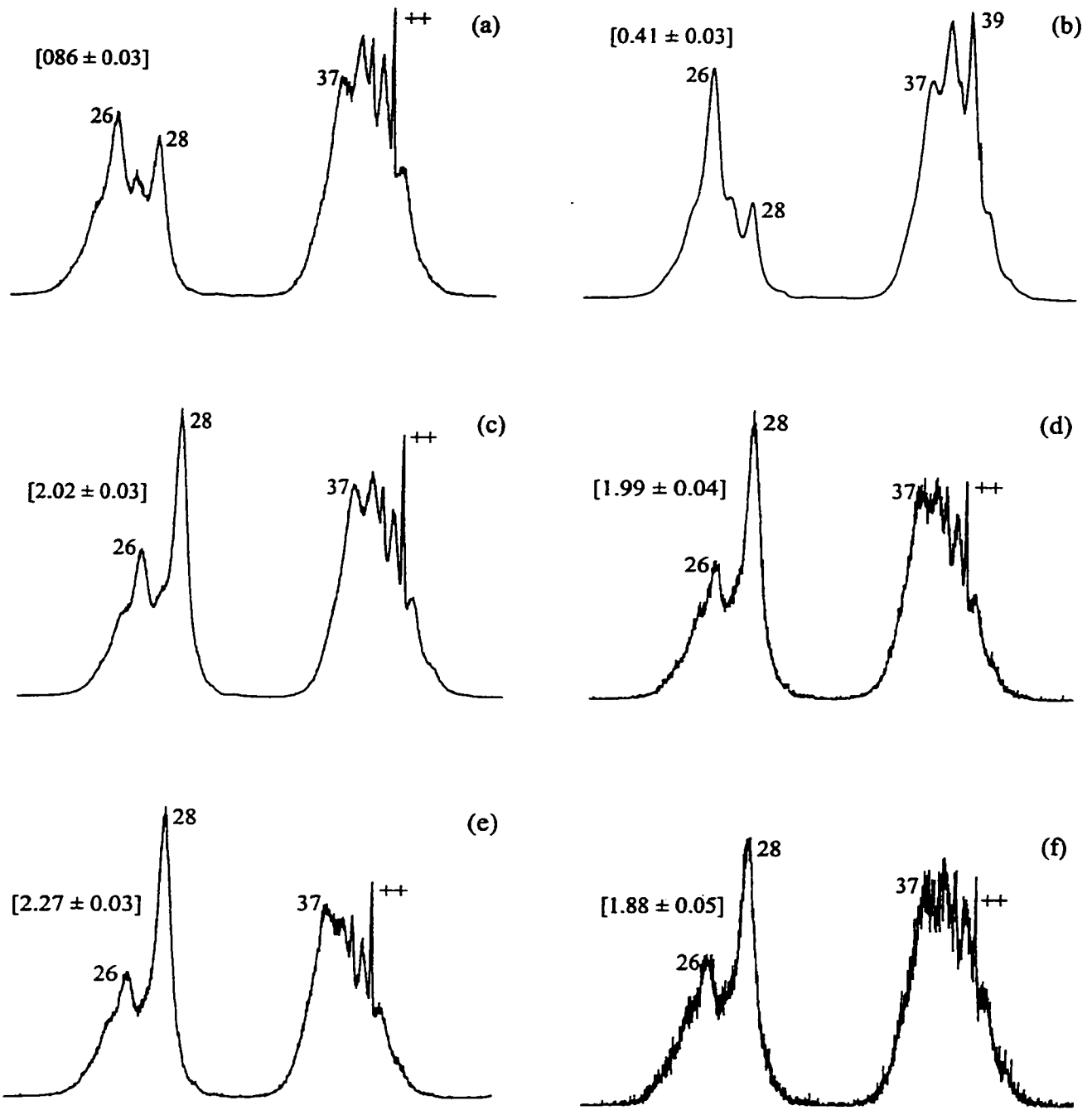

Figure 3.1: Partial CID mass spectra of ionized pyridine and its hydrogen shift isomers : (a) ionized pyridine-2-ylidene, $\mathbf{1}^{\bullet+}$; (b) ionized pyridine, $\mathbf{2}^{\bullet+}$; (c) and (d) ionized pyridine-3-ylidene, $\mathbf{1}^{\bullet+}$, generated from $\mathbf{I}^{\bullet+}$ and $\mathbf{II}^{+}$, respectively (see Scheme 3.1); (e) ionized pyridine-4-ylidene, $\mathbf{4}^{\bullet+}$; (f) NR/CID mass spectrum of the survivor ions from $\mathbf{3}^{\bullet+}$ (see text).

Computations.

In view of the previous detailed discussion of the potential energy surfaces (PESs) of **1**, $\mathbf{1}^{\bullet+}$, **2** and $\mathbf{2}^{\bullet+}$ in Chapter 2 and of related theoretical work on the C_5H_5N-PES [7] as well as for ionized pyridine $\mathbf{2}^{\bullet+}$ [37-41], a brief presentation of our present theoretical findings (summarized in Table 3.1 and Figure 3.2) will suffice. First of all, note that the B3LYP/6-31G** and CCSD(T)/ANO-TZP energetic data are generally in good agreement. The largest deviation amounts to approximately 7 kcal/mol. The quality of the results can be assessed by a comparison of the experimentally well known adiabatic ionization energy of pyridine (**2**) of 214.9 kcal/mol with the corresponding value predicted at CCSD(T)/ANO-TZP and B3LYP/6-31G** of 210.0 and 203.7 kcal/mol, respectively. Similarly, the experimental T_0 for the $^1A_1 \rightarrow {}^3B_1$ excitation of 84.8 kcal/mol is well reproduced at CCSD(T)/ANO-TZP (84.0 kcal/mol), while the B3LYP/6-31G** result is slightly smaller (81.8 kcal/mol). It is a general trend that the singlet/triplet excitation energies as well as the ionization energies are consistently larger by approximately 3-4 and 7 kcal/mol, respectively, at the CCSD(T)/ANO-TZP level as compared to B3LYP/6-31G**.

For neutral, singlet C_5H_5N, pyridine **2** is by far the most stable species, followed by **1** (43.4 kcal/mol, CCSD(T)). The isomers **3** and **4** are higher still, almost 60 kcal/mol above **2**. However, significant activation barriers hinder the unimolecular, spontaneous isomerization into pyridine. The lowest of these barriers is between **1** and **2** and is still more than 40 kcal/mol above **1**. For the triplets and the cationic (S = 1/2) species, there is no isomer with a comparably unique energetical advantage as pyridine for the neutral singlets. All four isomers, i.e. the triplets of **1** - **4** and the radical cations $\mathbf{1}^{\bullet+}$ - $\mathbf{4}^{\bullet+}$, are almost isoenergetic, their relative stabilities differ by not more than 1.4 and 4.9 kcal/mol for the neutral triplets and the cationic doublets, respectively. The same applies to the barriers for the respective 1,2-hydrogen migrations. They are all of comparable height, between 50 and 60 kcal/mol on both PESs. Further, we note that on all three PESs, **1** - **4** are genuine minima with positive definite Hessian matrices.

Table 3.1. Calculated energies for selected C_5H_5N neutrals, radical cations and transition structures for 1,2-hydrogen migrations.

		E_{rel} [kcal/mol][a]	
Species	ZVPE [kcal/mol]	B3LYP/6-31G**	CCSD(T)/ANO-TZP
1 (singlet)	55.6	46.8	43.4
TS **1/2** (singlet)	51.3	85.1	85.5
2 (singlet)	55.8	0.0[b]	0.0[c]
TS **1/3** (singlet)	51.3	120.2	118.6
3 (singlet)	54.8	61.2	57.8
TS **3/4** (singlet)	51.3	127.5	126.6
4 (singlet)	55.1	63.1	59.6
1 (triplet)	53.3	82.4	83.5
TS **1/2** (triplet)	49.4	133.8	135.7
2 (triplet)	52.3	81.8	84.0
TS **1/3** (triplet)	49.9	131.9	136.3
3 (triplet)	52.7	81.6	82.9
TS **3/4** (triplet)	49.7	138.9	141.6
4 (triplet)	53.4	81.9	82.6
$\mathbf{1}^{\bullet+}$	56.1	204.2	208.1
TS $\mathbf{1}^{\bullet+}/\mathbf{2}^{\bullet+}$	54.5	264.3	271.3
$\mathbf{2}^{\bullet+}$	54.2	203.1	210.0
TS $\mathbf{1}^{\bullet+}/\mathbf{3}^{\bullet+}$	52.0	271.4	277.3
$\mathbf{3}^{\bullet+}$	56.3	203.5	207.4
TS $\mathbf{3}^{\bullet+}/\mathbf{4}^{\bullet+}$	52.1	268.6	274.1
$\mathbf{4}^{\bullet+}$	56.3	201.3	205.1

[a] Corrected for ZPVE. [b] E_{tot} = -248.29260 Hartree. [c] E_{tot} = -247.71758 Hartree.

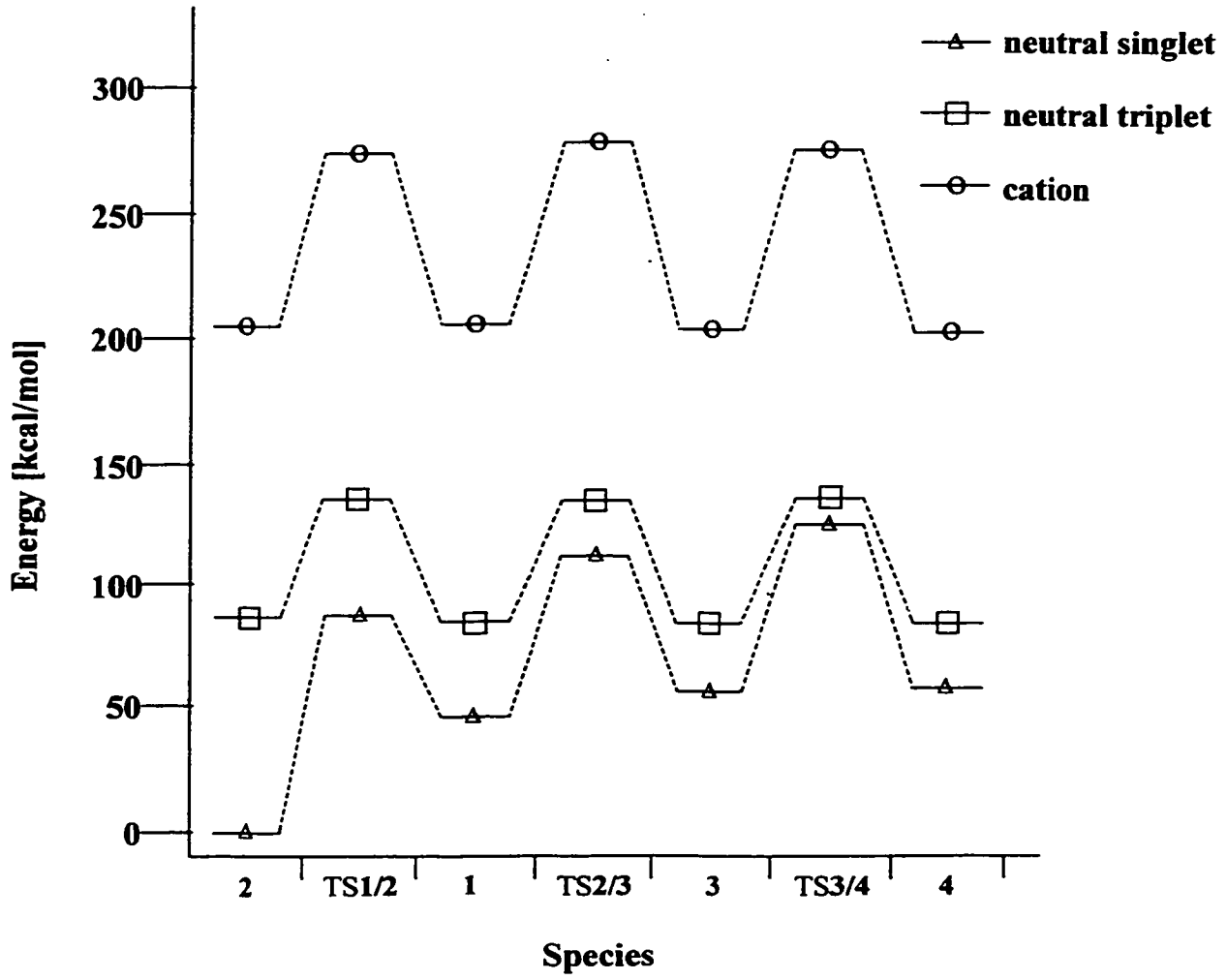

Figure 3.2: Schematic potential energy surface for the neutral and cationic C_5H_5N isomers [CCSD(T)/ANO-TZP//B3LYP/6-31G** level of theory].

Finally, the large barriers to isomerization, indicated by the computational and experimental results, clearly point to the possibility of directly observing the ylide isomers of pyridine, i.e. **1**, **3** and **4**, in the condensed phase under appropriate conditions, i.e. by low temperature matrix isolation. As pointed out by Shevlin *et al.* [7,8], direct observation in solution is more problematic due to facile, intermolecularly catalyzed isomerizations.

References

[1] D. Schröder and H. Schwarz, *Int. J. Mass Spectrom. Ion Processes* **1995**, *146/147*, 183.

[2] R.A. Moss, *Acc. Chem. Res.* **1989**, *22*, 15.

[3] R A. McClelland, *Tetrahedron* **1996**, *52*, 6823.

[4] P. Dyson and D.L. Hammick, *J. Chem. Soc.* **1937**, 1724.

[5] M.R.F. Ashworth, R.P. Daffern and D.L. Hammick, *J. Chem. Soc.* **1937**, 809.

[6] D.J. Lavorato, J.K. Terlouw, T.K. Dargel, W. Koch, G.A. McGibbon and H. Schwarz, *J. Am. Chem. Soc.* **1996**, *118*, 11898.

[7] C.J. Emanuel and P.B. Shevlin, *J. Am. Chem. Soc.* **1994**, *116*, 5991.

[8] W. Pan and P.B. Shevlin, *J. Am. Chem. Soc.* **1997**, *119*, 5091.

[9] M. Plisnier and R. Flammang, *Chim. Nouv.* **1990**, *8*, 893.

[10] F.W. McLafferty, *Int. J. Mass Spectrom. Ion Processes* **1992**, *118/119*, 211.

[11] F. Tureček, *Org. Mass Spectrom.* **1992**, *27*, 1087.

[12] N. Goldberg and H. Schwarz, *Acc. Chem. Res.* **1994**, *27*, 347.

[13] G.A. McGibbon, C.A. Kingsmill and J.K. Terlouw, *Chem. Phys. Lett.* **1994**, *222*, 129.

[14] G.A. McGibbon, P.C. Burgers and J.K. Terlouw, *Int. J. Mass Spectrom. Ion Processes* **1994**, *136*, 191.

[15] C.E.C.A. Hop, H. Chen, P.J.A. Ruttink and J.L. Holmes, *Org. Mass Spectrom.* **1991**, *26*, 697.

[16] G. Schaftenaar, R. Postma, P.J.A. Ruttink, P.C. Burgers, G.A. McGibbon and J.K. Terlouw, *Int. J. Mass Spectrom. Ion Processes* **1990**, *100*, 521.

[17] C. Wesdemiotis and F.W. McLafferty, *J. Am. Chem. Soc.* **1987**, *109*, 4760.

[18] D. Süzle, T. Drewello, B.L.M. van Baar and H. Schwarz, *J. Am. Chem. Soc.* **1988**, *110*, 8330.

[19] R. Feng, C. Wesdemiotis and F.W. McLafferty, *J. Am. Chem. Soc.* **1987**, *109*, 6521.

[20] W.J. Bouma, P.C. Burgers, J.L. Holmes and L. Radom, *J. Am. Chem. Soc.* **1986**, *108*, 1767.

[21] G.A. McGibbon, J. Hrušák, D.J. Lavorato, H. Schwarz and J.K. Terlouw, *Chem. Eur. J.* **1997**, *3*, 232.

[22] G.A. McGibbon, C. Heinemann, D.J. Lavorato and H. Schwarz, *Angew. Chem. Int. Ed. Engl.* **1997**, *36*, 1478.

[23] *Gaussian 94* (Revision B.2), M.J. Frisch, G.W. Trucks, H.B. Schlegel, P.M.W. Gill, B.G. Johnson, M.A. Robb, J.R. Cheeseman, T.A. Keith, G.A. Petersson, J.A. Montgomery, K. Raghavachari, J.B. Foresman, J. Cioslowski, B.B. Stefanov, A. Nanayakkara,

M. Challacombe, C.Y. Peng, P.Y. Ayala, W. Chen, M.W. Wong, J.L. Andres, E.S. Replogle, R. Gomperts, R.L. Martin, D.J. Fox, J.S. Binkley, D.J. DeFrees, J. Baker, J.J.P. Stewart, M. Head-Gordon, C. Gonzalez and J.A. Pople, Gaussian, Inc., Pittsburgh PA, **1995**.

[24] R.G. Parr and W. Yang, *Density Functional Theory of Atoms and Molecules*, Oxford University Press, Oxford 1989.

[25] a) A.D. Becke, *J. Chem. Phys.* **1993**, *98*, 1372.
b) A.D. Becke, *J. Chem. Phys.* **1993**, *98*, 5648.

[26] P.J. Stephens, F.J. Devlin. C.F. Chabalowski and M.J. Frisch, *J. Phys. Chem.* **1994**, *98*, 11623.

[27] For a competent review on these techniques, see: W.J. Hehre, L. Radom, P.v.R. Schleyer and J.A. Pople, *Ab Initio Molecular Orbital Theory*, Wiley Interscience, New York, **1986**.

[28] P.R. Taylor, in Lecture *Notes in Quantum Chemistry* II, B.O. Ross (ed.), Springer, Berlin, **1994**.

[29] T.J. Lee and G.E. Scuseria, in *Quantum Mechanical Electronic Structure Calculations with Chemical Accuracy*, S.R. Langhoff (ed.), Kluwer Academic Publishers, Dordrecht **1995**.

[30] R.J. Bartlett and J.F. Stanton, in *Reviews in Computational Chemistry*, Volume 5, K P. Lipkowitz and D.B. Boyd (eds.), VCH, New York, **1994**.

[31] MOLPRO is a package of *ab inito* programs written by H.-J. Werner and P.J.Knowles, with contributions from J. Almlöf, R.D. Amos, M.J.O. Deegan, S.T. Bert, C. Hampel, W. Meyer, K. Peterson, R. Pitzer, A.J. Stone, P.R. Taylor and R. Lindh.

[32] J. Almlöf and P.R. Taylor, *J. Chem. Phys.* **1987**, *86*, 4070.

[33] K. Pierloot, B. Dumez, P.-O. Widmark and B.O. Roos, *Theor. Chim. Acta* **1995**, *90*, 87.

[34] P.C. Burgers, J.L. Holmes and J.K. Terlouw, *J. Am. Chem. Soc.* **1984**, *106*, 2762.

[35] P.C. Burgers, J.K. Terlouw, T. Weiske and H. Schwarz, *Chem. Phys. Lett.* **1986**, *132*, 69.

[36] L.I.M. Spiessens and M.J.O. Antennis, *Bull. Soc. Chim. Belg.* **1980**, *89*, 205.

[37] G.F. Tantardini and M. Simonetta, *Int. J. Quant. Chem.* **1981**, *20*, 705.

[38] I.C. Walker, M.H. Palmer and A. Hopkirk, *Chem. Phys.* **1990**, *141*, 365.

[39] H. Nakano, T. Nakajima and S. Obara, *Chem. Phys. Lett.* **1991**, *177*, 458.

[40] J.B. Foresman, M. Head-Gordon, J.A. Pople and M.J. Frisch, *J. Phys. Chem.* **1992**, *96*, 135.

[41] M.P. Fulscher, K. Andersson and B.O. Roos, *J. Phys. Chem.* **1992**, *96*, 9204.

CHAPTER 4

The Thiazole Ylide: A Frequently Invoked Intermediate is a Stable Species in the Gas Phase

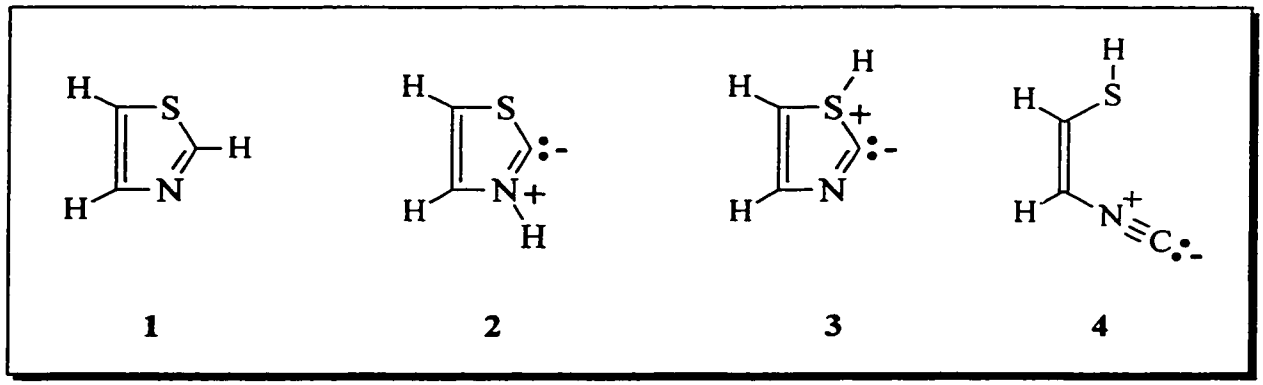

1 2 3 4

In this Chapter, the 1,2-hydrogen shift isomer of thiazole (**1**), 2,3-dihydrothiazol-2-ylidene (**2**) and its radical cation, have been identified as stable species in the gas phase using a combination of mass spectrometric experiments and computational chemistry. A further examination of the C_3H_3NS potential energy surface indicates that 1,2-dihydrothiazol-2-ylidene (**3**) is unstable and quickly undergoes ring cleavage to form the open chain species HSCH=CHNC (**4**). However, the computational results do predict that the ionic counterpart of **3**, as well as that of **4**, to be a stable entities. The facile interconversion of the neutral and ionic C_3H_3NS isomers is hindered by the presence of substantial isomerization barriers, thus accounting for their stability in the dilute gas phase.

The work described has been published previously in an article under the same title: G.A. McGibbon, J. Hrušák, D.J. Lavorato, H. Schwarz and J.K. Terlouw, Chem. Eur. J., 1997, 3, 232-236.

Introduction

Thiamin (Vitamin B_1) is a coenzyme essential to several biochemical processes [1]. The decarboxylation of pyruvic acid to acetaldehyde exemplifies its involvement in the catalytic cycles of many carbon-carbon bond forming and breaking reactions [2]. The enzymatic activity has been suggested to stem from the relatively easy deprotonation of the thiazolium ring to form an active, thiazolium ylide intermediate. Breslow's fundamental studies [3] on model systems laid foundations for this current understanding of thiamin action. Despite a considerable body of other supportive experimental work [1,4-9], including the recent synthesis and characterization of a few metallo-carbene complexes [10-12], the direct observation of free thiazolium-2-ylides seems to remain an elusive goal.[†] In contrast, closely related five-membered ring heterocycles of the imidazol-2-ylidene family proved to be isolatable compounds [13,14], although the parent species itself was only recently generated and characterized as a gaseous molecule [15]. More highly substituted members of this class have been probed spectroscopically in the gas phase [16]. Among related heterocycles, oxazole-2-ylidene has similarly been observed [17] in neutralization-reionization mass spectrometry (NRMS) [18] experiments.

Since these latter types of species are biochemically less significant than the thiazole ylides, it is important to address this deficit. This Chapter discuss the successful identification of the parent 2,3-dihydrothiazol-2-ylidene, **2**, using the technique of NRMS. Although not identical to the suggested active form of thiamin, this structure is the simplest model compound for the vitamin. While extensive computational studies have been carried out on imidazol-2-ylidene [14,19,20] much less information is available for the thiazole ylides [20-24]; quantum chemical calculations of the hybrid density functional theory [25] type have been used investigate aspects of the C_3H_3NS potential energy surface relevant to the characterization of thiazol-2-ylidenes and their

---

[†] The preparation of a stable thiazole ylide has recently been reported in solution: A.J. Arduengo III, J.R. Goerlich and W.J. Marshall, *Liebigs Ann. Recl.* **1997**, 365.

radical cations [26]. It should be mentioned that the issue of "aromaticity" [27] in five-membered ring heterocycles has long attracted attention [28]. Aromatic stabilization energies determined using ab initio calculations incorporating perturbation theory (MP2) [20,21] apparently indicated that **2** is less stabilized than imidazole-2-ylidene, and the exact extent of its aromatic stabilization has continued to be the subject of controversy [14,19]. Given the difficulties inherent to establishing unambiguously the exact extent of aromatic stabilization in **2**, notwithstanding the recent presentation of calculated magnetic susceptibility anisotropy data [21], the discussion is limited to comparisons of its structural features and energies relative to its isomers.

Results and Discussion

Mass Spectrometry.

Generation of $\mathbf{2}^{\bullet+}$ might be accomplished analogously with previous carbene radical cation "gas phase syntheses" [17,18] by dissociative electron ionization (EI) of an appropriately substituted thiazole such as the readily available 2-acetylthiazole (Scheme 4.1), which has a sizeable $C_3H_3NS^{\bullet+}$ peak at m/z 85 in its EI mass spectrum.

The proper identification of neutral species by NRMS requires that one can confidently establish the parent ion structure. Details of neutralization-reionization (NR) mass spectrum acquisition [29] and other tandem mass spectrometric experiments [30] used to generate and characterize C_3H_3NS ions and neutrals are given in the Experimental section.

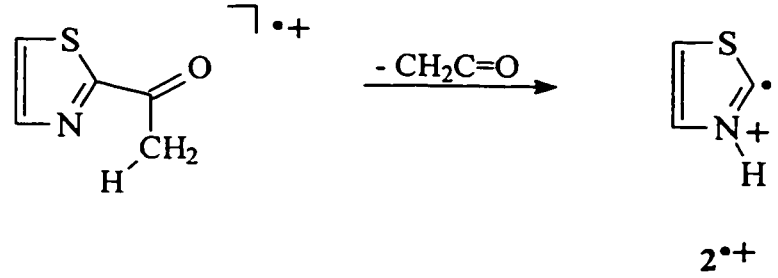

$\mathbf{2}^{\bullet+}$

Scheme 4.1

The collision-induced dissociation (CID) mass spectrum of the m/z 85 ions obtained according to Scheme 4.1 was compared to that of thiazole radical cations $\mathbf{1}^{\bullet+}$, which are produced simply by 70 eV EI of thiazole [31] (Figure 4.1). The m/z 85 ions generated from the two precursors give rise to reasonably similar spectra except for two crucial differences. First, only the m/z 85 ions that are expected to have the ylide ion structure produce a peak at m/z 73 ($C_2H_3NS^{\bullet+}$), which formally corresponds to the extrusion of the ylidic carbon atom from the ring. Secondly, the peak at m/z 59 ($HNCS^{\bullet+}$) provides definite evidence for a structure that can easily lose acetylene, that is, $\mathbf{2}^{\bullet+}$ [32]. Ion $\mathbf{3}^{\bullet+}$, although disfavoured energetically compared to $\mathbf{2}^{\bullet+}$ (see Table 4.1), could also provide m/z 59 ions ($HSCN^{\bullet+}$ or $C_2H_3S^+$) [33]. However, an MS/MS/MS experiment [33] confirmed the identity of the ions as $HNCS^{\bullet+}$ [34]. Ring cleavage in $\mathbf{1}^{\bullet+}$ would lead to the ion $N{=}CH\text{-}S^{\bullet+}$, which undoubtedly is higher in energy and this process is therefore not observed. Furthermore, the near absence of the m/z 59 peak in the CID mass spectrum of $\mathbf{1}^{\bullet+}$ effectively rules out the possibility that isomerization to ionized thiazole by a 1,2-hydrogen shift occurs to a significant extent prior to undergoing dissociation. Perhaps not surprisingly, an analogous situation is demonstrated by the imidazole/imidazol-2-ylidene radical cation system where the two isomers with otherwise similar CID mass spectra are clearly distinguished on the basis of the acetylene elimination reaction [15]. Depending upon thermochemical considerations, it may be that this is a generic differentiating feature for simple five-membered ring heterocyclic molecular ions and their ionic 2-ylide isomers. Although, such a generalization clearly has limits, as demonstrated by the challenge of identifying the pyridine-2-ylide ion which is a six-membered ring heterocycle [35].

Encouraged by the indications that the dissociative ionization of 2-acetylthiazole does produce m/z 85 radical cations of structure $\mathbf{2}^{\bullet+}$, neutralization-reionization mass spectrometry (NRMS) [18] was employed to attempt to generate and characterize the neutral ylide **2**. Ideally, near vertical electron transfer to the ion should yield the desired neutral. However, the internal energy content of the neutral so produced will be

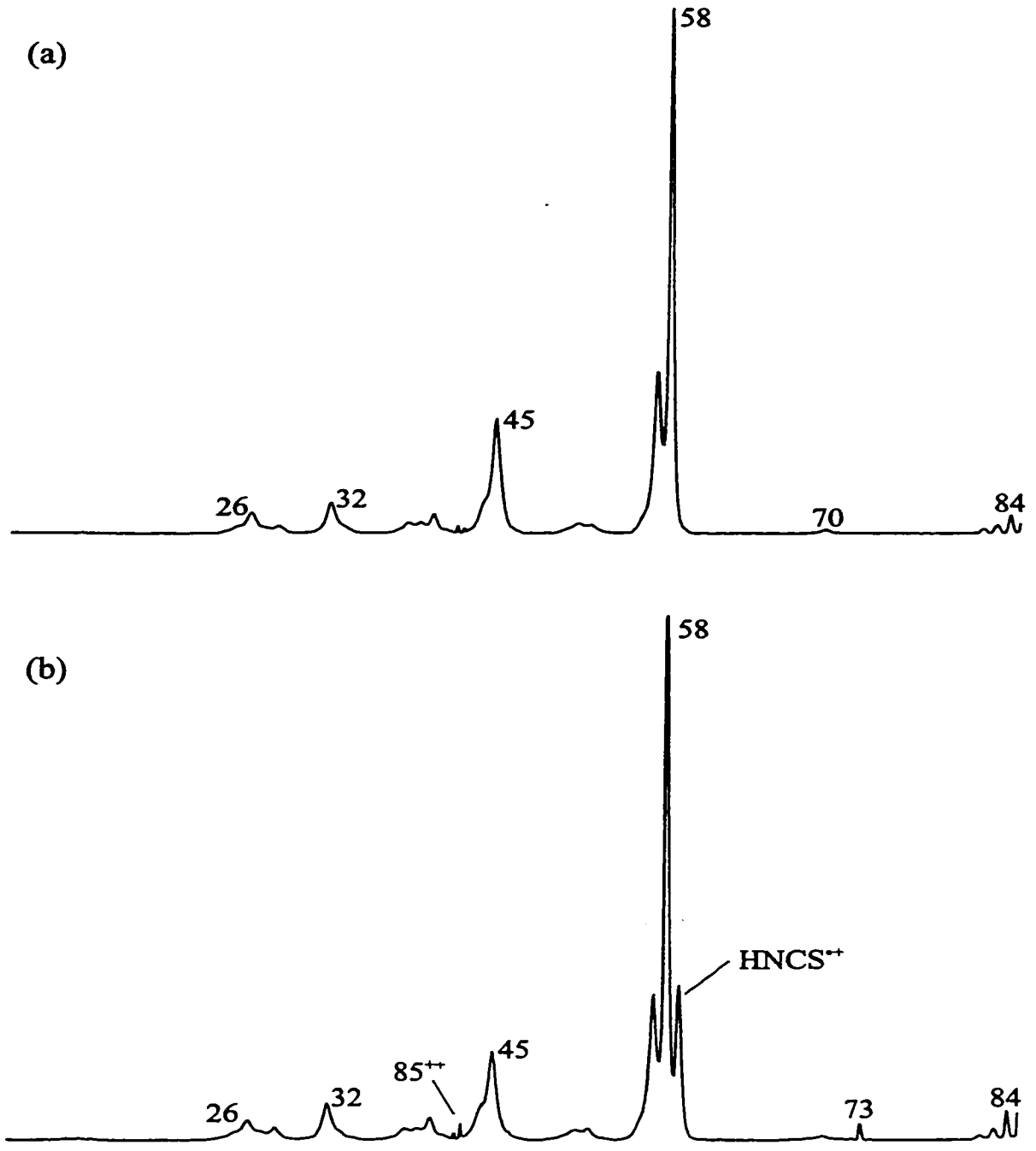

Figure 4.1: CID mass spectra of the m/z 85 ions generated from (a) ionized thiazole, $\mathbf{1}^{\bullet+}$ and (b) ionized 2-acetylthiazole, $\mathbf{2}^{\bullet+}$.

dependent upon the Franck-Condon overlap between the ion and neutral. If the energy barrier to isomerization in the neutral molecules is less than their minimum bond dissociation energy then rearrangement of excited neutral molecules is possible and may occur. In such a case, subsequent reionization would lead to a mixture of ions and as a result, to NR mass spectra that do not match the corresponding CID mass spectra.

The neutralization-reionization (NR) mass spectra of the two ions $\mathbf{1}^{\bullet+}$ and $\mathbf{2}^{\bullet+}$ are quite similar to the corresponding CID mass spectra and both exhibit survivor signals at m/z 85. The observation of recovery peaks is consistent with the computational predictions (see below) provided that the ions generated from 2-acetylthiazole do have structure $\mathbf{2}^{\bullet+}$ as opposed to $\mathbf{3}^{\bullet+}$, since the latter are not expected to yield stable species upon neutralization. More importantly, the distinguishing peaks at m/z 59 and 73 again appear only in the spectrum assigned to $\mathbf{2}^{\bullet+}$. Because of the absence of unique peaks for the thiazole structure itself, an absolute assessment as to whether or not the ion $\mathbf{1}^{\bullet+}$ is also generated from 2-acetylthiazole is prevented. However, the m/z 85 ions from 2-acetylthiazole were analyzed after NR by CID [35] (spectrum not shown) and they again showed a substantial m/z 59 peak so we conclude that the majority of the ions have the structure $\mathbf{2}^{\bullet+}$. Thus, it is clear that 2,3-dihydrothiazol-2-ylidene, **2**, is formed by one-electron reduction of $\mathbf{2}^{\bullet+}$ in the gas phase and that **2** does not readily isomerize to the neutral thiazole structure **1**.

The search for stationary points corresponding to the thiazole isomers **1** - **3**, their radical cations and the connecting transition structures of the 1,2-hydrogen shifts was conducted on a 6 processor SGI-POWER-Challenge computer using the Gaussian 94 program package [36]. Analytical frequency calculations confirmed the assignment of stable or transition structures based on the correct number of eigenvalues of the Hessian matrix, 0 or 1 respectively. The geometric parameters and energies of the structures were obtained with the 6-31G** basis set using the standard hybrid density functional theory option (HF/DFT) designated B3LYP [37]. Relative energies were corrected for non-scaled zero-point vibrational energy (ZPVE) contributions. The energy data and $\langle S^2 \rangle$

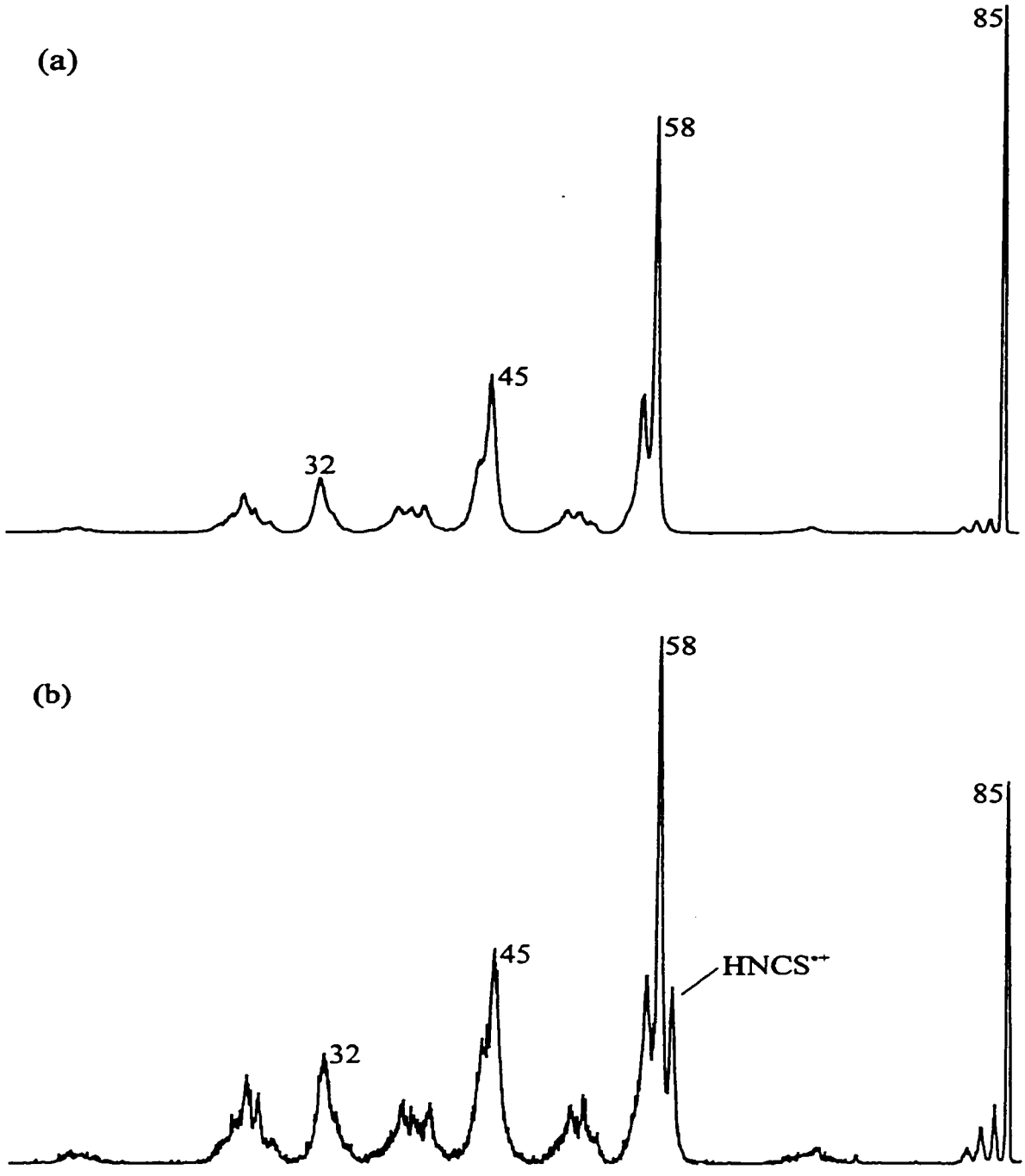

Figure 4.2: NR mass spectra of the m/z 85 ions generated from (a) ionized thiazole, $\mathbf{1}^{\bullet+}$ and (b) ionized 2-acetylthiazole, $\mathbf{2}^{\bullet+}$.

expectation values of the open shell systems are collected in Table 4.1. The latter show that the B3LYP wave functions do not suffer appreciably from spin contamination [38]. Table 4.2 contains the geometric details for the structures shown in Figure 4.3. According to the B3LYP calculations, thiazole **1** (^{1}A') is planar, with C-S bonds (1.737 Å and 1.731 Å) of almost equal length and a typical C=C double bond. This result is remarkably close

Table 4.1: Calculated energies[a] for selected C_3H_3NS neutrals,[b] radical cations and transition structures.

(a) Neutrals

	B3LYP/6-31G**$_S$	ZPVE$_S$	ΔE_{T-S}	ZPVE$_T$	$\langle S^2\rangle_T$	E_{rel}
1	-569.05184	34.7	69.5	31.9	2.000	0
2	-569.00160	34.7	63.2	33.1	2.007	31.5
4	-568.99175	31.5				34.5
TS1/2	-568.93010	30.7	58.7	29.9	2.021	72.4
TS1/4	-568.95724	30.2				54.9

(b) Ions

	B3LYP/6-31G**	ZPVE	$\langle S^2\rangle$	IE_a	E_{rel}
$\mathbf{1}^{\bullet+}$	-568.71800	33.6	0.750	9.04	0
$\mathbf{2}^{\bullet+}$	-568.70386	34.9	0.750	8.11	10.2
$\mathbf{3}^{\bullet+}$	-568.62938	31.9	0.750		53.9
$\mathbf{4}^{\bullet+}$	-568.67165	31.5	0.750	8.71	27.0
$\mathbf{TS1}^{\bullet+}/\mathbf{2}^{\bullet+}$	-568.61342	30.8	0.758	8.62	62.8
$\mathbf{TS1}^{\bullet+}/\mathbf{3}^{\bullet+}$	-568.60249	30.3	0.759	9.66	69.2

[a] Total energies are in Hartree, zero-point vibrational energies (ZPVE), triplet-singlet gap energies (ΔE_{T-S}) and relative energies of singlet species (E_{rel}) are in kcal/mol while ionization energies (IE_a) in eV. [b] Subscripts S and T are used to indicate values for singlet and triplet state neutral species.

Table 4.2: Optimized B3LYP geometries for selected C_3H_3NS neutrals,[a] radical cations and transition structures.

Structure	Angles (degrees)					Bond Lengths (Å)					
	SC(2)N	C(2)NCC	NCC	CCS	C(2)XH[c]	S-C(2)	C(2)-N	N-C	C=C	C-S	X-H[c]
$\mathbf{1}_{expt.}$[b]	115.2	110.1	115.8	109.6	121.3	1.713	1.304	1.372	1.367	1.713	
$\mathbf{1}_S$	115.2	110.4	116.1	109.8	121.5	1.750	1.300	1.377	1.365	1.733	1.083
$\mathbf{1}_T$	112.4	110.5	114.8	115.6	130.1	1.848	1.406	1.294	1.452	1.746	1.088
$\mathbf{1}^{\bullet+}$	114.8	110.9	115.1	111.5	120.5	1.820	1.308	1.339	1.450	1.672	1.086
$\mathbf{2}_S$	103.6	120.9	111.3	108.5	118.2	1.742	1.312	1.399	1.349	1.755	1.013
$\mathbf{2}_T$	113.5	108.3	114.9	113.0	118.8	1.780	1.390	1.401	1.348	1.778	1.022
$\mathbf{2}^{\bullet+}$	115.5	112.6	111.5	111.8	123.5	1.682	1.352	1.398	1.356	1.755	1.019
$\mathbf{3}^{\bullet+}$	110.6	117.0	113.4	110.7	94.1	1.834	1.216	1.419	1.306	1.803	1.368
$\mathbf{4}_S$	95.8	175.6	122.9	123.8	162.0	3.806	1.201	1.355	1.398	1.696	1.353
$\mathbf{4}^{\bullet+}$	95.6	179.3	122.9	122.0	164.2	3.788	1.183	1.374	1.342	1.762	1.346
$\mathbf{TS1}_S/\mathbf{2}_S$	116.0	110.8	112.5	113.2	60.0	1.731	1.324	1.385	1.377	1.737	1.308
$\mathbf{TS1}_T/\mathbf{2}_T$	115.3	105.6	118.2	113.4	60.2	1.784	1.431	1.392	1.357	1.786	1.339
$\mathbf{TS1}^{\bullet+}/\mathbf{2}^{\bullet+}$	108.3	115.3	113.3	112.7	60.7	1.768	1.372	1.397	1.362	1.740	1.316
$\mathbf{TS1}_S/\mathbf{4}_S$	93.6	130.1	114.9	116.5	23.3	2.650	1.196	1.392	1.366	1.714	1.979
$\mathbf{TS1}^{\bullet+}/\mathbf{3}^{\bullet+}$	110.4	116.9	114.0	116.8	49.4	1.885	1.245	1.371	1.373	1.740	1.529

[a] Subscript S and T are used to indicate the multipicity (singlet and triplet) of the neutral species. [b] Compare ref. [39]. [c] X = C(2) for structures **1**, X = N for structures **2** and **TS1/2**, and X = S for structures $\mathbf{3}^{\bullet+}$, **4**, $\mathbf{TS1}^{\bullet+}/\mathbf{3}^{\bullet+}$ and **TS1/4**.

to the structure of **1** determined by microwave spectroscopy [39]. In its triplet state **1** is non-planar. As well as having a hydrogen atom out-of-plane, the ring skeleton exhibits some torsion (~ 10°) and by comparison with the singlet state structure all the bonds except C(4)-N are longer with the SC(2)N angle narrowing slightly to accommodate the change. The triplet-singlet gap is large, 69.5 kcal/mol including zero-point vibrational energy contributions. Ionization of **1** yields a planar C_s structure with bond lengths and angles intermediate between neutral thiazole in its singlet and triplet states. According to the DFT calculations the separation of **1** from $\mathbf{1}^{\bullet+}$ is smaller than the experimentally determined ionization potential for thiazole, 9.51 eV [40]. The difference is somewhat smaller for imidazole [15,41], and for the imidazole carbene [14a,19f] where theory and experiment concur.

Like **1**, the ylide **2** (^{1}A') is also planar; its C=C bond is shorter and its C-N bond is a little longer whereas the C-S distances are about the same. In contrast to Sauer's structure for **2** derived using a single-determinant [20], the B3LYP derived structure (Figure 4.3) has longer (by at least 0.02 Å) C-S bonds and shorter C(2)-N and C=C bonds (by 0.043 and 0.01 Å respectively), although the SC(2)N angle is virtually the same. On going to the triplet state of **2** the SC(2)N angle widens noticeably from 103.6° to 113.5° and the two adjacent heteroatom-carbon bonds are lengthened. Upon ionization, further widening of the SC(2)N angle to 115.5° occurs, but while the associated C-N bond becomes slightly longer in $\mathbf{2}^{\bullet+}$, the C(2)-S bond is actually shortened to 1.682 Å and the other C-N and C-S bonds remain essentially unchanged. The geometry changes from singlet **2** are consistent with substantial localization of the HOMO at C(2). Energetically, reduction of the ions favours the formation of singlet **2** in the NRMS experiments, although considering the similarity of the SC(2)N angles, in $\mathbf{2}^{\bullet+}$ and in triplet **2**, the possibility of some endothermic neutralization to the latter cannot be ruled out on the basis of geometric differences.

The transition structure **TS1/2** possesses features one expects for a 1,2-hydrogen shift and has a typical associated frequency (~ 2000 cm^{-1}) for this type of process [42].

The energy required to surmount the barrier is 72.4 kcal/mol coming from **1**. Similarly, **TS1**$^{\bullet+}$/**2**$^{\bullet+}$, the corresponding structure for the ions, lies 62.8 kcal/mol above **1**$^{\bullet+}$.

According to the present calculations there is a stable radical cation **3**$^{\bullet+}$ that has a cyclic structure but curiously there seems to be no corresponding neutral molecule; optimization attempts led instead to spontaneous ring-opening and eventually to structure **4**. The ionized counterpart of the latter, **4**$^{\bullet+}$, is also lower in energy than the cyclic ion **3**$^{\bullet+}$ by 27 kcal/mol. The deprotonated counterpart of **4** has been proposed to rationalize reactions of thiazole with bases in both solution [43] and gas phase chemistry [44].

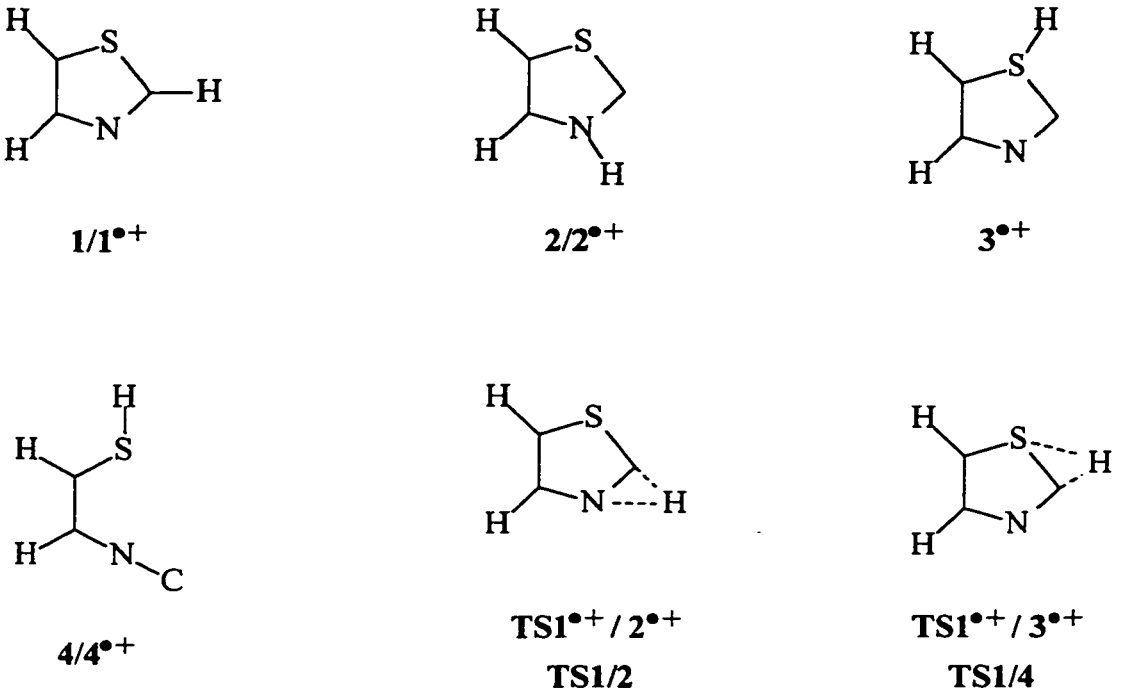

Figure 4.3: Optimized B3LYP/6-31G** geometries of selected C_3H_3NS molecules, radical cations, and their connecting transition state structures (see also Table 4.2 for detailed geometries).

The transition structures **TS1/4** and **TS1**$^{\bullet+}$/**3**$^{\bullet+}$ determined for 1,2-hydrogen shifts from C(2) to the sulfur atom should lie high enough in energy (20.4 and 15.3 kcal/mol relative to **4** and **3**$^{\bullet+}$) that the stable isomers should be observable under appropriate conditions.

If the enthalphy of formation of thiazole and its ionization energy were well established it should be possible to evaluate ΔH_f (**2**) and ΔH_f (**2**$^{\bullet+}$) from the computed energy differences between the various species. However, the Lias compendium [32] indicates that ΔH_f (**1**) = 37 ± 2 kcal/mol is an estimated value. If we rely on this estimate together with our calculated difference between **1** and **2**, it puts ΔH_f (**2**) = 68.5 kcal/mol. Using the calculated energy difference between ylide **2** and its radical cation we estimate ΔH_f (**1**$^{\bullet+}$) as 256 kcal/mol with an uncertainty of several kcal/mol. The energy difference between the two neutrals can be combined with ΔH_f ($C_3H_4NS^+$) = 187 kcal/mol, from the experimental proton affinity of thiazole, PA(**1**) = 216.5 kcal/mol [45]. However, note that the value PA(**2**) = 247 kcal/mol thus obtained is quite different from the 254.7 kcal/mol predicted by Sauer's calculations [20]. Further calculations and experiments are necessary to alleviate this discrepancy.

The stability of the gaseous thiazole ylide **2**, a model compound of Vitamin B_1, provides support of mechanisms of thiamin action involving ylidic intermediates. The high barriers to isomerization indicated by the computational and experimental results point to the possibility of directly observing **2** in the condensed phase under appropriate conditions, for example, by low temperature matrix isolation.

References

[1] R. Kluger, *Chem. Rev.* **1987**, *87*, 863.

[2] L.O. Krampitz, *Thiamin Diphosphate and Its Catalytic Functions*, Marcel Dekker: New York, **1970**.

[3] a) R. Breslow, *J. Am. Chem. Soc.* **1958**, *80*, 3719.
b) R. Breslow, *Chem. Ind.* **1957**, 893.
c) R. Breslow, *J. Am. Chem. Soc.* **1957**, *80*, 3719.

[4] A. Dondoni, A.W. Douglas and I. Shinkai, *J. Org. Chem.* **1993**, *58*, 3196.

[5] F.G. Bordwell and A.V. Satish, *J. Am. Chem. Soc.* **1991**, *113*, 985.

[6] M.W. Washabaugh and W.P. Jencks, *J. Am. Chem. Soc.* **1989**, *111*, 674.

[7] T. Matsumoto, M. Ohishi and J. Inoue, *J. Org. Chem.* **1985**, *50*, 603.

[8] H. Stetter, *Angew. Chem. Int. Ed. Engl.* **1976**, *15*, 639.

[9] P. Haake, L.P. Bauscher and W.B. Miller, *J. Am. Chem. Soc.* **1969**, *91*, 1113.

[10] Au complex: H.G. Raubenheimer, F. Scott, M. Roos and R. Otte, *J. Chem. Soc., Chem. Commun.* **1990**, 1722.

[11] Cu complex: H.G. Raubenheimer, S. Cronje, P. van Rooyan, P.J. Olivier and J.G. Toerien, *Angew. Chem. Int. Ed. Engl.* **1994**, *33*, 672.

[12] Li complex: G. Boche, C. Hilf, K. Harms, M. Marsch and J.C.W. Lohrenz, *Angew. Chem. Int. Ed. Engl.* **1996**, *34*, 487.

[13] For a précis of the "incredible renaissance" in this area, see: M Regitz, *Angew. Chem. Int. Ed. Engl.* **1996**, *35*, 725 and references contained therein.

[14] For new theoretical insights, see: a) C. Heinemann, T. Müller, Y. Apeloig and H. Schwarz, *J. Am. Chem. Soc.* **1996**, *118*, 2023.
b) C. Boehme and G. Frenking, *J. Am. Chem. Soc.* **1996**, *118*, 2039.

[15] G.A. McGibbon, C. Heinemann, D.J. Lavorato and H. Schwarz, *Angew. Chem. Int. Ed. Engl.* **1997**, *35*, 725.

[16] P. Chen, *personal communication*

[17] T. Wong, J.W. Warkentin and J.K. Terlouw, *Int. J. Mass Spectrom. Ion Processes* **1990**, *115*, 33.

[18] Recent reviews: a) M. Plisnier and R. Flammang, *Chim. Nouv.* **1990**, *8*, 893.

b) F.W. McLafferty, *Int. J. Mass Spectrom. Ion Processes* **1992**, *118/119*, 211.

c) F. Turecek, *Org. Mass Spectrom.* **1992**, *27*, 1087.

d) N. Goldberg and H. Schwarz, *Acc. Chem. Res.* **1994**, *27*, 347.

[19] a) R. Gleiter and R. Hoffmann, *J. Am. Chem. Soc.* **1968**, *90*, 5457.

b) D.A. Dixon and A.J. Arduengo, *J. Phys. Chem.* **1991**, *95*, 4180.

c) J. Cioslowski, *Int. J. Quant. Chem., Quant. Chem. Symp.* **1993**, *27*, 309.

d) C. Heinemann and W. Thiel, *Chem. Phys. Letters* **1994**, *217*, 11.

e) A.J. Arduengo III, D.A. Dixon, D.A. Harlow, K.K. Kumashiro, C. Lee, W.P. Power and K.W. Zilm, *J. Am. Chem. Soc.* **1994**, *116*, 6361.

f) A.J. Arduengo III, H. Bock, H. Chen, M. Denk, D.A. Dixon, J.C. Green, W.A. Herrmann, N.L. Jones, M. Wagner and R. West, *J. Am. Chem. Soc.* **1994**, *116*, 6641.

g) R.W. Alder, P.R. Allen and S.J. Williams, *J. Chem. Soc., Chem. Commun.* **1995**, 1267.

[20] R.R. Sauers, *Tetrahedron Lett.* **1996**, *37*, 149.

[21] G. Boche, P. Andrews, K. Harms, M. Marsch, K.S. Rangappa, M. Schimeczek and C. Willeke, *J. Am. Chem. Soc.* **1996**, *118*, 4925.

[22] R. Grigg, L. Wallace and J.O. Morley, *J. Chem. Soc., Perkin Trans. 2* **1990**, 51.

[23] F. Geijo, F. Lopez-Calahorra and S. Olivella, *J. Heterocyclic Chem.*, **1984**, *21*, 1785.

b) H.S. Aldrich, W.L. Alworth and N.R. Clement, *J. Am. Chem. Soc.* **1978**, *100*, 2362.

[24] R. Gleiter and R. Hoffmann, *J. Am. Chem. Soc.* **1968**, *90*, 5457.

[25] R.G. Parr, W. Yang, *Density Functional Theory of Atoms and Molecules*, Oxford University Press, Oxford **1989**.

[26] As long ago as 1865 even the structures of the "normal" isomeric forms of thiazole were the subject of lively debate, see: A. Hantzsch and J.H. Weber, *Ber. Dtsch. Chem. Ges.* **1887**, *20*, 3118.

[27] For an up-to-date perspective on definitions and criteria for characterizing aromaticity see: P.v.R. Schleyer and H. Jiao, *Pure Appl. Chem.* **1996**, *68*, 209 and references therein.

[28] a) R.C. Haddon, *J. Am. Chem. Soc.* **1978**, *101*, 1979.

b) A.R. Katritzky, P. Barcynski, G. Musumarra, D. Pisano and M. Szafran, *J. Am. Chem Soc.* **1989**, *111*, 7.

c) P.v.R. Schleyer, P.K. Freeman, H. Jiao and B. Goldfuss, *Angew. Chem Int. Ed. Engl.* **1995**, *34*, 337.

[29] H.F. van Garderen, P.J.A. Ruttink, P.C. Burgers, G.A. McGibbon and J.K. Terlouw, *Int. J. Mass Spectrom. Ion Processes* **1992**, *121*, 159.

[30] K.L. Busch, G.L. Glish and S.A. McLuckey, *Mass Spectrometry/Mass Spectrometry, Techniques and Applications of Tandem Mass Spectrometry*, VCH, New York, **1988**.

[31] a) G.M. Clarke, R. Grigg and D.H. Williams, *J. Chem. Soc. B* **1966**, 339.
b) K.J. Klobe, J.J.V. Houte and J.V. Thuijl, *Org. Mass Spectrom.* **1972**, *6*, 1363.

[32] $\Sigma\Delta H_f$ ($HN{=}C{=}S^{\bullet+} + C_2H_2$) = 314 kcal/mol; S.G. Lias, J.E. Bartmess, J.F. Liebman, J.L. Holmes, R.D. Levin and W.G. Mallard, *J. Phys. Chem. Ref. Data, Supplement 1*, **1988**.

[33] Based on the enthalpy difference between $CH_3NCS^{\bullet+}$ and $CH_3SCN^{\bullet+}$, the products $HSCN^{\bullet+}$ + C_2H_2 are expected to require ~ 337 kcal/mol. The alternative dissociation is estimated to need more energy, $\Sigma\Delta H_f$ ~ 348 kcal/mol, since ΔH_f ($CN^{\bullet}$) = 104 kcal/mol and computations (experimental data not being available) put protonated thiirene 40 kcal/mol above $H_3C{-}C{=}S^{\bullet+}$, for which ΔH_f = 204 kcal/mol.

[34] P. Kambouris, M. Plisnier, R. Flammang, J.K. Terlouw and C. Wentrup, *Tet. Lett.* **1991**, *32*, 1487.

[35] D.J. Lavorato, J.K. Terlouw, T. Dargel, W. Koch, G.A. McGibbon, H. Schwarz, *J. Am. Chem. Soc.* **1996**, *118*, 11898.

[36] Gaussian 94 (Revision B.2), M.J. Frisch, G.W. Trucks, H.B. Schlegel, P.M.W. Gill, B.G. Johnson, M.A. Robb, J.R. Cheeseman, T.A. Keith, G.A. Petersson, J.A. Montgomery, K. Raghavachari, J.B. Foresman, J. Cioslowski, B.B. Stefanov, A. Nanayakkara, M. Challacombe, C.Y. Peng, P.Y. Ayala, W. Chen, M.W. Wong, J.L. Andres, E.S. Replogle, R. Gomperts, R.L. Martin, D.J. Fox, J.S. Binkley, D.J. DeFrees, J. Baker, J.J.P. Stewart, M. Head-Gordon, C. Gonzalez and J.A. Pople, Gaussian, Inc., Pittsburgh PA, **1995**.

[37] a) S.J. Vosko, L. Wilk and M. Nusair, *Can. J. Chem.* **1980**, *58*, 1200.
b) A.D. Becke, *Phys. Rev. A* **1988**, 38, 5648.
c) C. Lee, W. Yang and R.G. Parr, *Phys. Rev. B* **1988**, *37*, 785.
d) A.D. Becke, *J. Chem. Phys.* **1993**, *98*, 1372.
e) A.D. Becke, *J. Chem. Phys.* **1993**, *98*, 5648.

[38] J. Baker, A. Scheiner and A. Andzelm, *Chem. Phys. Letters* **1993**, *216*, 1.

[39] J. Liebscher, *Houben-Weyl, Methoden der Organischen Chemie*, E8b, III-2, E. Schaumann (ed.), Georg Thieme, Stuttgart, **1994**, 1.

[40] P. Rademacher, K. Kowski and A. Müller, *J. Mol. Struct.* **1993**, *296*, 111.

[41] J. Main-Bobo, S. Olesik, W. Gase, T. Baer, A.A. Mommers and J.L. Holmes, *J. Am. Chem. Soc.* **1986**, *108*, 677.

[42] B.F. Yates, W.J. Bouma and L. Radom, *Tetrahedron*, **1986**, *42*, 6225.

[43] J.V. Metzger, *Thiazole and its Derivatives*, Part 1, A. Weissberger and E.C. Taylor (eds), **1986**, pp. 117-121.

[44] Deprotonated thiazole anions were characterized by mass spectrometry: G.W. Adams, J.H. Bowie and R.N. Hayes, *Int. J. Mass Spectrom. Ion Processes* **1992**, *114*, 163.

[45] A revised PA(1) was obtained by re-evaluating the value from: M. Meot-Ner, L.W. Sieck, *J. Am. Chem. Soc.* **1991**, *113*, 4448 using the PA scale of: J.E. Szulejko, T.B. McMahon, *J. Am. Chem. Soc.* **1993**, *115*, 7839.

CHAPTER 5

Imidazol-2-ylidene: Generation of a Missing Carbene and its Dication by Neutralization-Reionization and Charge-Stripping Mass Spectrometry

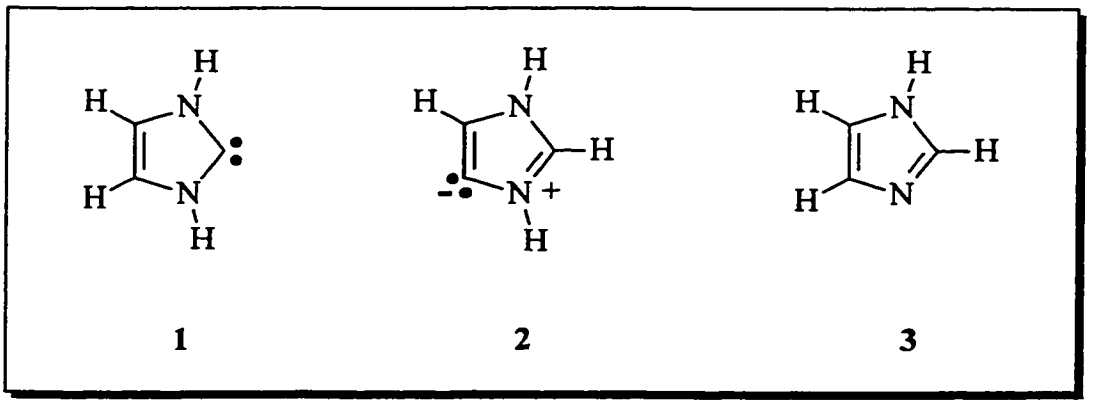

1 2 3

This short Chapter describes the experimental and computational results obtained in the study of the two hydrogen-shift isomers of imidazole (**3**), imidazol-2-ylidene (**1**) and imidazol-4-ylidene (**2**). These novel isomers along with their corresponding ionic counterparts have been identified as stable species in the gas phase using the method of neutralization - reionization mass spectrometry and related techniques. Relative and transition state energies for the neutral and ionic species obtained, using hybrid Hartree-Fock/density functional theory, indicate that each of the isomers exist in a deep potential well thus hindering their facile interconversion.

The work described here has been published previously in an article under the same title: G.A. McGibbon, C. Heinemann, D.J. Lavorato and H. Schwarz, Angew. Chem. Int. Ed. Engl., 1997, 36, 1478-1482.

Introduction

There are many simple molecules that have been studied by quantum chemical methods sufficiently often and thoroughly enough that they take on an aura of familiarity but nevertheless still manage to elude experimental observation. Among the most famous of these is O=C=C=O [1]. A more recent candidate is imidazol-2-ylidene **1**, the parent compound of a carbene family with members that proved stable enough to be isolated [2]. Although imidazolylidenes have been studied for over three decades [3], the theoretical scrutiny of **1** has recently intensified [4]. While computational investigations have concentrated on **1**, to-date all the aminocarbenes [2,4d-f,5] and related compounds [4d,6] observed in condensed phases possess non-hydrogen substituents on the nitrogen atoms. Unsubstituted aminocarbenes have been reported in the gas phase [7], for example the acyclic carbenes H_2N-C-NH_2 and H_2N-C-OH as well as the heterocyclic isomers of oxazole, pyridine and thiazole were prepared and characterized using neutralization-reionization mass spectrometry (NRMS) [8]. The latter method is particularly suitable for the identification of molecules that are susceptible to intermolecular isomerization but relatively stable toward unimolecular rearrangement since the experiments are performed on solitary gaseous species. This approach may be a route to **1** and to imidazol-4-ylidene **2**, the 1,2-hydrogen shift isomers of imidazole **3**. Earlier computations predicted that neutral **1** and **3** are separated by a substantial tautomerisation barrier as are their radical cations [4h,9]. Similarly, the hybrid Hartree-Fock/density functional theory calculations (B3LYP/6-31G**) [10] conducted in this study indicate that a barrier of 36 kcal/mol restricts the exothermic (50 kcal/mol) isomerization **2** $\rightarrow$ **3** and that the apparently isoenergetic ions $\mathbf{2}^{\bullet+}$ and $\mathbf{3}^{\bullet+}$ are separated by a barrier of 56 kcal/mol [11]. In light of this, it would seem that **1** and **2** are targets suitable for generation and characterization by NRMS if precursor molecules can be found (Scheme 5.1).

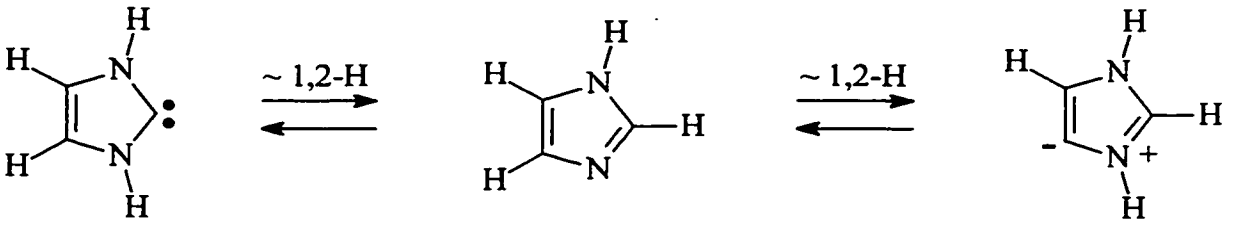

	TS1/3		TS2/3	
1: 29.0	68.8	3: 0.0	85.0	2: 48.8
$1^{\bullet+}$: 0.0	66.7	$3^{\bullet+}$: 14.0	69.6	$2^{\bullet+}$: 13.6

Scheme 5.1: Calculated (B3LYP/6-31G**) relative energies of imidazol-2-ylidene **1**, imidazole **3**, and imidazol-4-ylidene **2**, their interconnecting transition states and their respective radical cations.

It was presumed that the ion $\mathbf{1}^{\bullet+}$ could be generated analogously to previous gas phase syntheses of carbene radical cations by dissociative electron ionization (EI) of an appropriately substituted imidazole. Indeed, the readily available imidazol-2-carboxaldehyde (**I**) seemed a good initial choice since it has a sizeable peak at m/z 68 (corresponding to $[C_3,H_4,N_2]^{\bullet+}$) in its 70 eV EI mass spectrum, which could correspond to $\mathbf{1}^{\bullet+}$ produced from the molecular ion following a formal 1,3-hydrogen shift and decarbonylation (Scheme 5.2). The ionized diester dimethyl imidazole-4,5-dicarboxylate ($\mathbf{II}^{\bullet+}$) could generate $\mathbf{2}^{\bullet+}$ by the more complicated sequence of reactions shown in Scheme 5.3. Radical cations $\mathbf{3}^{\bullet+}$ are obtained simply by EI (70 eV) of imidazole and have been the subject of a number of mass spectrometric studies [12].

A careful comparison of the data from the collision-induced dissociation (CID) mass spectra in Table 5.1 and the charge-stripping (CS) mass spectra in Table 5.2 reveals that two new m/z 68 $[C_3,H_4,N_2]^{\bullet+}$ ions, distinguishable from imidazole do exist. At first glance, the tabulated CID mass spectra do not seem greatly different, which is perhaps

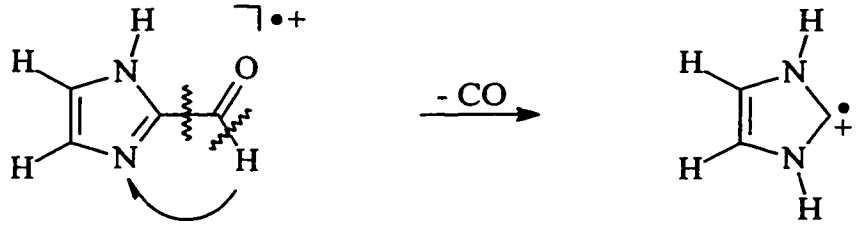

$I^{\bullet+}$ $1^{\bullet+}$

Scheme 5.2: Interpretation of the signal at m/z 68 in the EI (70 eV) mass spectrum of imidazole 2-carboxaldehyde $I^{\bullet+}$: $1^{\bullet+}$ could form from the molecular ion by a formal 1,3 hydrogen shift and decarbonylation.

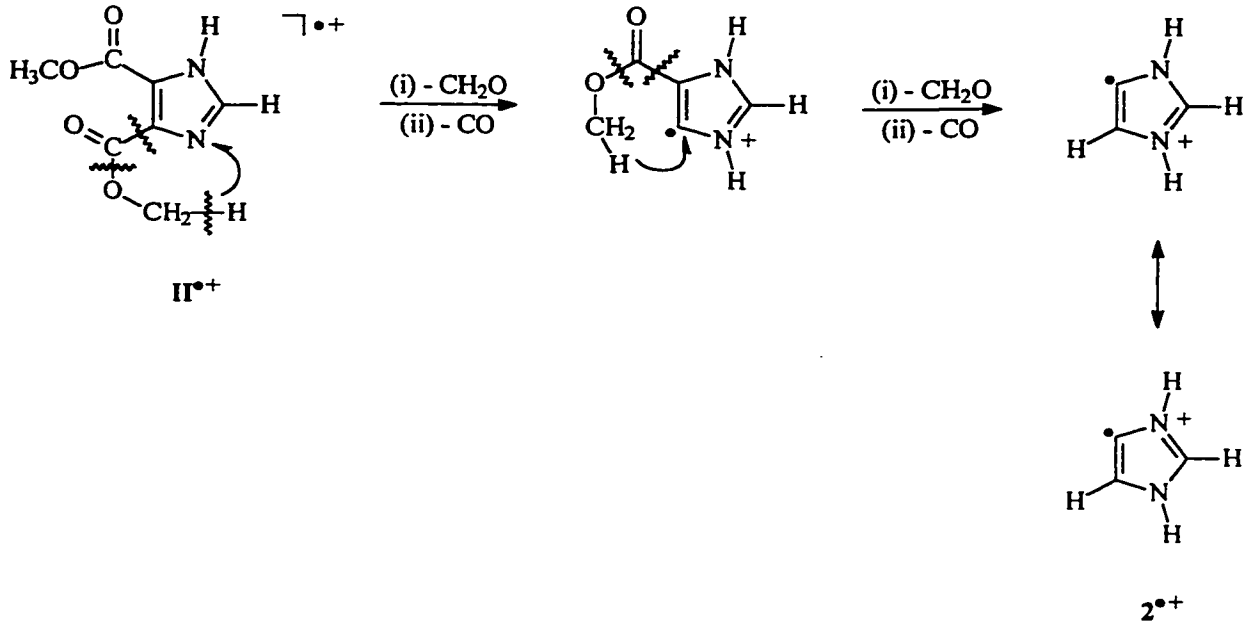

$II^{\bullet+}$ $2^{\bullet+}$

Scheme 5.3: Possible reaction sequence to $2^{\bullet+}$ starting from the ionized dimethyl imidazole-4,5-dicarboxylate, $II^{\bullet+}$.

not surprising in light of the structural similarity of the isomers and their complicated fragmentation pathways [12]. Nevertheless, the spectrum obtained from precursor $\mathbf{I}^{\bullet+}$ is distinguished by an intense peak at m/z 42 (see Table 5.1) that is attributed to the loss of acetylene and thus taken as a strong indication of the carbene ion structure $\mathbf{1}^{\bullet+}$. This process has been shown to occur for the closely related thiazol-2-ylidene radical cation [7e] and it is surmised that in this case ionized diimide $HN{=}C{=}NH^{\bullet+}$ is the product ion. However, attempts to demonstrate this experimentally are thwarted by the fact that

Table 5.1: CID mass spectra of m/z 68 $[C_3H_4N_2]^{\bullet+}$ ions generated from $\mathbf{I}^{\bullet+}$, $\mathbf{II}^{\bullet+}$ and imidazole.[a]

Precursor	$\mathbf{I}^{\bullet+}$		$\mathbf{II}^{\bullet+}$		imidazole	
Spectrum (*m/z*)	CID	NR/CID	CID	NR/CID	CID	NR/CID
42	24	21	1	3	1	3
40	39	32	45	39	52	44
39	10	12	17	13	13	14
38	7	8	10	10	11	10
29	1	3	5	6	1	1
27	8	8	8	10	9	9
26	5	5	3	6	5	6
25	2	3	2	3	2	4
24	1	1	2	2	1	1
16	0	0	2	2	0	0
15	0	1	2	2	0	1
14	1	3	1	2	1	3
13	1	3	1	1	1	3
12	1	1	0	0	1	1

[a] Intensities based on peak heights normalised to $\Sigma = 100$. Peaks containing metastable contributions have been omitted.

isomeric CH_2N_2 radical cations are very difficult to distinguish [13]. In any case, intense signals at m/z 42 are not expected from $\mathbf{2}^{\bullet+}$ and they are not present in the CID mass spectrum of the imidazole radical cation. Indeed, the m/z 68 ions from both $\mathbf{II}^{\bullet+}$ and imidazole are similar in the respect that there is almost no signal to be seen at m/z 42 and in terms of the relative abundances of the other fragments in their CID mass spectra; however, there are some notable differences between the two spectra: a considerably enhanced (5 % of total CID intensity) fragment peak at m/z 29 and a weak peak at m/z 16 is observed only in the spectrum of the ions from $\mathbf{II}^{\bullet+}$, which is an indication that these ions have a structure different from $\mathbf{1}^{\bullet+}$ or $\mathbf{3}^{\bullet+}$.

The existence of $\mathbf{1}^{\bullet+}$ and $\mathbf{2}^{\bullet+}$ is further endorsed by the CS mass spectral data in Table 5.2. Quite different intensity ratios for the dications at m/z $68^{++}/67^{++}/66^{++}$ are observed in all three spectra and in contrast to $\mathbf{3}^{\bullet+}$ the CS peaks are much more intense than the CID peaks for both of the new ions. The larger susceptibility of the ions $\mathbf{1}^{\bullet+}$ and especially $\mathbf{2}^{\bullet+}$ to charge-stripping is typical for ylide ions as compared to mundane

Table 5.2. Charge-stripping mass spectra of m/z 68 $[C_3H_4N_2]^{\bullet+}$ ions generated from $\mathbf{I}^{\bullet+}$, $\mathbf{II}^{\bullet+}$ and imidazole.[a]

Precursor	$\mathbf{I}^{\bullet+}$		$\mathbf{II}^{\bullet+}$		imidazole	
Spectrum	CS	NR/CS [b]	CS	NR/CS [b]	CS	NR/CS [b]
Ion						
68^{++}	100	100	100	100	100	94
67^{++}	5	40	9	39	33	100
66^{++}	2	10	2	5	8	30
CS Eff.[c]	0.60	0.48	1.11	1.02	0.32	0.17

[a] Relative abundance are from peak heights. [b] NR/CS refers to dications formed from neutralized ions (see text). [c] Charge-stripping efficiency as measured by the peak height ratio of 68^{++} relative to that of the nearby m/z 39 peak in the CID mass spectrum.

isomers [14]. The differences in the CS and CID mass spectra of the three isomers show that ions $\mathbf{1}^{\bullet+}$ and $\mathbf{2}^{\bullet+}$ do not easily isomerize to $\mathbf{3}^{\bullet+}$. Given that the fragmentation mechanisms of even the well-known ion $\mathbf{3}^{\bullet+}$ are still largely speculative [12], we avoid dwelling further on these differences. Thus, the three isomers can be differentiated by CID and CS mass spectrometry, therefore, it still remains to be demonstrated that the corresponding neutral molecules are stable in NRMS experiments.

When the individual NR mass spectra of distinguishable isomers match their respective CID mass spectra in appearance and contain observable recovery ion signals it is easy to conclude that the neutral molecules are stable. On this basis, the existence of **1** is strongly suggested since its NR mass spectrum (Figure 5.1a) contains both the signature peak at m/z 42, and as the base peak, the recovery signal at m/z 68. The evidence is less clear-cut for **2** because the relative intensities of the peaks in the NR mass spectrum are not quite the same as in the CID mass spectrum. Note, however, that the m/z 12-16 cluster patterns are unique and the weak but observable dication peaks denoted "++" in Figure 5.1 are very informative. The relative abundance of the dication at m/z 68^{++} is once again most noticeable for $\mathbf{2}^{\bullet+}$ and the largest peak that is attributed to a dication at m/z 67^{++} is again generated by $\mathbf{3}^{\bullet+}$. To probe the existence of **2** and **1** in more detail, the collision-induced dissociation behaviour of the reionized species with m/z 68 was investigated (see Figure 5.1). Note that this type of experiment, denoted as NR/CID, requires a multi-sector mass spectrometer and high sensitivity [7].

To assist direct comparisons of the m/z 68 ions, their NR/CID and CID mass spectra have been tabulated together in Table 5.1. An inspection quickly reveals the similarity of the NR/CID to the CID mass spectra for the three sets of ions, especially in regard to the key peaks at m/z 42 and 29. Scrutiny of the NR/CID mass spectra reveals that the m/z 40 peaks are likely diminished because of extensive fragmentation into smaller ions, which probably reflects a change to a higher internal energy distribution in the radical cations themselves after NR [7b]. This is consistent with the increased dissociation observed for the dications produced by charge-stripping of the m/z 68 ions

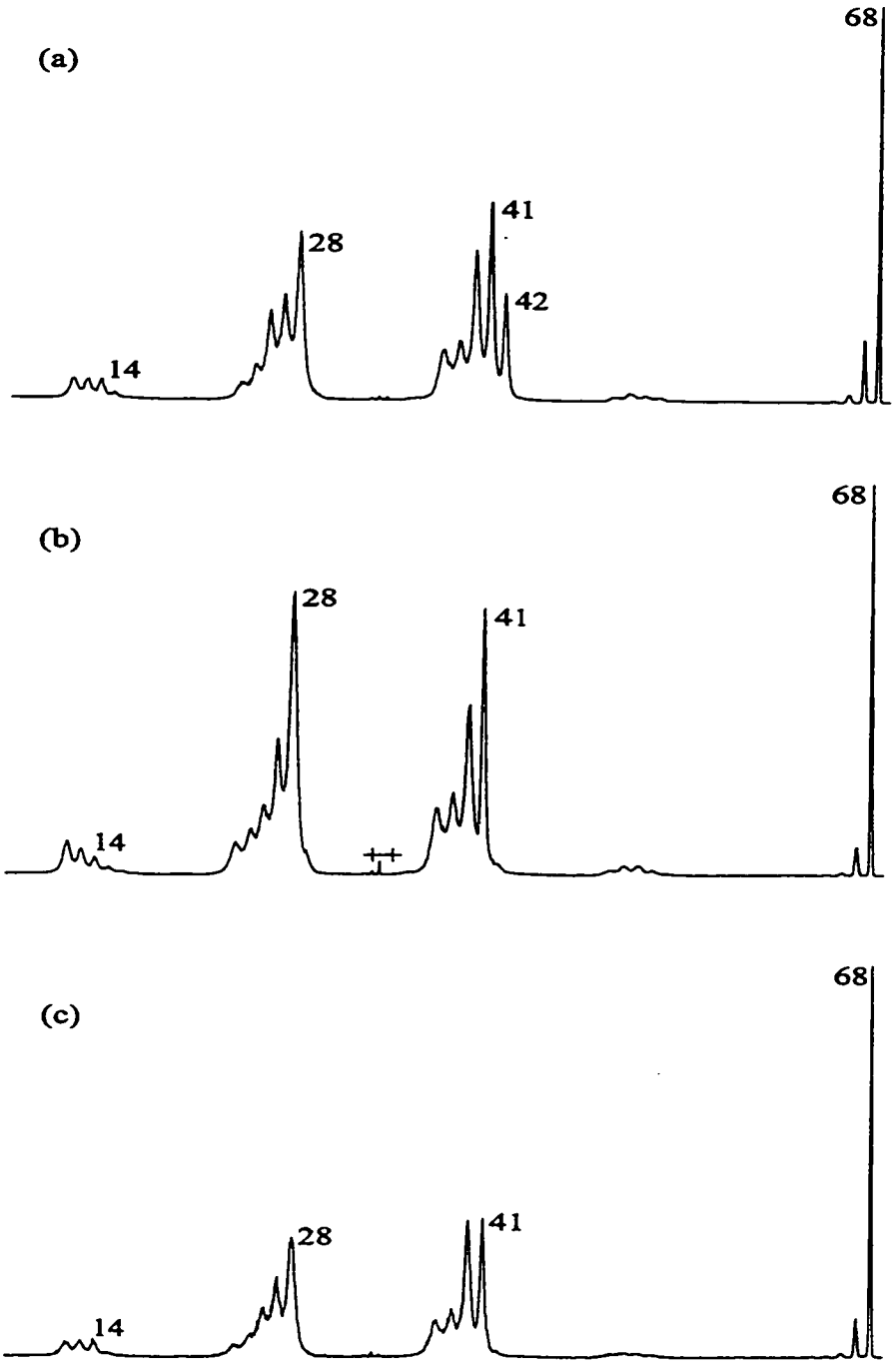

Figure 5.1: 10 keV NR mass spectra of the m/z 68 ions generated from (a) ionized imidazole-2-carboxaldehyde **I**, (b) ionized dimethyl imidiazole-4,5-dicarboxylate **II** and (c) ionized imidazole.

(see the NR/CS mass spectra in Table 5.2). Taking this into account, the CS efficiencies of the recovery ions and of the ions not subjected to NR are comparable. These facts lead to the conclusion that a significant portion of the neutral molecules **1** and **2** are able to survive structurally intact during the microsecond transit time between the neutralization and reionization cells in NRMS experiments.

In summary, the existence of imidazol-2-ylidene (**1**) and imidazol-4-ylidene (**2**), their radical cations and dications, have been demonstrated through tandem mass spectrometric experiments and are supported by high level quantum chemical calculations.

References

[1] For a review, see: J.A. Berson, D.A. Birney, W.P. Dailey and J.F. Liebman in *Modern models of bonding and delocalization* (Eds.: J.F. Liebman, A. Greenberg) VCH, Wienheim, **1987**. Recent attempts to identify C_2O_2 through mass spectrometry are summarized in: D. Schröder and H. Schwarz, *Int. J. Mass Spectrom. Ion Processes* **1995**, *146/147*, 183.

[2] Since the first isolation of "stable" carbenes: A.J. Arduengo III, R.L. Harlow and M. Kline, *J. Am. Chem. Soc.* **1991**, *113*, 361., the field has expanded rapidly and a précis of the "incredible renaissance" in this area can be found in: M. Regitz, *Angew. Chem. Int. Ed. Engl.* **1996**, *35*, 725 and M. Regitz, *Angew. Chem.* **1996**, *108*, 791.

[3] Reviews: a) H.-W. Wanzlick, *Angew. Chem.* **1962**, *74*, 129 and H.-W. Wanzlick, *Angew. Chem. Int. Ed .Engl.* **1962**, *1*, 75.
b) R.W. Hoffmann, *Angew. Chem. Int. Ed. Engl.* **1968**, *80*, 823 and R.W. Hoffmann, *Angew. Chem. Int. Ed. Engl.* **1968**, *7*, 754.
c) J. Hocker, R. Merten, *Angew. Chem. Int. Ed. Engl.* **1972**, *84*, 1022 and J. Hocker, R. Merten, *Angew. Chem. Int. Ed. Engl.* **1972**, *11*, 964.

d) M. Driess and H. Grützmacher, *Angew. Chem. Int. Ed. Engl.* **1996**, *108*, 900 and M. Driess, H. Grützmacher, *Angew. Chem. Int. Ed. Engl.* **1996**, *35*, 829.

[4] a) R. Gleiter and R. Hoffmann, *J. Am. Chem. Soc.* **1968**, *90*, 5457.

b) F. Geijo, F. Lopez-Calahorra and S. Olivella, *J. Heterocyclic Chem.* **1984**, *21*, 1785.

c) R. Grigg, L. Wallace and J.O. Morley, *J. Chem. Soc. Perkin Trans. 2* **1990**, 51.

d) D.A. Dixon and A. J. Arduengo III, *J. Phys. Chem.* **1991**, *95*, 4180.

e) A.J. Arduengo III, D.A. Dixon, D.A. Harlow, K.K. Kumashiro, C. Lee, W.P. Power and K.W. Zilm, *J. Am. Chem. Soc.* **1994**, *116*, 6361.

f) A.J. Arduengo III, H. Bock, H. Chen, M. Denk, D.A. Dixon, J.C. Green, W.A. Herrmann, N.L. Jones, M. Wagner and R. West, *J. Am. Chem. Soc.* **1994**, *116*, 6641.

g) J. Cioslowski, *Int. J. Quant. Chem., Quant. Chem. Symp.* **1993**, *27*, 309.

h) C. Heinemann and W. Thiel, *Chem. Phys. Letters* **1994**, *217*, 11.

i) C. Heinemann, T. Müller, Y. Apeloig and H. Schwarz, *J. Am. Chem. Soc.* **1996**, *118*, 2023.

j) C. Boehme and G. Frenking, *J. Am. Chem. Soc.* **1996**, *118*, 2039.

k) R.R. Sauers, *Tetrahedron Lett.* **1996**, *37*, 149.

l) A.J. Arduengo III, J.R. Goerlich and W.J. Marshall, *Liebigs Ann./Receuil,* **1997**, 305.

[5] a) R.W. Alder, P.R. Allen and S.J. Williams, *J. Chem. Soc., Chem. Commun.* **1995**, 1267.

b) A.J. Arduengo III, J.R. Goerlich and W.J. Marshall, *J. Am. Chem. Soc.* **1995**, *117*, 11027.

c) *Methoden der Organischen Chemie (Houben-Wey)*, 4th ed. 1952-, Bd. E19b, **1989**.

[6] Nitrene: a) G. Boche, P. Andrews, K. Harms, M. Marsch, K.S. Rangappa, M. Schimeczek and C. Willeke, *J. Am. Chem. Soc.* **1996**, *118*, 4925.

Fulvalene: b) T.A. Taton and P. Chen, *Angew. Chem. Int. Ed. Eng.* **1996**, *35*, 1101.

[7] a) G.A. McGibbon, C.A. Kingsmill and J.K. Terlouw, *Chem Phys. Letters* **1994**, *222*, 129.

b) G.A. McGibbon, P.C. Burgers and J.K. Terlouw, *Int. J. Mass Spectrom. Ion Processes* **1994**, *136*, 191.

c) T. Wong, J. Warkentin and J.K. Terlouw, *Int. J. Mass Spectrom. Ion Processes* **1990**, *115*, 33.

d) D.J. Lavorato, J.K. Terlouw, T. Dargel, W. Koch, G.A. McGibbon and H. Schwarz, *J. Am. Chem. Soc.* **1996**, *118*, 11898.

e) G.A. McGibbon, J. Hrušák, D.J. Lavorato, H. Schwarz and J.K. Terlouw, *Chem. Eur. J.* **1997**, *3*, 232.

[8] For a recent review, see: N. Goldberg and H. Schwarz, *Acc. Chem. Res.* **1994**, *27*, 347.

[9] V.Q. Nguyen and G. Turecek, *J. Mass Spectrom.* **1996**, *31*, 1173.

[10] *Gaussian94* (Revision B.3), M.J. Frisch, G.W. Trucks, H.B. Schlegel, P.M.W. Gill, B.G. Johnson, M.A. Robb, J.R. Cheeseman, T.A. Keith, G.A. Petersson, J.A. Montgomery, K. Raghavachari, J.B. Foresman, J. Cioslowski, B.B. Stefanov, A. Nanayakkara, M. Challacombe, C.Y. Peng, P.Y. Ayala, W. Chen, M.W. Wong, J.L. Andres, E.S. Replogle, R. Gomperts, R.L. Martin, D.J. Fox, J.S. Binkley, D.J. DeFrees, J. Baker, J.J.P. Stewart, M. Head-Gordon, C. Gonzales and J.A. Pople, Gaussian Inc., Pittsburgh PA, **1995**.

[11] According to the present calculations Frank-Condon type neutralization of the radical cations at their optimzed geometries results in vibrationally excited molecules **1-3**, but the energy deposited (9.9, 8.7, and 11.9 kcal/mol, respectively) is insufficient to enable their interconversion.

[12] a) J.H. Bowie, R.G. Cooks, S.O. Lawesson and G. Schroll, *Aust. J. Chem.* **1967**, *20*, 1613.
b) R. Hodges and M. Grimmet, *Aust. J. Chem.* **1968**, *21*, 1086.
c) K.J. Klebe, J.J. Houte and J. van Thuijl, *Org. Mass Spectrom.* **1971**, *5*, 1101.
d) J. van Thuijl, K.J. Klebe and J.J. Houte, *Org. Mass Spectrom.* **1972**, *6*, 1363.
e) G. Bouchoux and Y. Hoppilliard, *Org. Mass Spectrom.* **1977**, *12*, 196.
f) J. Main-Bobo, S. Olesik, W. Gase, T. Baer, A.A. Mommers and J.L. Holmes, *J. Am. Chem. Soc.* **1986**, *108*, 106.

[13] B.L.M. van Baar, Ph.D. Thesis, University of Utrecht, **1988**, Chapter 1.

[14] J.L. Holmes, F.P. Lossing, J.K. Terlouw and P.C. Burgers, *J. Am. Chem. Soc.* **1982**, *104*, 2931.

CHAPTER 6

Pyrazine Diradicals, Carbenes, Ylides and Distonic Ions Probed by Theory and Experiment

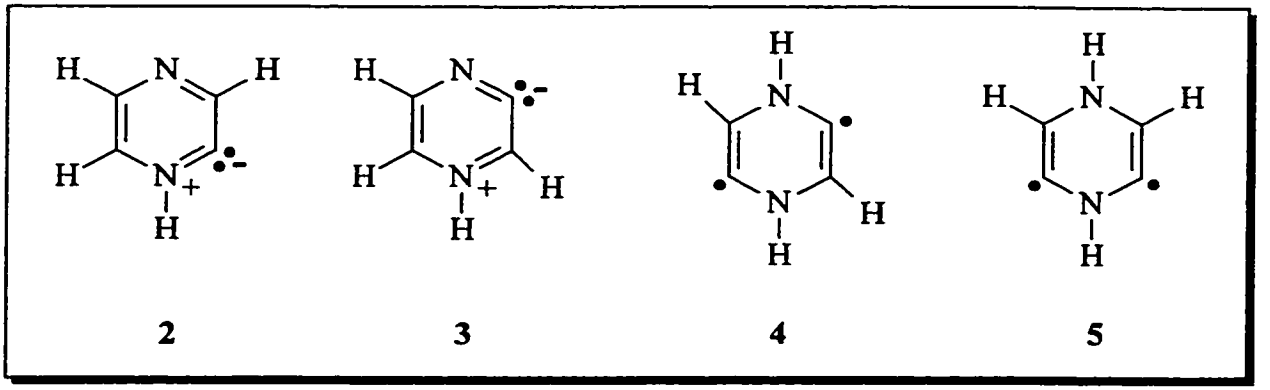

2 3 4 5

In this chapter, three hydrogen shift isomers of pyrazine (**1**) have been determined to be stable species in the gas phase using the technique of neutralization-reionization /collision-induced dissociation mass spectrometry. Included in this set of isomers are the two ylides, pyrazine-2-ylidene (**2**) and pyrazine-3-ylidene (**3**), and the 2,5-diradical of pyrazine **4**. The potential energy surface (PES) relating to pyrazine and its isomers has also been investigated computationally. The results indicate that all four neutral species as well as their corresponding radical cations, $\mathbf{1}^{\bullet+}$-$\mathbf{4}^{\bullet+}$, correspond to minima on the PES and are separated by sizable barriers. In addition, the 2,6-diradical of pyrazine **5** and its corresponding radical cation $\mathbf{5}^{\bullet+}$ have also been identified computationally and are predicted to be stable entities in the gas phase.

The work described here has been published previously in an article under the same title: T.K. Dargel, W. Koch, D.J. Lavorato, G.A. McGibbon, H. Schwarz, and J.K. Terlouw, Int. J. Mass Spectrom., 1999, 185/186/187, 925-930.

Introduction

There seems a near ubiquitous interest of chemists in nitrogen heterocycles. The biochemical importance of such species diminishes in no way the fascination of physical and organic chemists with their intrinsic structures, properties and dynamics [1,2]. In the latter context, desmotropy [3], the process of isolating individual tautomers or isomers, is an ever popular endeavor. The molecules most sought after in this respect are often those that represent classes of reactive intermediates, such as the carbene or ylide isomers of the imidazoles [4] that were eventually obtained by Arduengo and co-workers [5]. Sometimes, as is the case for the parent imidazolylidene ($C_3H_4N_2$) [6,7], the gas phase is the refuge of certain fugitive heterocyclic intermediates. The related thiazolylidene (C_3H_3NS) [8] and pyridinylidene (C_5H_5N) [7,9], are only a couple of many interesting species generated and characterized in the gas phase only via the technique of neutralization-reionization mass spectrometry (NRMS) [10,11]. Nevertheless, many other species exist only as "virtual molecules": viable according to sophisticated quantum chemical computations but experimentally unobserved.

The present work focuses on identifying molecules and radical cations in the [$C_4H_4N_2$] six-member ring system relating to pyrazine and its hydrogen-shift isomers. To this end, a combined experimental/computational approach was used relying on hybrid Hartree-Fock/density functional theory and a variety of tandem mass spectrometry experiments (metastable ion, collision-induced dissociation and neutralization-reionization mass spectrometry). Attention was directed particularly toward the neutral isomers of pyrazine **1** that are shown in Scheme 1: the α-ylide **2**, the β-ylide **3**, the 2,5-diradical **4** and the 2,6-diradical **5**.

Stationary points corresponding to neutral molecules **1** to **5** in the lowest singlet and triplet states, the corresponding doublet states of the radical cations [12] and the transition structures for their interconversions by 1,2-hydrogen shifts were located at the B3LYP/TZVP level of theory. In addition to **1**, three viable isomers **2** - **4** were experimentally generated through one-electron reduction of their radical cations in NRMS experiments [10]. Structure characterization of the ions and neutrals in this system is not

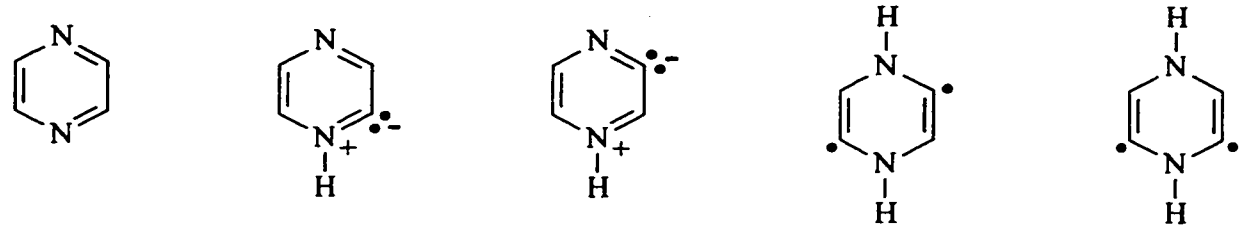

1 2 3 4 5

Scheme 6.1: $C_4H_4N_2$ species considered: pyrazine **1**, the α-ylide **2**, the β-ylide **3**, the 2,5-diradical **4** and the 2,6-diradical **5**.

facile and it proved advantageous to perform, specifically on the ions that survived the neutralization-reionization process, collision-induced dissociation experiments. These are denoted as NR/CID experiments [11].

Theoretical Procedure

The calculations of the structures, energies and frequencies were performed on IBM/RS6000 workstations and a CRAY Y-MP using the Gaussian 94 program package [13]. The accuracy of the hybrid density functional approach in this regard was previously demonstrated for pyridine and its ylide (see Chapter 2) by comparison of B3LYP with complete active space SCF (CASSCF) and highly correlated coupled cluster (CCSD(T)) type calculations [9,14]. In all cases, the CCSD(T) and B3LYP results were in very good agreement. Therefore, it was decided to use the B3LYP hybrid density functional theory (DFT) option employing Becke's [15] empirical three-parameter fit for mixing HF and DFT exchange-energy terms as implemented [16] in Gaussian 94 for the present study on the neutral and ionic $[C_4,H_4,N_2]$ species. All the neutral species and their respective radical cations are identified as genuine minima characterized by a positive definite Hessian matrix. Initial geometry optimizations were performed with the standard 6-31G** basis set [17]. Subsequently, Ahlrichs' polarized TZVP basis set [18] was used to improve the quality of the results. All data in the following correspond to B3LYP/TZVP geometries and energies corrected for zero-point vibrational energy (ZPVE) contributions. No scaling of the ZPVE

was performed for the B3LYP fundamentals. For the open shell species the unrestricted Kohn-Sham scheme was employed. The $<S^2>$ expectation value of the non-interacting Kohn-Sham determinant was in all cases very close to the exact values.

Results and Discussion

The computational strategy is very similar to the one described in Chapter 2 for the related hydrogen-shift isomers of pyridine [9,14] and the discussion can therefore be kept brief. Stable structures were computed for **1** - **5** as neutral molecules and radical cations. The computed total and zero-point vibrational energies are summarized in Table 6.1. The B3LYP/TZVP derived neutral and ionic $[C_4H_4N_2]$ potential energy surfaces are depicted in Figure 6.1.

As expected, pyrazine is the most stable species on the neutral potential energy surface. For the ylides **2** and **3**, the B3LYP energy differenes with respect to **1** amount to 45.2 and 65.0 kcal/mol using the TZVP basis set. For the less stable diradicals **4** and **5**, elevations above **1** of 83.5 and 89.6 kcal/mol, respectively, are obtained. The ground state singlet **1** (^1A_g) is calculated to be 70.8 kcal/mol more stable than the lowest lying triplet state ($^3B_{3u}$), compared to an experimental value of 76.7 kcal/mol [19]. For **2**, that is pyrazine-2-ylidene, the singlet-triplet energy gap is much smaller amounting to only 29.1 kcal/mol. By comparison, this energy difference is 35.6 kcal/mol for pyridine-2-ylidene [9] and 78 kcal/mol for imidazol-2-ylidene [20]. As radical cations, the isomers are more similar in stability, akin to the results obtained recently for the hydrogen-shift isomers of pyridine. The radical cation of pyrazine, $\mathbf{1}^{\bullet+}$ still represents the most stable isomer, but is followed by $\mathbf{3}^{\bullet+}$ (6.6 kcal/mol), $\mathbf{2}^{\bullet+}$ (12.7 kcal/mol), $\mathbf{4}^{\bullet+}$ (52.7 kcal/mol), and finally, $\mathbf{5}^{\bullet+}$ (49.1 kcal/mol). As indicated in Figure 6.1, there are large barriers connected to the 1,2-hydrogen shift transition states interconnecting the various isomers. In all cases, be it the neutral or the cationic potential surface, these barriers are higher than 40 kcal/mol. Thus, the calculations predict that the unimolecular spontaneous isomerization into the most thermodynamic stable isomer **1** or $\mathbf{1}^{\bullet+}$ will be hindered and under appropriate conditions all of these species should be observable in the gas phase.

Table 6.1: Total [E_h] and relative [E_{rel}, kcal/mol] energies for species **1-5** and $\mathbf{1}^{\bullet+}$-$\mathbf{5}^{\bullet+}$ as computed at B3LYP/TZVP. Relative intensities are corrected for zero-point vibrational energies (ZPVE).

Species	Singlet	ZPVE	E_{rel}	Triplet	ZPVE	E_{rel}
$C_4H_4N_2$						
1	-264.4031	48.0	0.0	-264.2835	43.7	70.8
2	-264.3311	48.0	45.2	-264.2814	45.9	74.3
3	-264.2973	46.6	65.0	-264.2917	46.0	67.9
4	-264.2693	47.5	83.5	-264.2320	45.5	104.9
5	-264.2602	47.9	89.6	-264.2366	46.0	102.6
TS 1/2	-264.2589	43.6	86.0	-264.1916	41.7	126.3
TS 2/3	-264.2031	43.1	120.6	-264.1883	42.4	129.2
TS 3/5	-264.1699	42.9	141.2	-264.1544	41.9	149.9
TS 4/5	-264.1619	43.0	146.3	-264.1480	42.6	154.4
TS 2/4	-264.1923	43.3	127.6	-264.1585	41.8	147.3

Species	Doublet	ZPVE	E_{rel}
$C_4H_4N_2^{\bullet+}$			
$\mathbf{1}^{\bullet+}$	-264.0668	46.1	0.0
$\mathbf{2}^{\bullet+}$	-264.0499	48.1	12.7
$\mathbf{3}^{\bullet+}$	-264.0601	48.4	6.6
$\mathbf{4}^{\bullet+}$	-263.9851	47.5	52.7
$\mathbf{5}^{\bullet+}$	-263.9916	47.9	49.1
TS $\mathbf{1}^{\bullet+}/\mathbf{2}^{\bullet+}$	-263.9561	43.0	66.4
TS $\mathbf{2}^{\bullet+}/\mathbf{3}^{\bullet+}$	-263.9298	43.8	83.7
TS $\mathbf{3}^{\bullet+}/\mathbf{5}^{\bullet+}$	-263.9077	43.5	97.3
TS $\mathbf{4}^{\bullet+}/\mathbf{5}^{\bullet+}$	-263.8793	43.1	114.7
TS $\mathbf{2}^{\bullet+}/\mathbf{4}^{\bullet+}$	-263.9132	43.5	93.9

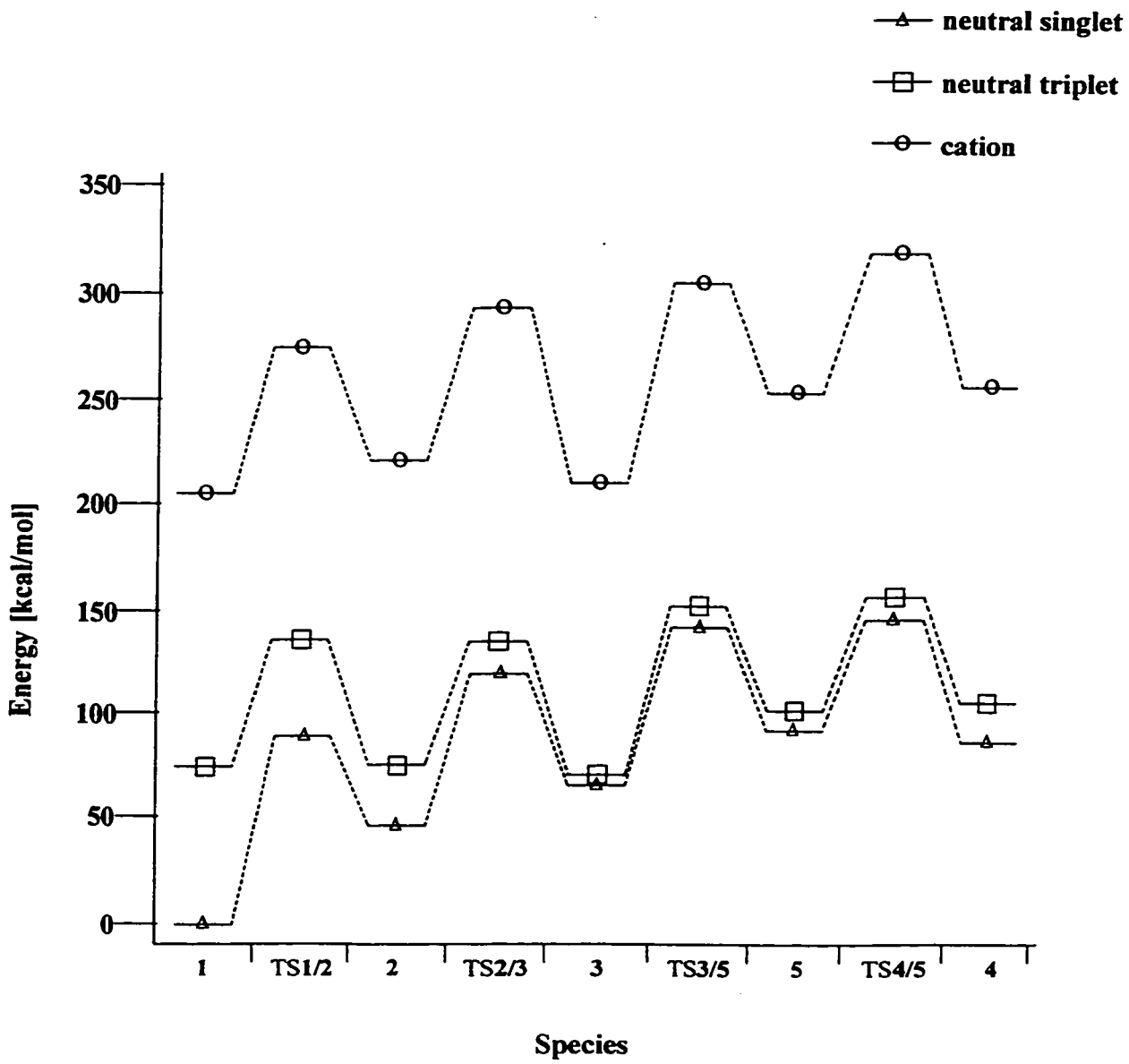

Figure 6.1: Potential Energy Surface for selected $C_4H_4N_2$ and $C_4H_4N_2^{\bullet+}$ isomers as computed at the B3LYP/TZVP level of theory.

Pyrazine and several of its derivatives have been investigated using tandem mass spectrometry methods [21] in the attempt to generate and characterize the $[C_4H_4N_2]$ isomers that the computations predicted would be stable in both their cationic and neutral forms. Generation of $\mathbf{1}^{\bullet+}$ is easily accomplished by electron ionization (EI) of pyrazine [22]. The other isomeric structures $\mathbf{2}^{\bullet+}$, $\mathbf{3}^{\bullet+}$ and $\mathbf{4}^{\bullet+}$ were anticipated from methyl pyrazine -2-carboxylate, dimethyl pyrazine-2,3-dicarboxylate and dimethyl pyrazine-2,5-dicarboxylate, respectively as summarized in Scheme 6.2 [9,14,23]. The structures of these potentially isomeric ions were first probed by metastable ion and collision-induced dissociation (CID) mass spectrometry experiments. The metastable ion results are summarized in Table 6.2 and the CID mass spectra are shown in Figure 6.2.

Pyrazine has been the subject of many mass spectrometry based investigations and a great deal of information is available about the ionization of **1** [22,24]. For $\mathbf{1}^{\bullet+}$ the dissociation reaction of lowest energy requirement is loss of HCN.[†] In fact, the metastable ion mass spectrum of each ion is dominated by a peak at m/z 53 that corresponds to [C,H,N] elimination. However, the kinetic energy release values ($T_{0.5}$) were obtained for the m/z 53 peaks [25] and found that they were not the same for all the ions (Table 6.2, values in parentheses). The differences reveal that $\mathbf{1}^{\bullet+}$ is certainly distinguishable prior to loss of [C,H,N], which is in agreement with the computed barrier height, $\mathbf{TS1}^{\bullet+}$-$\mathbf{2}^{\bullet+}$. Furthermore,

---

[†] Thermodynamic data other than the IP of pyrazine ions is apparently lacking a certain consensus since the appearance energy for $C_3H_3N^{\bullet+}$ ions is measured as 12.81 eV [22d], 13.00 [22b] and 11.97 (or 12.00 eV) [22a]. The latter value(s) used in conjunction with RRKM theory suggested a critical energy of 2.7 eV for HCN loss for ionized pyrazine and indicated a loose transition state consistent with rate determining ring cleavage. Direct fragmentation from an electronically excited state would have a high RRKM rate because of the low critical energy involved. The fact that the reaction takes place in the metastable time frame at energies > 2 eV above threshold, points to the participation of these states in dissociative ionization, followed by internal conversion to the electronic ground state rather than direct fragmentation from the ionized ground state. Buff and Dannacher [22a] stated: "With respect to the initially populated electronic states of the parent cation, we can thus conclude that excitation to high vibrational levels of the second electronic state or population of the third electronic state is required in order to dissociate pyrazine to $C_3H_3N^{\bullet+}$ + HCN".

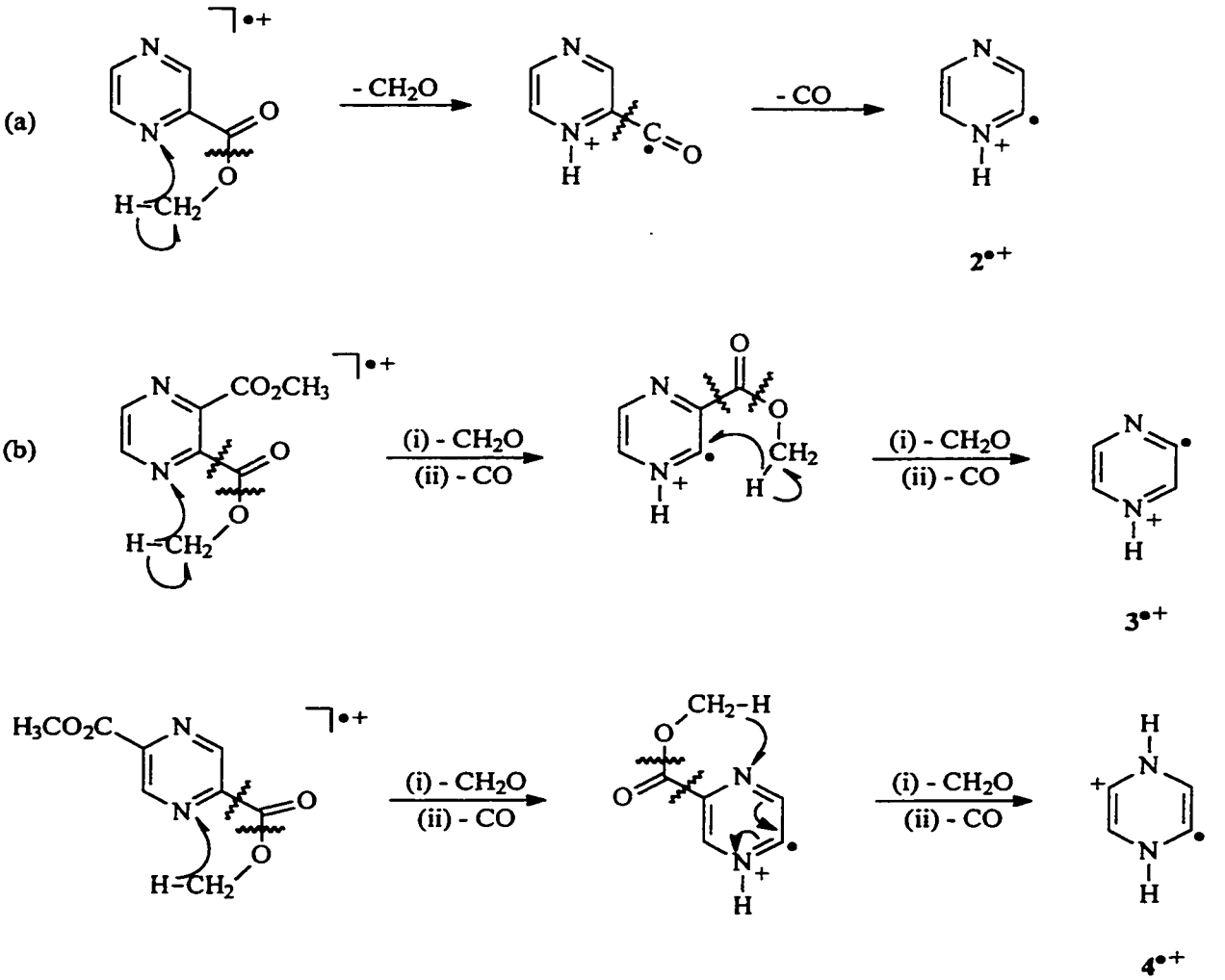

Scheme 6.2: Routes to generate (a) $2^{\bullet+}$ from ionized methyl pyrazine-2-carboxylate, (b) $3^{\bullet+}$ from ionized dimethyl pyrazine-2,3-dicarboxylate and (c) $4^{\bullet+}$ from ionized dimethyl pyrazine-2,5-dicarboxylate.

neither of these metastable ions communicate with the ion $4^{\bullet+}$; this is the only isomer that cannot eliminate HCN directly and it has the highest ratio of m/z 52 to m/z 53. Both $2^{\bullet+}$ and $3^{\bullet+}$ can eliminate HCN directly and the barrier separating them is predicted by the calculations to be quite a bit higher than $\mathbf{TS1}^{\bullet+}/2^{\bullet+}$ so the identical $T_{0.5}$ values for the ions generated from methyl pyrazine-2-carboxylate and dimethyl pyrazine-2,3-dicarboxylate might be an unusual coincidence. Alternatively, it could be indicative that $2^{\bullet+}$ and $3^{\bullet+}$ share a common (excited state) dissociation pathway or intermediate [25]. Discerning between

various possibilities would seem to require other types of experiments than ours [26].

Table 6.2 Metastable ion mass spectra of $C_4H_4N_2^{\bullet+}$ ions.

$C_4H_4N^{\bullet+}$ Ion	$\mathbf{1}^{\bullet+}$	$\mathbf{2}^{\bullet+}$	$\mathbf{3}^{\bullet+}$	$\mathbf{4}^{\bullet+}$
53	100	100	100	100
$(T_{0.5})$ [a]	(22.8)	(36.2)	(36.2)	(30.8)
52	2	5	10	20
29	-	-	-	2
28	-	2	4	3
26	2	2	3	-

[a] $T_{0.5}$ values are in meV and refers to the peak at m/z 53 (loss of H,C,N).

In CID experiments, the collision event gives the ions enough internal energy to isomerize but commonly dissociation takes place even more rapidly, i.e. before isomerization occurs. Thus, the differences between isomeric ions are more often manifested in CID mass spectra than MI mass spectra. However, gross spectral differences may not show up for collisionally activated ions $\mathbf{1}^{\bullet+}$-$\mathbf{4}^{\bullet+}$ since their basic similarity in ring structure leaves few unique dissociation channels available to the isomeric ions. Indeed, the CID mass spectra of the $C_4H_4N_2^{\bullet+}$ ions are similar to one another, but completely different from other known acyclic isomers [27]. However, an examination of the spectra in Figure 6.2 leaves no doubt though that the m/z 80 ions from the esters are not pyrazine radical cations $\mathbf{1}^{\bullet+}$. The latter ions are characterized by an intense m/z 26 fragment ion, consistent with the presence of the acetylene moiety (HCCH) embedded in the pyrazine ring. Furthermore, certain peaks are notably weak or by comparison they are more prominent in the spectra of the other isomer(s) e.g., m/z 28 ($HNCH^+$) and the doubly-charged ions at m/z 39.5 and m/z 40, which arise from charge-stripping. It should be noted though that the diagnostic use of the m/z 38-40 region is complicated by the juxtaposition of CID and

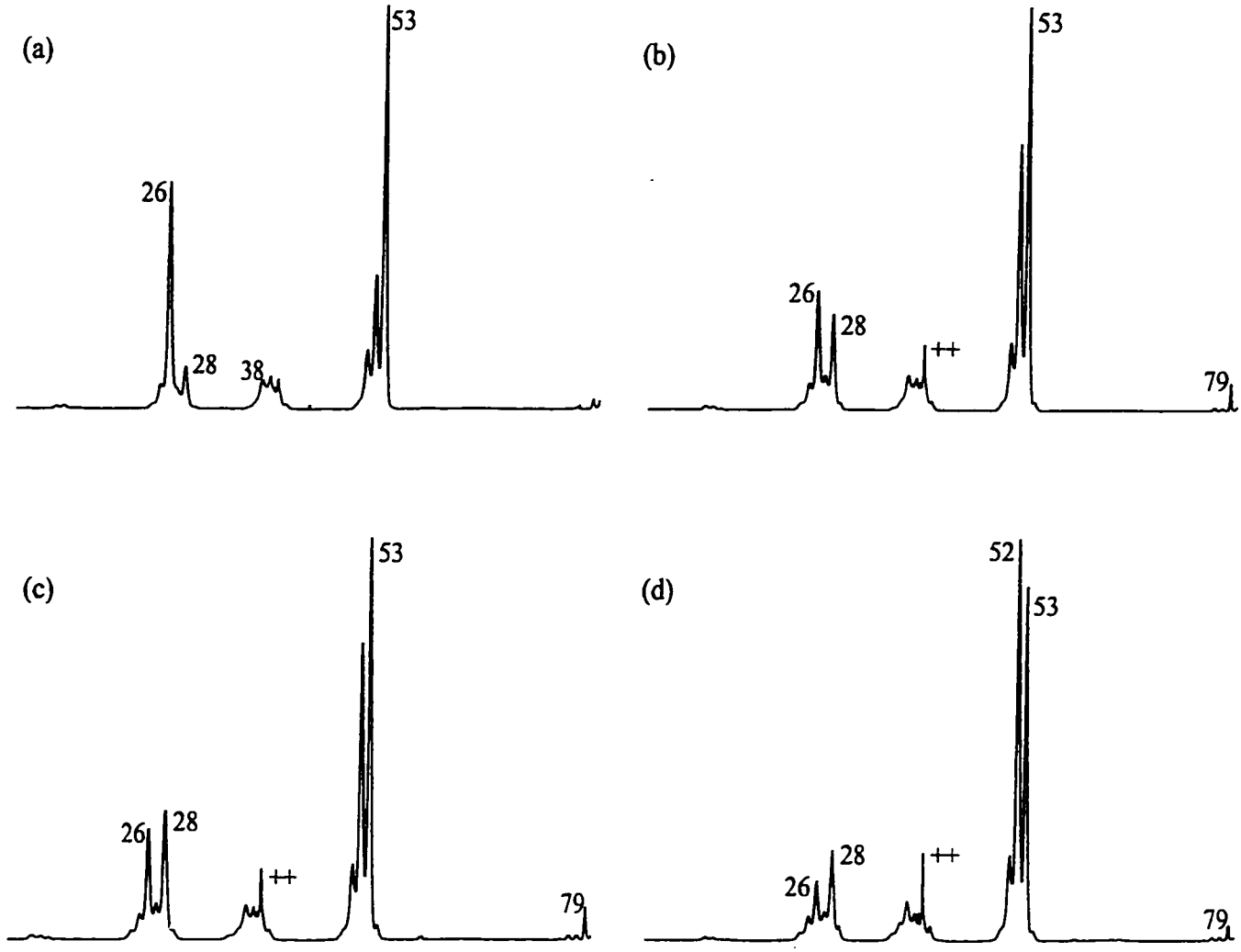

Figure 6.2: 10 keV CID (2ffr/O_2) mass spectra of $C_4H_4N_2^{\bullet+}$ ions (m/z 80) generated from ionized (a) pyrazine, (b) methyl pyrazine-2-carboxylate, (c) dimethyl pyrazine-2,3-dicarboxylate, and (d) dimethyl pyrazine-2,5-dicarboxylate.

charge-stripping peaks. Finally, the very weak cluster at m/z 12-15 appears to signal the presence or absence of C, CH, N and NH units to some extent. Even with these points in mind, the assignment of structures to the ions of Figure 6.2 (b-d) is challenging. However, the latter spectrum does show features consistent with the structure of ion $\mathbf{4}^{\bullet+}$, which would presumably rapidly oust the extant H-N=C-H segments as either charged or neutral fragments (loss of 28 amu). In accordance with this, note that m/z 52 is more intense than m/z 53 (loss of HCN/HNC) and the ratio of m/z 26 : 28 is the smallest for the ions from the 2,5-diester. According to the pathway suggested in Scheme 6.2, the m/z 81 ions of composition $C_4H_3DN_2$ produced from the CD_3 labelled monoester derivative of pyrazine should have the deuterium atom bonded to the nitrogen atom. If the unlabelled compound yielded ions $\mathbf{2}^{\bullet+}$ then these m/z 81 ions should be α-ylide cations that are isotopically substituted with deuterium on the nitrogen atom, which could be expected to fragment preferentially to $HCND^+$ (m/z 29) and other characteristic species. Indeed, the peak of m/z 28 is largely shifted to m/z 29 in the CID spectrum of the labelled ions but it is not feasible to assess the extent of H/D mixing prior to dissociation from an analysis of only these two spectra.

The neutralization-reionization (NR) mass spectra of the ions from the four precursors appear in Figure 6.3. They all contain abundant recovery signals at m/z 80 corresponding to stable $C_4H_4N_2$ molecules. It is further apparent that the NR mass spectra differ from one another, although their lack of close resemblance to the individual CID mass spectra makes any definitive statement about the neutral structures untenable at this juncture. The structural evidence provided by the m/z 12-15, 26, 28, 52 and 53 intensities is limited, but not altogether uninformative. For instance, the intense m/z 26 peak is featured again after NR of $\mathbf{1}^{\bullet+}$ and the m/z 52 : 53 ratio is still unique after NR of $\mathbf{4}^{\bullet+}$. However, the NR mass spectra of $\mathbf{2}^{\bullet+}$ and $\mathbf{3}^{\bullet+}$ are more similar to each other than their CID spectra. Some of the uncertainties in structure assignment can be obviated by obtaining the CID mass spectra of only the recovery ions, i.e. those m/z 80 ions that survived the process: $C_4H_4N_2^{\bullet+}$ → $C_4H_4N_2$ → $C_4H_4N_2^{\bullet+}$. The advantages and constraints of this approach have been previously discussed in the Introduction section.

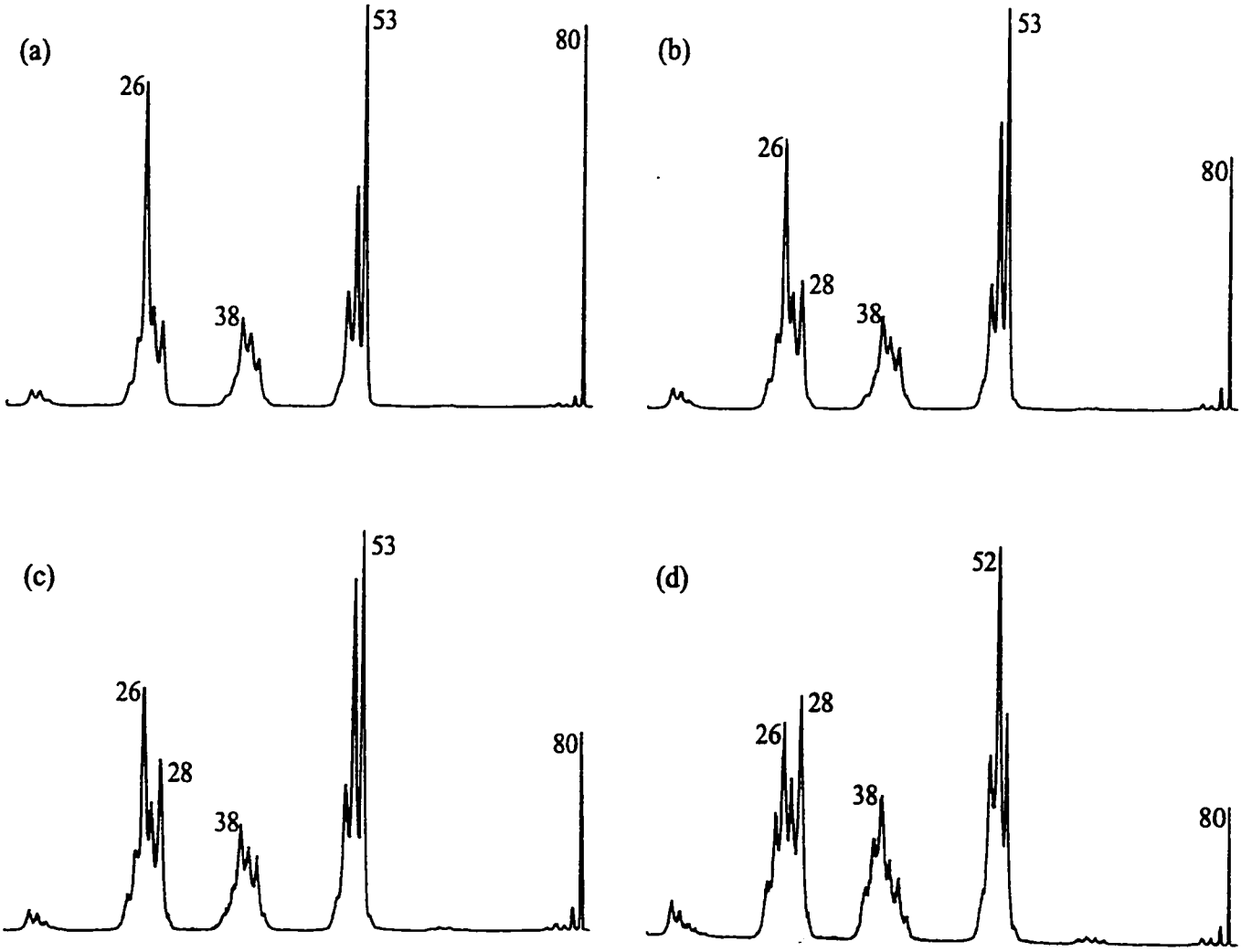

Figure 6.3: 10 keV NR (N,N-dimethylaniline/O_2) mass spectra of m/z 80 ions generated from ionized (a) pyrazine, (b) methyl pyrazine-2-carboxylate, (c) dimethyl pyrazine-2,3-dicarboxylate, and (d) dimethyl pyrazine-2,5-dicarboxylate.

For direct comparison, each NR/CID mass spectrum of reionized $C_4H_4N_2$ neutrals is shown paired with its corresponding third-field free region CID mass spectrum of source generated m/z 80 ions in Figure 6.4. A decisive trait shared by all sets is that each NR/CID spectrum is similar to the CID spectrum. The spectra of pyrazine ions are immediately distinguishable among the four sets of spectra. It also becomes apparent from an inspection of the pairs of spectra that the other ions still differ from one another after NR. The sets of spectra display characteristic m/z 26:28 ratios and except for the ions from dimethyl pyrazine-2,3-dicarboxylate they are the same within experimental uncertainty. As has been argued before [9], this similarity implies that the primary ion beam consisted almost entirely of a single isomeric species, which was neutralized and reionized without inducing isomerization of a substantial fraction of the ion or neutral population. The situation is more complicated for the ions from the remaining precursor since they appear to be altered following neutralization and reionization. The MI and CID peak ratios, especially 26:28:38, ensure that we have been dealing with at least four $C_4H_4N_2^{\bullet+}$ isomers. However, the m/z 80 ion flux obtained from dimethyl pyrazine-2,3-dicarboxylate may not be pure, i.e. consist of a single isomer. Simultaneous co-generation of $\mathbf{1}^{\bullet+}$ (a small amount) or $\mathbf{2}^{\bullet+}$ could explain the increase in m/z 26 following NR. Alternatively, the possibility that a portion of the ions $\mathbf{3}^{\bullet+}$ can isomerize to $\mathbf{1}^{\bullet+}$ or $\mathbf{2}^{\bullet+}$ after NR could be entertained. However, the stability of $\mathbf{3}^{\bullet+}$ and the high barriers (vide supra) make this less attractive than the co-generation option. Could neutrals **3** isomerize as well or instead? Remarkably, the β-ylide S_0 and T_0 energy surfaces are almost isoenergetic and the calculations indicate that Franck-Condon type reduction actually favours entry to the triplet state manifold. However, in neither case would ground state ions produce neutrals with sufficient energy to isomerize. Furthermore, the deep energy well on the ionic surface makes it unlikely that reionization from either state would give ions $\mathbf{3}^{\bullet+}$ that isomerize. To gain further insight another experiment was performed. The m/z 80 ions, which were produced by the spontaneous loss of CO from m/z 108 ions generated by dimethyl pyrazine-2,3-dicarboxylate in the ion source, were subjected to CID. The resulting (MI/CID) mass spectrum (not shown) was compared with the CID mass spectrum of source generated m/z 80 ions having the appropriate velocity. The

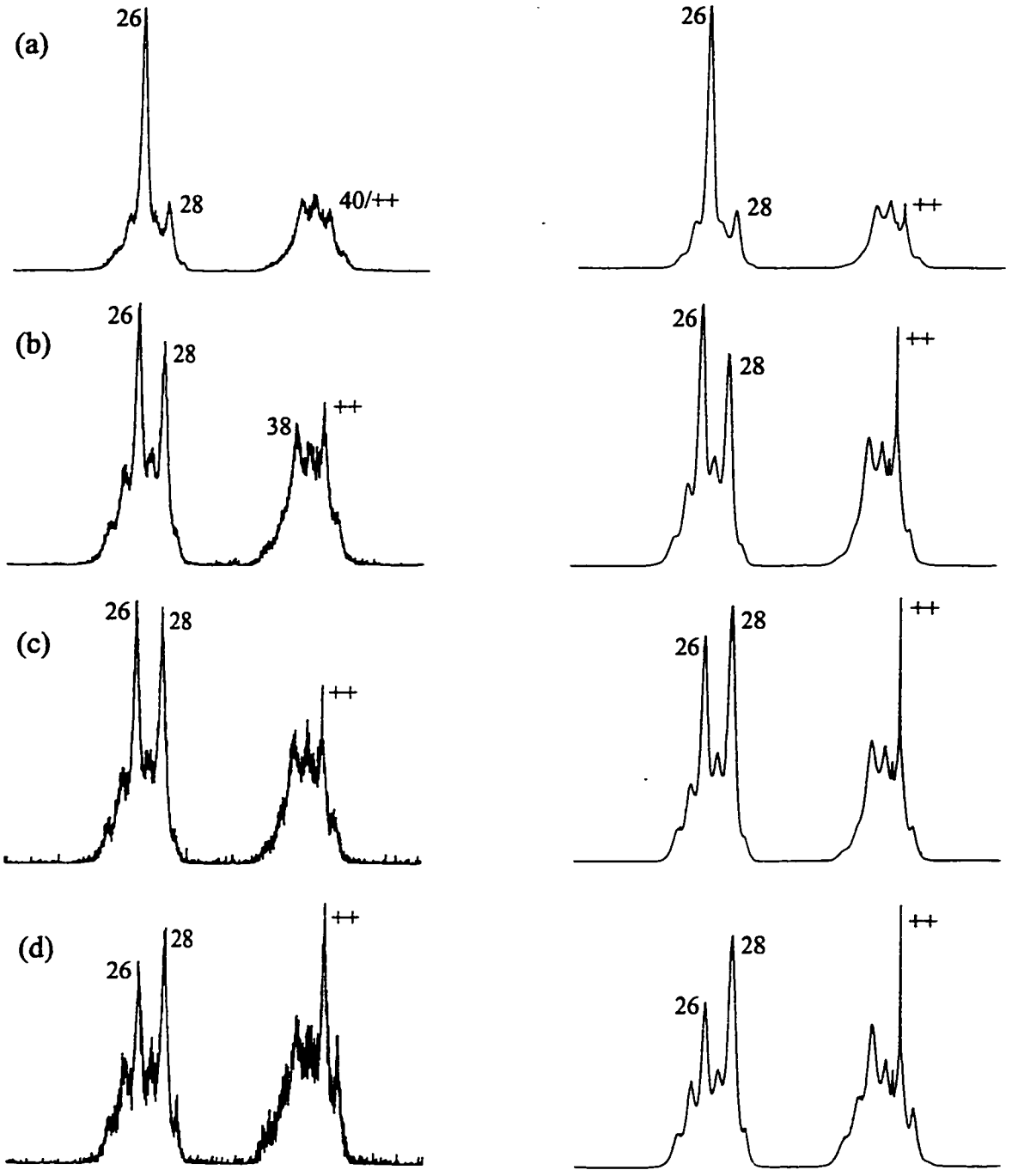

Figure 6.4: 10 keV NR/CID mass spectra (left) and comparative CID mass spectra (right) of the m/z 80 ions generated from ionized (a) pyrazine, (b) methyl pyrazine-2-carboxylate, (c) dimethyl pyrazine-2,3-dicarboxylate, and (d) dimethyl pyrazine-2,5-dicarboxylate.

metastable m/z 108 precursor ions will have a narrow distribution of internal energy and in fragmentation favor the production of the most stable products. The product m/z 80 ions in the MI/CID experiment are expected to be relatively cold and will only be able to isomerize post-collision. The MI/CID mass spectrum shows an increased m/z 26:28 ratio, which is thus consistent with the co-generation hypothesis wherein a small proportion (~10 %) of $\mathbf{1}^{\bullet+}$ is formed along with $\mathbf{3}^{\bullet+}$.

In summary, a combination of tandem mass spectrometry experiments and quantum chemical calcuations have allowed the generation and characterization of three new isomers of pyrazine as their solitary radical cations and neutral molecules. It is hoped that this study will provide impetus for future spectroscopic and matrix isolation studies.

References

[1] K.K. Innes, I.G. Ross and W.R. Moomaw, *J. Mol. Spectr.* **1988**, *132*, 492.

[2] J. Elguero, C. Marzin, A.R. Katritzky and P. Linda, *The Tautomerism of Heterocycles, Adv. Hetrocyclic Chem.*, Suppl. 1 Academic Press: New York, 1976.

[3] A German term used in NMR studies according to reference 2.

[4] H.-W. Wanzlick, Angew. *Chem. Int. Ed. Engl.* **1962**, *1*, 75.

[5] a) A.J. Arduengo III, R.L. Harlow, M.J. Kline, *J. Am. Chem. Soc.* **1992**, *114*, 5530.
b) M. Regitz, *Angew. Chem. Int. Ed. Engl.* **1996**, *35*, 725.

[6] G.A. McGibbon, D.J. Lavorato, C. Heinemann and H. Schwarz, *Angew Chem. Int. Ed. Eng.* **1997**, *36*, 1478.

[7] V.Q. Nguyen and F. Turecek, *J. Mass Spectrom.* **1996**, *31*, 1173.

[8] G.A. McGibbon, J. Hrušák, D.J. Lavorato, H. Schwarz and J.K. Terlouw, *Chem. Eur. J.* **1997**, *3*, 232.
b) G. Maier, *Angew. Chem* **1997**, *109*, 1788.
A stable thiazole ylide has just been reported in solution: A.J. Arduengo III, J.R. Goerlich and W.J. Marshall, *Liebigs Ann. Recl.* **1997**, 365.

[9] D.J. Lavorato, J.K. Terlouw, T.K. Dargel, W. Koch, G.A. McGibbon and H. Schwarz, *J. Am. Chem. Soc.* **1996**, *118*, 11898.

[10] N. Goldberg and H. Schwarz, *Acc. Chem. Res.* **1994**, *27*, 347.

[11] a) C.A. Shalley, G. Hornung, D. Schröder and H. Schwarz, *Chem. Soc. Rev.*, **1998**, *27*, 91.
b) C.A. Shalley, G. Hornung, D. Schröder and H. Schwarz, *Int. J. Mass Spectrom. Ion Processes* **1998**, *172*, 181.

[12] We also computed the lowest lying quartet states of the radical cations. However, they turned out to be too high in energy to be of any relevance and will therefore not be considered in this study.

[13] *Gaussian 94* (Revision B.3); M. Frisch, G.W. Trucks, H.B. Schlegel, P.M.W. Gill, B.G. Johnson, M.A. Robb, J.R. Cheeseman, T.A. Keith, G.A. Petersson, J.A. Montgomery, K. Raghavachari, M.A. Al-Laham, V.G. Zakrzewski, J.V. Ortiz, J.B. Foresman, C.Y. Peng, P.Y. Ayala, W. Chen, M.W. Wong, J.L. Andres, E.S. Replogle, R. Gomperts, R.L. Martin, D.J. Fox, J.S. Binkley, D.J. DeFrees, J. Baker, J.P. Stewart, M. Head-Gordon, C. Gonzales and J.A. Pople, Gaussian Inc., Pittsburgh PA, **1995**.

[14] D.J. Lavorato, J.K. Terlouw, G.A. McGibbon, T.K. Dargel, W. Koch and H. Schwarz, *Int. J. Mass Spectrom.* **1998**, *179/180*, 7.

[15] a) A.D. Becke, *J. Chem. Phys.* **1993**, *98*, 1372
b) A.D. Becke, *J. Chem. Phys.* **1993**, *98*, 5648.

[16] P.J. Stephens, F.J. Devlin, C.F. Chabalowski and M.J. Frisch, *J. Phys. Chem.* **1994**, *98*, 11623.

[17] For a competent review on these techniques, see: W.J. Hehre, L. Radom, P.v.R. Schleyer and J.A. Pople, *Ab Initio Molecular Orbital Theory*, Wiley Interscience, New York, **1986**.

[18] A. Shäfer, C. Huber and R. Ahlrichs, *J. Phys.* **1994**, *100*, 5829.

[19] K. Herzberg, *Molecular Spectra and Molecular Structure*, Vol. III, Krieger, Malabar, FL, **1991**.

[20] C. Heinemann, T. Müller, Y, Apeloig and H. Schwarz, *J. Am. Chem. Soc.* **1996**, *118*, 2023.

[21] K.L. Busch, G.L. Glish and S.A. McLuckey, *Mass Spectrometry/Mass Spectrometry, Techniques and Applications of Tandem Mass Spectrometry*, VCH, New York, **1988**.

[22] a) R. Buff and J. Dannacher, *Int. J. Mass Spectrom. Ion Processes* **1984**, *62*, 1.
b) L. Asbrink, C. Fridh, B.Ö. Jonsson and E. Lindholm, *Int. J. Mass Spectrom. Ion Phys.* **1972**, *8*, 229.
c) R. Gleiter, E. Heilbronner and V. Hornung, *Helv. Chim. Acta.* **1972**, *55*, 255.
d) J. Momigny, J. Urbain and H. Wankenne, *Bull. Soc. Roy. Sci. Liége* **1965**, *34*, 337.

[23] P.H. Chen, *J. Org. Chem.* **1976**, *41*, 2973.

[24] Ground state ionization requires 9.29 eV according to a ZEKE ($\nu = 74908\ cm^{-1}$) and several photoelectron spectroscopic measurements. We calculate for this process 9.15 eV.

[25] J.L. Holmes and J.K. Terlouw, *Org. Mass Spectrom.* **1980**, *15*, 383.

[26] High resolution spectroscopic measurements are desirable though CID emission measurements might suffice, see: J.L. Holmes, P.M. Mayer and A.A. Mommers, *Int. J. Mass Spectrom. Ion Processes* **1994**, *135*, 213.

[27] E.K. Chess, R.L. Lapp and M.L. Gross, *Org. Mass Spectrom.* **1982**, *17*, 475.

CHAPTER 7

Identifying Ylide Ions and Methyl Migrations in the Gas Phase: The Decarbonylation Reactions of Simple Ionized N-Heterocycles

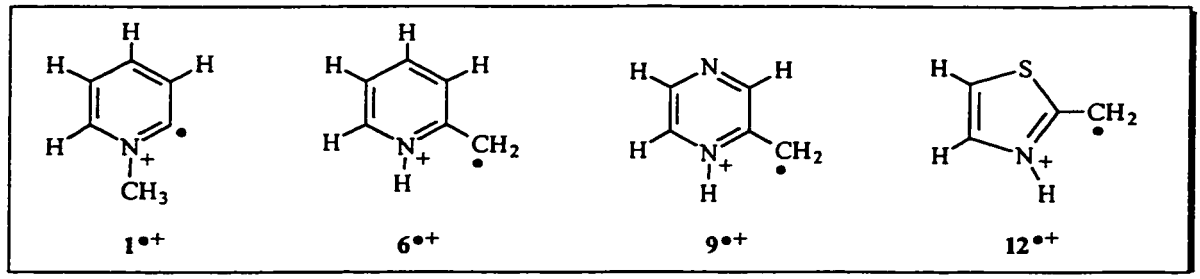

This Chapter describes the decarbonylation reactions of ionized 2-acetylpyridine, 2-acetylpyrazine and 2-acetylthiazole using a variety of mass spectrometric techniques. In particular, the structure of the resultant product ions have been identified as 2-methylene-1,2-dihydropyridine, $\mathbf{6}^{\bullet+}$, 2-methylene-1,2-dihydropyrazine, $\mathbf{9}^{\bullet+}$, and 2-methylene-2,3-dihydro-thiazole, $\mathbf{12}^{\bullet+}$, respectively. This result refutes proposals in the older literature that the decarbonylation would involve a methyl transfer yielding the 2-methyl substituted species. Literature proposals for a methyl transfer in the dissociation of ionized dimethyl pyridine-2,3-dicarboxylate and methyl pyridine-4-carboxylate were also examined, but could not be substantiated either. However, the proposed gas phase synthesis of the N-methylpyridinium ylide $\mathbf{1}^{\bullet+}$ did provide evidence for a genuine methyl migration.

Exploratory quantum chemical calculations indicate that $\mathbf{6}^{\bullet+}$ and $\mathbf{12}^{\bullet+}$ are among the most stable isomers in the $C_6H_7N^{\bullet+}$ and $C_4H_5NS^{\bullet+}$ systems. Their neutral counterparts, however, are considerably less stable : **6** is calculated to be 27 kcal/mol higher in energy than **2**. Nevertheless, from neutralization-reionization experiments it follows that the neutral counterparts of the ionized decarbonylation products **6**, **9**, and **12** are stable molecules on the microsecond timescale. Significant 1,3-hydrogen shift barriers hinder the interconversion of both the ions and the neutrals into their 2-methyl substituted counterparts, thus accounting for their stability in the dilute gas phase.

The results described in this Chapter have been submitted for publication in an article under the same title: David J. Lavorato, Lorne M. Fell, Graham A. McGibbon, Semia Sen, Johan K. Terlouw and Helmut Schwarz, Int. J. Mass Spectrom., 1999.

Introduction

A profusion of mass spectrometric methods is available for the determination of structures and elucidation of reaction pathways for gaseous ions and molecules [1]. Several of these, including tandem sector and Fourier transform ion cyclotron resonance (FT-ICR) mass spectrometries, have been aimed at characterizing six-membered ring containing N-heterocyclic $C_6H_7N^{\bullet+}$ isomers including the methyl pyridines **2**$^{\bullet+}$- **4**$^{\bullet+}$ [2] and the N- and 2-methylene pyridinium ylides **5**$^{\bullet+}$ and **6**$^{\bullet+}$ [3-6]. The recognition of six structural isomers was not precluded by the limited number of distinguishing features in collision-induced dissociation (CID) [7], charge-stripping (CS) and neutralization-reionization (NR) [8] mass spectrometry experiments [4-6]. However, despite the application of this battery of techniques and even chemometric methods of analysis [4,5], further innovation is still required to demonstrate to what extent the various isomeric ions may be capable of interconversion and to confirm that they have indeed stable (non-isomerizing) neutral counterparts for the less common C_6H_7N molecules. In this context, it should be noted that the radical cation, $C_5H_4NCH_3^{\bullet+}$, **1**$^{\bullet+}$, has appeared among several

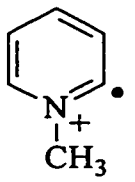

1$^{\bullet+}$

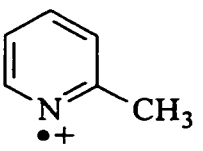

2$^{\bullet+}$

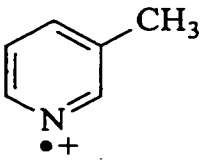

3$^{\bullet+}$

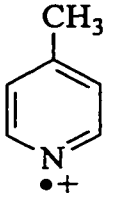

4$^{\bullet+}$

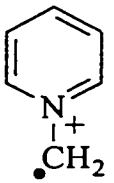

5$^{\bullet+}$

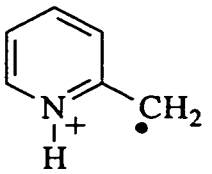

6$^{\bullet+}$

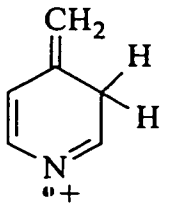

7$^{\bullet+}$

proposals accounting for the dissociation of 2-substituted pyridines by methyl group transfer [9,10]. Furthermore, loss of CO from ionized 2-acetylpyridine has been reported [11,12] but without any structural characterization of the product ion. In light of the attention devoted to the chemistry of other 2-keto pyridines [12] and related 2-carboxylic acid [13] and ester derivatives [14], it seems prudent to probe the $C_6H_7N^{\bullet+}$ (m/z 93) ions from 2-acetylpyridine.

There are additional systems immediately pertinent to the study of methyl migrations and structures of N-heterocycles. For example, closely related to the methyl pyridine radical cations are ionized methylpyrazine, **8**$^{\bullet+}$, and two of its distonic isomers, the 2-methylene pyrazinium ion **9**$^{\bullet+}$, and the 5-methylpyrazinium ion **10**$^{\bullet+}$. Another consists of the set of isomeric $C_4H_5NS^{\bullet+}$ species including ionized 2-methylthiazole, **11**$^{\bullet+}$, the methylene dihydrothiazoles, **12**$^{\bullet+}$ and **13**$^{\bullet+}$, and the N-methyl and S-methyl ylide ions, **14**$^{\bullet+}$ and **15**$^{\bullet+}$.

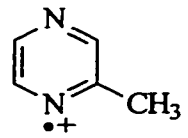

8$^{\bullet+}$

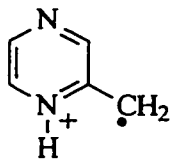

9$^{\bullet+}$

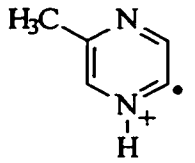

10$^{\bullet+}$

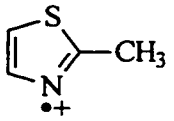

11$^{\bullet+}$

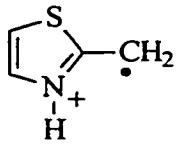

12$^{\bullet+}$

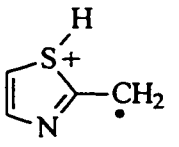

13$^{\bullet+}$

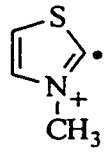

14$^{\bullet+}$

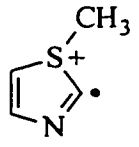

15$^{\bullet+}$

As a means to obtain additional structural and mechanistic insight on these N-heterocycles, we have employed the multiple collision technique of neutralization-

reionization/collision-induced dissociation (NR/CID) mass spectrometry [15]. The application of NR/CID as a structural assignment tool offers advantages in systems where isomeric ions (and neutrals) are not easily distinguished by the separate application of either CID and/or NR mass spectrometry. This may occur for several reasons: (i) mixtures of ions may be generated from ionized precursor molecules, (ii) the isomeric ions (or neutrals) may interconvert either spontaneously or as a result of the collision process prior to fragmenting, (iii) the ions may access only a limited number of dissociation channels, which do not result in fragment ions bearing unique mass-to-charge values, or (iv) in NR experiments reionized neutral fragments may interfere. The third scenario may often be interrogated by performing MS/MS experiments, and through isotopic labelling experiments, whereas the occurrence of the first two is usually more difficult to identify.

With this in mind, we report here an analysis of CID and NR/CID experiments on the above mentioned systems aided by selected *ab initio* calculations. Literature proposals involving methyl migration in substituted pyridine, pyrazine [16] and thiazole [17] radical cations have also been re-examined. On one hand, we were not able to find support for an earlier postulate for methyl transfer in the dissociation of dimethyl-2,3-pyridinedicarboxylate but on the other hand found evidence of the missing N-methylpyridinium ylide ion $\mathbf{1}^{\bullet+}$ [10]. The decarbonylation of ionized 2-acetylpyrazine and 2-acetylthiazole appears to proceed analogously to that of the 2-acetylpyridine ion, yielding the 2-methylene radical cation derivatives rather than the 1-methyl or 2-methyl substituted species.

Computational Methods

The computations were performed with the Gaussian 94 series of programs [18] on workstations at the TU-Berlin and McMaster University. Geometries were optimized using the standard basis set 6-31G* and vibrational frequencies estimated with the popular hybrid density functional method B3LYP [19], employing Becke's empirical three-parameter fit for mixing the Hartree-Fock and density functional exchange terms.

All structures had no negative eigenvalues, and the data presented are corrected for zero-point vibrational energy (ZPVE) contributions. The ZPVE were scaled by a factor of 0.9806 [20] for the B3LYP fundamentals. The $<S^2>$ expectation value of the non-interacting Kohn-Sham determinant was in all cases very close to the exact values.

Results and Discussion

Generation and characterization of C_6H_7N isomers.

As first reported by Ferretti and co-workers [11a], dissociative electron ionization (EI) of 2-acetylpyridine produces in its normal mass spectrum ions at m/z 93 by the loss of CO. To investigate the structure of the resulting $C_6H_7N^{\bullet+}$ ions, i.e. to differentiate these ions from their isomers, the technique of collision-induced dissociation was employed. Seven cyclic $C_6H_7N^{\bullet+}$ isomers were generated via EI of the appropriate substituted pyridine precursors. The cations $\mathbf{2}^{\bullet+}$ - $\mathbf{4}^{\bullet+}$ were realized by simple electron ionization of their neutral counterparts while $\mathbf{1}^{\bullet+}$, $\mathbf{5}^{\bullet+}$, $\mathbf{6}^{\bullet+}$ and $\mathbf{7}^{\bullet+}$ were obtained by dissociative EI of methyl pyridine-2-thiocarboxylate [10], bis(ethoxycarbonyl)pyridinium methylide [5,21], 2-propylpyridine [5], and 4-pyridylacetic acid, respectively.

The CID mass spectra of the putative ions $\mathbf{1}^{\bullet+}$ - $\mathbf{7}^{\bullet+}$ obtained in the third field free region of the three sector magnetic deflection instrument, are presented in Figure 7.1. In basic agreement with the study of Flammang and co-workers [5], the spectra of the 2-methylpyridine ion $\mathbf{2}^{\bullet+}$ (Figure 7.1a) and its methylene isomer $\mathbf{6}^{\bullet+}$ (Figure 7.1b) are similar but they do exhibit characteristic differences [22]. Perhaps the most structure diagnostic of these is the CH_2 loss peak at m/z 79 in the spectrum of the 2-methylene isomer $\mathbf{6}^{\bullet+}$. Furthermore, several fragment ion clusters show differences in their relative abundance: for example the m/z 26 ($C_2H_2^{\bullet+}$) : 28 (CH_2N^+) peak intensity ratio is 1.5 for $\mathbf{2}^{\bullet+}$ and 0.8 for $\mathbf{6}^{\bullet+}$. The enhanced m/z 28 (H-C≡N-H$^+$) intensity is characteristic of a pyridine ring bearing a N-H moiety [15,23]. The more intense charge stripping peak (++) at m/z 46.5 in Figure 7.1b is further revealing of the ylide structure of $\mathbf{6}^{\bullet+}$.

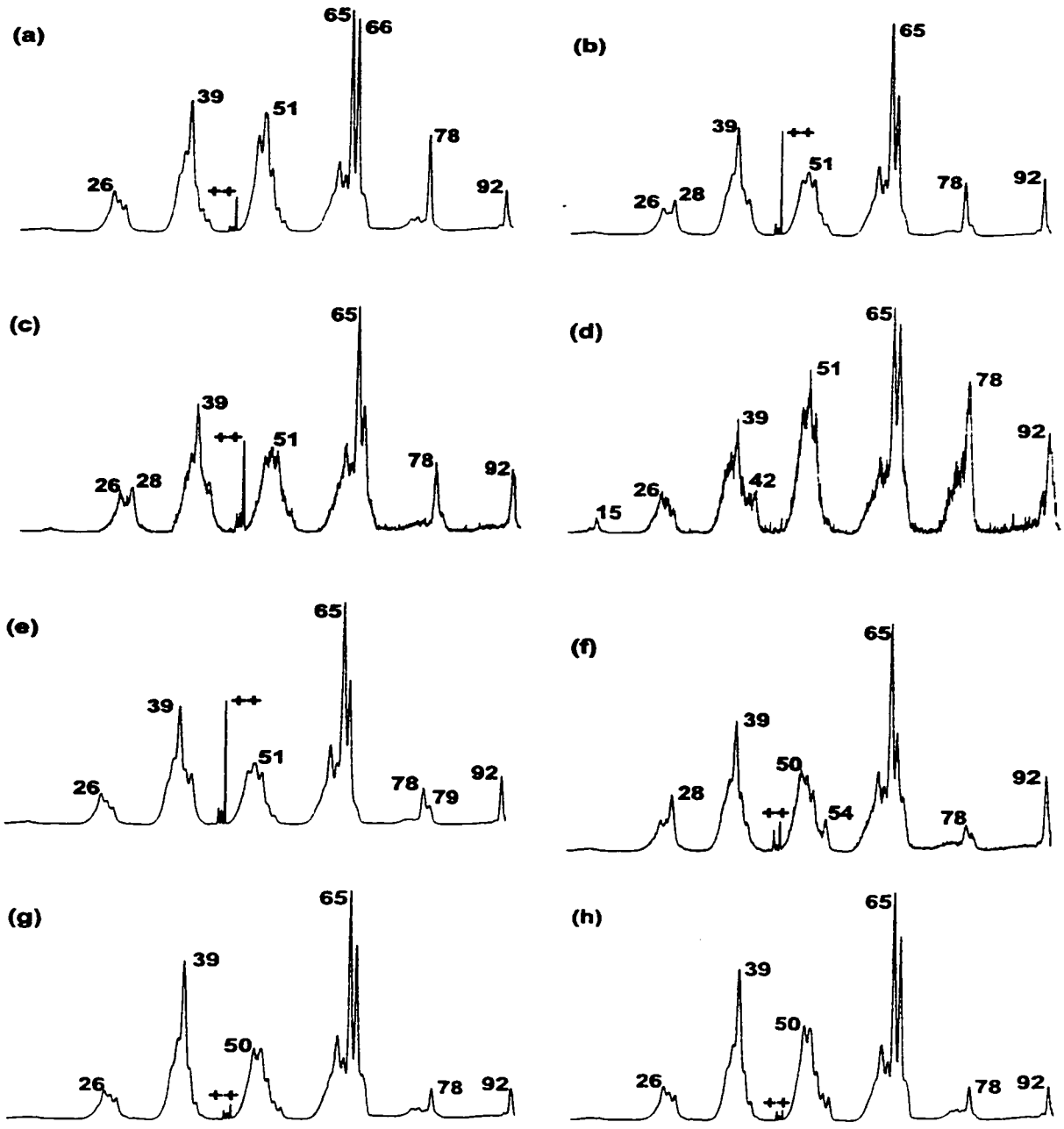

Figure 7.1: CID mass spectra (3ffr, 7 keV ions, collision gas O_2) of $C_6H_7N^{\bullet+}$ (m/z 93) ions generated from (a) ionized 2-methylpyridine, (b) ionized 2-acetylpyridine or 2-propylpyridine, (c) metastable 2-acetylpyridine ions (d) metastable methyl pyridine-2-thiocarboxylate ions, (e) ionized bis(ethoxycarbonyl)pyridinium methylide, (f) metastable 4-pyridylacetic acid ions, (g) ionized 3-methylpyridine, and (h) ionized 4-methylpyridine.

The N- methylene ylide ion $\mathbf{5}^{\bullet+}$ (Figure 7.1e) is characterized by an even lower m/z 78 (- CH_3) : 79 (- CH_2) peak intensity ratio, a result of the N-C bond proffered for cleavage. The arguments presented above also account for its fairly high m/z 26 : 28 peak intensity ratio, 1.75, and the intense charge stripping peak at m/z 46.5.

The remaining isomers of conventional structure, 3- and 4-methylpyridine ($\mathbf{3}^{\bullet+}$ and $\mathbf{4}^{\bullet+}$) exhibit, see Figures 7.1g and 7.1h, only weak doubly-charged ion peaks and they are easily distinguished from $\mathbf{2}^{\bullet+}$ on the basis of the reduced m/z 78 intensity [2], as is also observed in their normal mass spectra. However, differentiation of $\mathbf{3}^{\bullet+}$ and $\mathbf{4}^{\bullet+}$ on the basis of their CID mass spectra is clearly not possible.

The decarbonylation reaction of the 2-acetylpyridine ion has been proposed to yield ion $\mathbf{1}^{\bullet+}$, via a 1,3 methyl shift to the ring nitrogen [12]. However, the source generated product ions yield a CID mass spectrum which is superimposable upon that of Figure 7.1b, indicating that the ion generated is $\mathbf{6}^{\bullet+}$. Next, the structure of the m/z 93 ions generated from metastable 2-acetylpyridine ions was probed. The metastable ion/collision-induced dissociation sequence provides a MI/CID mass spectrum, Figure 7.1c, identical to the CID mass spectrum of the source generated ions, Figure 7.1b, thus indicating that the decarbonylation yields isomerically pure ions $\mathbf{6}^{\bullet+}$. A possible mechanism for its generation from ionized 2-acetylpyridine ($\mathbf{I}^{\bullet+}$) is presented in Scheme 7.1 along with that proposed earlier for its generation from ionized 2-propylpyridine ($\mathbf{II}^{\bullet+}$) [5,12]. In both cases the initial step involves the transfer of a hydrogen radical to the ring nitrogen. For 2-propylpyridine this is followed by C_2H_4 loss via a McLafferty rearrangement while 2-acetylpyridine, decarbonylates by an ipso [24] type rearrangement.

We further note that the decarbonylation reaction is associated with a large reverse activation energy. Metastable 2-acetylpyridine ions lose CO with a kinetic energy release of 890 meV but this process is in competition with the loss of CH_2=C=O (metastable peak intensity ratio 10 : 1). The loss of ketene yields the α-ylide ion of pyridine and the activation energy for this process is ~ 26 kcal/mol [15]. A similar value must obtain for the decarbonylation but its calculated minimum energy requirement is 44

kcal/mol lower [25] and thus this process is indeed characterized by a high reverse activation energy.

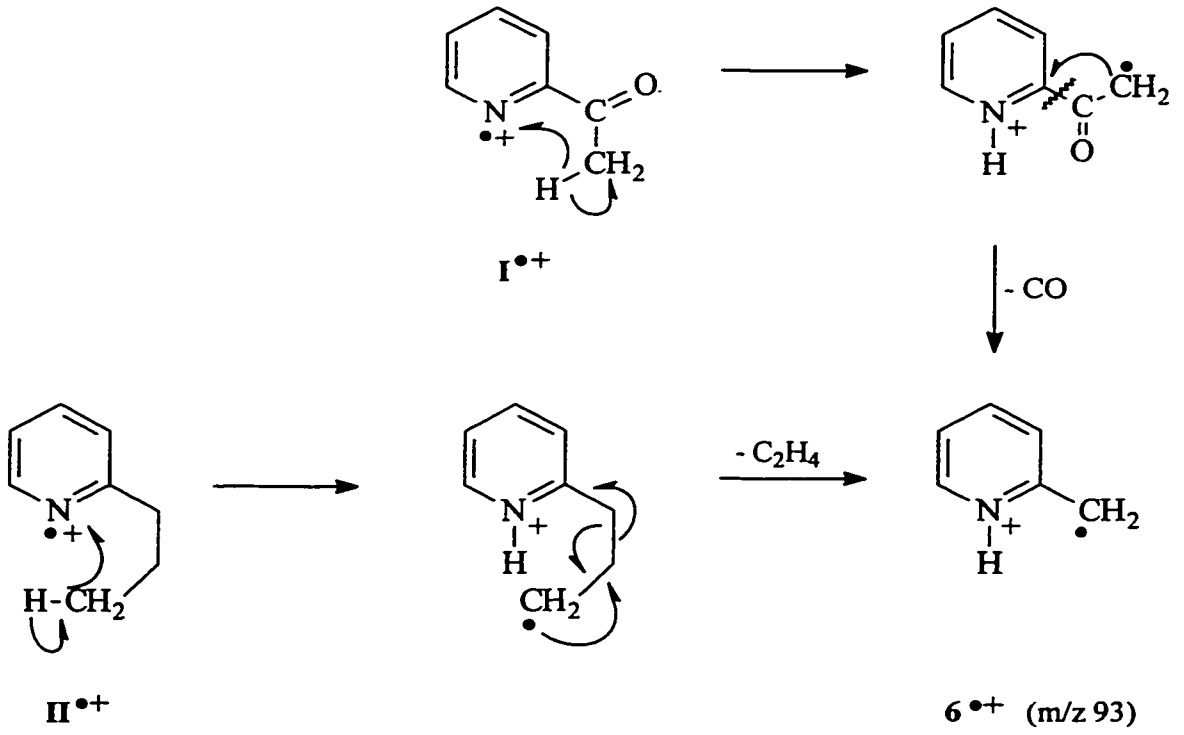

Scheme 7.1

Evidence for a true methyl migration was eventually obtained, thereby validating the (unverified) proposal by Budzikiewicz and co-workers [10] for the formation of the N-methyl ylide ion $\mathbf{1}^{\bullet+}$ from ionized methyl pyridine-2-thiocarboxylate, $\mathbf{III}^{\bullet+}$, as depicted in Scheme 7.2. Ions $\mathbf{1}^{\bullet+}$ are abundantly generated from the low energy (metastable) ions $\mathbf{III}^{\bullet+}$ by loss of COS. The CID mass spectrum (Figure 7.1d) of these ions is characterized by an intense $CH_3^{\bullet}$ loss (m/z 78) and tell-tale peaks at m/z 42 (CH_3NCH^+) and m/z 15 (CH_3^+). In the d_3-methyl isotopomer, m/z 42 is shifted to m/z 45 and m/z 15 to m/z 18, confirming the transfer of the intact methyl group.

Budzikiewicz [10] also proposed a methyl migration in the formation of the m/z 93 $C_6H_7N^{\bullet+}$ ions from dimethyl pyridine-2,3-dicarboxylate ions, $\mathbf{IV}^{\bullet+}$, as depicted in Scheme 7.2. However, loss of CO_2 from m/z 137 does not figure in either the MI or the CID mass spectrum of the m/z 137 ions in Scheme 7.2. Moreover, high resolution measurements showed that the *source* generated m/z 93 ions largely consist of $C_5H_3NO^{\bullet+}$ ions with only a small contribution of $C_6H_7N^{\bullet+}$. Corroborating this, the mass spectrum of the d_6-dimethyl isotopomer displays peaks at m/z 93 ($C_5H_3NO^{\bullet+}$) and m/z 97 ($C_6H_3D_4N^{\bullet+}$), with a ratio of 4 : 1. The CID mass spectrum of the labelled m/z 97 ions was obtained and despite the lack of reference spectra, it does indicate that a clean generation of the product ion shown in Scheme 7.2 is highly improbable.

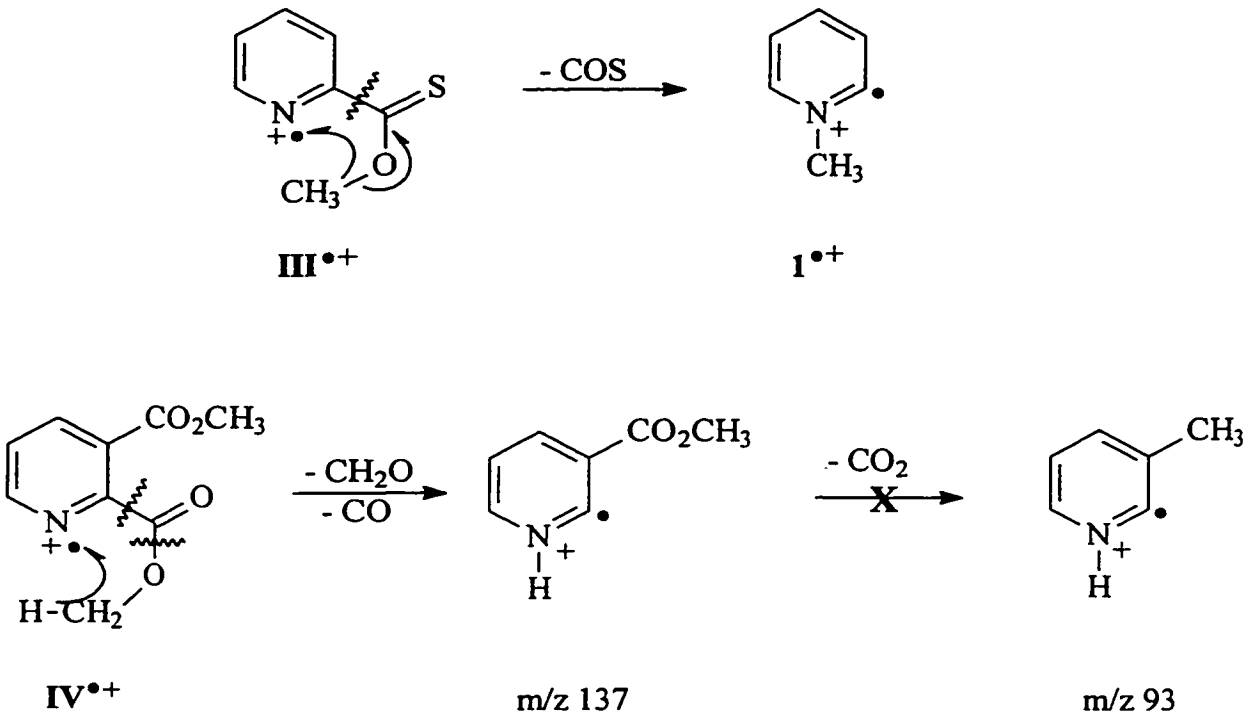

$\mathbf{III}^{\bullet+}$ $\mathbf{1}^{\bullet+}$ $\mathbf{IV}^{\bullet+}$ m/z 137 m/z 93

Scheme 7.2

The remaining isomer studied, $7^{\bullet+}$, was generated from ionized 4-pyridylacetic acid, $\mathbf{V}^{\bullet+}$, as depicted in Scheme 7.3. Careful analysis of spectra obtained at various ion source temperatures indicated that the source generated ions of putative structure $7^{\bullet+}$ were contaminated with 4-methylpyridine ions $4^{\bullet+}$ originating from thermal decarboxylation of the parent acid. An unadulterated ensemble of ions $7^{\bullet+}$ could be obtained from the unimolecular dissociation of metastable 4-pyridylacetic acid molecular ions. Their CID mass spectrum, see Figure 7.1f, is characterized by the lowest m/z 26 : 28 peak intensity ratio of the set, 0.63, and a relatively intense peak at m/z 79 (- CH_2) adjacent to a weak m/z 78 (- CH_3) signal. The presence of charge stripping peaks at m/z 46.5 and 45.5 of comparable abundance completes its structure characterization.[†]

To document another proposed methyl migration, the $C_6H_7N^{\bullet+}$ ions produced from methyl pyridine-4-carboxylate ($\mathbf{VI}^{\bullet+}$) were examined. In 1972, Neeter and Nibbering

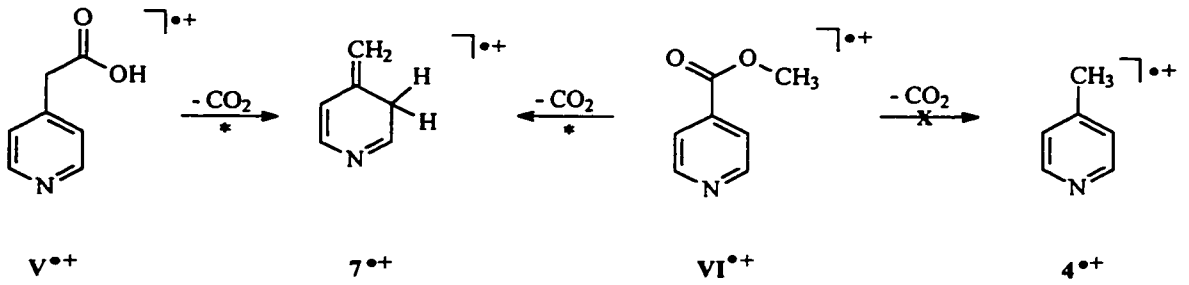

$\mathbf{V}^{\bullet+}$ $7^{\bullet+}$ $\mathbf{VI}^{\bullet+}$ $4^{\bullet+}$

Scheme 7.3

[†] Ions $7^{\bullet+}$ do not contain a pyridine ring bearing a N-H moiety. Nevertheless, the m/z 28 (H-C≡N-H$^+$) ion intensity is enhanced in the CID spectrum and this has led a reviewer to propose that ions $7^{\bullet+}$ are ionized 4-methylene-1,4-dihydropyridine. This possibility cannot be excluded, but we note that our proposal is based upon the structure diagnostic peak at m/z 54, rationalized by Flammang *et al.* [5] to originate from the direct bond cleavage $7^{\bullet+} \rightarrow$ H-C≡N-CH=CH_2^+ + H-C≡C-$CH_2^{\bullet}$. From a MS/MS spectrum and comparison with reference spectra [27] we conclude the m/z 54 ions likely have the proposed structure. Moreover, their major CID dissociation involves loss of C_2H_2 and formation of m/z 28 (H-C≡N-H$^+$) and this may explain the enhanced m/z 28 intensity in the spectrum of $7^{\bullet+}$.

[28] postulated that the decarboxylation of $\mathbf{VI}^{\bullet+}$ in the metastable time frame yields the 4-methylpyridine ion, see Scheme 7.3. However, we surmise that this is not the case since the resulting MI/CID mass spectrum of the product ion (not shown) is virtually identical with that presented in Figure 7.1f, indicating that $\mathbf{7}^{\bullet+}$ is the isomer produced. High resolution experiments showed that the *source* generated m/z 93 ions consist of a 1:1 mixture of $C_6H_7N^{\bullet+}$ and $C_5H_3NO^{\bullet+}$ ions. Thus, the CID mass spectrum (not shown) of these ions is that of a mixture and the structure of the weak *source* generated $C_6H_7N^{\bullet+}$ ions remains unresolved.

To further characterize the ions and to probe the stability of the elusive neutrals **5** and **6**, Flammang and co-workers have also reported the NR spectra of $\mathbf{2}^{\bullet+}$ - $\mathbf{7}^{\bullet+}$. One proposal from their study is that the intense "survivor ion" peaks in the spectra of $\mathbf{5}^{\bullet+}$ and $\mathbf{6}^{\bullet+}$ reflect the stability of their neutral counterparts. Evidence for this proposal comes from the presence of structure diagnostic signals in the NR spectra. However, consistent with our own observations (not shown), the intensity distribution of the various clusters of fragment ions in the NR spectra is considerably different from those in the CID spectra. One reason for this discrepancy (see Introduction) could be interference from reionized neutral fragments. To verify that these differences are not due to an isomerically impure initial beam of source generated ions and/or a partial isomerization upon neutralization, we have obtained the NR/CID spectrum of $\mathbf{5}^{\bullet+}$ and $\mathbf{6}^{\bullet+}$ along with that of the conventional isomer $\mathbf{2}^{\bullet+}$. These spectra are presented in Figure 7.2 along with the CID mass spectra (3ffr) of the corresponding source generated ions.

For ions $\mathbf{5}^{\bullet+}$ and $\mathbf{6}^{\bullet+}$, the NR/CID and CID mass spectra (Figures 7.2a,b and 7.2c,d) are closely similar, indicating (i) that the ions and their neutral counterparts are stable non-interconverting species in the gas phase and (ii) that the initial ion beams consisted of isomerically pure ions and (iii) that the structure diagnostic portions of the NR spectra are obscured by contributions from reionized neutral fragments. Note that when comparisons are made between the NR/CID and CID mass spectra, the signal at

m/z 66 (-H,C,N), which is largely of metastable origin and thus sensitive to the method of ion preparation, is not considered.

Interestingly enough, it is the NR/CID (Figure 7.2e) and the CID (Figure 7.2f) mass spectra of ionized 2-methylpyridine that exhibit a difference in the m/z 26 : 28 peak intensity ratio, such that the NR/CID spectrum of $\mathbf{2}^{\bullet+}$ could be argued to be that of a mixture of ions $\mathbf{2}^{\bullet+}$ and $\mathbf{6}^{\bullet+}$. Considering that the neutral counterpart of $\mathbf{2}^{\bullet+}$ is much more stable than that of $\mathbf{6}^{\bullet+}$ (see below), the possibility can be excluded that part of the neutralized ions **2** isomerize into **6**. Similarly, the possibility can be discarded that a significant fraction of the ions $\mathbf{2}^{\bullet+}$ generated by electron impact isomerizes into the more stable species $\mathbf{6}^{\bullet+}$, via a 1,3-H transfer. This is because the neutralization-reionization efficiency of $\mathbf{2}^{\bullet+}$ is four times greater than that of $\mathbf{6}^{\bullet+}$. It is therefore more likely that we are dealing with a significant degree of post-collisional isomerization upon *collisional* ionization of the neutral species **2**.

To test this hypothesis, a fast moving beam of *neutral* species **2** was produced in the second field free region from the 10 keV mass selected proton-bound dimer **2** via the collision-induced dissociation into $[\mathbf{2} + H]^+$ (5 keV) + **2** (5 keV). Using the deflector electrode, all ionic species were removed from the beam, thus allowing only the fast moving *neutrals* **2** to collide with O_2 in a second collision chamber, held at +2 kV. The resulting 7 keV m/z 93 ions were selectively transmitted into the third field free region and subjected to CID. The resulting partial CID mass spectrum, Figure 7.3a, resembles the NR/CID spectrum presented in Figure 7.3b, indicating that the common *collisional* ionization event is largely responsible for the significant degree of post collisional isomerization of $\mathbf{2}^{\bullet+}$ into $\mathbf{6}^{\bullet+}$. For comparison, the 7 keV CID mass spectrum of the source generated $\mathbf{2}^{\bullet+}$ ions is presented in Figure 7.3c. The 1,3-H transfer involved in the isomerization $\mathbf{2}^{\bullet+} \rightarrow \mathbf{6}^{\bullet+}$, undoubtedly imposes a high barrier (~ 50 kcal/mol) upon the reaction. However, one should also consider that ions $\mathbf{2}^{\bullet+}$ may contain up to 75 kcal/mol internal energy before any dissociation process becomes possible [29]. An increase in the average internal energy resulting from a *collisional* ionization event [31] could promote

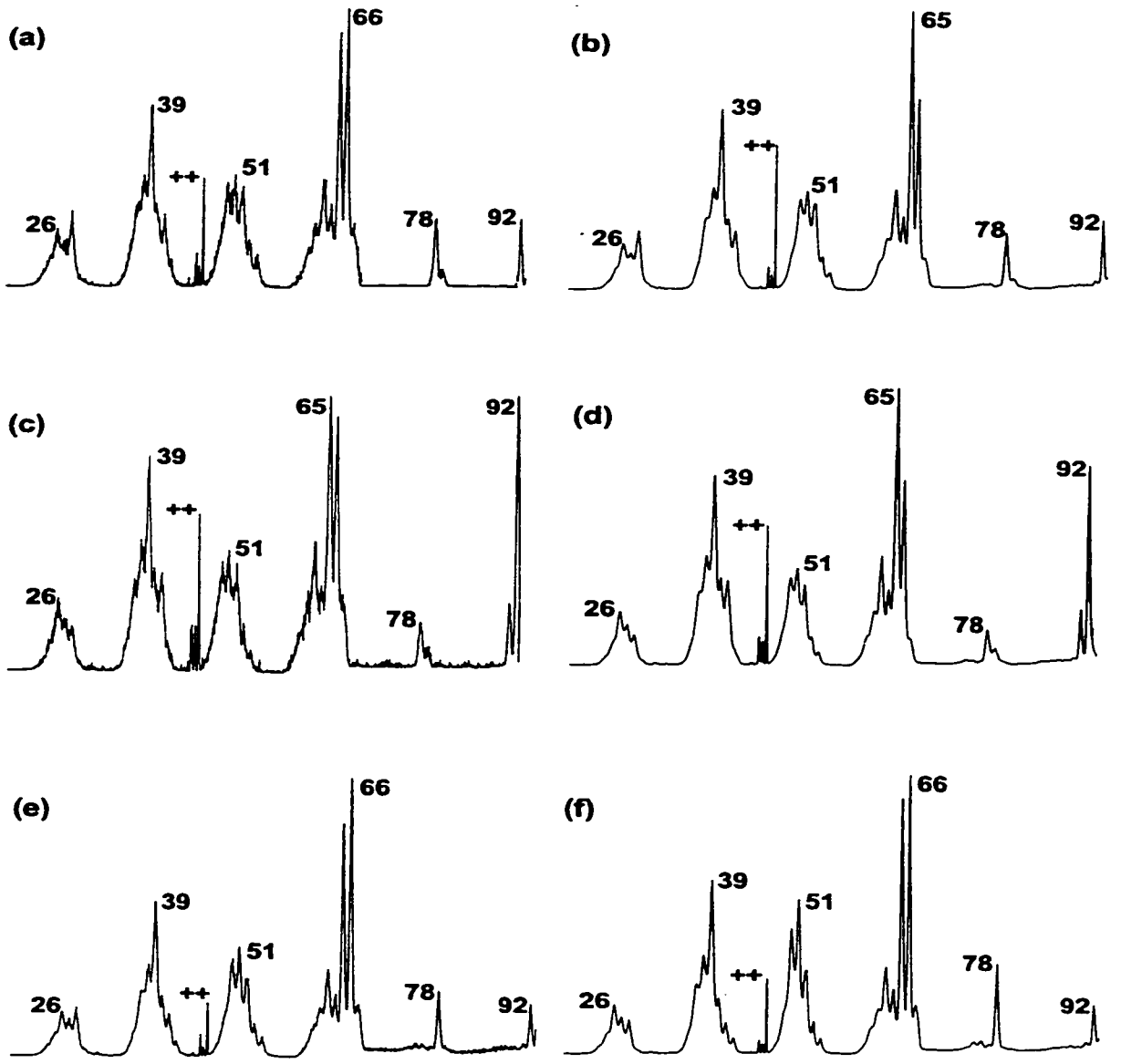

Figure 7.2: NR/CID and comparative CID mass spectra (3ffr, 10 keV ions, collision gas O_2) of $C_6H_7N^{\bullet+}$ (m/z 93) ions. Items (a) and (b): NR/CID and CID mass spectra of $C_6H_7N^{\bullet+}$ from ionized 2-acetylpyridine; items (c) and (d): NR/CID and CID mass spectra of $C_6H_7N^{\bullet+}$ from ionized bis(ethoxycarbonyl)pyridinium methylide; items (e) and (f): NR/CID and CID mass spectra of ionized 2-methylpyridine.

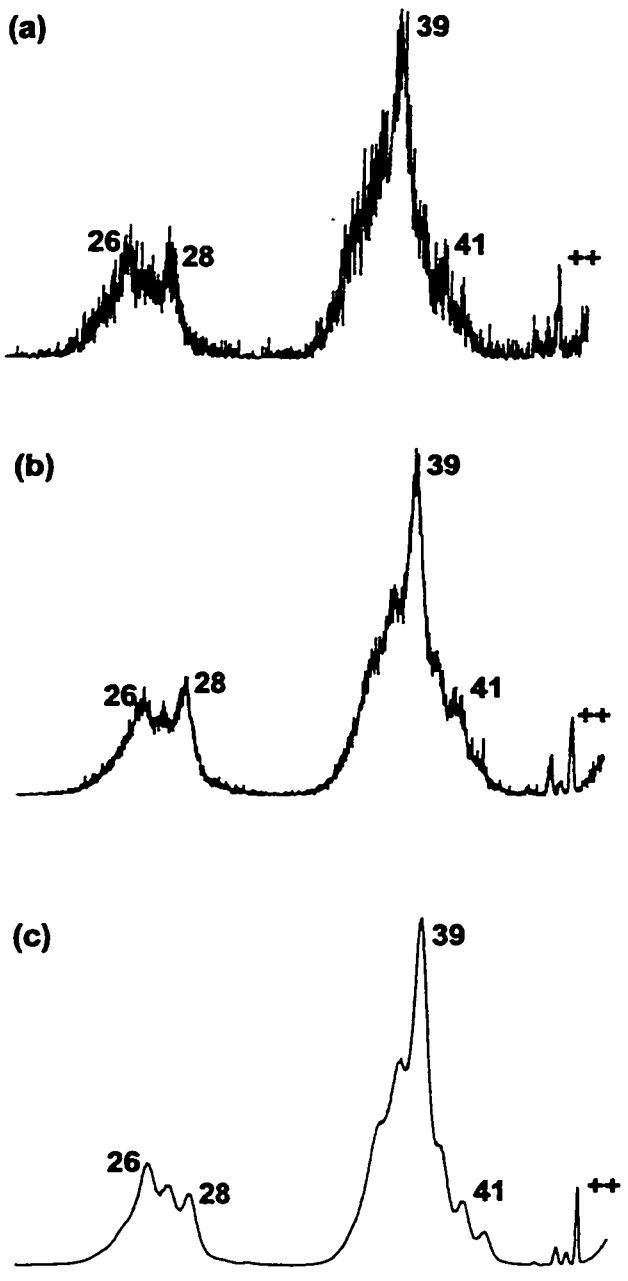

Figure 7.3: Partial CID mass spectra (3ffr, 7 keV ions, collision gas O_2) of the m/z 93 ions derived from (a) collisional ionization of 2-methylpyridine produced by the decomposition of its proton-bound dimer (see text for details), (b) neutralization-reionization of 2-methylpyridine ions and, (c) 2-methylpyridine subjected to electron ionization.

significant isomerization of $\mathbf{2}^{\bullet+}$, thus accounting for the observed differences in the NR/CID and CID mass spectra.

Finally, since ion $\mathbf{1}^{\bullet+}$ could only be obtained through the dissociation of metastable precursor ions, NR experiments were not feasible and thus its neutral counterpart remains unobserved.

To complement the experimental observations *ab initio* calculations were performed on four selected isomers viz. $\mathbf{1}^{\bullet+}$, $\mathbf{2}^{\bullet+}$, $\mathbf{5}^{\bullet+}$ and $\mathbf{6}^{\bullet+}$ as well as their neutral counterparts. The results are summarized in Table 7.1. Not surprisingly, the most stable species among the ionic isomers is not ionized 2-methylpyridine $\mathbf{2}^{\bullet+}$, but rather $\mathbf{6}^{\bullet+}$ which lies 24 kcal/mol lower in energy. The N-methylene isomer $\mathbf{5}^{\bullet+}$ is also more stable than $\mathbf{2}^{\bullet+}$, by 11 kcal/mol, but $\mathbf{1}^{\bullet+}$ is higher in energy, by 9 kcal/mol. These results are in fair agreement with a previous AM1 study [5] where $\mathbf{6}^{\bullet+}$ and $\mathbf{5}^{\bullet+}$ were found to be more stable than $\mathbf{2}^{\bullet+}$, by 33 and 10 kcal/mol, respectively. For the neutral counterparts, the relative stability of **6** and **2** is reversed, with **6** predicted to be 27 kcal/mol higher in energy than **2**, the most stable neutral of the set. Neutrals **1** and **5** are even higher in energy but, as could be experimentally verified for **5**, they do represent stable species on the potential energy surface. Although the isomeric ions and neutrals have considerably different stabilities, they must be separated by sizable barriers which hinder a facile intramolecular isomerization.

Table 7.1: Calculated energies for selected C_6H_7N and C_4H_5NS ions and neutrals at the B3LYP/6-31G* level of theory.[a]

Species	B3LYP	$<S^2>$	ZPVE [c]	E_{rel} [b]
$C_6H_7N^{\bullet+}$ Isomers				
1$^{\bullet+}$	-287.27836	0.778	75.1	9
2$^{\bullet+}$	-287.28911	0.756	73.3	0
5$^{\bullet+}$	-287.30982	0.775	74.6	-11
6$^{\bullet+}$	-287.33099	0.770	75.3	-24
C_6H_7N Isomers				
1	-287.51985		74.4	54
2	-287.60579		74.6	0
5	-287.53137		73.9	46
6	-287.56254		74.5	27
$C_4H_5NS^{\bullet+}$ Isomers				
11$^{\bullet+}$	-608.05434	0.759	50.0	19
12$^{\bullet+}$	-608.08632	0.769	51.5	0
13$^{\bullet+}$ [d]	-608.02955	0.776	50.6	35
14$^{\bullet+}$	-608.01100	0.761	51.5	42
15$^{\bullet+}$	-607.96166	0.759	49.7	77

[a] Total energies in Hartree, relative and zero-point vibrational energies are in kcal/mol.
[b] Relative energies include the ZPVE.
[c] ZPVE determined at B3LYP and scaled by 0.9806.
[d] Note that the optimized geometry of this ion represents an open chain structure, see text.

Generation and characterization of $C_5H_6N_2$ and C_4H_5NS isomers.

The decarbonylation of 2-acetylpyrazine and 2-acetylthiazole ions may be expected to occur analogously to that established for ionized 2-acetylpyridine. If so, the prominent m/z 94 and m/z 99 ions in their mass spectra should have the structures $\mathbf{9}^{\bullet+}$ and $\mathbf{12}^{\bullet+}$ rather than $\mathbf{8}^{\bullet+}$ (2-methylpyrazine) and $\mathbf{11}^{\bullet+}$ (2-methylthiazole), as proposed in the literature [16,17]. For the pyrazine system, this is confirmed by an analysis of the CID and NR/CID spectra presented in Figure 7.4. As with the $C_6H_7N^{\bullet+}$ system, the CID spectra of the ions generated by the loss of CO from the 2-acetyl precursor and the loss of C_2H_4 from the 2-propyl precursor are virtually identical. A representative spectrum is shown in Figure 7.4a. It is clearly characteristic of the 2-methylene structure $\mathbf{9}^{\bullet+}$ and, see Figure 7.4c, considerably different from that of the 2-methylpyrazine isomer $\mathbf{8}^{\bullet+}$. For $\mathbf{9}^{\bullet+}$ the structure diagnostic signals at m/z 80 and 47 (charge stripping peak) as well as the characteristic m/z 26 : 28 peak intensity ratio are reproduced in the CID spectrum, Figure 7.4b, of the intense survivor ion in the NR spectrum. Not only does this attest to the isomeric purity of the decarbonylation product, it also shows that 2-methylene-1,2-dihydropyrazine, **9**, is a stable, non-interconverting species in the dilute gas phase. For ion $\mathbf{8}^{\bullet+}$ the NR/CID and CID spectra are also closely similar and thus the post-collisional isomerization effect observed for 2-methylpyridine is clearly absent in the pyrazine analogue. Since the m/z 67 peak in the CID spectra contains a large MI contribution, it is not considered in the comparisons.

Another pyrazine ylide ion, $\mathbf{10}^{\bullet+}$, was also probed for the stability of its neutral counterpart. The ion was generated from the dissociative ionization of methyl-5-methylpyrazine-2-carboxylate, $\mathbf{VII}^{\bullet+}$, as depicted in Scheme 7.4 [32]. A distinct CID mass spectrum was obtained, see Figure 7.4e, which is closely similar, see Figure 7.4f, to the CID spectrum of the intense survivor peak in the NR spectrum. This leaves little doubt that 5-methyl-1,2-dihydropyrazine, **10**, is a stable species in the gas phase.

For the thiazole system, the decarbonylation of the 2-acetyl precursor and the C_2H_4 elimination from the 2-propyl precursor again yielded product ions of the same

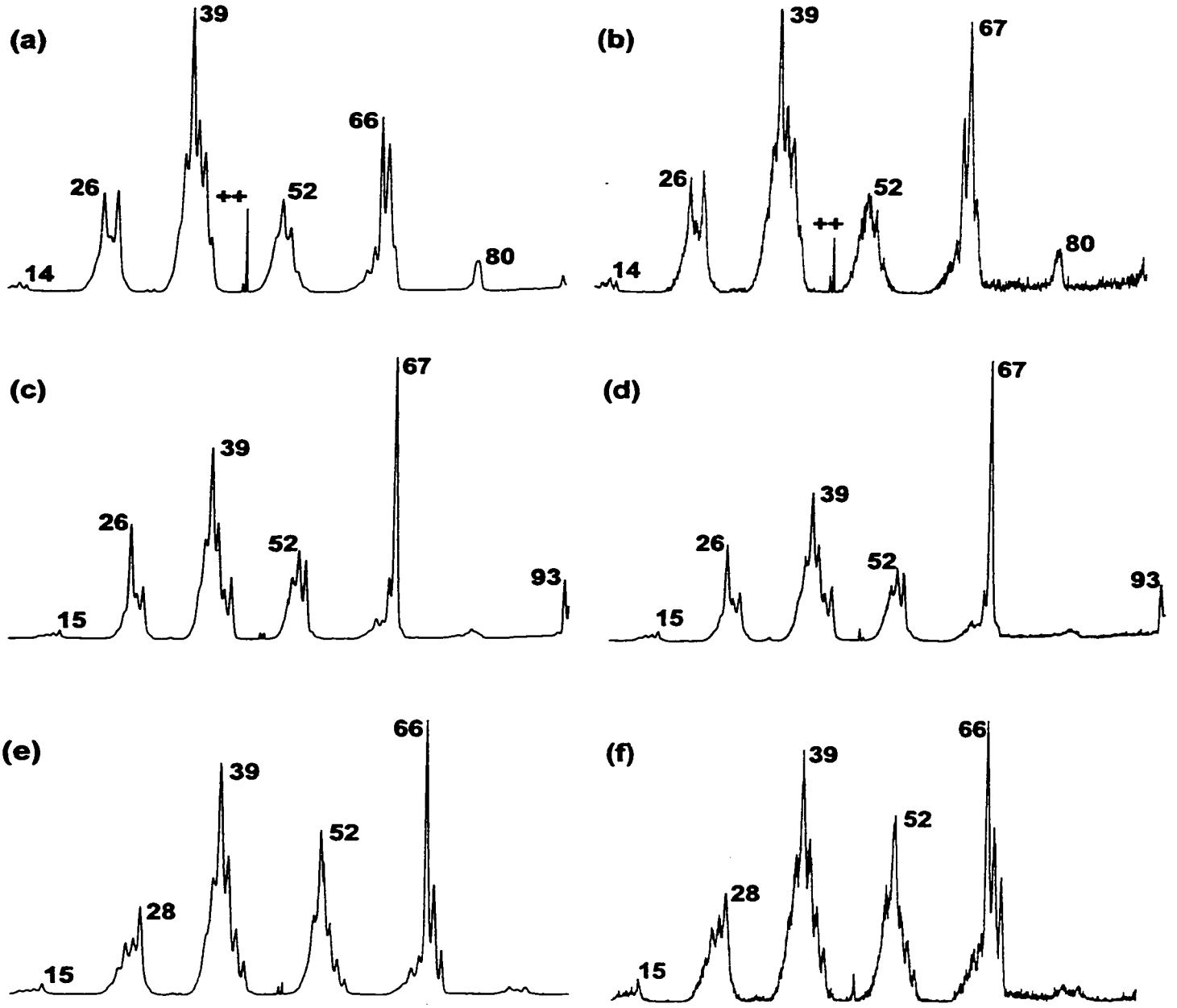

Figure 7.4: NR/CID and comparative CID mass spectra (3ffr, 10 keV, collision gas O_2) of $C_5H_6N_2^{\cdot+}$ (m/z 94) ions. Items (a) and (b): CID and NR/CID mass spectra of $C_5H_6N_2^{\cdot+}$ from ionized 2-acetylpyrazine or 2-propylpyrazine; items (c) and (d): CID and NR/CID mass spectra of ionized methylpyrazine; items (e) and (f): CID and NR/CID mass spectra of $C_5H_6N_2^{\cdot+}$ from ionized methyl-5-methylpyrazine-2-carboxylate. Spectra (e) and (f) are dominated by a peak at m/z 93 which is not shown because it is largely of metastable origin.

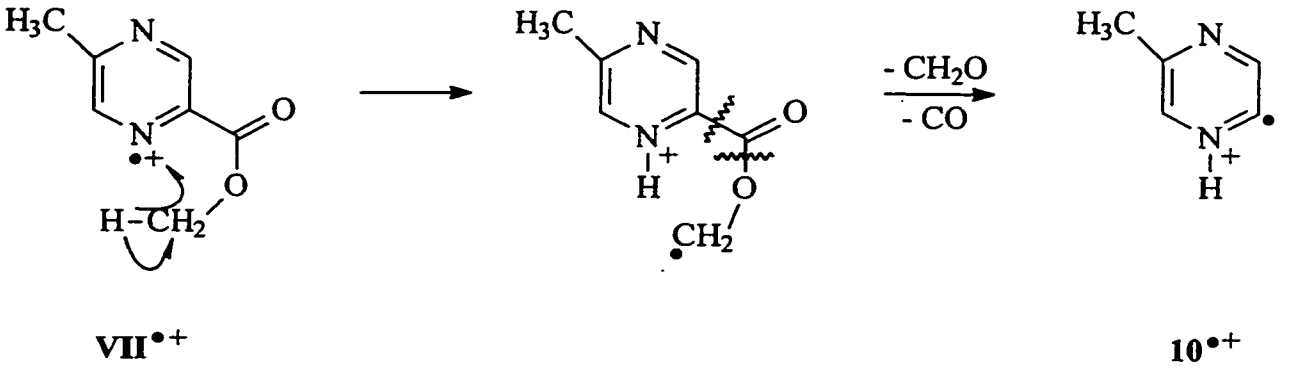

VII$^{\bullet+}$ **10**$^{\bullet+}$

Scheme 7.4

structure, as witnessed by their superimposable CID mass spectra. A representative spectrum is shown in Figure 7.5a. Unlike the situation with the pyridine and pyrazine analogues, this spectrum is markedly different from that of the 2-methyl substituted isomer **11**$^{\bullet+}$, see Figure 7.5b. The CID mass spectrum of the decarbonylation product ion is characterized by unique peaks at m/z 71 (loss of $CH_2N^{\bullet}$), m/z 59 (loss of C_2HN), m/z 54 (loss of $CHS^{\bullet}$) and an intense charge stripping peak at m/z 49.5. These CID features are compatible with the expected 2-methylene-1,2-dihydrothiazole structure **12**$^{\bullet+}$ but they do not necessarily rule out that the structurally related 2-methylene isomer **13**$^{\bullet+}$ is (co)-generated in the decarbonylation.

However, the computational results indicate that this is unlikely. Not only is **13**$^{\bullet+}$ found to undergo ring opening upon geometry optimization, but the resulting minimum energy structure, CH_2=C=N-C(H)=C(H)$SH^{\bullet+}$ lies 35 kcal/mol higher in energy than **12**$^{\bullet+}$. The N-methyl and S-methyl ylide isomers **14**$^{\bullet+}$ and **15**$^{\bullet+}$ retain their cyclic structure upon geometry optimization, but these species are even higher in energy, see Table 7.1. Thus, we conclude that the decarbonylation of 2-acetylthiazole occurs as established for the pyridine and pyrazine analogues and yields **12**$^{\bullet+}$ as the product ion. A NR experiment yielded intense "survivor" ions. Their CID spectrum appeared to be indistinguishable

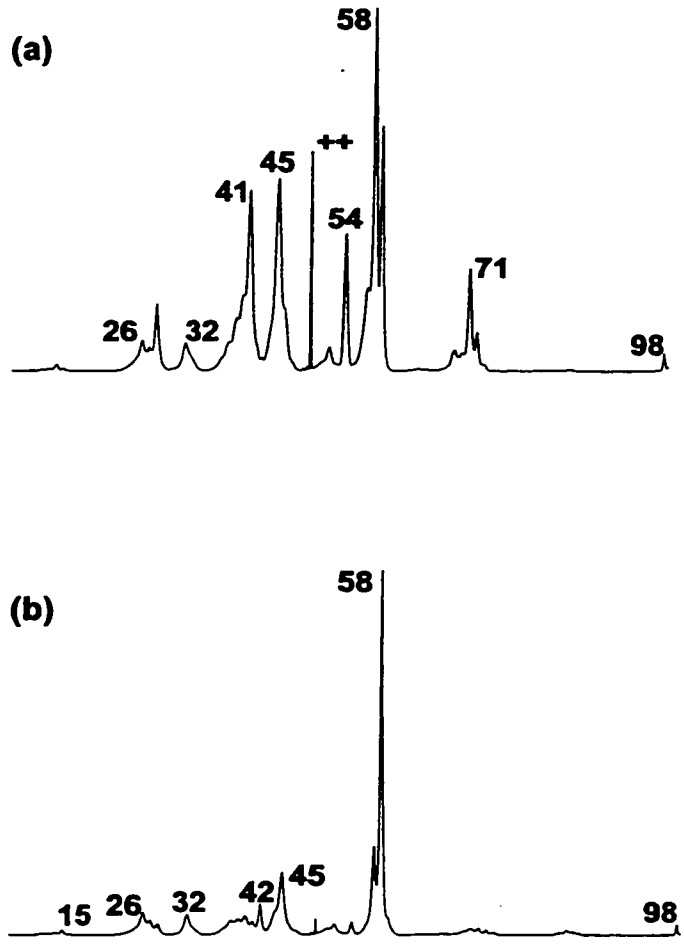

Figure 7.5: CID mass spectra (10 keV, collision gas O_2) of $C_4H_5NS^{\bullet+}$ (m/z 99) ions generated from ionized (a) 2-acetylthiazole or 2-propylthiazole, (b) 2-methylthiazole.

from that of the source generated ions (spectra not shown), confirming that 2-methylene-2,3-dihydrothiazole, **12**, is also a stable species in the rarefied gas phase.

References

[1] K.L. Busch, G.L. Glish and S.A. McLuckey, *Mass Spectrometry/Mass Spectrometry, Techniques and Applications of Tandem Mass Spectrometry*, VCH, New York, **1988**.

[2] a) K. Biemann, *Mass Spectrometry: Organic Chemical Applications*, McGraw-Hill, New York, NY, **1962**.

b) G. Spiteller, *Advances in Heterocyclic Chemistry*, Vol. 7., Academic Press, New York, NY, **1966**.

c) K.R. Jennings and J.H. Futrell, *J. Chem. Phys.* **1966**, *44*, 4115.

d) W.G. Cole, D.H. Williams and A.N.H. Yeo, *J. Chem. Soc. B.* **1968**, 1284.

e) N.M.M. Nibbering and T.J. de Boer, *Org. Mass Spectrom.* **1970**, *3*, 597.

[3] Review: A. Padwa, S.F. Hornbuckle, *Chem. Rev.* **1991**, *91*, 298.

[4] C.G. De Koster, J.J. van Houte and J. van Thuijl, *Int. J. Mass Spectrom. Ion Processes* **1990**, *98*, 235.

[5] R. Flammang, O. Thoelen, C. Quattrocchi and J.-L. Bredas, *Rapid Commun. Mass Spectrom.* **1992**, *6*, 135.

[6] S. Yu, M. Gross and K. Fountain, *J. Am. Soc. Mass Spectrom.* **1993**, *4*, 117.

[7] For a retrospective, see: R.G. Cooks, *J. Mass Spectrom.* **1995**, *30*, 1215.

[8] Recent reviews: a) F.W. McLafferty, *Int. J. Mass Spectrom. Ion Processes* **1992**, *118/119*, 211.

b) F. Tureček, *Org. Mass Spectrom.* **1992**, *27*, 1087.

c) N. Goldberg and H. Schwarz, *Acc. Chem. Res.* **1994**, *27*, 347.

d) C.A. Schalley, G. Hornung, D. Schröder and H. Schwarz, *Chem. Soc. Rev.* **1998**, *27*, 91.

e) C.A. Schalley, G. Hornung, D. Schröder and H. Schwarz, *Int. J. Mass Spectrom. Ion Processes* **1998**, *172*, 181.

[9] a) P.D. Michie and B.M. Johnson, *Org. Mass Spectrom.* **1983**, *18*, 202.

b) C.P. Whittle, M.J. Lacey and C.G. MacDonald, *Org. Mass Spectrom.* **1976**, *11*, 848.

c) D.L. von Minden, J.G. Liehr, M.H. Wilson and J.A. McCloskey, *J. Org. Chem.* **1974**, *39*, 285.

d) N. Neuner-Jehle, *Tetrahedron Lett.* **1968**, 2047.

e) C.P. Whittle, *Tetrahedron Lett.* **1968**, 3689.

f) Y. Rahamin, J. Sharvit, A. Mandelbaum and P. Sprecher, *J. Org. Chem.* **1967**, *32*, 3856.

[10] H. Budzikiewicz, E. Lange and W. Ockels, *Phosphorus and Sulfur* **1981**, *11*, 33.

[11] a) A. Ferretti and V.P. Flanagan, *J. Agr. Food Chem.* **1971**, *19*, 245.

b) M.D. Migahed and F.H. Abd El-Kader, *Int. J. Mass Spectrom. Ion Phys.* **1979**, *31*, 373.

[12] K.B. Tomer and C. Djerassi, *J. Org. Chem.* **1973**, *38*, 4152.

[13] a) R.J. Moser and E.V. Brown, *Org. Mass Spectrom.* **1970**, *4*, 555.

b) E.V. Brown and R.J. Moser, *J. Heterocycl. Chem.* **1971**, *8*, 189.

[14] P.H. Chen, *J. Org. Chem.* **1976**, *419*, 2973.

[15] D.J. Lavorato, J.K. Terlouw, T.K. Dargel, W. Koch, G.A. McGibbon and H. Schwarz, *J. Am. Chem. Soc.* **1996**, *118*, 11898 and references cited therein.

[16] a) J.J. Brophy and G.W.K. Cavill, *Heterocycles* **1990**, *14*, 477.

b) J.A. Maga and C.E. Sizer, *Fernarolis Handbook of Flavour Ingredients*, Vol. 1, C.R.C., Cleveland, Ohio, **1975**.

[17] G.M. Clarke, R. Grigg and D.H. Williams, *J. Chem. Soc. B* **1966**, 339.

[18] Gaussian 94 (Revision B.2): M.J. Frisch, G.W. Trucks, H.B. Schlegel, P.M.W. Gill, B.G. Johnson, M.A. Robb, J.R. Cheeseman, T.A. Keith, G.A. Peterson, J.A. Montgomery, K. Raghavachari, J.B. Foresman, J. Cioslowski, B.B. Stefanov, A. Nanayakkara, M. Challacombe, C.Y. Peng, P.Y. Ayala, W. Chen, M.W. Wong, J.L. Andres, E.S. Replogle, R. Gomperts, R.L. Martin, D.J. Fox, J.S. Binkley, D.J. DeFrees, J. Baker, J.J.P. Stewart, M. Head-Gordon, C. Gonzalez and J.A. Pople, Gaussian, Inc., Pittsburgh PA, **1995**.

[19] a) A.D. Becke, *J. Phys. Chem.* **1993**, *98*, 5648.

b) C. Lee, W. Yang and R.G. Parr, *Phys. Rev. B.* **1988**, *37*, 785.

[20] a) A.P. Scott and L. Radom, *J. Phys. Chem.* **1996**, *100*, 16502.

b) M.W. Wong, *Chem. Phys. Lett.* **1996**, *256*, 391.

[21] D.V. Bowen, P.W. Skett, J. Thorpe and A.O. Plunkett, *Org. Mass Spectrom.* **1984**, *19*, 285.

[22] The CID spectra reported in the present study are not identical to those reported in reference 5. However, a discussion of the variations that may be attributed to differing instrumental and experimental conditions would form an unnecessary digression in the context of this work.

[23] D. J. Lavorato, J.K. Terlouw, G.A. McGibbon, T.K. Dargel, W. Koch and H. Schwarz, *Int. J. Mass Spectrom. Ion Processes*, **1998**, *179/180*, 7.

[24] M. Tiecco, *Acc. Chem. Res.* **1981**, *18*, 16.

[25] $\Sigma\Delta H_f$ [pyridine-2-ylidene]$^{\bullet+}$ + ΔH_f [$CH_2C{=}O$] = 237 kcal/mol - 11.4 kcal/mol = 225.6 kcal/mol [15,26] whereas $\Sigma\Delta H_f$ [**6**$^{\bullet+}$] + ΔH_f [CO] = 208 kcal/mol - 26.4 kcal/mol = 181.6 kcal/mol [26]. ΔH_f [**6**$^{\bullet+}$] was estimated to be 208 kcal/mol, based on the ΔH_f [**2**$^{\bullet+}$] = 232 kcal/mol [26] and the difference in the relative energies of **6**$^{\bullet+}$ and **2**$^{\bullet+}$ presented in Table 7.1.

[26] S. Lias, J.E. Bartmess, J.F. Liebman, J.L. Holmes, R.D. Levin and W.G. Mallard, *J. Phys. Chem. Ref. 17*, **1988**, Supplement 1.

[27] W. Heerma, M.M. Sarneel and G. Dijkstra, *Org. Mass Spectrom.* **1986**, *21*, 681.

[28] R. Neeter and N.M.M. Nibbering, *Tetrahedron* **1972**, *28*, 2575.

[29] The MI spectrum of **2**$^{\bullet+}$ shows that the reactions of lowest energy requirement are the loss of HCN (m/z 66), C_2H_2 (m/z 67) and H$^{\bullet}$ (m/z 92). The activation energy for the latter process has been established as 77 kcal/mol, from an appearance energy measurement [30].

[30] T.F. Palmer and F.P.L. Lossing, *J. Am. Chem. Soc.* **1963**, *85*, 1733.

[31] S. Beranova and C. Wesdemiotis, *J. Am. Soc. Mass Spectrom.* **1994**, *5*, 1093.

[32] T.K. Dargel, W. Koch, D. J. Lavorato, J.K. Terlouw and H. Schwarz, *Int. J. Mass Spectrom. Ion Processes*, **1999**, *185/186/187*, 925.

CHAPTER 8

Observation of Pyrimidine-4-ylidene and Pyrimidine-2-ylidene Using Neutralization - Reionization Mass Spectrometry

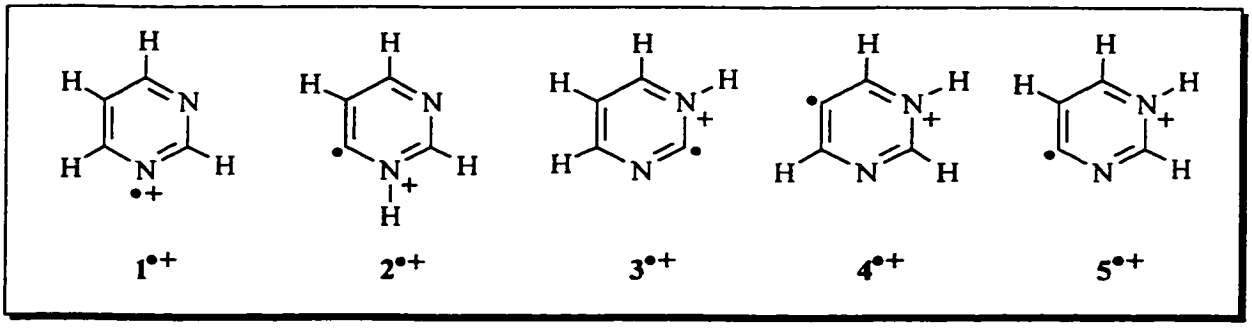

Ab initio calculations predict that ionized pyrimidine, $\mathbf{1}^{\bullet+}$, has four hydrogen shift isomers of comparable stability which reside in deep potential wells, *viz.* the ions $\mathbf{2}^{\bullet+}$ - $\mathbf{5}^{\bullet+}$ shown above. Three of these ions, $\mathbf{2}^{\bullet+}$ - $\mathbf{4}^{\bullet+}$, could be generated in the mass spectrometer and be identified on the basis of their collision-induced dissociation characteristics.

Ions $\mathbf{2}^{\bullet+}$ and $\mathbf{3}^{\bullet+}$ were obtained by dissociative electron impact ionization and subjected to neutralization - reionization mass spectrometry (NRMS). From collision-induced dissociation spectra of the intense survivor ions, it follows that their neutral ylide/carbene counterparts, i.e. pyrimidine-4-ylidene, **2**, and pyrimidine-2-ylidene, **3**, are viable chemical species in the rarefied gas phase. Ions $\mathbf{4}^{\bullet+}$ could only be generated by a collision-induced dissociation process and were therefore not amenable to NR experiments. A strategy to generate isomerically pure ions $\mathbf{5}^{\bullet+}$ could not be realized.

To assist in the interpretation of the experimental observations, the quantum chemical results summarized in the Appendix were used. These calculations were performed by T. Dargel of the TU Berlin group of Professors W. Koch and H. Schwarz in the context of a joint project whose results will be reported in the literature in due course.

Introduction

There are certain classes of molecules which attract a great deal of attention and appear to be constantly under study. A prime example are molecules which possess a pyrimidine moiety, a structural motif which appears in a number of biologically important species including the nitrogenous bases guanine, thymine, adenine, cytosine and the vitamin thiamin. As a consequence, numerous experimental and theoretical studies have been reported dealing with various intrinsic properties of pyrimidine and its derivatives [1-3]. Surprisingly, however, the so-called hydrogen shift isomers of pyrimidine have not been explicitly studied, although they have been invoked as reactive intermediates in solution chemistry. A case in point concerns the work of Dunn and co-workers [4] who studied the decarboxylation kinetics of pyrimidine-2-carboxylic acid in solution and proposed the ylide/carbene isomer pyrimidine-2-ylidene, **3**, as a short-lived reactive intermediate en route to the formation of pyrimidine. Such a reaction sequence is analogous to that postulated earlier by Hammick and co-workers [5,6] for the decarboxylation of pyridine-2-carboxylic acid, via the pyridine-2-ylidene intermediate.

A major obstacle in the study of such species in condensed phases concerns their rapid intermolecular isomerization into the thermodynamically much more stable heterocycles of conventional structure; even matrix isolation studies encounter such difficulties as demonstrated by Maier and co-workers in the characterization of 2,3-dihydrothiazol-2-ylidene [7]. Consequently, there are often advantages to study such reactive species in the gas phase where intermolecular reactions are essentially absent. The confines of a mass spectrometer offer such an environment and since the inception of neutralization-reionization (NR) mass spectrometry over twenty years ago [8], a technique which involves the one-electron reduction of their corresponding radical cations, numerous elusive species have been identified, including the archetypal carbenes $H_2N\text{-}\ddot{C}\text{-}OH$ [9], $H_2N\text{-}\ddot{C}\text{-}NH_2$ [10] and $CH_3\text{-}\ddot{C}\text{-}OH$ [11]. Further developments in both the NR methodology and computational chemistry made it possible to analyze more complex systems and in 1996 definitive evidence could be obtained for the structure and stability of the Hammick intermediate [12]. Several related species, including imidazol-2-ylidene

[13], 2,3-dihydrothiazol-2-ylidene [14], pyridine-3-ylidene [15] and the two pyrazine isomers pyrazine-2-ylidene and pyrazine-3-ylidene [16], could also be successfully identified using this approach. In this context, it is important to note that, whereas these neutral carbenes and ylides are much higher in energy than their molecular isomers, this is not true for the ionic counterparts. For example, for the pyridine system, theory and experiment [12] established that ionized pyridine and its α-ylide isomer have a comparable stability and are separated by high isomerization barriers. The combination of NRMS and computational chemistry also proved advantageous in a recent study of protonated pyrimidine's neutral counterpart, a proposed model compound in studies of DNA radiation damage [17].

Given the possibility to characterize reactive heterocyclic intermediates by the NR methodology, we set out to examine the structure and stability of the hydrogen shift isomers of pyrimidine, the most important of the diazines. *Ab initio* calculations, see Appendix, predict that ionized pyrimidine, $\mathbf{1}^{\bullet+}$, has four hydrogen shift isomers of comparable stability residing in deep potential wells, *viz.* the ions $\mathbf{2}^{\bullet+}$ - $\mathbf{5}^{\bullet+}$ shown below. Their neutral counterparts are also calculated to be stable and, although they lie 40 - 65 kcal/mol higher in energy than pyrimidine, isomerization is prevented by barriers in the 85 - 130 kcal/mol range. Thus, these pyrimidine-ylidenes should all be observable chemical species in the mass spectrometer, provided their ionic counterparts can be generated in an isomerically pure form.

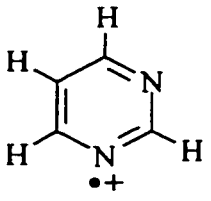

$\mathbf{1}^{\bullet+}$

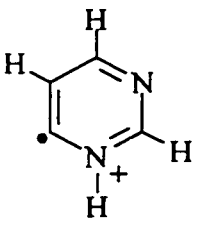

$\mathbf{2}^{\bullet+}$

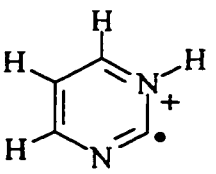

$\mathbf{3}^{\bullet+}$

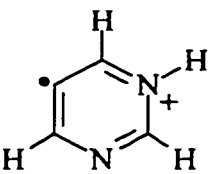

$\mathbf{4}^{\bullet+}$

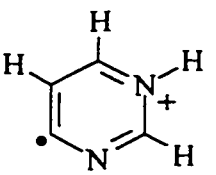

$\mathbf{5}^{\bullet+}$

Results and Discussion

To probe the stability of the above mentioned hydrogen shift isomers of pyrimidine with the neutralization - reionization (NR) methodology, it first becomes necessary to characterize the radical cations, $\mathbf{1}^{\bullet+}$- $\mathbf{5}^{\bullet+}$. The search for appropriate precursor molecules to the putative ions $\mathbf{2}^{\bullet+}$- $\mathbf{4}^{\bullet+}$ was straightforward but unfortunately a strategy to generate isomerically pure ions $\mathbf{5}^{\bullet+}$ could not be realized. Electron impact ionization of pyrimidine yields a simple mass spectrum dominated by molecular ions $\mathbf{1}^{\bullet+}$ and principal fragment ions at m/z 53 (loss of HCN) and m/z 26 ($C_2H_2^{\bullet+}$) [2a]. By analogy with earlier work on the pyridine [12] and pyrazine [16] systems, ions $\mathbf{2}^{\bullet+}$ and $\mathbf{3}^{\bullet+}$ should be obtainable by dissociative electron ionization of the appropriate methyl esters, *viz.* Methyl pyrimidine-4-carboxylate (**I**) and methyl pyrimidine-2-carboxylate (**II**). These two esters do indeed show a prominent m/z 80 peak in their conventional electron impact mass spectrum, which is cleanly shifted to m/z 81 in the spectra of the CD_3-labelled isotopomers, **I**-d_3 and **II**-d_3. As shown in Scheme 8.1, the proposed formation of $\mathbf{2}^{\bullet+}$ and $\mathbf{3}^{\bullet+}$ involves a 1,5-H transfer to a ring N atom followed by consecutive losses of CH_2O and CO. Ions $\mathbf{4}^{\bullet+}$ could not be generated by dissociative electron impact but collision-induced dissociation of protonated 5-bromopyrimidine, see Scheme 8.2, provided a viable alternative. Unfortunately, however, this method of ion preparation does not lend itself to NR experiments with the available instrumentation and thus the neutral counterpart of $\mathbf{4}^{\bullet+}$ could not be studied.

The isomeric cations $\mathbf{1}^{\bullet+}$- $\mathbf{4}^{\bullet+}$ were characterized using the technique of collision-induced dissociation (CID) mass spectrometry. Upon inspection of the CID mass spectra shown in Figure 8.1, it becomes immediately apparent that a number of common dissociation pathways exists of which loss of HCN, yielding the peak at m/z 53, is the most prominent. Nevertheless, there are characteristic differences between the spectra which enable isomer differentiation. The most significant are the m/z 26 ($C_2H_2^{\bullet+}$) : 28 ($HC{\equiv}NH^+$) peak intensity ratio and the intensity of the charge stripping peak, denoted as "++". For the pyrimidine radical cations $\mathbf{1}^{\bullet+}$ a high m/z 26 : 28 ratio, 3.33 ± 0.03, is

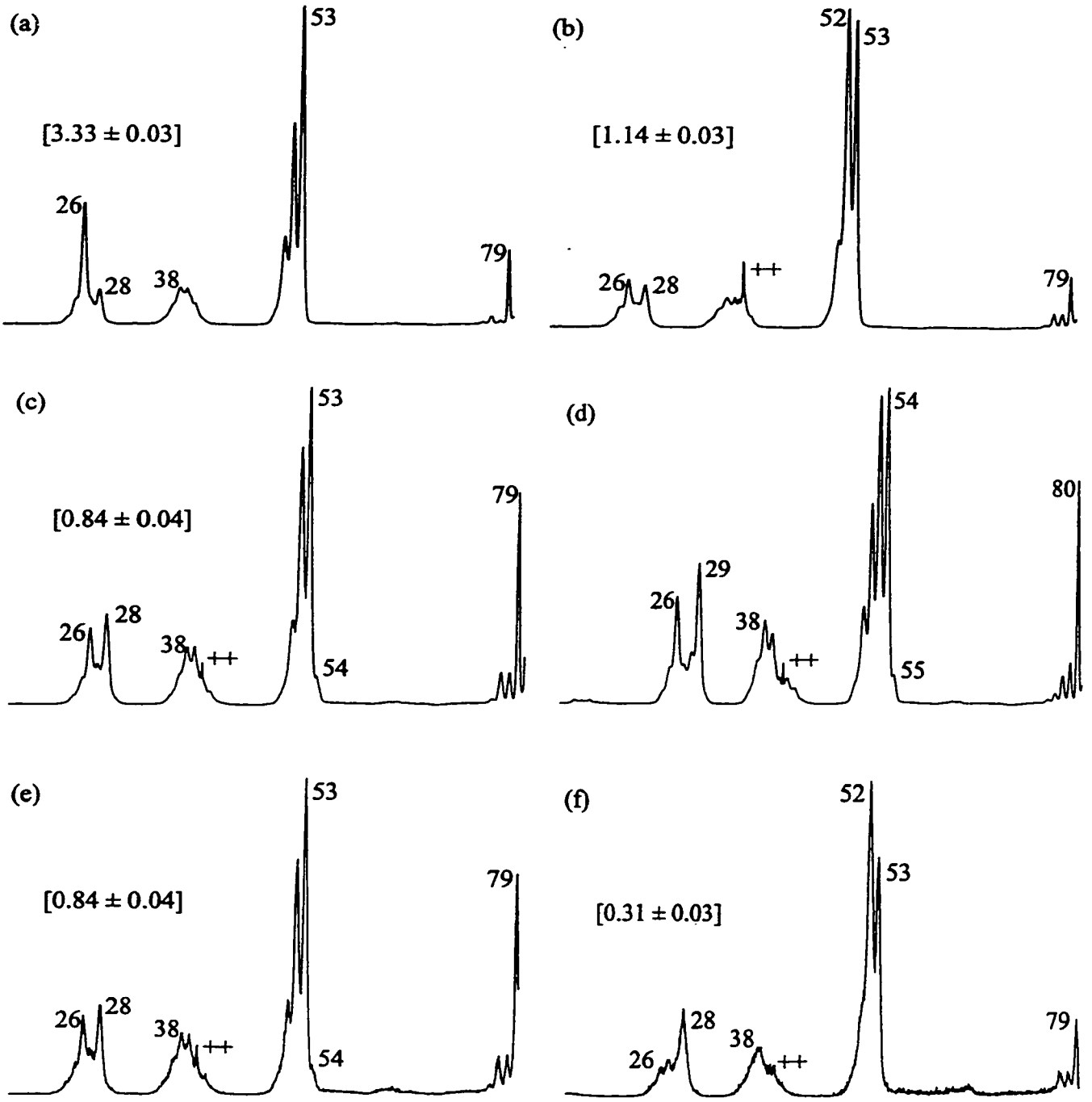

Figure 8.1: CID [O_2] mass spectra (7 keV, 3ffr) of the m/z 80 ions from (a) ionized pyrimidine ($1^{\bullet+}$); (b) ionized methyl pyrimidine-4-carboxylate, yielding $2^{\bullet+}$; (c) ionized methyl pyrimidine-2-carboxylate, yielding $3^{\bullet+}$; (d) d_3-methyl pyrimidine-2-carboxylate ions, yielding $3^{\bullet+}$-(N-D); (e) metastable m/z 108 ions from ionized methyl pyrimidine-2-carboxylate, yielding $3^{\bullet+}$; (f) collision-induced dissociation of protonated 5-bromopyrimidine, yielding $4^{\bullet+}$. Note that the m/z 26 : 28 ratios quoted in the spectra depend on the translational energy of the ions and also the field free region in which the ions dissociate (2ffr vs 3ffr, see Figures 8.3 and 8.4; the field free region 'effect' is due to differences in energy resolution.

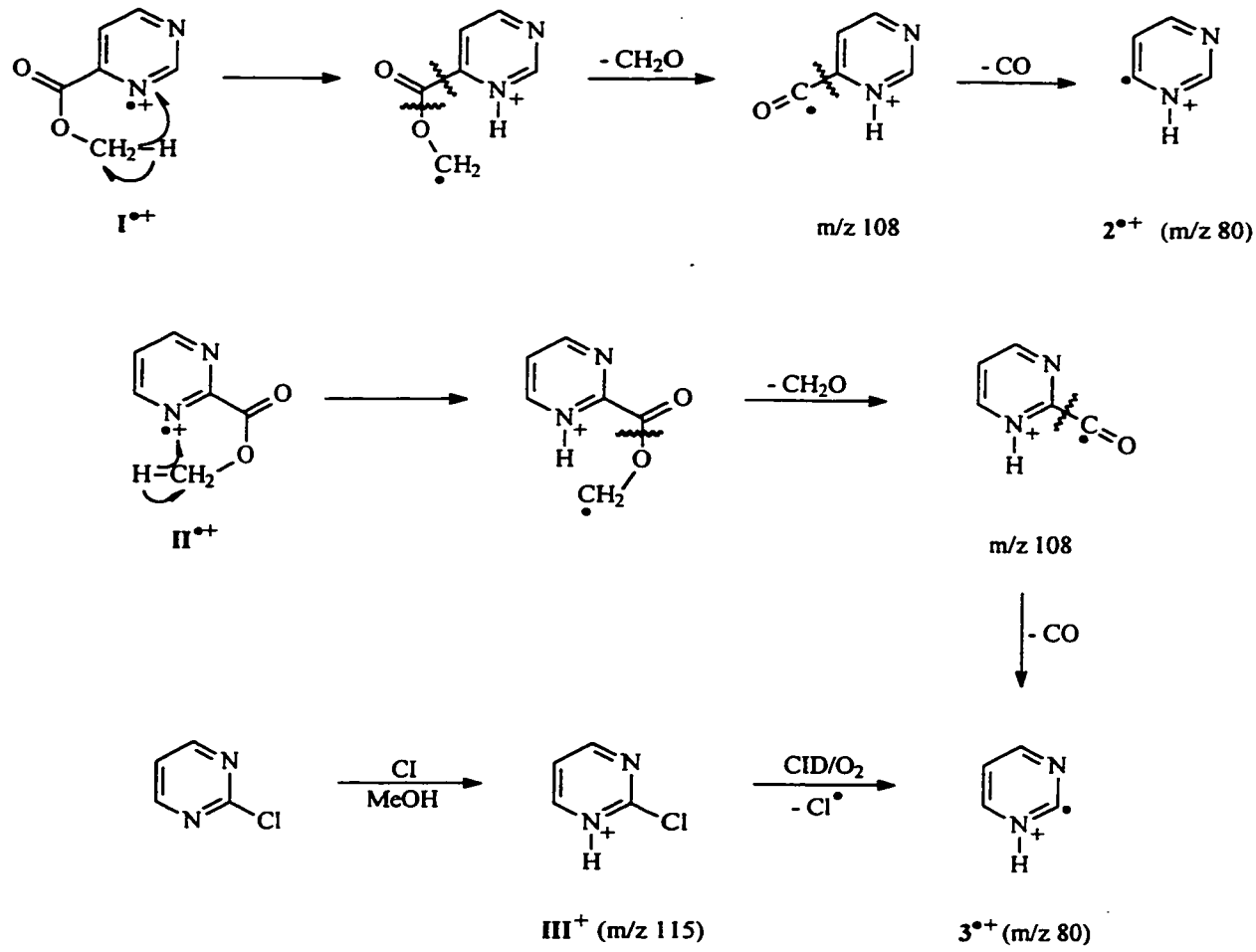

Scheme 8.1

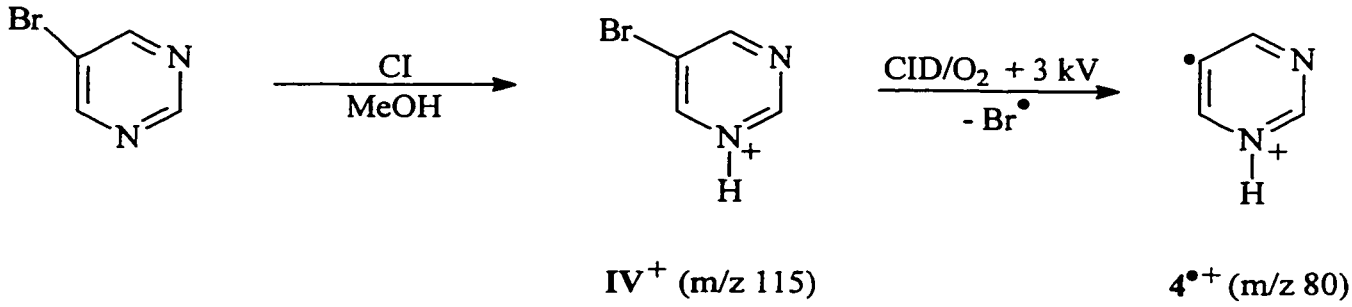

Scheme 8.2

observed and a charge stripping peak at m/z 40 is absent, see Figure 8.1a. In contrast, see Figure 8.1b, the CID spectrum of the putative ion $\mathbf{2}^{\bullet+}$ displays a m/z 26 : 28 ratio of 1.14 ± 0.03 and a sizable charge stripping peak indicative of an ylide structure. As documented in previous work on the pyridine [12] and pyrazine [16] systems, the ionic ylide isomers are more prone to produce m/z 28, H-C≡N^+-H, ions - via a high energy direct bond cleavage reaction - than their ionized parent heterocycles which have no -CH-NH- moiety. In agreement with this proposal, the CID spectrum of the m/z 81 ions from $\mathbf{I}$-d_3 shows a clean shift of m/z 28 to m/z 29, whereas m/z 26 remains unchanged.

The CID mass spectrum of $\mathbf{3}^{\bullet+}$, Figure 8.1c, again exhibits a structure diagnostic m/z 26 : 28 ratio, 0.83 ± 0.03, but compared to that of $\mathbf{2}^{\bullet+}$ the charge stripping peak is less intense. Of even greater structure diagnostic value is the peak at m/z 54. From a CID experiment in the 3ffr it follows that these m/z 54 ions have the elemental composition C_3H_4N [18] and thus they represent a highly structure specific loss of $^{\bullet}$CN.

Ions $\mathbf{3}^{\bullet+}$ also show, see Figure 8.1c, a prominent loss of $H^{\bullet}$. Surprisingly, the product generated is not the stable 2-pyrimidyl cation [19]. This is because (i) the CID mass spectrum of the isotopomer $\mathbf{3}^{\bullet+}$-(N-D), see Figure 8.1d, shows a specific loss of $H^{\bullet}$, not $D^{\bullet}$ and (ii) the CID spectrum of the $[\mathbf{3} - H]^+$ ions is dominated by the loss of HCN whereas the pyrimidyl cation - generated by loss of $Cl^{\bullet}$ from 2-chloropyrimidine [19] - loses both C_2H_2 and HCN to about the same extent. These observations make it highly unlikely that the six membered ring structure of $\mathbf{3}^{\bullet+}$ remains intact upon $H^{\bullet}$ loss. Guided by the results of exploratory *ab initio* calculations on the relative stability of the $[\mathbf{3} - H]^+$ product ions [20], we tentatively propose that the reaction occurs as indicated in Scheme 8.3.

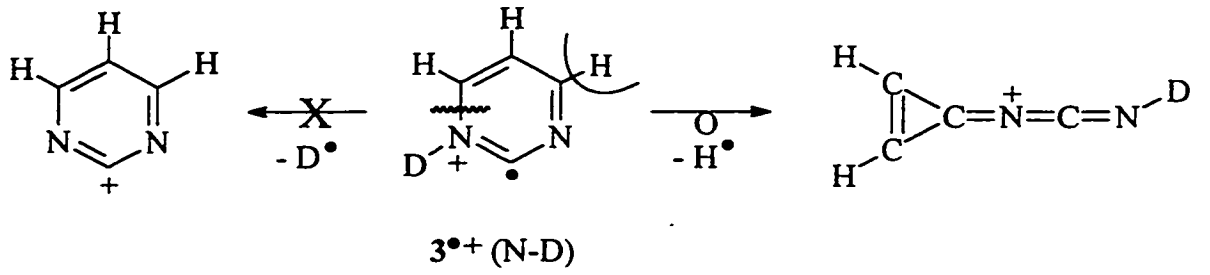

Scheme 8.3

Ions $3^{\bullet+}$ were also generated by a second independent method. Under chemical ionization conditions, using methanol as the reagent gas, 2-chloropyrimidine molecules were protonated, accelerated and subsequently transmitted into the 2ffr of the instrument. The fast moving ions $\mathbf{III}^{+}$, see Scheme 8.1, were then collided with oxygen and the resulting 7 keV m/z 80 ions generated upon loss of $Cl^{\bullet}$ were selectively transmitted into the 3ffr of the instrument and collided with oxygen. The resulting CID mass spectrum was indistinguishable from that obtained for the m/z 80 source generated ions from the ester $\mathbf{II}^{\bullet+}$, Figure 8.1c, confirming that a common ion, $3^{\bullet+}$, is produced in the two processes. Further attesting to our proposal that these ions also have a high isomeric purity is the observation that the CID spectrum of the *metastably* generated m/z 80 ions from the ester precursor, see Figure 8.1e, is virtually identical with the spectrum presented in Figure 8.1c.

The third hydrogen shift isomer, $4^{\bullet+}$, was generated by the chemical ionization - CID sequence described above for ion $3^{\bullet+}$, but using 5-bromopyrimidine (**IV**) as the precursor, see Scheme 8.2 [21]. The resulting CID spectrum, see Figure 8.1f, displays the lowest m/z 26 : 28 ratio of the set, 0.31 ± 0.04, in keeping with the fact that ions $4^{\bullet+}$ cannot generate m/z 26 ($HC{\equiv}CH^{\bullet+}$) ions by direct bond cleavage, whereas m/z 28, $HC{\equiv}NH^{+}$, can readily be generated.

The conclusions regarding the structural integrity of the ions $1^{\bullet+}$ - $4^{\bullet+}$ derived from the CID experiments are supported by the quantum calculations summarized in the

Appendix. Ionized pyrimidine, $\mathbf{1}^{\bullet+}$, is predicted to be the most stable isomer but the four hydrogen shift isomers $\mathbf{2}^{\bullet+}$ - $\mathbf{5}^{\bullet+}$ are only slightly higher in energy. Moreover, the five ions are separated by considerable 1,2-H shift barriers, in the 60 - 80 kcal/mol energy range, which prevents their facile isomerization.

Buff and Dannacher [2c], in a photoelectron-photoion coincidence study of diazine cations, have determined the critical energy for the loss of HCN from ionized pyrimidine. This process represents the dissociation reaction of lowest energy requirement for $\mathbf{1}^{\bullet+}$. It dominates, see Table 8.1, the MI spectrum and also, see Figure 8.1a, the CID mass spectrum. The measured critical energy, ~ 63 kcal/mol, dictates that the heat of formation of the resulting $C_3H_3N^{\bullet+}$ product ion is ≤ 293 kcal/mol. We also note that this critical energy is close to the calculated barriers for isomerization into the H-shift isomers $\mathbf{2}^{\bullet+}$ and $\mathbf{3}^{\bullet+}$, see Appendix. Therefore, it is conceivable that the MI spectra of the three species which, see Table 8.1, are all dominated by m/z 53, represent loss of HCN from a common reacting configuration. This, indeed, seems to be likely since the CID mass spectra of the *metastably* generated m/z 53 $C_3H_3N^{\bullet+}$ ions from $\mathbf{1}^{\bullet+}$, $\mathbf{2}^{\bullet+}$ and $\mathbf{3}^{\bullet+}$ are indistinguishable, see Figure 8.2a for a representative spectrum. The resulting m/z 53 product ion is clearly not ionized acrylonitrile (ΔH_f = 296 kcal/mol [22]) as proposed by Buff and Dannacher [2c]: its CID mass spectrum is shown in Figure 8.2b and is entirely different. Rather, we propose that the slightly more stable isomer $H_2C{=}C{=}C{=}N{-}H^{\bullet+}$ [23] is generated. The CID spectrum of this cumulene type isomer is expected to be dominated by loss of $H^{\bullet}$ to produce the protonated cyanoacetylene product ion $H{-}C{\equiv}C{-}C{\equiv}N{-}H^{+}$, the direct bond cleavage of lowest energy requirement calculated for this structure [24]. CID mass spectra of the m/z 54 ions generated by the *specific* collision-induced loss of HCN from the metastable m/z 81 ions of the N-D labelled isotopomers of $\mathbf{2}^{\bullet+}$ and $\mathbf{3}^{\bullet+}$ (generated from **I**-d_3 and **II**-d_3 respectively) were also obtained. These spectra appear to be indistinguishable, see Figure 8.2c for a representative spectrum, and although they

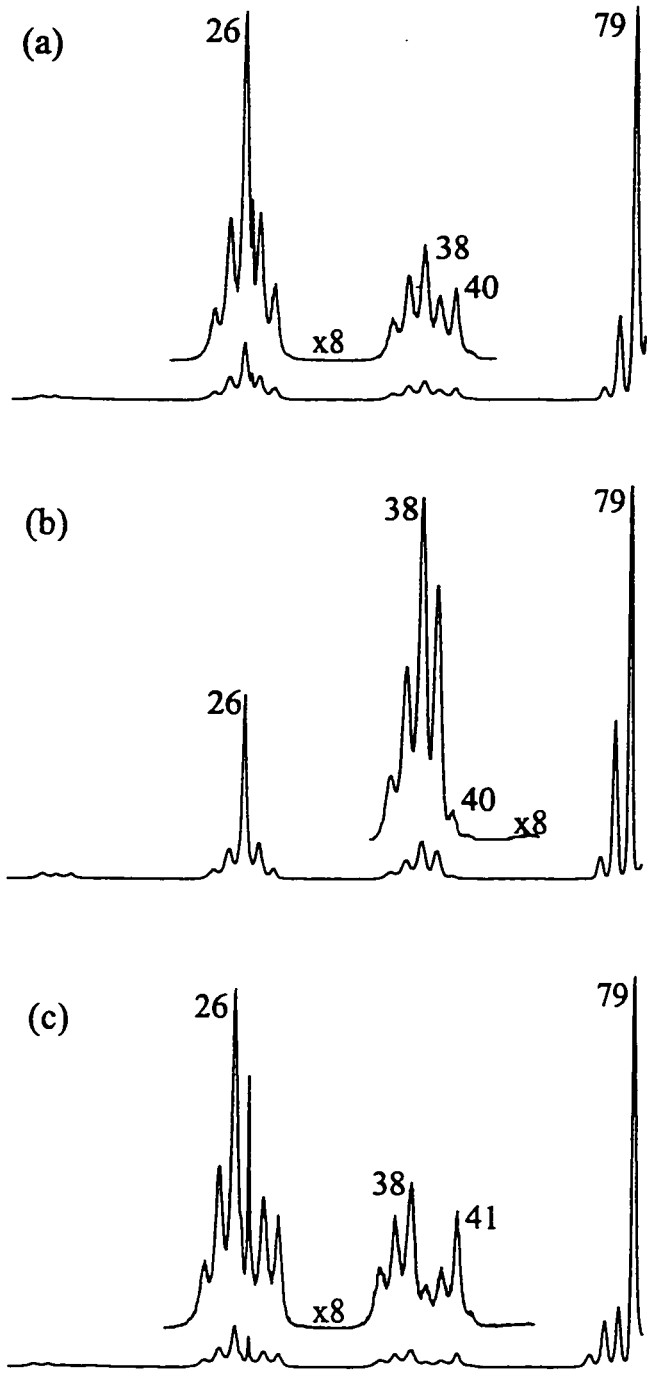

Figure 8.2: CID [O_2] mass spectra (7 keV, 3ffr) of m/z 53 $C_3H_3N^{\bullet+}$ ions generated from: (a) loss of HCN from 10 keV metastable ions $\mathbf{3}^{\bullet+}$; (b) electron impact ionization of acrylonitrile. Item (c) represents the CID spectrum of m/z 54 $C_3H_2DN^{\bullet+}$ ions generated by the specific loss of HCN from 10 keV metastable ions $\mathbf{3}^{\bullet+}$-(N-D).

attest to the structure assignment of the product ion, mechanistic proposals for the intriguing mechanism(s) for the loss of HCN from metastable ions $\mathbf{1}^{\bullet+}$ - $\mathbf{3}^{\bullet+}$ must await analysis of selected D [2d] and ^{13}C labelled isotopomers of $\mathbf{1}^{\bullet+}$.

Table 8.1: Metastable ion mass spectra of the m/z 80 ions $\mathbf{1}^{\bullet+}$- $\mathbf{3}^{\bullet+}$.

Isomer	$\mathbf{1}^{\bullet+}$	$\mathbf{2}^{\bullet+}$	$\mathbf{3}^{\bullet+}$
(m/z)			
54 [b]	–	–	3
53	100 (32) [a]	100 (13)	100 (32)
52 [b]	3	5	4
28 [b]	–	–	1
26 [b]	2	–	1

[a] Values in parentheses refer to $T_{0.5}$ values in the meV.

[b] Peak may contain a CID contribution from residual collision gas.

In any case, the picture that emerges from the experimental and computational results is that the H-shift isomers $\mathbf{2}^{\bullet+}$, $\mathbf{3}^{\bullet+}$ and $\mathbf{4}^{\bullet+}$ represent stable species on the $C_4H_4N_2^{\bullet+}$ potential energy surface which can be unambiguously characterized by their high energy collision-induced dissociation reactions into $C_2H_2^{\bullet+}$ and $H\text{-}C{\equiv}N\text{-}H^+$.

Following the successful characterization of the ionic isomers $\mathbf{1}^{\bullet+}$- $\mathbf{4}^{\bullet+}$ by CID, the NR spectra of $\mathbf{1}^{\bullet+}$- $\mathbf{3}^{\bullet+}$ were obtained to probe the structure and stability of the elusive species **2** and **3**. The NR spectra are presented in Figure 8.3, together with their CID spectra obtained at the same accelerating voltage. Clearly, the NR spectra of $\mathbf{1}^{\bullet+}$ and $\mathbf{2}^{\bullet+}$, which are both dominated by an intense survivor signal, show a fragment ion distribution similar to that of their corresponding CID spectra. Thus, it may be tentatively concluded that the neutral counterpart of $\mathbf{2}^{\bullet+}$ is a stable species in the gas phase. However, the

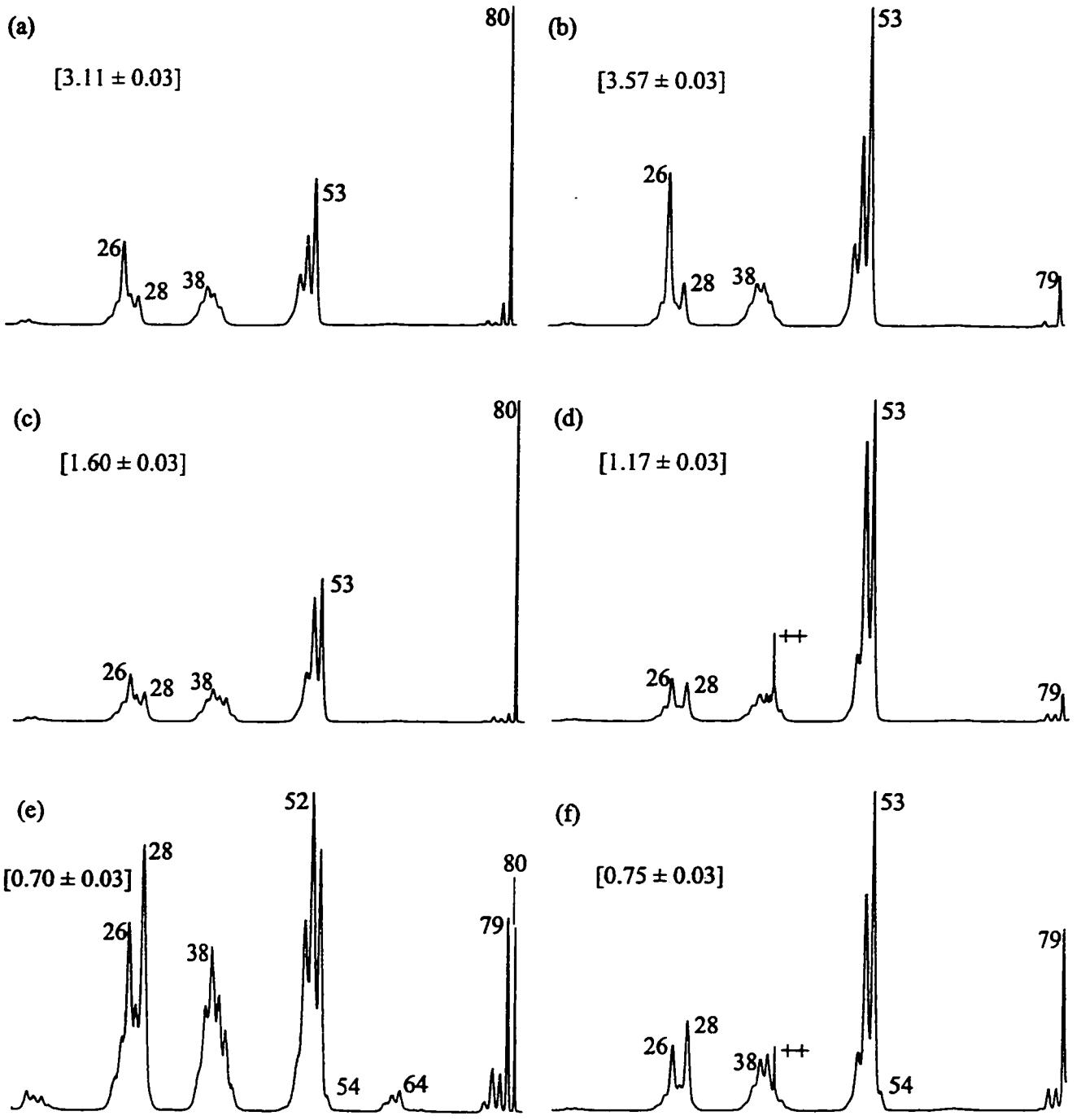

Figure 8.3: NR [NDMA/O_2] and comparative CID [O_2] mass spectra (8 keV, 2ffr) of ionized pyrimidine $\mathbf{1}^{\bullet+}$, items (a) and (b); ions $\mathbf{2}^{\bullet+}$ from methyl pyrimidine-4-carboxylate, items (c) and (d); and ions $\mathbf{3}^{\bullet+}$ from methyl pyrimidine-2-carboxylate, items (e) and (f).

structure characteristic m/z 26 : 28 ratios in the CID spectra of $\mathbf{1}^{\bullet+}$ and $\mathbf{2}^{\bullet+}$ are not exactly reproduced in the NR spectra and this raises the question whether a partial isomerization upon neutralization takes place. This point will be addressed in the next section where the CID spectra of the survivor ions in the NR spectra are examined.

The NR mass spectrum of $\mathbf{3}^{\bullet+}$, see Figure 8.3e, is considerably different from that of $\mathbf{1}^{\bullet+}$ and $\mathbf{2}^{\bullet+}$: its survivor ion signal is of only moderate intensity relative to the fragment ions. Nevertheless, the structure diagnostic m/z 26 : 28 CID ratio has remained virtually unchanged, 0.70 ± 0.03 versus 0.75 ± 0.03 in the NR mass spectrum. The tell-tale peak at m/z 54 is also present in the NR spectrum and thus it may be tentatively concluded that pyrimidine-2-ylidene is also a stable species in the gas phase. However, further analysis of the survivor ion structure is warranted here too, since the intensity distributions of the clusters at m/z 36-40 and m/z 51-54 in the NR spectrum are clearly different from those in the CID spectrum.

As argued before, [12-16], a CID experiment on the mass selected "survivor" ions in a NR spectrum may facilitate the interpretation of NR spectra contaminated with reionized neutral fragments from decomposition of the incipient neutral and/or neutrals generated by collision-induced dissociation. In addition, the technique provides a useful tool to probe the isomeric purity of the source generated ions subjected to the neutralization process and the structure integrity of the neutrals produced therefrom.

For ions $\mathbf{1}^{\bullet+}$ and $\mathbf{2}^{\bullet+}$, the (partial) NR/CID and corresponding CID mass spectra are shown in Figure 8.4. The pyrimidine radicals cations, $\mathbf{1}^{\bullet+}$, display NR/CID and CID mass spectra which are essentially superimposable. Thus, in agreement with the theoretical observations discussed above, the stable source generated ions $\mathbf{1}^{\bullet+}$ do not isomerize to any of their H-shift isomers $\mathbf{2}^{\bullet+}$ - $\mathbf{5}^{\bullet+}$. The partial NR/CID mass spectrum of $\mathbf{2}^{\bullet+}$ shows a m/z 26 : 28 ratio, 1.32 ± 0.05, which is slightly but significantly higher than the structure diagnostic ratio derived from the CID spectrum, 1.16 ± 0.03. The similarity of the two spectra confirms that the ions generated in the neutralization - reionization process are largely $\mathbf{2}^{\bullet+}$. The enhanced m/z 26 intensity in the NR/CID spectrum points to

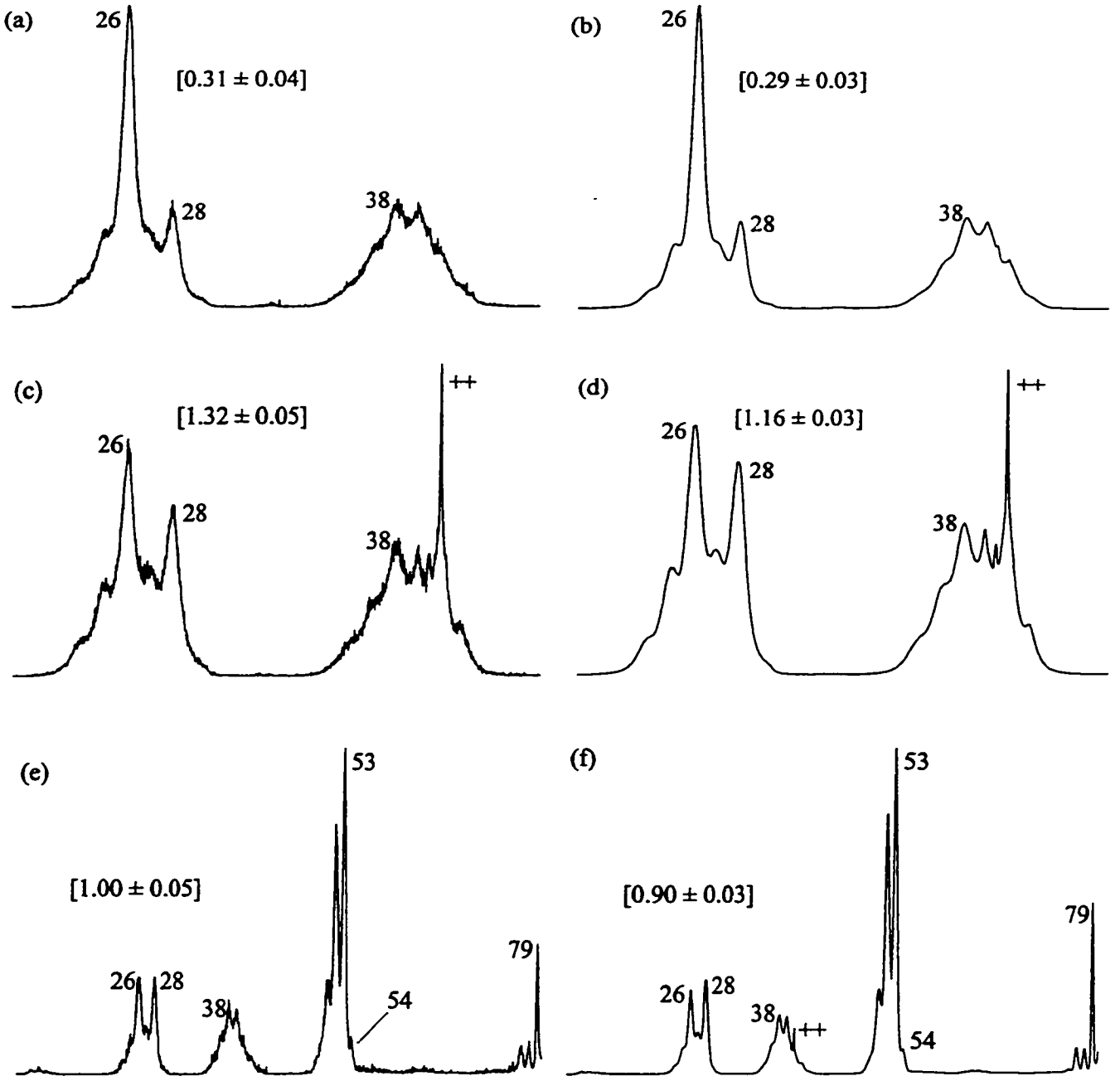

Figure 8.4: NR/CID [O_2] and comparative CID [O_2] mass spectra (8 keV, 3ffr) of m/z 80 ions $\mathbf{1}^{\bullet+}$ - $\mathbf{3}^{\bullet+}$. Items (a) and (b) partial NR/CID and CID spectra of ionized pyrimidine, $\mathbf{1}^{\bullet+}$; items (c) and (d) partial NR/CID and CID spectra of pyrimidine-4-ylidene ions, $\mathbf{2}^{\bullet+}$; items (e) and (f) NR/CID and CID spectra of pyrimidine-2-ylidene ions, $\mathbf{3}^{\bullet+}$.

the presence of a small fraction of pyrimidine radical cations. One possibility is that the initial ion beam is not isomerically pure, possibly because a minor fraction of the methyl pyrimidine-4-carboxylate thermally decomposes into pyrimidine prior to ionization. To test this hypothesis, the structure of the m/z 80 ions generated by loss of CO from *metastable* m/z 108 ions, see Scheme 8.1, was examined by collision-induced dissociation. The m/z 80 ions generated therefrom have a much lower internal energy content so that any spontaneous isomerization of the ions will be greatly suppressed. The resulting CID mass spectrum (result not shown) showed a m/z 26 : 28 ratio which is slightly, but significantly, lower than that of the source generated ions, 1.03 ± 0.04 versus 1.14 ± 0.03. This supports our proposal that the source generated m/z 80 ions from the ester do contain a small contribution from ionized pyrimidine, which we estimate to be ca. 5 percent [25]. Thus, we conclude that pyrimidine-4-ylidene, **2**, is indeed a stable, non-interconverting, species in the rarefied gas phase.

The above experiments further indicate that it is the singlet state of the ylide/carbene **2** which has been accessed, rather than the triplet state. From the theoretical results in the Appendix and the experimental ΔH_f (**1**), 47 kcal/mol [22], the ΔH_f of singlet **2** is assessed as 89 kcal/mol, while for the triplet state the ΔH_f is 133 kcal/mol. Combining this with ΔH_f ($\mathbf{2}^{\bullet+}$) = 268 kcal/mol (from ΔH_f ($\mathbf{1}^{\bullet+}$) = 260 kcal/mol [22] and the calculated energy difference between $\mathbf{1}^{\bullet+}$ and $\mathbf{2}^{\bullet+}$ given in the Appendix), ionization energies (IE) of ~ 7.7 eV and 5.8 eV are obtained for the singlet and triplet states of **2**. The first three vertical IEs of the neutralization agent, N,N-dimethylaniline (NDMA), are 7.5, 9.0 and 9.8 eV respectively [26]. Therefore, a close-to-resonant vertical electron transfer from NDMA to **2** is available for the formation of **2** (singlet), but not **2** (triplet). The optimized geometries of the ion and the neutral (see Appendix) are not greatly different and thus unfavourable Franck-Condon factors do not militate against the formation of the singlet either. To probe the stability of the triplet, a close-to-resonant neutralization with an atomic target like Li vapour (IE Li = 5.4 eV [22]) would be advantageous. Such experiments are planned as part of a future project.

The near resemblance of the NR/CID and CID spectra of $3^{\bullet+}$, compare Figures 8.4e and 8.4f, leaves little doubt that pyrimidine-2-ylidene, **3**, is a stable species in the gas phase too. A NR/CID spectrum of the isotopomer $3^{\bullet+}$-(N-D) was also obtained (spectrum not shown) and it, too, is closely similar to the CID spectrum of the source generated ions, see Figure 8.1d. There is a slight bias towards m/z 26 in the two NR/CID spectra, again indicative of the presence of a minor fraction of pyrimidine ions. However, unlike the situation with the ions $2^{\bullet+}$, there is no evidence that the primary beam of ions $3^{\bullet+}$ is contaminated with ions $1^{\bullet+}$. Although the possibility cannot be ruled out that a small fraction of the incipient neutral species **3** isomerizes into the more stable pyrimidine structure, it is more likely that the collisional *ionization* event promotes the isomerization [27]. The singlet and triplet states of **3** have ΔH_f values of 97 and 125 kcal/mol and IEs of 7.2 and 6.0 respectively (from the data in the Appendix). These values are close to those of **2**, as are the isomerization barriers for a 1,2-H transfer. The geometry differences between the ion and the neutral are again minor (see Appendix) and thus neutralization of **3** may reasonably be expected to yield the stable singlet structure. As with **2**, neutralization to the triplet state is unlikely. Also, dissociation of both **2** and **3** from their singlet state is fairly endothermic : loss of $H^{\bullet}$ from singlet **2** and **3** is calculated to be endothermic by 60 and 47 kcal/mol respectively (from ΔH_f **2**(s) = 89 kcal/mol and $\Sigma\Delta H_f$ [4-pyrimidyl]$^{\bullet}$ + $H^{\bullet}$ = 149 kcal/mol [1g, 22]; ΔH_f **3**(s) = 97 kcal/mol and $\Sigma\Delta H_f$ [2-pyrimidyl]$^{\bullet}$ + $H^{\bullet}$ = 144 kcal/mol [1g, 22]). Thus, there is little reason to assume that the neutralization of $2^{\bullet+}$ and $3^{\bullet+}$ yields neutrals with a greatly different internal energy distribution and isomerization/dissociation behaviour. Nevertheless, the NR spectrum of $3^{\bullet+}$ shows a much weaker survivor ion, see Figure 8.3e. This we (largely) attribute to the collisional *ionization* event : the degree of dissociation in the NR spectra of $3^{\bullet+}$ appears to be strongly dependent on the translational energy of the neutralized ion beam. For example, whereas the relative survivor ion intensity in the NR spectra of $1^{\bullet+}$ and $2^{\bullet+}$ decreases by a factor of 3 when the translational energy of the primary ion beam for neutralization is raised from 8 to 10 keV, the survivor ion in the NR spectrum of $3^{\bullet+}$

decreases by a factor of 8 ! Our interpretation is that considerably more internal energy is deposited in the collisional ionization of **3** than in that of **2** or **1** and that this causes a minor fraction of the incipient *ionized* neutrals **3** to isomerize into $\mathbf{1}^{\bullet+}$.

In summary, evidence has been provided that pyrimidine-4-ylidene (**2**) and pyrimidine-2-ylidene (**3**) in their singlet states are stable, non-interconverting species in the rarefied gas phase. The results further indicate that under appropriate conditions, i.e. low temperature matrix isolation, such species may also be accessible in the condensed phase.

References

[1] a) J.S. Murray, J.M. Seminario and P. Politzer, *J. Mol. Struct. (Theochem)* **1989**, *187*, 95 .

b) A. Hinchliffe, *J. Electron Spectrosc. Rel. Phenom.* **1977**, *10*, 415.

c) L. Asbrink, C. Fridh, B.O. Jonsson and E. Lindholm, *Int. J. Mass Spectrom. Ion Processes* **1972**, *8*, 215.

d) A. Castellan and J. Michl, *J. Am. Chem. Soc.* **1978**, *100*, 6824.

e) A. Hinchliffe and H.J. Soscũn, *J. Mol. Struct. (Theochem)* **1994**, *304*, 109.

f) N. J. Jones, G.B. Bacskay, J. C. Mackie and A. Doughty, *J. Chem. Soc. Faraday Trans.* **1995**, *91*, 1587.

g) J.H. Kiefer, Q. Zhang, R.D. Kern, J. Yao and B. Jursic, *J. Phys. Chem. A* **1997**, *101*, 7061.

[2] For studies of the dissociation chemistry of ionized pyrimidine see:

a) J.M. Rice, G.O. Dudek and M. Barber, *J. Am. Chem. Soc.* **1965**, *87*, 4569.

b) H. Ichikawa and M. Ogata, *J. Am. Chem. Soc.* **1973**, *95*, 806.

c) R. Buff and J. Dannacher, *Int. J. Mass Spectrom. Ion Processes* **1984**, *62*, 1.

d) F. Milani-Nejad and H. Stidham, *Spectrochimica Acta* **1975**, *31A*, 1433. This Raman study of various D-labelled isotopomers of pyrimidine also quotes their 70 eV electron impact mass spectra. Although these spectra show illogical peaks in the low mass region,

the conclusion seems to be warranted that loss of HCN from high energy pyrimidine ions involves cleavage of the C(2)-N(3) and C(4)-C(5) bonds. We also note that the CID mass spectrum of the source generated m/z 53 $[M\text{-}HCN]^{\bullet+}$ ions is entirely different from that of the metastable ions.

e) H. Perreault, L. Ramaley, F.M. Benoit, P.G. Sim and R.K. Boyd, *Org. Mass Spectrom.* **1992**, *27*, 89.

[3] For protonation studies of pyrimidine see:

a) V.Q. Nguyen and F. Tureček, *J. Am. Chem. Soc.* **1997**, *119*, 2280.

b) P. Mátyus, K. Fuji and K. Tanaka, *Tetrahedron* **1994**, *50*, 2405.

[4] G.E. Dunn, E.A. Lawler and B. Yamashita, *Can. J. Chem.* **1977**, *55*, 2478.

[5] P. Dyson and D.L. Hammick, *J. Chem. Soc.* **1937**, 1734.

[6] M.R.F. Ashworth, R.P. Daffern and D.L. Hammick, *J. Chem. Soc.* **1937**, 809.

[7] G. Maier and H.P. Reisenaue, *Angew. Chem.* **1997**, *109*, 1788.

[8] For recent reviews see:

a) N. Goldberg and H. Schwarz, *Acc. Chem. Res.* **1994**, *27*, 347.

b) C.A. Schalley, G. Hornung, D. Schröder and H. Schwarz, *Chem. Soc. Rev.* **1998**, *27*, 91.

[9] a) G.A. McGibbon, P.C. Burgers and J.K. Terlouw, *Int. J. Mass Spectrom. Ion Processes* **1994**, *136*, 191.

b) C.E.C.A. Hop, H. Chen, P.J.A. Ruttink and J.L. Holmes, *Org. Mass Spectrom.* **1991**, *26*, 697.

[10] G.A. McGibbon, C.A. Kingsmill and J.K. Terlouw, *Chem. Phys. Lett.* **1994**, *222*, 129.

[11] C. Wesdemiotis and F.W. McLafferty, *J. Am. Chem. Soc.* **1987**, *109*, 4760.

[12] D. Lavorato, J.K. Terlouw, T.K. Dargel, W. Koch, G.A. McGibbon and H. Schwarz, *J. Am. Chem. Soc.* **1996**, *118*, 11898.

[13] G.A. McGibbon, C. Heinneman, D.J. Lavorato and H. Schwarz, *Angew. Chem. Int. Ed. Engl.* **1997**, *36*, 1478.

[14] G.A. McGibbon, J. Hrušák, D.J. Lavorato, H. Schwarz and J.K. Terlouw, *Chem. Eur. J.* **1997**, *3*, 232.

[15] D.J. Lavorato, J.K. Terlouw, G.A. McGibbon, T.K. Dargel, W. Koch and H. Schwarz, *Int. J. Mass Spectrom. Ion Processes* **1998**, *179/180*, 7.

[16] T.K. Dargel, W. Koch, D.J. Lavorato, J.K. Terlouw and H. Schwarz, *Int. J. Mass Spectrom. Ion Processes* **1999**, *185/186/187*, 925.

[17] F. Tureček, *J. Mass Spectrom.* **1998**, *33*, 779.

[18] W. Heerma, M.M. Sarneel and G. Dijkstra, *Org. Mass Spectrom.* **1986**, *21*, 681.

[19] M. Carvalho, F.C. Gozzo, M.A. Mendes, R. Sparrapan, C. Kascheres and M.N. Eberlin, *Chem. Eur. J.* **1998**, *4*, 1161.

[20] Another possibility involves ring opening by cleavage of the N[3]-C[4] bond (see Appendix for atom numbering) followed by loss of H$^{\bullet}$ from C[5]. Our calculations indicate that the resulting product ion, H-C≡C-$^{+}$CH-N=C=N-H, is 11 kcal/mol higher in energy than the 2-pyrimidyl cation, whereas the ion depicted in Scheme 8.3 is of comparable stability (B3LYP/cc-pvdz level of theory). We further note that loss of H$^{\bullet}$ from the heteroatom in **3**$^{\bullet+}$ may involve a sizable reverse barrier.

[21] To facilitate a comparison with the other spectra, the first collision chamber was held at + 3000V, so that the m/z 80 ions **4**$^{\bullet+}$, generated from 10 keV m/z 159 precursor ions, possessed ca. 7 keV translational energy.

[22] S. Lias, J.E. Bartmess, J.F. Liebman, J.L. Holmes, R.D. Levin and W.G. Mallard, *J. Phys. Chem. Ref. Data 17*, **1988**, Supplement 1.

[23] CH_2=C=C=NH$^{\bullet+}$is calculated to be more stable than ionized acrylonitrile, CH_2=CH-C≡N$^{\bullet+}$, by 13 kcal/mol. The *a priori* plausible isomers H-C≡C-C(H)=N-H$^{\bullet+}$ and H-C=CH-C=N-H$^{\bullet+}$ lie higher in energy, by 17 and 6 kcal/mol respectively (B3LYP/cc-pvdz level of theory).

[24] $\Sigma\Delta H_f$ [H-C≡C-C≡N-H^{+} + H$^{\bullet}$] is 321 kcal/mol [22], whereas $\Sigma\Delta H_f$ [HC≡CH$^{\bullet+}$ + HCN] is 349 kcal/mol; the latter process dominates the CID and MI spectra of ionized acrylonitrile.

[25] Based upon a linear combination of the m/z 26 : 28 CID peak intensity ratios for **1**$^{\bullet+}$ and **2**$^{\bullet+}$ and considering that their relative neutralization-reionization efficiency is 1.8.

[26] A.D. Baker, D.P. May and D.W. Turner, *J. Chem. Soc. B* **1968**, 22.

[27] D.J. Lavorato, L.M. Fell, G.A. McGibbon, S. Sen, J.K. Terlouw and H. Schwarz, *Int. J. Mass Spectrom. Ion Processes* **1999**, submitted for publication.

Appendix

In the context of an ongoing joint project, T. Dargel and W. Koch have explored the potential energy surface of ionized pyrimidine and its hydrogen shift isomers, structures $\mathbf{1}^{\bullet+}$- $\mathbf{9}^{\bullet+}$ in Chart 1, as well as that of the corresponding neutrals. At a level of theory (B3LYP/TZVP) that has proven to be adequate for related species [7,16], the computations predict that the distonic ions $\mathbf{2}^{\bullet+}$- $\mathbf{5}^{\bullet+}$ have a stability comparable to that of the pyrimidine ion $\mathbf{1}^{\bullet+}$. Moreover, from transition state calculations, see Table 8.2, it follows that high barriers separate these stable ions. Thus, the isomeric ions $\mathbf{2}^{\bullet+}$- $\mathbf{5}^{\bullet+}$ should be viable chemical species and indeed, as described above, mass spectrometry based experiments lead to the generation and characterization of $\mathbf{2}^{\bullet+}$, $\mathbf{3}^{\bullet+}$ and $\mathbf{4}^{\bullet+}$ as stable species in the gas phase. Ions $\mathbf{5}^{\bullet+}$ have not been identified so far, one problem being that it is difficult to envisage precursor molecules that produce the ion free of its isomer $\mathbf{2}^{\bullet+}$. Also presented in Table 8.2 are the relative energies of four more hydrogen shift isomers $\mathbf{6}^{\bullet+}$- $\mathbf{9}^{\bullet+}$. These species lie, not unexpectedly considering their canonical structures, much higher in energy than $\mathbf{1}^{\bullet+}$- $\mathbf{5}^{\bullet+}$. They were primarily considered to verify that none of the more stable distonic isomers $\mathbf{2}^{\bullet+}$- $\mathbf{5}^{\bullet+}$ rearranges via a 1,2-hydrogen shift and indeed, as shown in Table 8.2, the connecting transition state energies are prohibitively high.

In the case of the neutrals, it follows from the results presented in Table 8.3 that **2** - **5** are stable species separated by high hydrogen shift barriers and lying some 50 kcal/mol higher in energy than the pyrimidine isomer. This confirms the interpretation of the experimental observations that **2** and **3** are stable carbene/ylide type species in the gas phase. As mentioned above, the procedure by which stable ions $\mathbf{4}^{\bullet+}$ are generated does not allow probing of its neutral, whereas ions $\mathbf{5}^{\bullet+}$ have not yet been obtained as isomerically pure species in the rarefied gas phase.

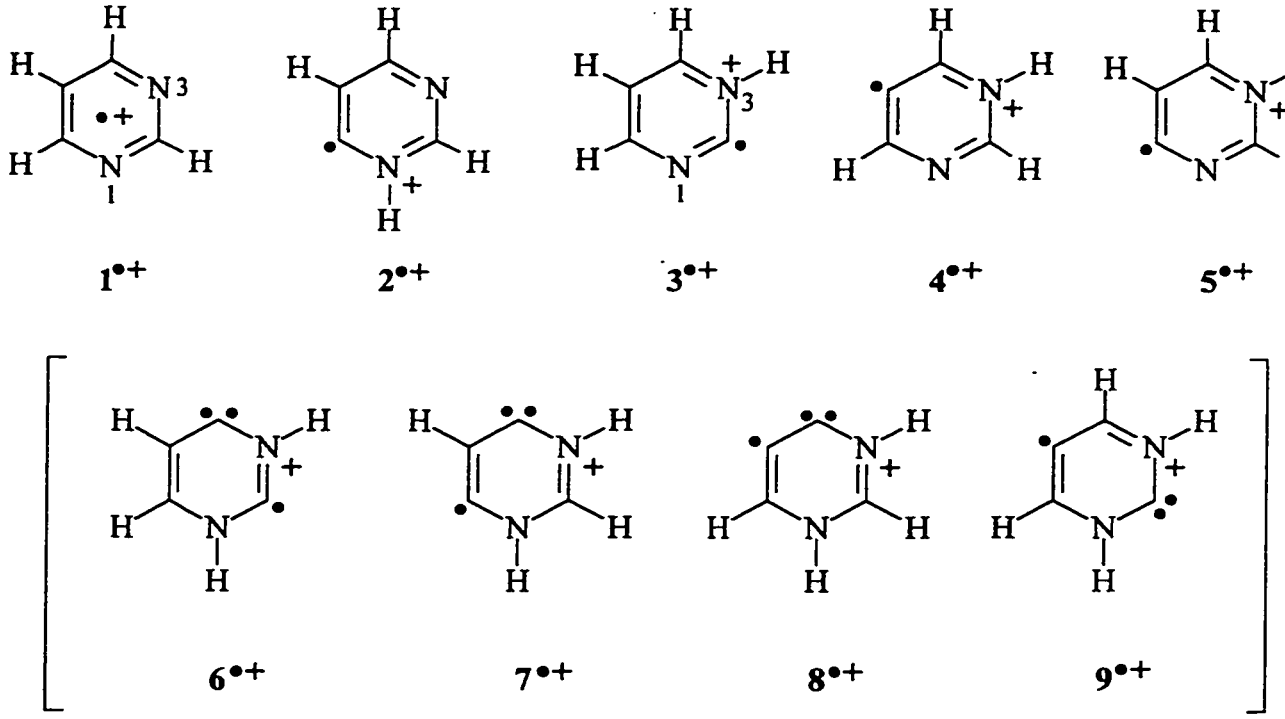

Chart 1

Table 8.2
Calculated energies (B3LYP/TZVP) for the $C_4H_4N_2^{\bullet+}$ radical cations **1**$^{\bullet+}$- **9**$^{\bullet+}$ and their isomerization barriers for 1,2-hydrogen migrations.

Species	Doublet (Hartree)	ZPVE (kcal/mol)	E_{rel}[a] (kcal/mol)
1$^{\bullet+}$	-264.07222	47.2	**0.0**
2$^{\bullet+}$	-264.06120	48.0	**7.7**
3$^{\bullet+}$	-264.06871	48.5	**3.5**
4$^{\bullet+}$	-264.06004	48.3	**8.8**
5$^{\bullet+}$	-264.07159	48.5	**1.7**
TS **1**$^{\bullet+}$/**2**$^{\bullet+}$	-263.96521	42.8	**62.8**
TS **1**$^{\bullet+}$/**3**$^{\bullet+}$	-263.95846	43.3	**67.5**
TS **2**$^{\bullet+}$/**4**$^{\bullet+}$	-263.94680	43.9	**75.4**
TS **4**$^{\bullet+}$/**5**$^{\bullet+}$	-263.94263	43.8	**77.9**
6$^{\bullet+}$	-264.01835	48.2	34.8
7$^{\bullet+}$	-263.99939	47.8	46.3
8$^{\bullet+}$	-263.99992	48.2	46.4
9$^{\bullet+}$	-264.00969	48.2	26.3
TS **3**$^{\bullet+}$/**6**$^{\bullet+}$	-263.91482	43.1	94.6
TS **2**$^{\bullet+}$/**6**$^{\bullet+}$	-263.93314	43.3	83.4
TS **2**$^{\bullet+}$/**7**$^{\bullet+}$	-263.92272	43.5	90.1
TS **7**$^{\bullet+}$/**8**$^{\bullet+}$	-263.87551	43.3	119.5
TS **4**$^{\bullet+}$/**8**$^{\bullet+}$	-263.91780	43.6	93.4
TS **5**$^{\bullet+}$/**6**$^{\bullet+}$	-263.93153	43.4	84.5
TS **4**$^{\bullet+}$/**9**$^{\bullet+}$	-263.92961	43.6	85.9
TS **6**$^{\bullet+}$/**9**$^{\bullet+}$	-263.90066	43.6	104.1

[a] Relative energies are corrected for zero-point vibrational energy (ZPVE) contributions.

Table 8.3
Calculated energies (B3LYP/TZVP) for the $C_4H_4N_2$ neutrals **1- 9** and their isomerization barriers for 1,2-hydrogen migrations.

Species	singlet (Hartree)	ZPVE (kcal/mol)	E_{rel}[a] (kcal/mol)	triplet (Hartree)	ZPVE (kcal/mol)	E_{rel}[a] (kcal/mol)
1	-264.40954	48.2	**0.0**	-264.28191	44.2	84.1
2	-264.34203	48.1	**42.3**	-264.28057	45.5	86.2
3	-264.32958	47.5	**49.5**	-264.29395	45.6	77.8
4	-264.31569	47.3	**58.1**	-264.28065	45.3	86.0
5	-264.30107	46.8	**66.7**	-264.28605	45.6	82.9
TS **1/2**	-264.26821	43.7	**84.2**	-264.18894	41.75	140.0
TS **1/3**	-264.26121	43.1	**88.0**			
TS **2/4**	-264.21474	43.6	**117.7**	-264.19532	42.2	136.4
TS **4/5**	-264.19488	43.0	**129.6**	-264.18125	42.3	145.3
6	-264.29133	48.3	74.3	-264.24428	46.2	109.7
7	-264.25636	47.7	95.7	-264.21843	45.6	125.4
8	-264.22633	46.5	113.3	-264.21160	45.3	129.3
9	-264.28012	47.6	80.7	-264.24237	45.8	110.4
TS **3/6**	-264.20455	43.6	124.1			
TS **2/6**	-264.21031	43.7	120.6	-264.16879	41.7	152.6
TS **2/7**	-264.19129	43.4	132.2	-264.15146	41.0	162.7
TS **7/8**	-264.13280	42.8	168.3	-264.10824	41.5	190.4
TS **4/8**	-264.16448	42.6	148.2	-264.13836	41.3	171.2
TS **5/6**	-264.18937	43.2	133.2	-264.16798	42.0	153.4
TS **4/9**	-264.20144	43.4	125.8	-264.16812	41.7	153.0
TS **6/9**	-264.17086	43.7	145.3	-264.15538	42.6	161.9

[a] Relative energies are corrected for zero-point vibrational energy (ZPVE) contributions.

Table 8.4
Selected calculated geometric parameters for **1** (singlet), **1** (triplet), and $\mathbf{1}^{\bullet+}$ (doublet) at the B3LYP/TZVP level of theory.[a]

Parameter	**1** (singlet)	**1** (triplet)	$\mathbf{1}^{\bullet+}$ (doublet)
C_2-N_3	1.337	1.320	1.328
C_5-N_3	1.339	1.392	1.322
C_5-C_9	1.393	1.392	1.399
H_1-C_2	1.088	1.085	1.083
H_7-C_5	1.089	1.082	1.090
H_{10}-C_9	1.085	1.087	1.084
C_2-N_4	1.140	1.410	1.410
N_4-C_6	1.282	1.282	1.282
C_6-C_9	1.454	1.454	1.454
C_6-H_8	1.091	1.091	1.091
N_3-C_5-C_9	122.4	118.3	120.1
C_5-C_9-C_6	116.5	118.2	114.3
N_3-C_2-N_4	127.4	118.0	113.9
N_3-C_5-H_7	116.5	117.1	117.1
C_5-C_9-H_{10}	121.8	121.8	121.8
N_4-C_6-H_8	119.2	119.2	119.2
C_6-C_9-H_{10}	121.8	121.8	121.8

[a] Bond lengths are in Å and angles in degrees.

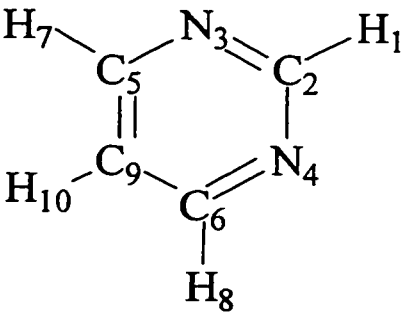

Table 8.5
Selected calculated geometric parameters for **2** (singlet), **2** (triplet), and $\mathbf{2}^{\bullet+}$ (doublet) at the B3LYP/TZVP level of theory.[a]

Parameter	**2** (singlet)	**2** (triplet)	$\mathbf{2}^{\bullet+}$ (doublet)
H_1-C_2	1.089	1.086	1.087
H_5-N_3	1.016	1.013	1.022
H_8-C_7	1.089	1.083	1.088
H_{10}-C_9	1.088	1.085	1.084
C_2-N_3	1.362	1.428	1.376
N_3-C_6	1.379	1.384	1.328
C_6-N_9	1.432	1.348	1.368
C_2-N_4	1.306	1.287	1.305
N_4-C_7	1.362	1.368	1.342
C_7-C_9	1.379	1.434	1.410
H_1-C_2-N_3	117.3	114.8	117.0
C_2-N_3-H_5	116.0	117.1	119.8
C_2-N_3-C_6	127.4	115.2	119.4
N_3-C_6-C_9	108.4	123.3	122.9
H_8-C_7-C_9	121.7	121.6	120.0
C_7-C_9-H_{10}	118.7	120.9	122.4
C_6-C_9-C_7	123.1	116.8	114.1
C_2-N_4-C_7	115.0	119.9	118.9
N_4-C_7-C_9	123.3	120.6	123.6
H_5-N_3-C_6-C_9	0.0	-24.8	0.0

[a] Bond lengths are in Å and angles in degrees.

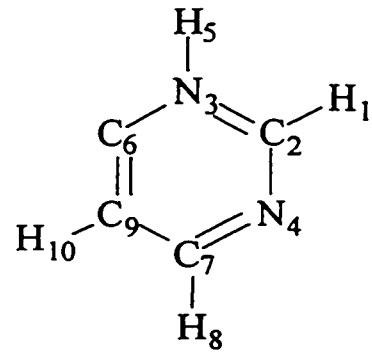

Table 8.6
Selected calculated geometric parameters for **3** (singlet), **3** (triplet), and $\mathbf{3}^{\bullet+}$ (doublet) at the B3LYP/TZVP level of theory.[a]

Parameter	**3** (singlet)	**3** (triplet)	$\mathbf{3}^{\bullet+}$ (doublet)
C_1-N_2	1.399	1.366	1.344
C_1-N_3	1.385	1.249	1.269
N_2-C_5	1.357	1.423	1.362
C_5-C_9	1.370	1.376	1.384
N_3-C_6	1.324	1.406	1.347
C_6-C_9	1.411	1.403	1.402
N_2-H_4	1.013	1.007	1.019
C_5-H_7	1.086	1.081	1.085
C_6-H_8	1.092	1.081	1.086
C_9-H_{10}	1.083	1.086	1.084
C_1-N_2-C_5	128.2	117.2	119.1
C_1-N_2-H_4	114.4	121.4	120.3
N_2-C_5-C_9	117.7	117.7	118.7
N_2-C_5-H_7	118.1	116.8	117.1
C_5-C_9-C_6	115.7	121.1	118.2
C_5-C_9-H_{10}	121.9	118.9	120.5
N_2-C_1-N_3	111.8	126.2	124.3
C_1-N_3-C_6	122.0	120.1	120.0
N_3-C_6-C_9	124.7	117.7	119.8
N_3-C_6-H_8	116.5	117.9	117.7

[a] Bond lengths are in Å and angles in degrees.

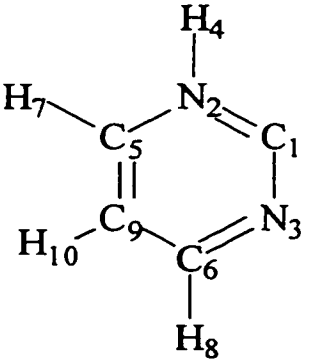

CHAPTER 9

Experimental

9.1 The VG Analytical ZAB-R

All tandem mass spectrometry-based experiments were performed at McMaster University using the VG Analytical ZAB-R instrument of $B(\perp Q)E_1E_2$ geometry (B = magnet, Q = quadrupole, E = electrostatic analyzer). This custom built mass spectrometer is a three sector instrument whose design is based on the standard, non-extended geometry of its predecessor the ZAB-2f [1].

The ion source, which is kept under high vacuum using a 160/170 Diffstak, is equipped with four inlet systems for sample introduction: i) a septum inlet used for compounds having very high vapour pressures, ii) an all glass heated inlet system (AGHIS), which can also be used as a very low pressure (VLVP) inlet, used for volatile compounds, iii) an all quartz direct insertion probe used for less volatile compounds and iv) a direct solid insertion probe used for solid samples which have very low vapour pressures. For involatile liquid samples, it is often useful to smear a sample on the tip of the quartz probe to obtain greater sensitivity. Both the AGHIS and quartz probe possess reservoirs from which the sample steadily evaporates/sublimes, consequently the temperature of bulk sample can easily be varied to obtain a desired source pressure.

Located in the first field free region (1ffr) of the instrument, there is a collision cell (cell 1). An Autospec magnet precedes the second field free region (ffr) housing which has the form of a rectangular box. This box [79 x 23 x 23 cm] has easily removable top and side panels. The box may be quickly isolated from its two 160/170 Diffstaks and the other sectors by using four valves. This enables rapid access to the collision chambers

and lens assemblies which are mounted to its "optical bench" type of internal base. The box contains three collision gas chambers, i.e. cells 2, 3 and 4, whose locations are shown in Figure 1.1. Cell 2 [30(l) x 3(w) x 14(h) mm] is a home-built chamber used for neutralization with organic vapours, such as N,N-dimethylaniline. Cell 3 [20(l) x 1(w) x 10(h) mm], which is electrically isolated to 5 keV and is preceded by a (de)-accelerating lens, is used for neutralization with permanent gases, such as cyclopropane. Cell 4 [20(l) x 1(w) x 10(h) mm], which is also electrically isolated and equipped with a y-focus/deflection lens assembly, is used for "standard" reionization and collision-induced dissociation (CID) experiments. These collision chambers are situated at distances of 240, 44 and 10 mm, respectively, from the focal point at the intermediate slit located next to the glass window which is situated on the top of the box. Immediately following the first electrostatic analyzer (E_1), there is a box type collector housing in which the 3ffr collision gas chamber is located in front of a small Autospec ESA (E_2, 5" radius, 72.5°). This housing contains two photomultiplier type detectors and a fifth 160/700 Diffstak is used to pump this region.

A Quadrupole mass analyzer (200 amu), with a channeltron electron multiplier detector, is mounted on one side of cell 3 - perpendicular to the flight path of the fast moving ion beam. The quadrupole is used to acquire spectra of ionized target molecules and their dissociation products resulting from the neutralization process of a mass selected ion beam [2]. This technique was not used in the context of the work described in the thesis.

9.2 Experimental Conditions

Unless otherwise stated, all mass spectra were obtained using electron impact ionization and were acquired under the following conditions: electron energy, 70 eV; emission current, 100-500 μA; source temperature 100-120 °C. The accelerating potential used in individual experiments is given in the Chapters. Source pressures, monitored by a remote ionization gauge, of 10^{-5} to 10^{-6} Torr were used.

The chemical ionization experiments carried out in this work used methanol vapour as the reagent gas at pressures of approximately 10^{-4} Torr. All other parameters were as indicated above.

The metastable ion (MI) mass spectra were obtained in the 2ffr of the instrument unless otherwise indicated. The kinetic energy release (KER) values were estimated from the width at half height ($T_{0.5}$) of the appropriate metastable peak, by means of a standard equation (see Chapter 1) and corrected for the width at half height of the main beam [3].

The collision-induced dissociation (CID) spectra were obtained in either the second or third ffr using O_2 (main beam transmittance - 80 %) as the collision target. The "MS/MS/MS" experiments, i.e. the MI/CID, CID/CID and NR/CID, were all obtained in the 3ffr again using O_2 (main beam transmittance - 80 %) to collisionally activate the ions.

The neutralization-reionization (NR) mass spectra were obtained in the 2ffr using either N,N-dimethylaniline (cell 2) or cyclopropane (cell 3) as the neutralization target (main beam transmittance - 70 %) and O_2 (cell 4, main beam transmittance - 80 %) as the reionization agent. For all NR experiments, a total analyzer pressure of 2-3 x 10^{-5} Torr was used. A positive deflector electrode is located between cells 3 and 4 to remove any remaining ions from the beam.

All spectra were recorded using a PC-based data system with ZABCAT software developed by Mommers Technologies Inc. (Ottawa, Canada). The quoted MI, CID and NR spectra are integrated data, complied from 2 - 5 individual scans while the MS/MS/MS spectra represent an accumulation of 25 - 35 individual scans.

The appearance energy (AE) obtained for the $C_5H_5N^{\bullet+}$ ions generated from metastable methylpicolinate molecular ions (see Chapter 2) was obtained by the comparative method of Burgers and Holmes [4] using the KRATOS MS 902S instrument located at the University of Ottawa.

9.3 Preparation of Precursor Molecules

Unless otherwise indicated, all precursor molecules were commercially available (Aldrich, Milwaukee, USA), and were used without further purification. The procedure for all synthesized precursor molecules is given below and is presented by Chapter. High resolution measurements were performed on all precursor molecules to verify the identity of the compound.

CHAPTER 2

Methyl picolinate was prepared according to literature procedures [5]. Concentrated sulfuric acid (1 mL, 0.019 mol) was slowly added to a cold (0 °C) solution of picolinic acid (4g, 0.032 mol) in methanol (7.3 mL, 0.175 mol). The mixture was then boiled under reflux for 3 hours and assumed a brown colour. The excess methanol was removed using a rotary evaporator. The solution was then cooled to 0 °C and 35 mL of ice was added. The mixture was then made alkaline with a saturated solution of sodium carbonate and the precipitate removed by cold filtration. The product was then extracted using 5 x 30 mL of diethyl ether, dried with anhydrous sodium sulfate and filtered. The ether was removed using a rotatory evaporator yielding 3.7 g (83 %) of a clear colourless oil. ^{1}H NMR (200 MHz, $CDCl_3$) δ: 3.94 (s, 3H), δ: 7.46 (ddd, 1H), δ: 7.81 (dt, 1H), δ: 8.03 (ddd, 1H), δ: 8.70 (dt, 1H); ^{13}C NMR (50 MHz, $CDCl_3$) δ: 52.8 (CH_3), 125.0, 126.8, 137.0, 147.7, 149.6, 165.6 (C=O).

Methyl picolinate (CD_3) was synthesized using the procedure described above. (1.35 g, 0.011 mol) of picolinic acid in (2.5 mL, 0.062 mol) of methanol-d_4 and (0.25 mL, 0.004 mol) sulfuric acid were used. This yielded 1.12 g (75 %) of a colourless oil. ^{1}H NMR (200 MHz, $CDCl_3$) δ: 7.42 (ddd, 1H), δ: 7.80 (dt, 1H), δ: 8.07 (ddd, 1H), δ: 8.73 (dt, 1H); ^{13}C NMR (50 MHz, $CDCl_3$) δ: 125.1, 126.9, 137.0, 147.8, 149.7, 165.6 (C=O).

CHAPTER 3

A sample of methyl-2-carboxypyridine-3-carboxylate was generously donated by Prof. David MacLean and was used without further purification. The -OD labelled isotopomer of methyl-2-carboxypyridine-3-carboxylate was obtained by an exchange reaction with CH_3OD. To obtain greater isotopic enrichment, the exchange reaction was performed a total of three times. In each case, the excess methanol was removed under vacuum.

CHAPTER 5

Dimethyl imidazole-4,5-dicarboxylate was prepared as previously described by Baxter and Spring [6]. 4,5-Imidazoledicarboxylic acid (2.1 g, 0.013 mol) was partially dissolved in cold (0 °C) concentrated sulfuric acid (12 mL, 0.230 mol). To this reaction mixture, anhydrous methanol (50 mL, 1.24 mol) was carefully added. The mixture was then boiled under reflux until all the starting material had dissolved (~ 15 min.). The excess methanol was removed using a rotary evaporator and the residue was taken up in 50 mL of distilled water and neutralized with a saturated solution of sodium carbonate. The precipitate was filtered and the filtrate concentrated. Crystallization of the product occurred upon cooling in a salt/ice bath yielding 1.5 g (63 %) of the ester m.p. = 195 - 197 (lit. [6] = 200 - 203). ^{1}H NMR (200 MHz, DMSO-d_6) δ: 3.79 (s, 6H), δ: 7.90 (s, 1H); ^{13}C NMR (50 MHz, DMSO-d_6) δ: 52.0 (CH_3), 136.3, 138.1, 161.2 (C=O).

CHAPTER 6

Methyl pyrazine-2-carboxylate was prepared as described by Spinner [7]. A solution of 2-pyrazinecarboxylic acid (1 g, 0.008 mol) in absolute methanol (4.9 mL, 0.121 mol) containing concentrated sulfuric acid (0.2 mL, 0.002 mol) was boiled under reflux for 8 hr. After adding 0.5 g of activated charcoal, the solution was filtered and washed with methanol. The filtrate was evaporated to ~ 2 mL and then diluted with 10 mL of distilled water. After saturating the solution with sodium chloride the mixture was neutralized with sodium carbonate and immediately extracted 5 times with 10 mL

portions of diethyl ether. The ethereal extract was dried over sodium sulfate, filtered, and concentrated. Upon cooling, the crystalline ester was obtained. The crystals were further purified by the addition of hot light petroleum ether to an existing diethyl ether solution until a very small amount of yellow oil separated. The colourless supernatant was decanted and immediately placed in an ice bath. Upon crystallization, 0.9 g (80 %) of the ester was obtained m.p. 57 - 58 °C (lit. [7] = 59 °C). ^{1}H NMR (200 MHz, $CDCl_3$) δ: 3.98 (s, 3H), δ: 8.67 (dd, 1H), δ: 8.72 (d, 1H), δ: 9.26 (d, 1H). ^{13}C NMR (50 MHz, $CDCl_3$) δ: 53.1 (CH_3), 143.2, 144.3, 146.2, 147.6, 164.3 (C=O).

Methyl pyrazine-2-carboxylate (CD_3) was synthesized using the procedure described above. (1.0 g, 0.008 mol) of 2-pyrazinecarboxylic acid in (4.9 mL, 0.121 mol) of methanol-d_4 and (0.2 mL, 0.002 mol) sulfuric acid were used. This yielded 0.81 g (73 %) of the labelled ester. ^{1}H NMR (200 MHz, $CDCl_3$) δ: 8.68 (dd, 1H), δ: 8.74 (d, 1H), δ: 9.28 (d, 1H). ^{13}C NMR (50 MHz, $CDCl_3$) δ: 143.2, 144.3, 146.2, 147.7, 164.3 (C=O).

Dimethyl pyrazine-2,3-dicarboxylate was prepared using the above procedure. A solution of 2,3-pyrazinedicarboxylic acid (1 g, 0.006 mol) in absolute methanol (10 mL, 0.244 mol) containing concentrated sulfuric acid (0.2 mL, 0.002 mol) was boiled under reflux for 15 hr. The result was 1.0 g of the diester (86 %) m.p. 55 - 57 °C (lit. [7] = 59.5 - 60 °C). ^{1}H NMR (200 MHz, $CDCl_3$) δ: 4.00 (s, 3H), δ: 8.74 (s, 1H). ^{13}C NMR (50 MHz, $CDCl_3$) δ: 53.4 (CH_3), 144.9, 145.5, 164.5 (C=O).

Dimethyl pyrazine-2,5-dicarboxylate was prepared in a two step synthesis as described by Schut and co-workers [8]. 2,5-Dimethylpyrazine (2.5 mL, 0.023 mol), pyridine (50 mL, 0.619 mol), selenium dioxide (12.5 g, 0.113 mol) and distilled water (7 mL, 0.389 mol) were boiled under reflux for 12 hr., the boiling solution assumed an orange-red colour after 20 minutes as selenium gradually precipitated. The mixture was allowed to cool to room temperature and the precipitate A, a mixture of selenium and

product, was filtered. The flask was rinsed out 3 times with 10 mL of a hot pyridine/water mixture (10:1). All the filtrates were combined and taken to dryness under vacuum. The brown coloured residue was dissolved in warm 2 M ammonium hydroxide (15 mL) to which concentrated HCl was added to give precipitate B. The combined precipitates A and B were washed three times with 15 mL portions of 2 M HCl, then with 3 times 20 mL of ice-cold water. The precipitates were then dissolved in 2 M ammonium hydroxide and concentrated HCl was added to the colourless solution to produce a white precipitate which was filtered and washed with 2 M HCl and ice-cold water. 2.1 g of 2,5-pyrazinedicarboxylic acid was obtained.

A mixture of anhydrous 2,5-pyrazinedicarboxylic acid (1 g, 0.006 mol), absolute methanol (34 mL, 0.840 mol) and concentrated sulfuric acid (0.5 mL, 0.010 mol) was boiled under reflux until a clear solution was obtained (~ 3 hr.). After standing overnight at -5 °C, the crystalline product was filtered off and washed twice with ice-cold methanol to yield 0.8 g of dimethyl pyrazine-2,5-dicarboxylate m.p. 167 - 168 °C (lit. [8] = 168.5 - 169 °C). ^{1}H NMR (200 MHz, $CDCl_3$) δ: 4.00 (s, 6H), δ: 9.18 (s, 2H). ^{13}C NMR (50 MHz, $CDCl_3$) δ: 52.7 (CH_3), 144.6, 144.8, 162.8 (C=O).

CHAPTER 7

Methyl pyridine-2-thiocarboxylate was prepared as outlined by Budzikiewicz and co-workers [9]. 2-Cyanopyridine (9.5 g, 0.093 mol) and anhydrous methanol (11.3 mL, 0.279 mol) were dissolved in toluene (30 mL, 0.315 mol). Anhydrous HCl was passed through the solution for 6 hr. while being cooled with a salt/ice bath. The white precipitate which was formed was filtered under nitrogen and dissolved in anhydrous pyridine (80 mL, 0.971 mol). Anhydrous H_2S was then passed through the solution for 6 hr. The pyridine was then distilled under vacuum and the residue was extracted with diethyl ether (20 mL x 6). The ether was removed with a rotary evaporator and 4 mL of a red liquid remained. To remove residual pyridine and toluene, the compound was chromatographed on a 4 mm silica plate using hexane. Approximately 400 uL of the compound was isolated. MS (E.I.) m/z: 153 ($M^{\bullet+}$, 50 %), 123 (100 %), 93 (60 %), 79 (70

%), 78 (90 %).

Bis(ethoxycarbonyl)pyridinium methylide was prepared as described by Bowen [10]. Diethylbromomalonate (3.5 mL, 0.021 mol) was dissolved in pyridine (1.7 mL, 0.021 mol) and was stirred at room temperature for 24 hr. The solid brown residue obtained was then dissolved in 10 mL of a saturated sodium carbonate solution. The product was extracted with 4 x 10 mL of chloroform. The chloroform layer was dried over magnesium sulfate and filtered. The chloroform was removed under vacuum to yield a yellow powder of bis(ethoxycarbonyl)pyridinium methylide. The product was recrystallized from acetone (2.5 g, 50 %) m.p. 170 - 171 °C (lit. [10] 170 - 171 °C). ^{1}H NMR (200 MHz, $CDCl_3$) δ: 1.26 (t, 6H), δ: 4.15 (quartet, 4H) δ: 7.67 (t, 2H), δ: 8.08 (t, 1H), δ: 8.58 (d, 2H). ^{13}C NMR (50 MHz, $CDCl_3$) δ: 14.8 (CH_3), 59.0 (CH_2), 97.9, 125.6, 140.9, 149.9, 165.1 (C=O).

Dimethyl pyridine-2,3-dicarboxylate was prepared using a similar method [11] to that of the mono ester, methyl picolinate. Concentrated sulfuric acid (0.4 mL, 0.009 mol) was slowly added to a cold (0 °C) solution of 2,3-pyridinedicarboxylic acid (5 g, 0.030 mol) in methanol (15 mL, 0.355 mol). The reaction mixture was then boiled under reflux for 28 hours. The excess methanol was removed using a rotary evaporator. The mixture was then cooled to 0 °C and neutralized using a saturated solution of sodium carbonate. The solution was filtered and the product was extracted using 5 x 30 mL of chloroform. The extract was dried with anhydrous sodium sulfate and filtered. The solvent was removed using a rotator evaporator yielding 5.0 g (85 %) of the diester. ^{1}H NMR (200 MHz, $CDCl_3$) δ: 3.90 (s, 3H), δ: 3.97 (s, 3H), δ: 7.46 (dd, 1H), δ: 8.14 (dd, 1H), δ: 8.73 (dd, 1H). ^{13}C NMR (50 MHz, $CDCl_3$) δ 52.9 (CH_3), 53.0 (CH_3), 124.8, 126.4, 137.5, 150.6, 151.7, 165.7 (C=O), 166.5 (C=O).

Dimethyl pyridine-2,3-dicarboxylate $(CD_3)_2$ was synthesized using the procedure described above. (1.35 g, 0.011 mol) of 2,3-pyridinedicarboxylic acid in (2.5 mL, 0.062

mol) of methanol-d_4 and (0.25 mL, 0.004 mol) sulfuric acid were used. This yielded 1.12 g (72 %) of the product. ^{1}H NMR (200 MHz, $CDCl_3$) δ: 7.46 (dd, 1H), δ: 8.14 (dd, 1H), δ: 8.73 (dd, 1H). ^{13}C NMR (50 MHz, $CDCl_3$) δ: 124.8, 126.4, 137.5, 150.6, 151.7, 165.7 (C=O), 166.5 (C=O).

Propylpyrazine was prepared as described by Behun and Levine [12]. Sodium metal (1.3 g, 0.056 mol) was carefully added to liquid ammonia (60 mL) contained in a 250 mL, three neck, round bottom flask equipped with a stirrer, dry ice condenser and dropping funnel. Once the sodium had completely reacted, methylpyrazine (5 g, 0.053 mol) was added. The blood-red solution of pyrazylmethyl sodium which resulted was stirred for 30 min. to ensure complete conversion of methylpyrazine to its anion. Bromoethane (3.9 mL, 0.053 mol) diluted in diethyl ether (4 mL, 0.038 mol) was then added over a twenty minute period and the reaction was stirred for 1 hr. The reaction was then quenched by the addition of ammonium chloride (5 g, 0.094 mol). The dry ice condenser was replaced by a water-cooled condenser and the ammonia was replaced with diethyl ether (30 mL). The reaction was then boiled under reflux for 3 min. to ensure that the ammonia had been completely removed. The resulting solution was then poured onto ice (30 mL), was made strongly acidic with concentrated HCl and extracted with 5 x 10 mL portions of ether. The ethereal extract was dried using magnesium sulfate, filtered and evaporated to yield 2.6 g (40 %) of product. ^{1}H NMR (200 MHz, $CDCl_3$) δ: 0.84 (t, CH_3), δ: 1.63 (dt, CH_2) δ: 2.66 (t, CH_2), δ: 8.26 (2, 1H), δ: 8.34 (dd, 1H), δ: 8.36 (d, 1H). ^{13}C NMR (50 MHz, $CDCl_3$) δ: 13.5 (CH_3), 22.4 (CH_2), 37.2 (CH_2), 141.9, 143.6, 144.4, 157.5.

Methyl-5-methylpyrazine-2-carboxylate was prepared using the procedure outlined above for dimethyl pyrazine-2,5-dicarboxylate (Chapter 6). 5-methylpyrazine-2-carboxylic acid, (4 g, 0.029 mol), absolute methanol (30 mL, 0.740 mol) and concentrated sulfuric acid (0.5 mL, 0.010 mol) were used to obtain 3.3 g (74 %) of the ester. ^{1}H NMR

(200 MHz, $CDCl_3$) δ: 2.66 (s, CH_3), δ: 4.01 (s, OCH_3), δ: 8.57 (s, 1H), δ: 9.18 (s, 1H). ^{13}C NMR (50 MHz, $CDCl_3$) δ: 21.9 (CH_3), δ: 52.9 (OCH_3), 140.5, 144.3, 145.3, 157.8, 164.6 (C=O).

CHAPTER 8

Methyl pyrimidine-4-carboxylate was prepared in a two step synthesis as described by Wong and co-workers [13]. 4-Methylpyrimidine (1.7 g, 0.018 mol) and sodium hydroxide (0.42 g, 0.011 mol) were dissolved in 10 mL of distilled water at 70 °C. A solution of $KMnO_4$ (6 g, 0.038 mol) in 60 mL of distilled water was added over 3 hr. to the above solution. The stirred solution was kept between 70 and 80 °C for the duration of the addition. After the addition was complete, the solution was allowed to stir for 3 more hours. The solution was not allowed to cool and the MnO_2 was filtered from the hot solution and washed with hot water. The filtrate and the washings were then concentrated to approximately 25 mL. Concentrated HCl was added to the solution to adjust the pH to 2-3. A white precipitate formed and the flask was cooled. 1.8 g (82 %) of 4-pyrimidinecarboxylic acid was obtained and was not further purified.

A solution of 4-pyrimidinecarboxylic acid (0.8 g, 0.006 mol), concentrated HCl (0.3 mL, 0.006) and methanol (30 mL, 0.653 mol) were boiled under reflux for 8 hr. The resulting solution was neutralized with sodium bicarbonate, concentrated, and extracted with 5 x 20 mL of ether. The combined extracts were dried over magnesium sulfate, concentrated and cooled to yield 0.6 g (72 %) of the ester m.p. 68 - 69 °C (lit. [13] = 70 - 71 °C). ^1H NMR (200 MHz, $CDCl_3$) δ: 4.02 (s, 3H), δ: 8.01 (dd, 1H), δ: 9.00 (d, 1H), δ: 9.39 (d, 1H). ^{13}C NMR (50 MHz, $CDCl_3$) δ: 53.4 (CH_3), 120.9, 154.6, 159.1, 159.2, 164.4 (C=O).

Methyl pyrimidine-4-carboxylate (CD_3) was synthesized using the procedure described above. (0.8 g, 0.006 mol) of 4-pyrimidinecarboxylic acid in (2.5 mL, 0.062 mol) of methanol-d_4 and (0.10 mL, 0.002 mol) sulfuric acid were used. This yielded 0.51

g (60 %) of the labelled ester. ^{1}H NMR (200 MHz, $CDCl_3$) δ: 8.00 (dd, 1H), δ: 8.98 (d, 1H), δ: 9.39 (d, 1H). ^{13}C NMR (50 MHz, $CDCl_3$) δ: 120.9, 154.6, 159.2, 159.3, 164.5 (C=O).

Methyl pyrimidine-2-carboxylate was prepared in a four step procedure. 2-chloropyrimidine was first converted to 2-cyanopyrimidine [14] in a two step process. The nitrile was then hydrolyzed to the carboxylic acid and ultimately esterified to the methyl ester [15].

To a cooled solution of 2-chloropyrimidine (3.4 g, 0.03 mol) and anhydrous benzene (60 mL, 0.672 mol) was added a solution of trimethylamine (2.1 g, 0.035 mol) in anhydrous benzene (15 mL, 0.163 mol). The reaction mixture was stirred for 30 min. at which time the cooling bath was removed and the solution was brought to room temperature. The resulting precipitate was filtered, washed with diethyl ether and dried under vacuum to yield 4.5 g (86 %) of the 2-pyrimidyltrimethylammonium chloride salt.

2-Pyrimidyltrimethylammonium chloride (4.5 g, 0.026 mol) was suspended in CH_2Cl_2 (40 mL, 0.502 mol). Over a period of 10 min., a solution containing $(CH_3CH_2)_4N^+CN^-$ (3.81 g, 0.03 mol) dissolved in CH_2Cl_2 (40 mL, 0.502 mol) was added with constant stirring. The reaction was stirred for a further 25 min. The reaction mixture was then shaken with 20 mL of distilled ice-cold water (3x). The CH_2Cl_2 layer was then dried using magnesium sulfate and filtered. The CH_2Cl_2 was removed using a rotary evaporator yielding 2.1 g (74 %) of 2-cyanopyrimidine.

A solution of 2-cyanopyrimidine (1.0 g, 0.009 mol) in 2 M NaOH (14 mL) was boiled under reflux for 2 hr. The pH of the solution was then adjusted (2.0 - 2.5) by the addition of 12 M HCl. The solution was then concentrated to approximately 10 mL. A 10 % cupric acetate solution was added and the resulting blue precipitate was filtered. The copper salt was then suspended in water and hydrogen sulfide was passed through the mixture. The copper sulphide was removed by filtration and the filterate was evapourated to dryness yielding 1.8 g (68 %) of 2-pyrimidinecarboxylic acid.

2-Pyrimidinecarboxylic acid (1.0 g, 0.008 mol) was dissolved in water,

neutralized with ammonia and precipitated as the silver salt by the addition of a solution of silver nitrate (1.2 M). The dry silver salt was suspended in CH_2Cl_2 and boiled under reflux together with CH_3I (2.0 g, 0.014 mol) for 2 hr. The mixture was filtered, the chloroform removed and the residue recrystallized from ethanol to yield 0.65 g (60 %) of the ester m.p. 96 - 97 °C (lit. [16] = 104 - 105 °C). ^1H NMR (200 MHz, $CDCl_3$) δ: 4.05 (s, 3H), δ: 7.48 (t, 1H), δ: 8.93 (d, 2H). ^{13}C NMR (50 MHz, $CDCl_3$) δ: 53.6 (CH_3), 123.1, 156.4, 157.7, 163.7 (C=O).

Methyl pyrimidine-2-carboxylate (CD_3) was synthesized using the procedure described above. (0.8 g, 0.006 mol) of 2-pyrimidinecarboxylic acid in (2.5 mL, 0.062 mol) of methanol-d_4 and (0.10 mL, 0.002 mol) sulfuric acid were used. This yielded 0.35 g (42 %) of the labelled ester. ^1H NMR (200 MHz, $CDCl_3$) δ: 7.47 (t, 1H), δ: 8.93 (d, 2H). ^{13}C NMR (50 MHz, $CDCl_3$) δ: 123.1, 156.5, 157.8, 163.7 (C=O).

References

[1] R.P. Morgan, J.H. Beynon, R.H. Bateman and B.N. Green, *Int. J. Mass Spectrom. Ion Phys.* **1978**, *28*, 171.

[2] T. Wong, J.K. Terlouw, T. Weiske and H. Schwarz, *Int. J. Mass Spectrom. Ion Processes* **1992**, *113*, R23.

[3] M.A. Baldwin, P.J. Derrick and R.P. Morgan, *Org. Mass Spectrom.* **1976**, *11*, 440.

[4] P.C. Burgers and J.L. Holmes, *Org. Mass Spectrom.* **1982**, *17*, 123.

[5] E. Bald, *Chemica Scripta* **1978/79**, *13*, 108.

[6] F. Baxter and J. Spring, *J. Chem. Soc.* **1945**, 233.

[7] K. Spinner, *Recueil* **1958**, *77*, 125.

[8] W.J. Schut, H.I.X. Mager and W. Berends, *Recueil* **1961**, *80*, 391.

[9] H. Budzikiewicz, E. Lange and W. Ockles, *Sulfur and Phosphorus* **1981**, *11*, 33.

[10] D.V. Bowen, W. Skett, J. Thorpe, and A.O. Plunkett, *Org. Mass Spectrom.* **1984**, *19*, 285.

[11] W.L.P. Armarego, B.A. Milloy and S.C. Sharma, *J. Chem. Soc.* **1972**, 2485.

[12] J.D. Behun and R. Levine, *J. Org. Chem.* **1961**, *26*, 3379.

[13] J.L. Wong, M.S. Brown and H. Rapoport, *J. Chem. Soc.* **1965**, 2398.

[14] F.H. Case and E. Koft, *J. Am. Chem. Soc.* **1959**, *95*, 803.

[15] S. Gronowitz, B. Norrman, B. Gestblom, B. Mathiasson and R.A. Hoffman, *Arkiv För Kemi* **1963**, *22*, 65.

[16] A. Holland, *Chem. and Ind.* **1954**, 786.

SUMMARY

The stability of the hydrogen shift isomers of a series of nitrogen containing heterocycles has been studied in the rarefied gas phase using a variety of tandem mass spectrometric techniques, isotopic labelling experiments and quantum chemical calculations. The heterocyclic systems examined include the five membered species thiazole and imidazole as well as the six membered species pyridine, pyrazine and pyrimidine.

The ionic hydrogen shift isomers studied are thermodynamically as stable as their parent isomer of conventional structure. They are accessible by dissociative electron ionization of a carefully chosen molecule. In the case of heterocyclic systems, precursors capable of 1,4- or 1,5-hydrogen migrations to the heteroatom are excellent candidates. For example, 2-pyridinecarboxylic acid and its methyl ester abundantly yield ionized pyridine-2-ylidene by respectively, the loss of CO_2 and the consecutive loss of CH_2O and CO. Other hydrogen shift isomers, including ionized pyridine-3-ylidene, thiazol-2-ylidene, imidazol-2-ylidene, imidazol-4-ylidene, pyrazine-2-ylidene, pyrazine-3-ylidene, pyrimidine-2-ylidene and pyrimidine-4-ylidene could also be generated using this strategy.

The characterization of a set of ionic isomers was accomplished using both MI and CID mass spectrometry. The isomers of each system yielded MI spectra dominated by a peak corresponding to the loss of m/z 27 [H,C,N]. The KER values associated with this loss differed for some isomers enabling their characterization. However, pairs of isomers such as ionized pyridine and pyridine-2-ylidene, ionized pyrazine-2-ylidene and pyrazine-3-ylidene and ionized pyrimidine and pyrimidine-2-ylidene, have identical KER values. This suggests that these isomers may communicate prior to the dissociation reaction of lowest energy requirement, a rearrangement. Indeed, the *ab initio* calculations indicate that the high barriers for isomerization of the isomers do lie below the dissociation threshold. Nevertheless, high energy CID reactions, see below, can be used to

differentiate the isomeric ions.

The ionized hydrogen shift isomers of thiazole and imidazole displayed characteristic dissociation pathways in their respective CID mass spectra. In contrast, the CID spectra of pyridine, pyrazine, pyrimidine and their hydrogen shift isomers could only be differentiated on the basis of relative peak intensities and the presence of charge stripping peaks. In particular, the ratio m/z 26 : 28 provided the most structure diagnostic information. The formation of these fragment ions requires that a considerable amount of internal energy be deposited in the precursor ions upon CID. Thus, differentiation of the isomers is possible even for systems in which the isomerization barrier lies lower in energy than the dissociation reaction of lowest energy requirement. These characterizations are possible because the rate of dissociation of these *high* energy ions is significantly faster than the rate of isomerization.

NR experiments showed that, despite their elevated enthalpies of formation, the neutral hydrogen shift isomers pyridine-3-ylidene, thiazol-2-ylidene, imidazol-2-ylidene, imidazol-4-ylidene, pyrazine-2-ylidene, pyrazine-3-ylidene, pyrimidine-2-ylidene and pyrimidine-4-ylidene are stable species on the microsecond timescale. CID experiments on the reionized neutrals were used to unambiguously establish the structure of the incipient molecules. Quantum chemical calculations revealed the presence of large isomerization barriers (> 40 kcal/mol) which hinders the facile interconversion of the isomers of a given system, thus accounting for their intrinsic stability in the gas phase. The calculations also indicate that the singlet carbenes/ylides are more stable than their triplet counterparts. The observed singlet-triplet (S-T) gap varied considerably depending upon the isomer and a clear trend could not be established for the hydrogen shift isomers studied. For example, the highest S-T gap was observed for imidazol-2-ylidene, 78 kcal/mol, while pyrazine-3-ylidene yielded the lowest, 3 kcal/mol.

The product ions of the decarbonylation reaction of ionized 2-acetylpyridine, 2-acetylpyrazine and 2-acetylthiazole were identified as ionized 2-methylene-1,2-dihydropyridine, 2-methylene-1,2-dihydropyrazine and 2-methylene-2,3-dihydrothiazole, respectively. This refutes proposals in the older literature that the decarbonylation would

involve a methyl transfer yielding the 2-methylpyridine, 2-methylpyrazine and 2-methylthiazole. Literature proposals for a methyl migration in the dissociation of ionized dimethyl pyridine-2,3-dicarboxylate and methyl pyridine-4-carboxylate were also examined, but could not be substantiated. However, the proposed gas phase synthesis of the N-methylpyridinium ylide from ionized methyl pyridine-2-thiocarboxylate provided evidence for a genuine methyl migration. Exploratory quantum chemical calculations indicated that ionized 2-methylene-1,2-dihydropyridine and ionized 2-methylene-2,3-dihydrothiazole are among the stable isomers on their respective potential energy surfaces. Their neutral counterparts, however, are considerably less stable. Nevertheless, from neutralization-reionization experiments it follows that the neutral counterparts of the ionized decarbonylation products are stable molecules on the microsecond timescale. Significant 1,3-hydrogen barriers hinder the interconversion of both the ions and the neutrals into their 2-methyl substituted isomers, thus accounting for their stability in the gas phase.